frontiers | Research Topics

# Current insights in Epigenetics and Epigenomics

**Edited by**
Steven Henikoff, Sharon Y. R. Dent, Raul Mostoslavsky, Ting Wang and Luca Comai

**Published in**
Frontiers in Epigenetics and Epigenomics

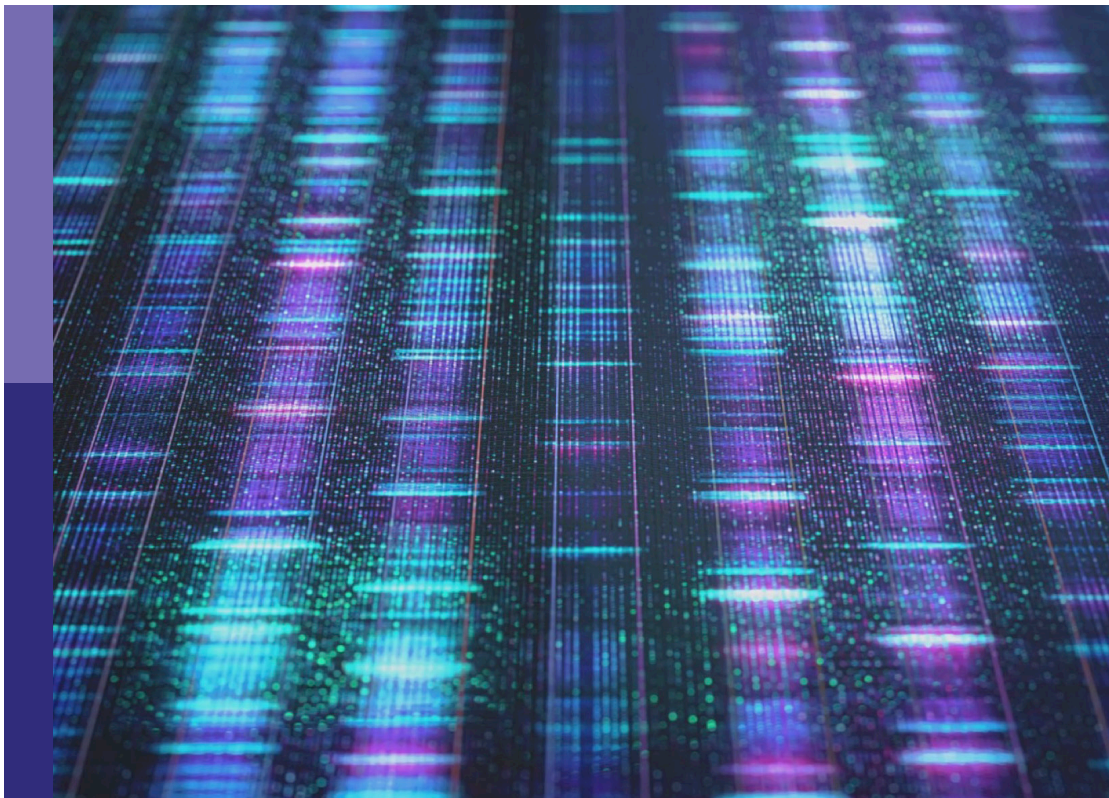

ISSN 1664-8714
ISBN 978-2-8325-6724-1
DOI 10.3389/978-2-8325-6724-1

**Generative AI statement**
Any alternative text (Alt text) provided alongside figures in the articles in this ebook has been generated by Frontiers with the support of artificial intelligence and reasonable efforts have been made to ensure accuracy, including review by the authors wherever possible. If you identify any issues, please contact us.

## About Frontiers

Frontiers is more than just an open access publisher of scholarly articles: it is a pioneering approach to the world of academia, radically improving the way scholarly research is managed. The grand vision of Frontiers is a world where all people have an equal opportunity to seek, share and generate knowledge. Frontiers provides immediate and permanent online open access to all its publications, but this alone is not enough to realize our grand goals.

## Frontiers journal series

The Frontiers journal series is a multi-tier and interdisciplinary set of open-access, online journals, promising a paradigm shift from the current review, selection and dissemination processes in academic publishing. All Frontiers journals are driven by researchers for researchers; therefore, they constitute a service to the scholarly community. At the same time, the *Frontiers journal series* operates on a revolutionary invention, the tiered publishing system, initially addressing specific communities of scholars, and gradually climbing up to broader public understanding, thus serving the interests of the lay society, too.

## Dedication to quality

Each Frontiers article is a landmark of the highest quality, thanks to genuinely collaborative interactions between authors and review editors, who include some of the world's best academicians. Research must be certified by peers before entering a stream of knowledge that may eventually reach the public - and shape society; therefore, Frontiers only applies the most rigorous and unbiased reviews. Frontiers revolutionizes research publishing by freely delivering the most outstanding research, evaluated with no bias from both the academic and social point of view. By applying the most advanced information technologies, Frontiers is catapulting scholarly publishing into a new generation.

## What are Frontiers Research Topics?

Frontiers Research Topics are very popular trademarks of the *Frontiers journals series*: they are collections of at least ten articles, all centered on a particular subject. With their unique mix of varied contributions from Original Research to Review Articles, Frontiers Research Topics unify the most influential researchers, the latest key findings and historical advances in a hot research area.

Find out more on how to host your own Frontiers Research Topic or contribute to one as an author by contacting the Frontiers editorial office: frontiersin.org/about/contact

# Current insights in Epigenetics and Epigenomics

**Topic editors**

Steven Henikoff — Fred Hutchinson Cancer Center, Howard Hughes Medical Institute, United States

Sharon Y. R. Dent — University of Texas MD Anderson Cancer Center/UT Health Houston Graduate School of Biomedical Sciences, United States

Raul Mostoslavsky — The Massachusetts General Hospital Cancer Center and Harvard Medical School, The Broad Institute of Harvard and MIT, United States

Ting Wang — Washington University in St. Louis, United States

Luca Comai — University of California, Davis, United States

**Citation**

Henikoff, S., Dent, S. Y. R., Mostoslavsky, R., Wang, T., Comai, L., eds. (2025). *Current insights in Epigenetics and Epigenomics*. Lausanne: Frontiers Media SA. doi: 10.3389/978-2-8325-6724-1

We are pleased to announce the inaugural release of our annual "Current Insights in Epigenetics and Epigenomics" collection in collaboration with the Epigenetics Society.

The goal of this Research Topic is to shed light on notable progress made in the epigenetics space, and on its future challenges to provide a thorough overview of the field. This article collection will inspire, inform, and provide direction and guidance to researchers in the field. We welcome submissions from our editorial board members, as well as members of the Epigenetics Society, and beyond.

We welcome forward-looking contributions from the editorial board, Epigenetic Society members, and conference attendees, that describe the state of the art, outlining recent developments and major accomplishments that have been achieved and that need to occur to move the field forward. Authors are encouraged to identify the greatest challenges in the sub-disciplines, and how to address those challenges.

# Table of contents

frontiers | Frontiers in Epigenetics and Epigenomics

TYPE Editorial
PUBLISHED 07 February 2025
DOI 10.3389/freae.2025.1566501



OPEN ACCESS

EDITED AND REVIEWED BY
Ian Maze,
Icahn School of Medicine at Mount Sinai, United States

*CORRESPONDENCE
Steven Henikoff,
steveh@fredhutch.org

RECEIVED 24 January 2025
ACCEPTED 27 January 2025
PUBLISHED 07 February 2025

CITATION
Henikoff S, Dent SYR, Mostoslavsky R, Wang T and Comai L (2025) Editorial: Current insights in Epigenetics and Epigenomics.
*Front. Epigenet. Epigenom.* 3:1566501.
doi: 10.3389/freae.2025.1566501



# Editorial: Current insights in Epigenetics and Epigenomics

Steven Henikoff[1,2]*, Sharon Y. R. Dent[3,4], Raul Mostoslavsky[5,6], Ting Wang[7] and Luca Comai[8]

[1]Basic Sciences Division, Fred Hutchinson Cancer Center, Seattle, WA, United States, [2]Howard Hughes Medical Institute, Chevy Chase, MD, United States, [3]Department of Epigenetics and Molecular Carcinogenesis and Center for Cancer Epigenetics, University of Texas MD Anderson Cancer Center, Houston, TX, United States, [4]University of Texas MD Anderson Cancer Center/UT Health Houston Graduate School of Biomedical Sciences, Houston, TX, United States, [5]The Krantz Family Center for Cancer Research, The Massachusetts General Hospital Cancer Center and Harvard Medical School, Boston, MA, United States, [6]The Broad Institute of Harvard and MIT, Cambridge, MA, United States, [7]Department of Genetics, Washington University in St. Louis, St. Louis, MO, United States, [8]Department of Plant Biology, University of California, Davis, Davis, CA, United States

KEYWORDS

**Epigenetics, Epigenomics, DNA methylation, chromatin, environment**

Editorial on the Research Topic
Current insights in Epigenetics and Epigenomics

We are starting this new year with our first full collection of selected papers, consisting of review and research articles that provide glimpses into some of the exciting current areas of research in the broad field of epigenetics and epigenomics. Below we highlight topics reviewed in this collection with examples of new research published in Frontiers in Epigenetics and Epigenomics during 2024.

No scientific topic has been more in the news than climate change and the increasing frequency of disasters that have resulted (Roe et al.). What might be the epigenetic and epigenomic consequences of disastrous events? An especially well-studied disaster resulting in epigenetic modifications was the Dutch Hunger Winter, the 1944-45 famine during the Nazi occupation of Holland, highlighted in a review article in this series (Bernasocchi and Mostoslavsky). Physiological and behavioral effects were observed in children exposed to starvation *in utero*, and the genetic and epigenetic mechanisms underlying the predisposition of chronic conditions such as obesity and diabetes is an expanding area of research.

Disasters such as earthquakes and droughts can have mental health effects and associated epigenetic modifications (Roe et al.). Nearly all of the epigenetic studies examined have measured DNA methylation, although plausible mechanisms for environmentally induced changes in DNA methylation affecting human behavior are lacking (Bird, 2024). Even in plants, where meiotically heritable and environmentally induced DNA methylation epialleles are well-documented, evidence for their evolutionary importance is inconclusive (Comai, 2023). Other epigenetic modifiers, especially small RNAs, have received relatively little attention despite their demonstrated importance in regulating physiological processes. For example, microRNAs are known to regulate differentiation by targeting specific sets of mRNAs for degradation (Razavi-Mohseni and Beer, 2024). There are thousands of microRNA genes in the human genome, and we expect to see more environmental studies focused on microRNAs, which won the 2024 Nobel Prize in Physiology and Medicine more than 3 decades after their discovery.

Environmental changes that affect diet can have metabolic impacts on synthesis of the universal methyl donor, S-adenosyl methionine, which in turn affects not only DNA methylation, but also histone methylation, modifications that condition the epigenomic landscape (Bernasocchi and Mostoslavsky). Vitamins and other dietary micronutrients can alter the activities of the DNMT family of DNA methyltransferases and the TET family of enzymes that oxidize 5-methylcytosine to modify and remove the DNA methyl mark (Leesang et al.). DNA methylation and silencing histone modifications may be inherited through multiple rounds of cell division, and changes in both modifications have important implications for our understanding of cancer and aging.

Although most attention in the chromatin field has been on histone modifications, histone variants are critical for maintaining the chromatin landscape, especially post-mitotically, when canonical S-phase-dependent histones are silent. In addition, specialized histone variants are critical for fundamental cellular processes, including chromosome segregation (CENP-A), transcriptional regulation (H2A.Z) and DNA repair (H2A.X). DNA double-strand breaks have long been known to trigger rapid phosphorylation of H2A.X, but what happens next depends on the genomic and epigenomic context of the break (Clerf et al.). Multiple repair pathways for homologous recombination and non-homologous end-joining require nucleosomes to be destabilized for the DNA repair machineries to gain access, and this is facilitated by increases in H2A.Z acetylation and incorporation of macroH2A.

The chromatin dynamics required to make DNA available for replication, transcription and repair are mediated by four major families of chromatin remodelers, which share structurally related ATP-dependent DNA translocase domains. Subunits of the SWI/SNF family of remodelers, which acts to clear enhancers and promoters of nucleosomes to facilitate engagement of RNA Polymerase II, and possibly histone acetylation as well (Zhang, 2024), are mutated in >20% of human cancers. Just how SWI/SNF complexes interact with transcription factors, such as the androgen receptor (AR) in prostate cancer, has been the subject of much recent research (Ordonez-Rubiano et al.). Transcription factors (TFs), such as AR, provide sequence and cell-type specificity for the action of chromatin regulatory complexes and modifications. Similarly, a group of TFs collectively known as Phytochrome Interacting Factors (PIFs) provide sequence specificity for "landscaping" the epigenome in plants (Ammari et al.), acting as recruiters of chromatin regulators. Networks of oncogenic transcription factors are the major drivers of cancer, either as oncogenes when up-regulated or as tumor suppressors when down-regulated. In one study in this series, the authors combined RNA sequencing and ATAC-seq with CUT&Tag chromatin profiling for active and silencing histone modifications to follow the time-course of epigenomic alterations after oncogene induction (Vasilopoulos and Martinez-Zamudio). Detailed maps of chromatin changes following induction may help to guide the development of therapies to favor senescence over uncontrolled proliferation.

Among the most difficult cancers to treat are Ewing's sarcomas (EWS), the subject of a clinical epigenomics study in this series (Patrizi et al., 2024). Deconvolution of DNA methylation bead-chip data from 32 EWS pediatric patients quantified the total numbers and percentages of immune cells in the tumors without requiring a tumor-specific signature. As the degree of immune infiltration correlates with longer survival, DNA methylation profiling may serve as a general cancer diagnostic. DNA methylation levels measured in peripheral blood can also be used as a disease diagnostic: As was reported in another clinical study in this series, the level of blood DNA methylation at the promoter of the corticotropin-releasing factor gene in Cushing's Syndrome patients correlated with amygdala volume and depression relative to healthy controls (Lee et al.). We look forward to further technological improvements in DNA methylation profiling (Deinichenko et al., 2024; Xu et al., 2024) and other epigenomic interrogation techniques, not only for disease diagnosis, but also for understanding fundamental principles of genetics and cell biology that epigenomic research can reveal.

## Author contributions

SH: Writing–original draft, Writing–review and editing. SD: Writing–review and editing. RM: Writing–review and editing. TW: Writing–review and editing. LC: Writing–review and editing.

## Funding

The author(s) declare that financial support was received for the research, authorship, and/or publication of this article. SH is an Investigator of the Howard Hughes Medical Institute. RM laboratory is supported by the Waxman Cancer Research Foundation, a Krantz Breakthrough Award and a NIH grant R01CA279173.

## Conflict of interest

The authors declare that the research was conducted in the absence of any commercial or financial relationships that could be construed as a potential conflict of interest.

The author(s) declared that they were an editorial board member of Frontiers, at the time of submission. This had no impact on the peer review process and the final decision.

## Generative AI statement

The author(s) declare that no Generative AI was used in the creation of this manuscript.

## Publisher's note

# References

Bird, A. (2024). Transgenerational epigenetic inheritance: a critical perspective. *Frontiers in Epigenetics and Epigenomics* 2. doi:10.3389/freae.2024.1434253

Comai, L. (2023). Triggers and mediators of epigenetic remodeling in plants. *Frontiers in Epigenetics and Epigenomics* 1. doi:10.3389/freae.2023.1188733

Deinichenko, K. A., Vynogradskaya, V. G., Grebnev, P. A., Mikova, V. M., Bobylev, D. O., Shaymardanov, A. M., et al. (2024). Benchmark of the Oxford Nanopore, EM-seq, and HumanMethylationEPIC BeadChip for the detection of the 5mC sites in cancer and normal samples. *Front. Epigenet. Epigenom.* 2. doi:10.3389/freae.2024.1362926

Patrizi, S., Vallese, S., Pedace, L., Nardini, C., Stracuzzi, A., Barresi, S., et al. (2024). Quantification of tumour-infiltrating immune cells through deconvolution of DNA methylation data in Ewing sarcomas. *Front. Epigenet. Epigenom. 2.* doi:10.3389/freae.2024.1427399

Razavi-Mohseni, M., and Beer, M. A. (2024). MicroRNAs provide negative feedback and stability in gene regulatory network models of cell-state transitions. *Front. Epigenet. Epigenom.* 2. doi:10.3389/freae.2024.1473789

Xu, X., Guo, Y., Liu, M., Hu, Y., and Li, S. (2024). Advancements in the clinical application of gene methylation for early cancer detection. *Front. Epigenet. Epigenom.* 2. doi:10.3389/freae.2024.1430294

Zhang, G. (2024). A hypothetical model: chromatin remodelers couple with acetyltransferases to trigger the elongation of RNA polymerase II (pol II). *Front. Epigenet. Epigenom.* 2. doi:10.3389/freae.2024.1439973

frontiers | Frontiers in Epigenetics and Epigenomics

TYPE Review
PUBLISHED 04 January 2024
DOI 10.3389/freae.2023.1337345



OPEN ACCESS

EDITED BY
Sharon Y. R. Dent,
University of Texas MD Anderson Cancer Center, United States

REVIEWED BY
Zhilian Jia,
City of Hope National Medical Center, United States
Tingting Yao,
Colorado State University, United States

*CORRESPONDENCE
Emily C. Dykhuizen,
edykhui@purdue.edu

RECEIVED 12 November 2023
ACCEPTED 05 December 2023
PUBLISHED 04 January 2024

CITATION
Ordonez-Rubiano SC, Strohmier BP, Sood S and Dykhuizen EC (2024), SWI/SNF chromatin remodelers in prostate cancer progression.
*Front. Epigenet. Epigenom.* 1:1337345.
doi: 10.3389/freae.2023.1337345



# SWI/SNF chromatin remodelers in prostate cancer progression

Sandra C. Ordonez-Rubiano[1], Brayden P. Strohmier[1], Surbhi Sood[1,2] and Emily C. Dykhuizen[1,2,3]*

[1]Department of Medicinal Chemistry and Molecular Pharmacology, Purdue University, West Lafayette, IN, United States, [2]Interdisciplinary Life Sciences-PULSe, Purdue University, West Lafayette, IN, United States, [3]Purdue Institute for Cancer Research, Purdue University, West Lafayette, IN, United States

Prostate cancer (PCa) is the most commonly diagnosed cancer and the second most common cause of cancer-related deaths in men in the US. The majority of PCa cases arise in the luminal cells of the prostate and develop into adenocarcinoma. Primary PCas are heterogeneous and have alterations in a variety of tumor suppressors and oncogenes; however, the vast majority are dependent on gene expression regulation by androgen receptor (AR), making it the focus for most targeted therapy development. As the incidence of PCa cases resistant to AR-targeted therapies rises, there is renewed attention on how additional genetic and epigenetic alterations contribute to PCa progression and resistance. In this review we summarize the efforts made over the past 20 years to dissect the function of the SWI/SNF chromatin remodelers in PCa. We mainly focus on how SWI/SNF complexes regulate different aspects of AR signaling, facilitate other key drivers in PCa, promote the advancement of the disease, and regulate the tumor microenvironment.

KEYWORDS

**SWI/SNF, BAF complex, prostate cancer, androgen receptor, neuroendocrine differentiation, tumor microenvironment, chromatin remodeling**

## 1 Introduction

Prostate cancer (PCa) is a highly prevalent malignancy with 1.4 million cases diagnosed worldwide in 2020 alone (Sung et al., 2021). Approximately 288,000 new cases and 34,700 PCa-associated deaths are estimated for 2023 in the US (Siegel et al., 2023). PCa initiates as prostatic intraepithelial neoplasia, wherein malignant cells grow toward the lumen of the prostate (Wang et al., 2018). If the cancer advances, most PCa cases develop into prostate adenocarcinoma, which originates from luminal or basal cells in the prostate (Wang et al., 2018). PCa is a hormone-driven malignancy; therefore, the majority of the available therapies focus on disrupting hormone-related pathways (Wang et al., 2018; Teo et al., 2019; Litwin and Tan, 2017). Uncommon types of PCa include squamous carcinoma, which is derived uniquely from basal cells, and neuroendocrine carcinoma, which may arise from prostate neuroendocrine cells or as a result of resistance to treatment (Wang et al., 2018). As the malignancy progresses to metastatic disease, bone metastases are the most common, followed by lung and liver (Wang et al., 2018) (Figure 1).

The Gleason scoring system is the international standard to score prostatic carcinomas from tissue biopsies (Gleason and Mellinger, 1974; Litwin and Tan, 2017). Combined with the evaluation of serum prostate-specific antigen (PSA) levels, the stage and grade of the cancer, the Gleason score is used to assign PCa patients to one of 5 risk groups: very low, low, intermediate, high or very high risk (Mohler et al., 2016). The therapeutic approach to very low risk patients is active surveillance and surgical removal of localized carcinoma (Wang

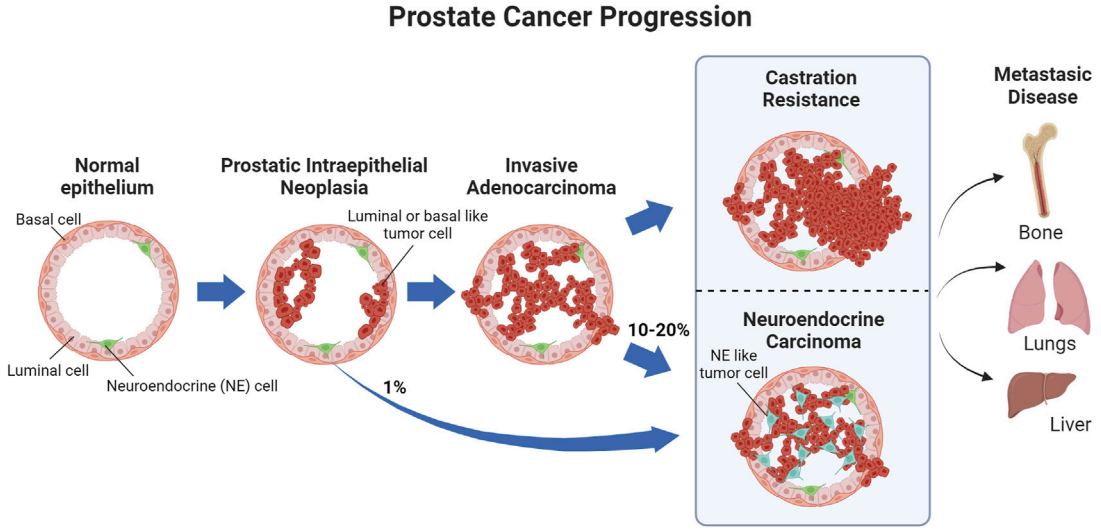


FIGURE 1
PCa progression. Prostatic intraepithelial neoplasias primarily develop into invasive carcinomas, while approximately 1% develop into neuroendocrine carcinoma. As the invasive carcinoma advances and stops responding to treatment, it becomes castration resistant, with 10–20% of castration-resistant tumors emerging through neuroendocrine differentiation. Metastatic PCa, primarily in the bone, can occur before or after castration resistance.

**TABLE 1 Summary of PCa cell-based models mentioned in this review.**

| Cell line | Type | AR expression | References |
|---|---|---|---|
| RWPE-1 | Non-cancerous prostate epithelium | High | Bello et al. (1997), Saranyutanon et al. (2020) |
| LNCaP | Castration-sensitive PCa | High | Horoszewicz et al. (1980), Bokhoven et al. (2003), Saranyutanon et al. (2020) |
| R1-AD1 | Castration-sensitive PCa | High | Li et al. (2013), Nyquist et al. (2013) |
| C4-2/C4-2B | CRPC | High | Thalmann et al. (1994), Saranyutanon et al. (2020) |
| DU145 | CRPC | Low | Stone et al. (1978); Bokhoven et al. (2003); Alimirah et al. (2006); Saranyutanon et al. (2020) |
| LNCaP-AI | CRPC | Low | Yasumizu et al. (2020) |
| PC3 | CRPC | Low | Kaighn et al. (1979); Bokhoven et al. (2003); Alimirah et al. (2006); Saranyutanon et al. (2020) |
| VCaP | CRPC | High | Korenchuk et al. (2001); Bokhoven et al. (2003); Saranyutanon et al. (2020) |
| 22Rv1 | CRPC | High | Sramkoski et al. (1999); Bokhoven et al. (2003); Saranyutanon et al. (2020) |
| NCI-H660 | Neuroendocrine PCa | Low | Carney et al. (1985); Johnson et al. (1989); Bokhoven et al. (2003) |

et al., 2018; Litwin and Tan, 2017). Most therapies for higher risk groups are based on androgen deprivation therapy (ADT), which generally includes chemical castration with the adjunct use of androgen receptor (AR) antagonists. Other common treatments include radical prostatectomy, chemotherapy, immunotherapy, and radiotherapy (Wang et al., 2018; Desai, McManus, and Sharifi, 2021). Resistance to ADT leads to castration-resistant PCa (CRPC), which may emerge either before or after the metastatic stage (Wang et al., 2018; Desai et al., 2021). Cell line models representing the different stages of PCa disease and responsiveness to hormones commonly used in pre-clinical research are summarized in Table 1.

The frequency and grouping of genomic aberrations vary depending on the stage of the disease (He et al., 2022). Hormone sensitive stages are characterized by *SPOP*, *MED12,* and *FOXA1* mutations, the *TMPRSS2::ERG* gene fusion, and *PTEN* deletions or mutations (Abeshouse et al., 2015; He et al., 2022). As the disease advances, the frequency of *TP53* deletions or mutations and *MYC* amplification or overexpression increases (Abeshouse et al., 2015; Quigley et al., 2018; He et al., 2022). CRPC presents with *AR* amplification, mutation, overexpression and/or enhanced signaling, and *APC* deletions or mutations (Abeshouse et al., 2015; Fraser et al., 2017; He et al., 2022). Finally, as the disease advances into the metastatic stage, *RB1* deletions and mutations, *CTNNB1* amplification or overexpression, and *CDK12*, *BRCA1*, *BRCA2*, and *ATM* deletions or mutations become more frequent (Abeshouse et al., 2015; Fraser et al., 2017; Stopsack et al., 2020; He et al., 2022). Overall, regardless of the stage of the disease, mutations

or deletions of well stablished tumor suppressors (*PTEN*, *SPOP*, *TP53*, *BRCA1/2*, and *RB1*) or genes that encode for proteins involved in DNA damage repair (*ATM*) and cell cycle control (*MED12*, *CDK12*, and *APC*) are common; while genes that are transcriptional regulators (*FOXA1*, *TMPRSS2::ERG* fusion, *MYC*, *AR*, and *CTNNB1*) present with gain-of-function, amplification or overexpression.

Epigenetic regulators are currently in the spotlight as alternative therapeutic targets in PCa; however, the epigenetic landscape is not fully defined for the various PCa stages. Most epigenetic characterization has focused on histone methylation/acetylation, and DNA hypermethylation (Stelloo et al., 2018; Sugiura et al., 2021; He et al., 2022). The repressive histone marks H3K9me2 and H3K9me3 are reduced in malignant tissues compared to healthy tissues in part as result of overexpression of LSD1, a histone demethylase, which cooperates with AR to promote the expression of cell cycle-associated genes (Metzger et al., 2005; He et al., 2022). In contrast, histone deacetylases, which silence gene expression, are also overexpressed in PCa and their expression is correlated with higher Gleason scores (Weichert et al., 2008). Similarly, the H3K27me3 repressive marks are increased in PCa, which is driven by EZH2 overexpression (Park et al., 2021; He et al., 2022). In terms of DNA hypermethylation, 22% of PCa tumors have been shown to be associated with this feature and DNA methyl transferase inhibitors such as azacytidine and decitabine have been in clinical trials for PCa (He et al., 2022; Zhao et al., 2020). Hypermethylation may result in part from a loss in CTCF (CCCTC-binding factor) in a subset of PCa cases (Damaschke et al., 2020). CTCF is a chromatin insulator and its high expression is, paradoxically, also correlated with a worse prognosis in PCa (Höflmayer et al., 2020) and has been implicated in binding to single nucleotide polymorphisms associated with increased PCa risk (Tian et al., 2023; Guo et al., 2018). CTCF cooperates with cohesin to establish a 3D chromatin architecture consisting of chromatin loops and topologically associating domains, which is important for gene insulation as well as enhancer-promoter interactions that are increased for many genes during PCa progression (Ramanand et al., 2020). For instance, AR binds primarily at enhancers and induces chromatin looping with the *KLK3* promoter to facilitate RNA polymerase II binding (Wanget al., 2005). Many of these loops, which increase in number during PCa progression, require CTCF binding to domain boundaries within the *KLK* family locus (Khoury et al., 2020). Additional transcriptional drivers of PCa similarly rely on enhancer-driven transcription, implicating similar changes in genome organization during PCa progression, which may similarly be dependent on CTCF. Metastatic PCa is also characterized by a general increase in chromatin accessibility (Stelloo et al., 2015), which may facilitate rapid changes in genome organization during progression and provide transcriptional plasticity for the development of therapy resistance.

Chromatin accessibility is facilitated by chromatin remodelers, which mobilize nucleosomes on DNA to repress or activate target genes (Clapier et al., 2017). The SWI/SNF multi-subunit complexes (also called BRG/BRM-associated (BAF) complexes) are ATP-dependent chromatin remodelers important in development and disease (Clapier et al., 2017). Three biochemically distinct SWI/SNF complexes have been defined up to date: canonical BAF (cBAF), polybromo-associated BAF (PBAF), and the non-canonical GLTSCR1/1L-BAF (GBAF or ncBAF) (Alpsoy and Dykhuizen, 2018; Gatchalian et al., 2018; Mashtalir et al., 2018; Wang et al., 2019) (Figure 2). Variations in SWI/SNF subcomplexes that result from cell type-specific expression of paralogs have also been defined: for example, embryonic stem cell-specific BAF (esBAF) (Ho et al., 2009), neural progenitor BAF (npBAF) and neuronal BAF (nBAF) (Wu et al., 2007; Cenik and Shilatifard, 2020; Son and Crabtree, 2014) (Figure 2). All BAF subcomplexes contain a catalytic motor module comprised of the ATPase SMARCA2/4 (SWI/SNF related, Matrix associated, Actin dependent Regulator of Chromatin, subfamily A, member 2/4) connected via its HSA (Helicase-SANT–Associated) domain to ACTL6A or B (actin-like 6A/B), ACTB (β-actin), and BCL7A/B/C (B-cell CLL/lymphoma 7 protein family member A/B/C). This motor module is connected to a core comprised of a dimer of SMARCC1/2 subunits, and SMARCD1/2/3 (Mashtalir et al., 2018; Alpsoy and Dykhuizen, 2018; Gatchalian et al., 2018; Wang et al., 2019; Cenik and Shilatifard, 2020; Son and Crabtree, 2014; He et al., 2021; Dietrich et al., 2023). The incorporation of ARID1A/B, ARID2, or GLTSCR1/1L on to the core seeds the assembly of additional subunits to form cBAF, PBAF, or GBAF (Figure 2). Subunits unique to a particular complex are involved in modulating enzymatic remodeling activity, recognizing DNA/histone substrates, recruiting additional transcriptional regulators or promoting heterotypic phase separation (Kuang et al., 2021; Davis et al., 2023; Patil et al., 2023). The HUGO Gene names and the many aliases of SWI/SNF subunits are listed in Table 2.

Subunits of the SWI/SNF complex are mutated in around 20% of cancers and several are recognized as tumor suppressors (Kadoch et al., 2013; Shain and Pollack, 2013); however, SWI/SNF mutations are infrequent in PCa. Instead, as described below, aberrant expression of multiple subunits is found in PCa and is often associated with a specific stage. In this review, we summarize the often-conflicting roles of SWI/SNF complexes in PCa, where both tumor suppressive and promoting roles have been reported for several subunits. We focus on how the SWI/SNF complexes facilitate the activity of different PCa key drivers and dependencies such as AR and FOXA1, their stage-dependent functions as the disease advances, and the role they play in the increasingly essential tumor microenvironment (TME).

## 2 SWI/SNF complexes and androgen receptor (AR)-mediated transcription

The central regulator in PCa is AR, a ligand-dependent nuclear transcription factor that contains an N-terminal domain (NTD), a DNA-binding domain (DBD), a C-terminal ligand-binding domain (LBD), and a hinge region that connects the DBD and the LBD (reviewed in Dai et al., 2017). When unbound, AR is found in the cytoplasm with chaperone proteins (i.e., HSP90) that prevent its degradation. When AR binds to an androgen ligand, mainly dihydrotestosterone (DHT), it undergoes a conformational change leading to its dissociation from the chaperones, homodimerization, and translocation to the nucleus. There it associates with transcriptional coregulators that facilitate its binding to androgen response elements (AREs) in enhancers and promote looping with

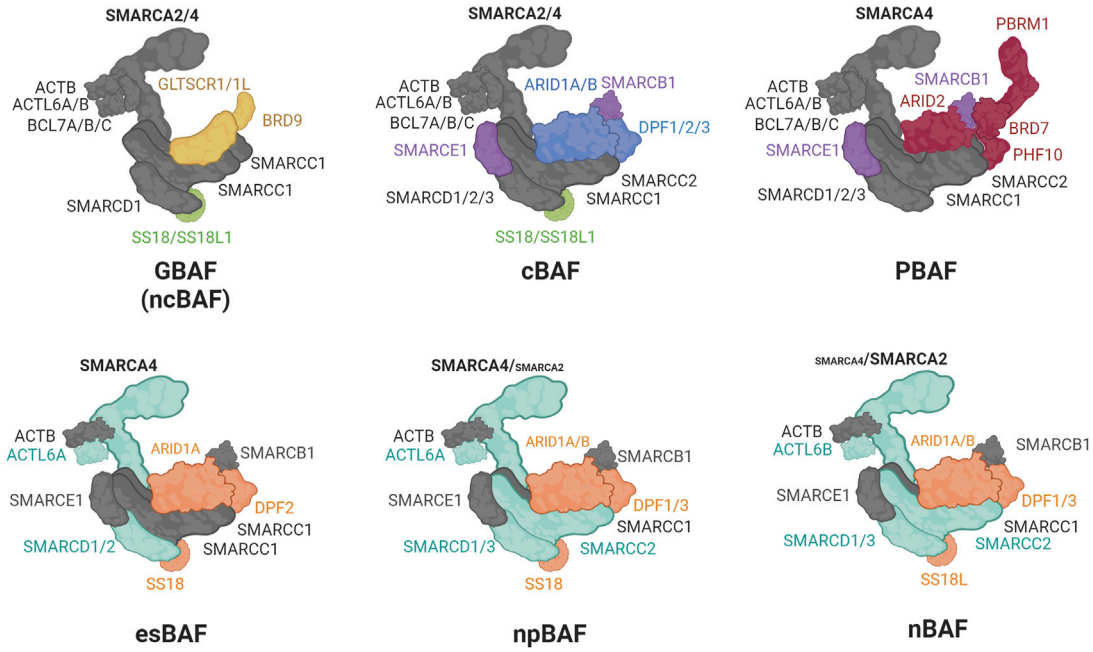


FIGURE 2
Composition of the SWI/SNF complexes. In gray: shared core subunits, in light green: subunits shared by GBAF and cBAF; in purple: subunits shared by cBAF and PBAF; in yellow: GBAF unique subunits; in blue: cBAF unique subunits; in red: PBAF unique subunits; in cyan: motor and core subunits whose paralogs interchange between esBAF, npBAF, and nBAF; in orange: accessory subunits whose paralogs interchange between esBAF, npBAF, and nBAF.

promoters to allow for transcription of genes important for cell survival and cell proliferation (Figure 3) (Royen et al., 2012; Shafi et al., 2013; Dai et al., 2023). AR is not typically altered during the initiation of PCa; however, the dependency of PCa on AR-mediated transcription has made it the major focus of therapies.

## 2.1 Early studies investigating AR dependence on SWI/SNF

Initial studies investigating SWI/SNF involvement in AR-mediated transcription utilized ectopic expression of AR and exogenous activity reporters such as probasin pARR2-luciferase, PSA-luciferase, and the mouse mammary tumor virus promoter-driven luciferase (MMTV) (Inoue et al., 2002; Marshall et al., 2003; Link et al., 2005; Klokk et al., 2007; Kikuchi et al., 2009; Jin et al., 2018). In these systems, the ATPase subunit SMARCA2 is recruited by AR for chromatin remodeling and AR reporter activity (Y. Dai et al., 2008; Klokk et al., 2007; Marshall et al., 2003). In Smarca2$^{-/-}$ mice, however, AR activity is not affected (Shen et al., 2008), raising a question of SMARCA2 dependence in PCa. In a small patient cohort, SMARCA2 levels were increased in PCa samples compared to normal tissue (Sun et al., 2007); however, according to large scale genomics and proteomic studies, contrary to what had been originally reported, SMARCA2 levels are decreased in PCa patients compared to normal prostate tissue (Shen et al., 2008; Muthuswami et al., 2019) and SMARCA2 expression is inversely correlated with the advancement of the disease.

Other reporter studies identified a dependency on SMARCA4 for AR activity (Huang et al., 2003), which were further characterized to interact using co-immunoprecipitation (Li et al., 2006), and other techniques (Lempiäinen et al., 2017; Paltoglou et al., 2017; Stelloo et al., 2018; Launonen et al., 2021). SMARCA4 associates with AR when the NTD is associated with the LBD (Li et al., 2006), which is a stronger interaction if the polyglutamine (polyQ) tract located in the NTD is shorter (Q. Wang et al., 2004) (Figure 4). The polyQ tract is encoded by a series of CAG triplets located in exon 1 of *AR* which may vary in length between individuals (He et al., 2020). AR with shorter polyQ tract is associated with an increase in AR transcriptional activity and higher risk and aggressiveness in PCa (He et al., 2020), implicating SMARCA4 in promoting AR activity and PCa advancement. Some early studies found SMARCA4 upregulated in PCa samples (Sun et al., 2007) and unlike SMARCA2, this upregulation has been confirmed in larger datasets (Muthuswami et al., 2019).

The core subunit SMARCC1 was one of the first subunits other than the ATPase subunits established to be important for AR signaling (Wang et al., 2004; Link et al., 2005; Hong et al., 2005) (Figure 4). This function is typically dependent on the ATPase; however, one study concludes that Smarcc1 can promote an AR luciferase reporter through an ATPase subunit-independent association between Smarcc1 and AR (Hong et al., 2005). Proteomic analyses consistently identified the ATPases, SMARCC1, and other SWI/SNF subunits with AR, (Lempiäinen et al., 2017; Paltoglou et al., 2017; Stelloo et al., 2018; Launonen et al., 2021; Ban et al., 2021); however, the absence of the ATPase subunits in this study might indicate that AR association with SWI/SNF is not necessarily mediated through the ATPase module.

**TABLE 2 HUGO names of the SWI/SNF subunits in alphabetical order, the complex(es) they are part of, and their aliases.**

| HUGO name | Associated complex | Other aliases |
|---|---|---|
| ACTB | All | β-actin |
| ACTL6A | All | BAF53A, SMARCN1 |
| ACTL6B | All | BAF53B, SMARCN2 |
| ARID1A | cBAF | BAF250a |
| ARID1B | cBAF | BAF250b |
| ARID2 | PBAF | BAF200, Zipzap/p200 |
| BCL7A | All | SMARCJ1 |
| BCL7B | All | SMARCJ2 |
| BCL7C | All | SMARCJ3 |
| BICRA | GBAF | GLTSCR1 |
| BICRAL | GBAF | GLTSCR1L |
| BRD7 | PBAF | - |
| BRD9 | GBAF | - |
| DPF1 | cBAF | BAF45B |
| DPF2 | cBAF | BAF45D |
| DPF3 | cBAF | BAF45C |
| PBRM1 | PBAF | BAF180 |
| PHF10 | PBAF | BAF45A |
| SMARCA2 | cBAF and GBAF | BRM |
| SMARCA4 | All | BRG1 |
| SMARCB1 | cBAF and PBAF | BAF47, INI-1, SNF5 |
| SMARCC1 | All | BAF155, SRG3 |
| SMARCC2 | cBAF and PBAF | BAF170 |
| SMARCD1 | All | BAF60A |
| SMARCD2 | cBAF and PBAF | BAF60B |
| SMARCD3 | cBAF and PBAF | BAF60C |
| SMARCE1 | cBAF and PBAF | BAF57 |
| SS18 | cBAF and GBAF | SYT, SMARCL1 |
| SS18L1 | cBAF and GBAF | CREST, SMARCL2 |

The last subunit identified in these early studies is SMARCE1, a subunit shared by cBAF and PBAF. It is required for endogenous AR activity and immunoprecipitates with endogenous AR independent of ligand binding (Link et al., 2005). Later studies showed that SMARCE1 is temporarily recruited to AREs and, in biochemical assays, binds to the DBD and hinge region of AR (Link et al., 2008). Inhibition of the interaction between SMARCE1 and AR using an AR N-terminal peptide abrogates AR activity and reduces AR-dependent PCa proliferation, indicating SMARCE1 promotes AR activity (Link et al., 2005). After these early studies, the role for several other subunits in AR signaling has been reported. In the following sections, we describe the different aspects of AR signaling that require SWI/SNF.

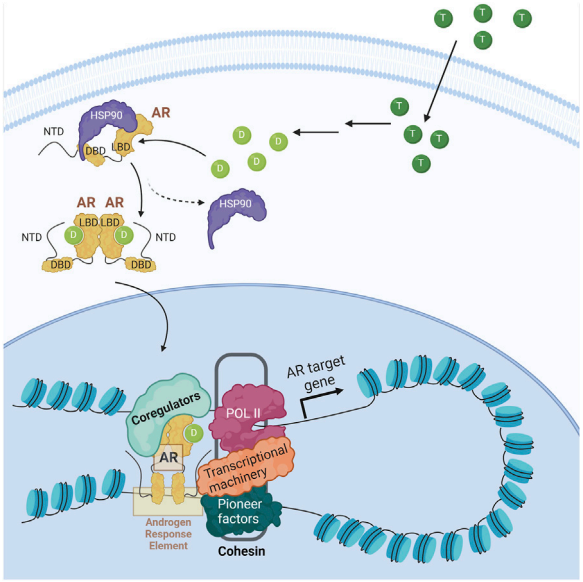


FIGURE 3
Androgen receptor signaling. Upon entering the cell, testosterone (dark green circle) is metabolized into dihydrotestosterone (light green circle), the main AR ligand. Upon ligand binding, AR is released from the chaperone (i.e., HSP90), dimerizes and translocates to the nucleus where, along with coregulators and RNA polymerase II (POL II), promotes AR target genes expression.

## 2.2 SWI/SNF subunits interact with AR

Via distinct methodologies, proteomic studies in PCa cells have confirmed that AR interacts with multiple SWI/SNF subunits (Lempiäinen et al., 2017; Paltoglou et al., 2017; Stelloo et al., 2018; Launonen et al., 2021; Ban et al., 2021) (Table 3). SMARCA4 was identified in all studies while SMARCA2 was not, perhaps due to its reduced expression in PCa. As for the shared core subunits, SMARCC1/2, SMARCD1/2/3, and ACTL6A were identified, as were SMARCB1 and SMARCE1, shared by cBAF and PBAF. cBAF-specific subunits ARID1A/B and PBAF-specific subunits PBRM1 and ARID2 were identified; however, GBAF subunits SS18/SS18L1, GLTSCR1/1L, and BRD9, were not. These data indicate that PBAF and cBAF function as direct AR coactivators, while the role of GBAF in PCa is independent from a direct interaction with AR.

Considering the strong data supporting SWI/SNF association with AR, understanding the biochemical basis for this association is important for deciphering the role of SWI/SNF in CRPC. Most AR inhibitors target the c-terminal LBD; however some forms of CRPC express constitutively active AR variants without the LBD (Li et al., 2013). Alternate strategies for these cancers include the development of drugs targeting the NTD (Ji et al., 2023; Dai etbal., 2023). One NTD inhibitor is VPC-220010, which inhibits the association between AR and several important co-regulators to reduce proliferation of LNCaP and 22Rv1 cells (Ban et al., 2021). VPC-220010 inhibits the androgen-dependent interaction between AR and SMARCC1, SMARCC2, SMARCD1, SMARCD2, and SMARCA2, but not SMARCA4 (Ban et al., 2021). This indicates

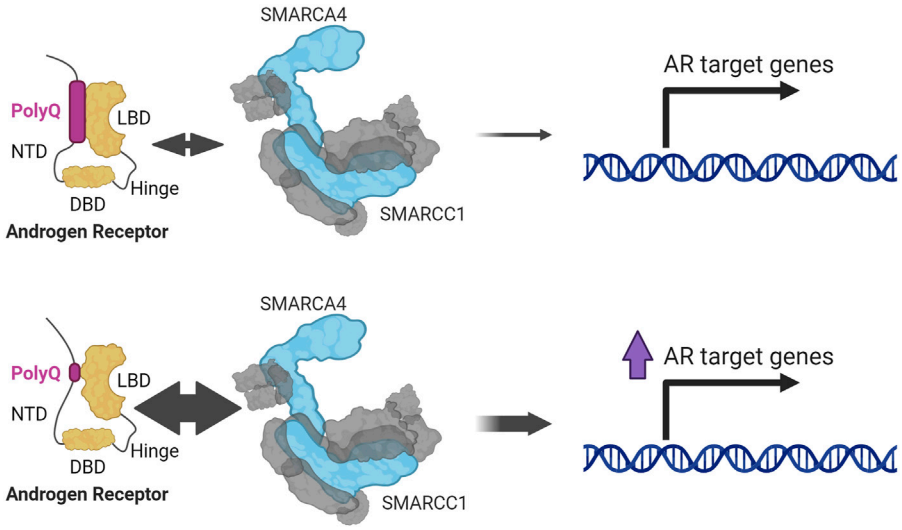


FIGURE 4
SMARCA4 and SMARCC1 interact with AR through the interaction between its NTD (N-terminal domain) and LBD (ligand binding domain). This interaction is stronger the shorter the polyglutamine tract (PolyQ) (Li et al., 2006; Wang et al., 2004).

**TABLE 3 Summary of proteomic studies evaluating binding to SWI/SNF subunits to AR. Blue shade indicates the subunit was present in the proteomic analysis (Lempiäinen et al., 2017; Paltoglou et al., 2017; Stelloo et al., 2018; Launonen et al., 2021; Ban et al., 2021).**

| | Lempiäinen (2017) | Paltoglou (2017) | Stelloo et al. (2018) | Launonen et al. (2021) | Ban et al. (2021) |
|---|---|---|---|---|---|
| Cells | HEK293T - ectopic AR | R1-AD1 | LNCaP | VCaP | LNCaP |
| Technique | proximity-dependent biotin identification | RIME | RIME | ChIP-SICAP | RIME |
| Subunit | | | | | |
| *Shared core subunits* | | | | | |
| SMARCA2 | ■ | | | ■ | ■ |
| SMARCA4 | ■ | ■ | ■ | ■ | ■ |
| SMARCC1 | ■ | ■ | ■ | ■ | ■ |
| SMARCC2 | ■ | | ■ | ■ | ■ |
| SMARCD1 | ■ | ■ | | ■ | ■ |
| SMARCD2 | | ■ | ■ | ■ | ■ |
| SMARCD3 | | ■ | | ■ | |
| ACTL6A | | | | ■ | |
| *cBAF unique subunits* | | | | | |
| ARID1A | ■ | ■ | ■ | ■ | ■ |
| ARID1B | ■ | ■ | | ■ | ■ |
| *PBAF and cBAF shared subunits* | | | | | |
| SMARCB1 | ■ | ■ | | ■ | ■ |
| SMARCE1 | ■ | ■ | ■ | ■ | ■ |
| *PBAF unique subunits* | | | | | |
| PBRM1 | | | | ■ | ■ |
| ARID2 | | ■ | | | |

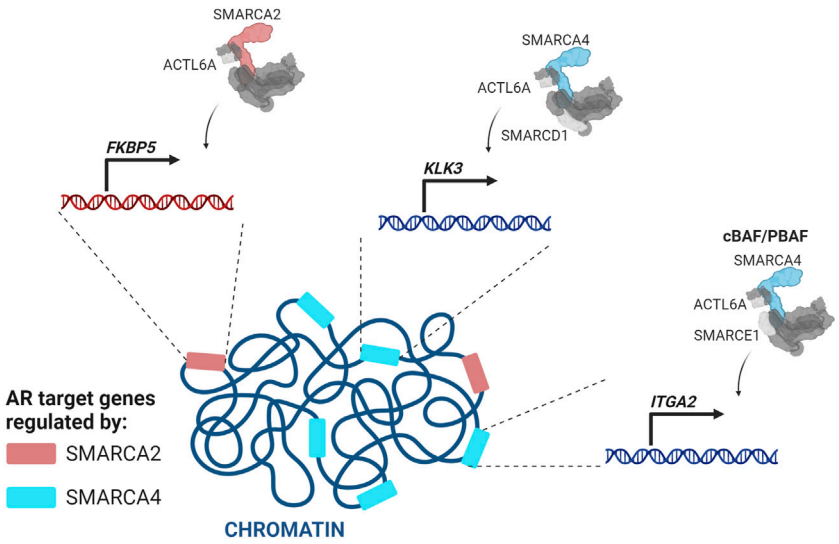


FIGURE 5
SMARCA4-and SMARCA2-containing SWI/SNF complexes regulate different sets of AR target genes (Makkonen et al., 2009; Balasubramaniam et al., 2013; Jin, Kim, and Jeong, 2018; Wijngaart et al., 2009; S. Liu et al., 2017).

that SWI/SNF associates with AR through the NTD, but the interaction between SMARCA4 and AR may occur through the LBD, as previously demonstrated (Li et al., 2006). While SWI/SNF association is likely stronger for wild type AR, it may also contribute to the activity of AR splice variants in CRPC.

## 2.3 AR target gene expression regulation by SWI/SNF

In the vast majority of PCas the genes *KLK3* (PSA), *KLK2*, *TMPRSS2*, *FKBP5*, *NKX3.1*, *LSD1*, and *UBE2C* are upregulated by AR (Takayama and Inoue, 2013). A SMARCA2/4 dual degrader reduces AR target gene expression in multiple PCa cell lines (Xiao et al., 2022). Core subunits shared by all three SWI/SNF complexes (ACTL6A, SMARCD1, and SMARCC1) or cBAF and PBAF complexes (SMARCE1 and SMARCD2) are similarly required for AR target gene expression (S. Liu et al., 2017; Wijngaart et al., 2009; Sun et al., 2011; Ertl et al., 2023). cBAF complexes, which are the most abundant, are thought to be the primary dependency (Xiao et al., 2022). Several studies implicate SMARCA4 as the primary ATPase for AR gene regulation. SMARCA4 and SMARCC1 regulate the second largest number of androgen-dependent AR target genes after p300, with a significantly larger number than SMARCA2 (S. Liu et al., 2017) (Figure 5). Confirming a role for SMARCA4 as the major AR co-regulator, ACTL6A is recruited to two AREs of *KLK3* with SMARCA4, but not SMARCA2 (Jin, Kim, and Jeong, 2018) (Figure 5) and SMARCA4, but not SMARCA2, was enriched at the second intron of the AR target gene *ITGA2* (Balasubramaniam et al., 2013). At the *FKBP5* locus in VCaP cells, three validated AREs have high SMARCA2, but not SMARCA4, enrichment (Ban et al., 2021), indicating that SMARCA2 may be required for at least a subset of AR target genes (Lempiäinen et al., 2017; Ban et al., 2021; Launonen et al., 2021) (Figure 5). Supporting a role for both ATPases in PCa, loss of both SMARCA4 and SMARCA2 is required for decreased chromatin accessibility at enhancers, including those occupied by AR (Xiao et al., 2022).

## 2.4 Bromodomain (BD)-containing proteins and AR regulation

In PCa the most studied bromodomain-containing proteins are the BET (bromodomain and extra-terminal domain) proteins, primarily BRD4 (Urbanucci and Mills, 2018); however, the BDs on SWI/SNF subunits such as BRD9, SMARCA4, SMARCA2, PBRM1, and BRD7 are also important for AR activity.

BRD9, a unique subunit of the GBAF complex, is required for proliferation of AR-positive cell lines, and high GBAF subunit expression correlates with a decrease in tumor-free survival in patients (Alpsoy et al., 2021). BRD9 regulates the expression of AR target genes in both androgen-responsive and CRPC cell lines (Alpsoy et al., 2021) through association with BRD4. BRD9 colocalizes with BRD4 and CTCF at multiple genomic sites including at AR target genes (Alpsoy et al., 2021). This is presumably to facilitate chromatin looping and enhancer activation; however, further studies are needed to define the function of GBAF in PCa.

A role in CTCF-mediated looping in PCa may extend to other SWI/SNF subcomplexes as subunits from all three SWI/SNF complexes immunoprecipitate with CTCF (Valletta et al., 2020). Using publicly available datasets for Hi-C chromosomal contacts, histone modifications, DNA methylation, and nucleosome positioning in LNCaP cells (Giles et al., 2019), SMARCA4 was associated more with "actively marked" chromatin and CTCF enrichment than SMARCA2, which was more associated with

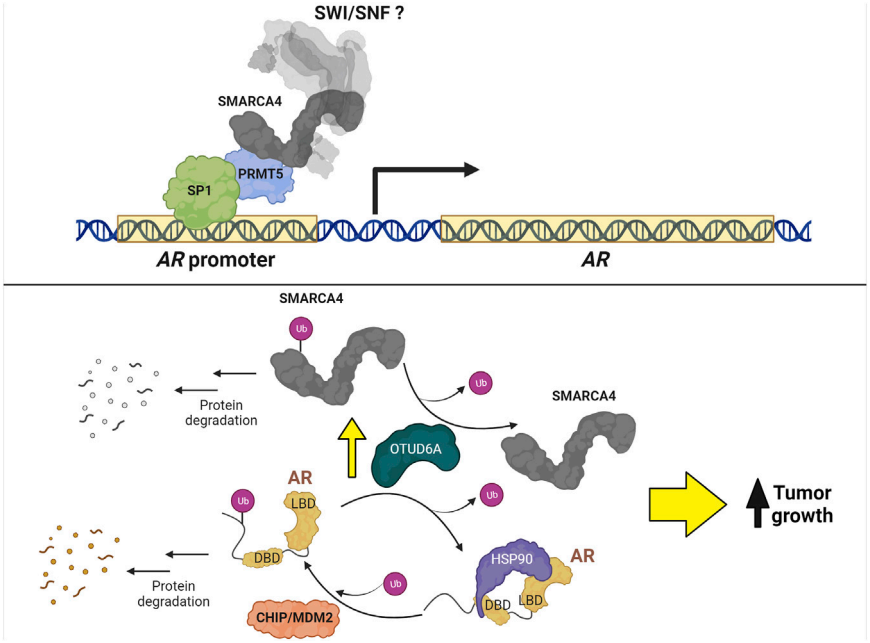


FIGURE 6
Regulation of AR expression in PCa. Top: PRMT5 forms a complex with SP1 and SMARCA4 to promote *AR* transcription. Bottom: MDM2 and CHIP ubiquitinate AR to promote protein degradation. Conversely, the protein levels of AR and SMARCA4 are upregulated by OTUD6A-mediated deubiquitination, thereby increasing tumor growth.

"repressively marked" chromatin (Giles et al., 2019). This is in accordance with the model that SMARCA4-containing SWI/SNF complexes target different sites than SMARCA2-containing complexes. Further studies focused on the loci where unique subunits colocalize with CTCF upon AR activation in PCa cells could shed light on the mechanism by which SMARCA2 and SMARCA4 regulate different sets of AR target genes.

Another BD-containing protein explored in PCa is TRIM24, which promotes AR signaling and has increased expression in CRPC (Groner et al., 2016). BRD7, a PBAF subunit, interacts with TRIM24 to limit TRIM24-induced AR transcriptional activity in a luciferase reporter assay (Kikuchi et al., 2009); however, this interaction was not studied at an endogenous level. In our recent work, BRD7 knockdown reduces proliferation of AR-dependent PCa cell lines and BRD7 BD inhibition in LNCaP cells downregulates the expression of AR target genes (Ordonez-Rubiano et al., 2023). Similarly, in the near-haploid HAP1 cells loss of BRD7 or ARID2 leads to reduction in genes involved in response to testosterone and dehydroepiandrosterone (Schick et al., 2019). Further supporting a role for PBAF in PCa, PBRM1 is almost 10 times more highly expressed in PCa than in benign prostatic hyperplasia (Mota et al., 2019). LNCaP cells (AR-dependent) have higher PBRM1 levels compared to PC-3 (AR-independent), DU145 (AR-independent), and RWPE-1 (normal prostate) cells (Mota et al., 2019). Supporting a role for PBAF in AR-mediated function, a PBRM1-selective BD inhibitor reduced the growth of LNCaP cells but not PC-3 and RWPE-1 cells (Shishodia et al., 2022). Overall, increasing evidence supports PBAF in the positive regulation of AR signaling; however, the mechanism by which this occurs is unexplored.

## 2.5 Regulation of AR expression and protein stability by SWI/SNF

Most studies focus on the regulation of AR-mediated transcription, but fewer studies investigate the regulation of AR itself. Consequently, little is known about the function of SWI/SNF in AR expression regulation except that long term loss of SWI/SNF results in a decrease in AR, which could be direct or indirect (Xiao et al., 2022). SMARCA4 is associated with Protein arginine methyltransferase 5 (PRMT5) and SP1 at the *AR* promoter where PRMT5 is required for transcription (Deng et al., 2017); however, whether AR transcription is dependent on chromatin remodeling by SMARCA4 has not been determined (Figure 6).

The regulation of AR stability has been a subject of investigation for many years. For example, CHIP (C-terminus of Hsp70-interacting protein) (Sarkar et al., 2014) and MDM2 (mouse double minute 2 homolog) (Gaughan et al., 2005; Giridhar et al., 2019) ubiquitin ligases promote AR degradation via proteasomal activity, while the long non-coding RNA PCBP1-AS1 prevents AR degradation by stabilizing a complex formed between AR and the deubiquitinase USP22 (Zhang et al., 2021); however, no connection has been made between these ubiquitin-mediated processes and SWI/SNF. In contrast, OTUD6A (ovarian tumor deubiquitinase 6A), a deubiquitinase amplified in PCa patients that promotes tumor growth in mice, deubiquitinates both SMARCA4 at K27 and AR at K11 to prevent their degradation by the proteasome (Fu et al., 2022) (Figure 6). Although promising as a strategy to promote degradation of SMARCA4 and AR simultaneously in PCa cells, no OTUD6A inhibitor has been developed.

## 2.6 Other AR coregulators and their relationship with SWI/SNF

AR transcriptional coregulators are mainly involved in four different roles: chromatin/histone modification, co/chaperone, scaffolding, and transcription machinery assembly (Leach, Fernandes, and Bevan, 2022). These components can be classified as coactivators or corepressors depending on their function in regulating AR transcriptional activity (Heemers and Tindall, 2007; Leach, Fernandes, and Bevan, 2022). There is increasing evidence supporting target gene-specific coregulator activity, wherein next generation sequencing techniques reveal that individual AR coregulators can have positive, negative, or no effects on specific AR target genes (Leach et al., 2022; Liu et al., 2017). This observation aligns with the SWI/SNF roles discussed in previous sections, in particular, that SMARCA4- and SMARCA2-containing complexes regulate separate sets of AR target genes. In this section we discuss the relationship between SWI/SNF and three less defined AR coregulators: ZMIZ1, ZMIZ2, and HMGB1.

ZMIZ1 and ZMIZ2 (Zinc Finger MIZ-Type Containing 1/2) are members of the protein inhibitor of activated STAT (PIAS) family of proteins that promote the activity of multiple signaling pathways, including AR (Lomelí, 2022). Immunoprecipitation studies indicate that SMARCA4 and SMARCE1 interact with ZMIZ2 and cooperate to promote AR transcriptional activity (Huang et al., 2005). The ability of ZMIZ1 to promote the activity of AR with short polyQ tract is enhanced by SMARCA4 and SMARCE1 (X. Li et al., 2011), further supporting the role of SWI/SNF in promoting transcriptional activity of AR with short polyQ tract.

High-mobility group box 1 (HMGB1) is an architectural chromatin-binding factor that facilitates transcription, recombination, and DNA damage repair (Xue et al., 2021) and *HMGB1* single nucleotide polymorphisms may predict PCa progression (Chou et al., 2020). HMGB1 can also be released from cells and its co-expression with the inflammatory receptor Receptor for Advanced Glycation End products (RAGE) correlates with progression and worse overall survival in PCa patients (Zhao et al., 2014). SMARCA4 co-immunoprecipitates with HMGB1 in both PC-3 and LNCaP cells, and colocalizes with HMGB1 in the nucleus (Lv et al., 2019). HMGB1 regulates SMARCA4 expression, and by inducing SMARCA4 expression in the AR-negative PC-3 cells, HMGB1 promotes epithelial-mesenchymal transition (EMT) (Lv et al., 2019). HMGB1 also directly interacts with AR and can reactivate AR signaling (Chen et al., 2022) indicating that SMARCA4 cooperates with HMGB1 to facilitate AR signaling in early stages of PCa, while in advanced CRPC, SMARCA4 cooperates with HMGB1 to promote a different set of genes involved in EMT. Comparing whole genome sequencing data between models of hormone sensitive and castration resistant disease could shed light on how this reprogramming may be occurring.

# 3 The interplay between SWI/SNF complexes and genetic drivers of PCa

While there is no universal genetic driver of PCa, several factors are mutated or altered in a significant portion of patients to drive the initiation and progression of PCa development and represent dependencies in PCa. Hereby we summarize discoveries on how SWI/SNF is involved in these additional events.

## 3.1 TMPRSS2::ERG fusion

ETS (E-26 transformation-specific)-related gene (ERG) is an oncogenic transcription factor that is overexpressed in multiple cancers such as Ewing's sarcoma, hematologic malignancies, and PCa (Adamo and Ladomery, 2016). Multiple gene fusions are present in PCa, the most frequent being TMPRSS2::ERG (Lorenzin and Demichelis, 2022). The TMPRSS2::ERG fusion gene in PCa was first reported in 2005 as a recurrent chromosomal rearrangement in patients (Tomlins et al., 2005) which increases ERG expression to induce ERG target gene expression (Fujita and Nonomura, 2018; Z. Wang et al., 2017; Tomlins et al., 2005). Since then, it has been established as a urinary biomarker of poor prognosis of PCa patients (Laxman et al., 2006; Sanda et al., 2017). IP-MS identified cBAF subunits as ERG interactors (Fu et al., 2021; Sandoval and Pulice, 2018). ChIP-Seq studies indicate that ERG dictates the overall targeting of cBAF, and that, conversely, the binding of ERG to chromatin depends on cBAF activity (Sandoval and Pulice, 2018). Moreover, SMARCA4 knockdown in organoids derived from prostate epithelia from *Pten*$^{+/-}$, *Tmprss2::ERG*$^{+}$ mice prevents basal-to-luminal transition, suggesting the interplay between SWI/SNF and TMPRSS2::ERG could drive PCa oncogenesis. The TMPRSS2::ERG fusion gene is thought to promote cell cycle progression, as knocking down *ERG* leads to $G_0/G_1$ cell cycle arrest in VCaP cells (Wang et al., 2017). Whether the TMPRSS2::ERG—SWI/SNF interaction drives such function in cell cycle progression of PCa cells remains to be elucidated.

## 3.2 FOXA1

Forkhead box A1 (FOXA1) is a pioneer factor that is recruited to chromatin in the presence of the H3K4me1 and H3K4me2 histone marks and induces chromatin accessibility at loci with reduced DNA methylation (Lupien et al., 2008; Sérandour et al., 2011). FOXA1 is highly mutated in PCa and drives PCa progression by poising sites for AR binding (Barbieri et al., 2012; Gerhardt et al., 2012) and promoting promoter-enhancer loops at PCa specific genes (Rhie et al., 2019). In addition to AR, FOXA1 is the most enriched transcription factor at SMARCA4 promoter binding sites in LNCaP cells. At the promoters of the AR target genes *KLK2* and *PCAT1*, FOXA1 binding is dependent on SMARCA4 (Giles et al., 2021). Supporting this, PCa cells with high AR and FOXA1 expression are dramatically more sensitive to the SMARCA2/4 degrader AU-15330 compared to cells that lack AR and FOXA1 (Xiao et al., 2022). Treatment of these cells with AU-15330 reduces chromatin accessibility and subsequent binding of both AR and FOXA1 to the enhancers of essential genes (Xiao et al., 2022).

## 3.3 HOXB13

Homeobox protein Hox-B13 (HOXB13) is a transcription factor highly expressed in the prostate involved in its development and maintenance (Kim et al., 2010; Brechka et al., 2017). HOXB13 has demonstrated to be a prognostic marker for PCa with increased

expression of AR-variant 7 target genes (Chen et al., 2018; Kim et al., 2020). In LNCaP cells SMARCA4 binding did not enrich for FOXA1 or HOXB13 at AR binding sites (S. Stelloo et al., 2018), while in VCaP cells ATAC-seq analyses indicated FOXA1 and HOXB13 binding motifs were enriched in sites dependent on SMARCA4 for accessibility (Launonen et al., 2021). These results indicate that SMARCA4 may be required for FOXA1 and HOXB13 binding primarily in a CRPC setting.

# 4 SWI/SNF complexes regulate PCa progression

SWI/SNF complexes regulate gene expression in a context-dependent manner, wherein their activity is dependent on the genetic background and disease stage (Kadoch et al., 2013; Cenik and Shilatifard, 2020; Mittal and Roberts, 2020). We described above the role of SWI/SNF in early stages of PCa that are dependent on AR and driven by transcriptional drivers such as TMPRSS2::ERG and FOXA1. In this section we will focus on two additional contexts: progression to the metastatic stage and therapy resistance, including lineage plasticity-associated neuroendocrine differentiation (NED).

## 4.1 SWI/SNF and the emergence of metastatic phenotypes

Other key driver events in PCa include loss of tumor suppressors TP53 and PTEN (Abeshouse et al., 2015; Robinson et al., 2015) and overexpression of EZH2 (Park et al., 2021). CRISPR Cas9-based screening revealed a synthetic lethal relationship between PTEN and SMARCA4 where ablation of SMARCA4 reduced growth of PTEN-null 22Rv1 PCa cells while having no effect in cells expressing wildtype PTEN (Ding et al., 2019). These results were further corroborated in a mouse model where SMARCA4 was demonstrated to be critical for progression of PCa tumors to invasive stages in $Pten^{PC-/-}$ mice (Ding et al., 2019).

In metastatic PCa, SMARCA4 has been connected to the expression of long-chain fatty acid elongase 3 (ELOVL3), which is involved in the synthesis of C20-C24 saturated and mono-unsaturated neutral very long-chain fatty acids (Westerberg et al., 2004). In PCa models, a metastatic phenotype can be induced with androgens (Lin et al., 2018) and TGF-β (Mirzaei et al., 2022). Under these conditions, SMARCA4 promotes migration and invasion of DU145 cells by interacting with p300 and the nuclear receptor RORγ at the *ELOVL3* promoter to induce transcription. Based on a general role for RORγ in cholesterol biosynthesis, SWI/SNF chromatin remodeling may be supporting metastasis and invasion in PCa by regulating the expression of genes involved in lipid metabolism and androgen synthesis (Stuchbery et al., 2017; Zou et al., 2022); however, mechanistic studies would be required to confirm this function genome-wide.

The role of other SWI/SNF subunits in metastatic PCa is less defined, with only a few subunits investigated so far. SMARCE1 is upregulated in prostatic intraepithelial neoplasia compared with benign prostatic hyperplasia tissues and promotes androgen-independent expression of genes involved in cell migration and metastasis (Balasubramaniam et al., 2013). BRD7, a PBAF-specific subunit is overexpressed in the AR-negative cell lines DU145 and PC-3 cells, and the knockdown of BRD7 leads to reduced cell proliferation, migration and invasion (Liang et al., 2019). This could indicate that, in contrast to the cBAF dependency for enhancer-mediated transcription, metastatic gene signatures may be more dependent on PBAF complexes; however, mechanistic studies are required to dissect the roles of distinct SWI/SNF subcomplexes in PCa metastasis.

## 4.2 Treatment-emergent neuroendocrine prostate cancer

Normal prostate architecture consists of luminal cells, basal cells, and interspersed neuroendocrine (NE) cells that surround the lumen (Figure 1). The vast majority of PCa are adenocarcinomas that arise from the luminal cells. Upon prolonged treatment with AR signaling inhibitors, a few of the cancer cells adapt and transdifferentiate to a NE-like state, which is a lineage plasticity event that involves cellular, molecular, and morphological identity changes (Davies et al., 2018; Davies et al., 2023). This transdifferentiation is an important contributor to the development of treatment-emergent neuroendocrine PCa (TE-NEPC) (Beltran et al., 2016), which is a subset of CRPC (10–20%) that is aggressive, AR null, transcriptionally unique, and treatment-resistant, with a median survival of 1 year (Aggarwal et al., 2018; Abida et al., 2019) (Figure 1). Of note, while TE-NEPC is different from focal NEPC (a small cell PCa subtype that arises directly from NE cells of normal prostate) (Small et al., 2016), in the clinic, it is difficult to distinguish between them, as they both present with low PSA levels and the expression of classical NE markers such as CD56, chromogranin A, synaptophysin, and neuron specific enolase (Aggarwal et al., 2014). Tumor tissue matched whole-exome sequencing showed that loss of *RB1* and *TP53* are distinguishing features of TE-NEPC compared to CRPC (Beltran et al., 2016). The somatic landscape of CRPC and TE-NEPC are similar to one another suggesting that epigenetic mechanisms drive the clonal evolution of TE-NEPC from the adenocarcinoma under the selection pressure of anti-androgen therapy (Beltran et al., 2016). Efforts are being made to identify the epigenetic drivers of this process, including SWI/SNF, with an eye on reversing or combating drug resistance (Cheng and Wang, 2021).

The conversion between cell-type specific mammalian SWI/SNF complex subunit configuration is well-established during development. In the differentiation from embryonic stem cells to terminally differentiated neurons, the cBAF subunits (ACTL6A, DPF2, SMARCD1/2, SMARCC1, SMARCA4, and SS18) are exchanged with paralogues (ACTL6B, DPF1/3, SMARCD1/3, SMARCC2, SMARCA2, and SS18L1; respectively) (Olave et al., 2002; Lessard et al., 2007; Ho, Ronan, et al., 2009) (Figure 2). To some extent, this developmental SWI/SNF configuration switch is recapitulated during the transition from CRPC to TE-NEPC (Cyrta et al., 2020), wherein a few neuronal SWI/SNF subunits (DPF1, SS18L1, and ACTL6B) are upregulated both at mRNA and protein levels in a TE-NEPC patient cohort. In contrast to a decrease during neuronal differentiation, SMARCA4 expression is increased in TE-NEPC, and its expression positively correlates to the expression of *SYP* (neuroendocrine marker) and *SOX2* (pluripotency marker) (Cyrta et al., 2020). This suggests that unique SWI/SNF complexes play a role in emergence of TE-NEPC.

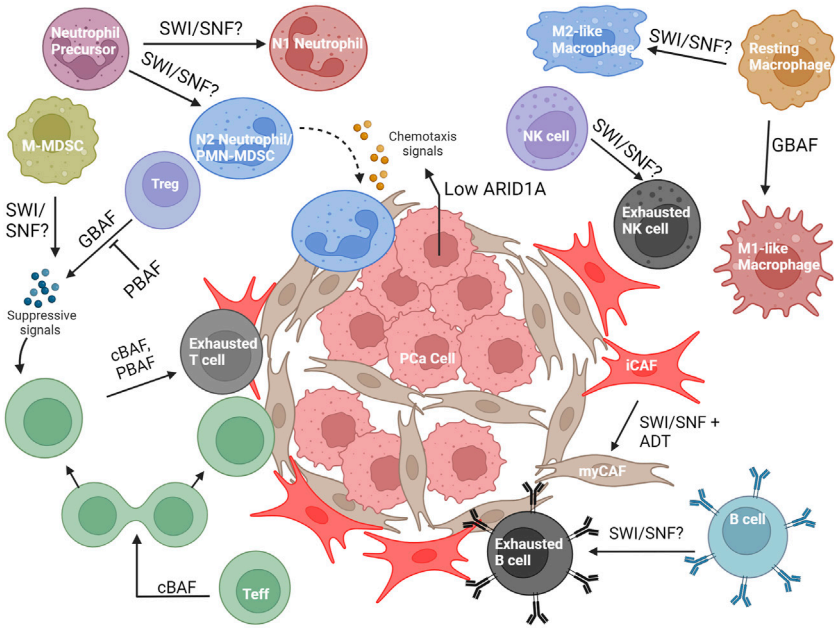


FIGURE 7
Overview of the known and possible roles SWI/SNF may have in the PCa microenvironment. Abbreviations: PCa, prostate cancer; ADT, androgen-deprivation therapy; Teff, T effector cell; Treg, T regulatory cell; NK cell, Natural killer cell; PMN-MDSC, Polymorphonuclear myeloid-derived suppressor cell; M-MDSC, Mononuclear myeloid-derived suppressor cell; iCAF, inflammatory carcinoma-associated fibroblast; myCAF, myofibroblastic carcinoma-associated fibroblast.

Some potential mechanistic understanding of SWI/SNF in NEPC has been revealed through the study of Mucin 1 (MUC1), which is expressed as two separate, non-covalently bound, parts: the N-terminus (MUC1-N) involved in cell-cell adhesion, and the C terminus (MUC1-C) involved in cell signaling and transcription (Kufe, 2023). MUC1 is overexpressed specifically in androgen-independent and neuroendocrine PCa cell lines (LNCaP-AI, DU-145, and NCI-H660) (Yasumizu et al., 2020) and reduced *MUC1-C* expression results in increased expression of AR target genes and decreased expression of NE and pluripotency genes (Yasumizu et al., 2020). MUC1-C binds directly to genomic sites near *SMARCA4*, *ARID1A*, *PBRM1*, *ARID2,* and *BRD7* (Hagiwara et al., 2021; Hagiwara et al., 2021). Reduction in nuclear expression of MUC1-C via genetic knockdown or chemical inhibition using the MUC1-C dimerization inhibitor, GO-203, results in decreased expression of cBAF and PBAF, but not GBAF subunits (Hagiwara et al., 2021; Hagiwara et al., 2021). In addition, MUC1-C co-immunoprecipitates with PBRM1 and directly cooperates with PBAF to regulate the expression of NRF2 target genes (Hagiwara et al., 2021). Although these studies provide evidence that SWI/SNF subunits play a role in TE-NEPC, the mechanistic interplay within the sub-complexes remains to be elucidated.

# 5 The crosstalk between SWI/SNF complexes and the tumor microenvironment (TME) in PCa

The prostate TME contains carcinoma-associated fibroblasts (CAFs) and several types of immune cells, including but not limited to, T cells, B cells, NK cells, macrophages, myeloid-derived suppressor cells (MDSCs), and neutrophils (Kwon et al., 2021; Palano et al., 2022) (Figure 7). These cell types all display plasticity and can differentiate into multiple subtypes with different effects on tumor growth and therapy resistance. Because of this, both immune cells and CAFs could be dependent on epigenetic modulation by SWI/SNF for pro or anti-tumorigenic function. Moreover, the effects of SWI/SNF within the cancer cells, including the perturbation of specific subunits, can change the interaction between the PCa and the immune microenvironment (Li et al., 2022; Hagiwara et al., 2022).

## 5.1 Carcinoma associated fibroblasts (CAFs)

CAFs are a heterogenous group of fibroblasts that have differing and overlapping functions to support the tumor cells and the greater microenvironment (Glabman, Choyke, and Sato, 2022). Although many subtypes of CAFs exist, the two most common are myofibroblastic CAFs (myCAFs) and inflammatory CAFs (iCAFs). myCAFs have high expression of α-smooth muscle actin (α-SMA), low expression of inflammatory cytokines, and are responsive to TGF-β. iCAFs are defined by high IL-6 and IL-11 expression and low α-SMA expression (Glabman et al., 2022). myCAFs support cancer growth by producing an extracellular matrix that protects tumor cells from immune attack and therapeutics, while iCAFs secrete inflammatory cytokines to sequester immune cells from tumor and encourage immune exhaustion (Elyada et al., 2019). While initially discovered in pancreatic cancer (Öhlund et al., 2017; Biffi et al., 2019; Elyada

et al., 2019), single-cell RNA sequencing (scRNA-seq) studies have shown these CAF signatures in several other solid tumor cancers (Chen et al., 2020; Wu et al., 2020), including PCa (Wang et al., 2023). iCAF and myCAF fibroblast signatures were identified in genetically-engineered mouse models of PCa with clusters that appear to be transitioning between iCAF and myCAF (Wang et al., 2023), consistent with other studies indicating that CAFs can interconvert (Biffi et al., 2019; Elyada et al., 2019). Blocking androgen signaling in these fibroblasts encouraged conversion to a myCAF-like state, which induce castration resistance through the actions of SPP1 (secreted phosphoprotein 1) (Wang et al., 2023). This CAF conversion was dependent on the transcription factor SOX4; knockdown of *Sox4* in CAFs reduced myCAF-related gene expression and tumor resistance to androgen signaling blockade. In addition, SOX4 associates with SMARCA4, SMARCC1, and ARID1A (via co-IP), with SOX4 and SMARCA4 both binding at the *Spp1* locus (via ChIP-qPCR). In a SOX4 overexpression CAF model, knockdown of *SMARCA4* significantly reduced transcription of myCAF-related genes while not changing iCAF-related gene transcript levels (Wang et al., 2023), suggesting that the interconversion from iCAFs to myCAFs in PCa is dependent on SWI/SNF function. This implicates SWI/SNF as a potential target to inhibit anti-androgen therapy resistance mediated by myCAFs.

## 5.2 Immune cells

There has been very little investigation into the roles of SWI/SNF in the immune cells specifically found in the PCa microenvironment, such as monocytic MDSC (M-MDSC) and polymorphonuclear MDSC (PMN-MDSC). However, in some relevant immune cells, the dependencies on SWI/SNF may be applicable to the PCa microenvironment. We have highlighted the studies performed on immune cell types potentially relevant to the PCa TME below.

### 5.2.1 Macrophages

In the TME, macrophages can have both a pro-inflammatory (M1-like) or anti-inflammatory (M2-like) role (Palano et al., 2022). M1-like macrophages inhibit tumor growth by recruiting adaptive immune cells, whereas M2-like macrophages promote cancer growth by immune suppression, vascularization of the tumor, and promoting metastasis (Palano et al., 2022). In macrophage development, SWI/SNF complexes are known to control lineage-determining transcription factors (LDTFs) (Gatchalian et al., 2020), as demonstrated by *Arid1a* knockout mice decreasing chromatin accessibility to the LDTFs PU.1, RUNX1, GATA, and CSF-1 (L. Han et al., 2019). Furthermore, LDTFs recruit SWI/SNF subunits to enhancers of macrophage-specific genes, such as PU.1 recruiting SMARCC1 and SMARCB1 to the *Il12b* and *Il1a* loci in mature macrophages (McAndrew et al., 2016). SWI/SNF is recruited to other pro-inflammatory early and late response genes (Ramirez-Carrozzi et al., 2006; Liu et al., 2023), through AKIRIN2 (Tartey et al., 2014), KDM2B (Zhou et al., 2020) or the non-coding RNA transcript from *Cox2* (LincRNA-Cox2) (Hu et al., 2016), and cooperates with p300 to increase expression of DNA repair enzymes that control DNA damage from macrophage activity (Pietrzak et al., 2019).

GBAF specifically has been found to be important for macrophage function. BRD9 is important for inflammatory gene expression in bone marrow-derived macrophages treated with lipopolysaccharide (LPS) and BRD9 inhibitors can enhance the anti-inflammatory response mediated by dexamethasone-induced glucocorticoid receptor activity (Wang et al., 2021). Similarly, bone marrow-derived macrophages require BRD9 for the expression of secondary response genes in the IFN pathway when stimulated with the endotoxin Lipid A via cooperation with the ISGF3 transcription factor complex, which regulates interferon-stimulated genes (Ahmed et al., 2022). Given these findings, SWI/SNF is clearly important for proinflammatory (M1-like) macrophage function, which would support an anti-tumorigenic role for SWI/SNF in PCa; however, it is unknown whether SWI/SNF is also important for anti-inflammatory M2-like macrophage function, which could implicate SWI/SNF in a pro-tumorigenic role. Additionally, SWI/SNF has not been investigated specifically in the context of PCa, where pro-tumorigenic M2-like macrophages are prevalent (Han et al., 2022).

### 5.2.2 Neutrophils

Neutrophils are granulocytic polymorphonuclear phagocytes that serve a role in the innate immune system (Wang, Zhang, and Gao, 2022). Similar to macrophages, neutrophils can differentiate into both a proinflammatory (N1) and an anti-inflammatory (N2) phenotype (Wang et al., 2022). The N1 neutrophils exert anti-tumorigenic activity by releasing factors that support cytotoxicity, such as reactive oxygen species (ROS), Fas, and ICAM-1, while N2 neutrophils support tumor growth by releasing factors such as MMP9, VEGF, CCL2, and CXCL4 (Wang et al., 2022). For clarification, N2 neutrophils and PMN-MDSCs are considered to be the same cell type by some, but this is currently debated in the field (Antuamwine et al., 2023). In metastatic PCa, an increased neutrophil-lymphocyte ratio was associated with poorer outcomes (Su et al., 2019), implicating neutrophils as a potential therapeutic target; however, very few studies have investigated the role of SWI/SNF in their function, and none have addressed this role in the context of PCa. In development, the differentiation from promyelocytes to neutrophils corresponds with a decrease in PBAF subunit expression and an upregulation of an inactive PHF10 isoform (PHF10Ss) without the tandem PHDs in the C-terminal region (Viryasova et al., 2019). Additionally, SMARCD2 (found in cBAF and PBAF) is required for the binding and activity of CCAAT-enhancer binding protein-epsilon (CEBPε), which upregulates the expression of secondary and tertiary granule genes important during neutrophil maturation and granule function (Priam et al., 2017). This corroborates the clinical finding that patients with SMARCD2 mutations are associated with defects in neutrophil function (Witzel et al., 2017; Schim van der Loeff et al., 2021). The role of SWI/SNF in the context of tumor-associated neutrophils has not been explored, and from a therapeutic perspective, it would be important to determine whether SWI/SNF-driven chromatin remodeling plays a role in the differentiation to N1 and N2 phenotypes (Wang et al., 2018).

### 5.2.3 T cells

As in many cancers, T cells have a prominent role in PCa. $CD4^+$ T cells can have an anti-tumorigenic role (Th1), pro-tumorigenic role (Treg), or a mixture of both (Th2, Th17). $CD8^+$ T cells are

important for an anti-tumor response, but can differentiate to an exhausted state, with reduced cytotoxic function (Wang et al., 2022). Lastly, memory T cell (Tmem) generation is important for immunosurveillance, maintaining an anti-tumor immune response, and facilitating the response to immunotherapies (Liu et al., 2020). SWI/SNF has been extensively studied in T cell development and has numerous dependencies (Wurster and Pazin, 2012), including lineage-specific differentiation (De et al., 2011; F. Zhang and Boothby, 2006, 1; Letimier et al., 2007; Wurster and Pazin, 2008; Lee et al., 2020; Chaiyachati et al., 2013); however, to remain in the cancer context as much as possible, we will focus on SWI/SNF function post-activation in this review and highlight several different roles for SWI/SNF that have recently been identified.

*Treg*: In a genome-wide screen of activated $CD4^+$ T regulatory cells (Tregs), expression of *Foxp3*, the master transcription factor of Tregs, was reduced upon loss of GBAF subunits (BRD9, GLTSCR1/1L), and increased upon loss of PBAF subunits (BRD7, ARID2, PBRM1, and PHF10) (Loo et al., 2020). Furthermore, loss of GBAF or PBAF-specific subunits, respectively, decreased and increased suppression activity of Tregs when co-cultured with T effector cells (Teff). Treatment with the molecular degrader dBRD9 was able to recapitulate these effects seen in BRD9 knockout (Loo et al., 2020), highlighting a druggable target that could increase the antitumor immune response in solid tumors.

*Tmem:* Memory T cell (Tmem) formation has also been investigated in two recent major studies (Guo et al., 2022; McDonald et al., 2023) In the first study, a genome-wide CRISPR screen in ovalbumin peptide-specific OT-1 T cells identified an increase in Tmem generation with loss of *Arid1a* and *Smarcd2* prior to activation. It was concluded that upon activation, cBAF and c-Myc are asymmetrically distributed upon T cell division; cells with lower amounts of cBAF and c-Myc became Tmem, and cells with high amounts became Teff. Additionally, it was demonstrated that *ex vivo* treatment with the cBAF inhibitor BD98 in $CD8^+$ T cells and in CAR T cells resulted reduced tumor growth in mouse models (A. Guo et al., 2022), suggesting a druggable target in the cancer setting. The second study utilized a lymphocytic choriomeningitis virus (LCMV)-specific $CD8^+$ T cell clone with a floxed *Arid1a* allele and *Gzmb-Cre*$^+$ such that *Arid1a* knockout occurs right at the point of activation instead of prior to activation. With this model, it was found that Teff cell expansion was dependent on *Arid1a* as cBAF was required for maintaining chromatin accessibility for the enhancers of transcription factors important for early activation and effector differentiation, such as *Tbx21* (T-bet) and *Zeb2* (McDonald et al., 2023). Furthermore, this loss of chromatin accessibility at the point of activation effected Tmem cells as well. While Tmem generation was not changed, cytokine production by circulating Tmem cells was impaired and tissue-resident Tmem cells were reduced. (McDonald et al., 2023). To summarize, upon activation, if cBAF has been previously knocked out prior to activation, naïve T cells will prefer maturing to the memory phenotype due to the absence of cBAF. If cBAF is knocked out right at the point of activation, then enhancer regions at the loci of important transcription factors, such as T-bet, are reduced. This causes dysfunctional Tmem activity, reduced Teff population, and reduced tissue-resident Tmem cells (Figure 8A). Both studies showed cBAF was important for differentiation and proliferation of Teff cells (Guo et al., 2022; McDonald et al., 2023). From these results, more questions arise of the exact role of cBAF in T cell activation and how that role changes temporally.

*Exhausted T cells:* The process of T cell exhaustion is dependent on SWI/SNF as well. $CD4^+$ T cells that were exhausted via breast cancer cell coculture had increased SMARCA4 binding to the *CD274* locus and increased PD-L1 expression (Jancewicz et al., 2021). In a genome-wide CRISPR screen of mouse $CD8^+$ T cells *in vitro, Arid1a* was required for the transition to the exhausted state, and deletion thereof increased T cell persistence (Belk et al., 2022). Moreover, in solid tumor xenograft experiments, T cell-specific *Arid1a* deletion increased overall survival and decreased tumor burden (Belk et al., 2022). These observations were later corroborated in a separate study where an *in vitro* genome-wide CRISPR screen of overstimulated murine $CD8^+$ T cells showed major depletion of *Arid1a* and *Dpf2* knockouts in T cells with high PD-1 and TIM-3, indicating exhaustion (Battistello et al., 2023). Guide RNAs for *Smarcc1, Smarca4, Arid2, Pbrm1,* and *Arid1b* were also depleted, albeit to a lesser extent. Increased T cell persistence was observed in pan-SWI/SNF and cBAF-specific subunit-knockout $CD8^+$ T cells after 9 days of activation. Furthermore, pretreatment of $CD8^+$ T cell and CAR T cells with inhibitors/degraders of SMARCA4/2 decreased the number of exhausted T cells and increased persistence in solid tumor models as well (Battistello et al., 2023).

Using $CD4^{CRE+}$ $Cas9^+$ LCMV infection model, an *in vivo* genome-wide CRISPR screen found PBAF subunits (mainly *Arid2* and *Pbrm1*) important for blocking the transition of early progenitor exhausted state in $CD8^+$ T cells to an intermediate exhausted state and inducing the transition of the intermediate to terminally exhausted state (Baxter et al., 2023). Thus, blocking PBAF subunits caused an accumulation of this intermediate exhausted T cell state, which is "effector-like." It was also found that knocking out *Arid1a* led to less intermediate and more terminally exhausted T cells. Moreover, concomitant loss of PBAF in the T cells improved treatment response in the B16 melanoma model with PD-1 antibody blockade (Baxter et al., 2023). In a separate study, *Arid2*$^{fl/fl}$ *Vav*Cre mice (*Arid2* conditional deletion in hematopetic cells) infected with LCMV had an increased fraction of Teff and decreased progenitor and terminally exhausted T cells, suggesting that PBAF inhibition can reverse progenitor exhausted T cells back to effector T cells. In agreement, the same effect was observed for T cells in the B16 melanoma model (Kharel et al., 2023). The discrepancy between these studies is intriguing; Baxter et al. essentially showed PBAF inhibits the transformation from a progenitor exhausted state to an intermediate "effector-like" state while promoting the effector-like state to the terminally exhausted state, while Kharel et al. suggested that PBAF promotes the whole effector to exhausted transition (Figure 8B). The discrepancy may be due to the differences in the models. It is also possible the intermediate exhausted population may be more similar to T effector cells than initially thought. Questions still arise, however, on the epigenetic changes occurring during the transition from effector T cells to terminally exhausted T cells and how SWI/SNF controls these changes.

### 5.2.4 B cells

The biology of tumor-infiltrating B cells is currently a young field; however, there are some established roles in the TME. After

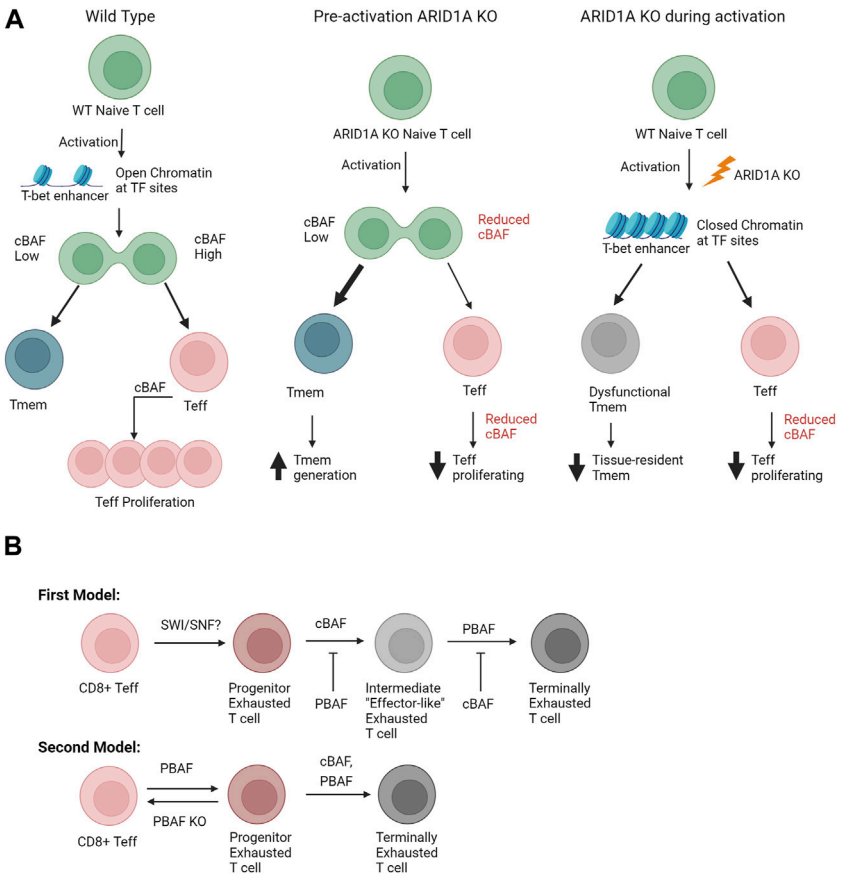


FIGURE 8
**(A)** Comparison of different modalities to study cBAF in memory T cell formation. The middle pathway is similar to the work performed by (A. Guo et al., 2022). The reduced cBAF before activation leads to a lower amount of Teff proliferation and increased amount of Tmem generation; this is thought to be due to the asymmetric expression of cBAF upon cell division after activation. The right pathway summarizes the work performed by (McDonald et al., 2023). Knocking out ARID1A at the point of activation leads to a decrease in transcription factors important for T cell activation and differentiation, such as Tbx21 (T-bet). This in turn leads to a reduced Teff population and a dysfunctional circulating Tmem population and a decreased tissue-resided Tmem population. **(B)** Suggested exhaustion models of SWI/SNF driven exhaustion. The first model is based on (Baxter et al., 2023). The second model is based on (Kharel et al., 2023). Both models loosely support the findings from (Belk et al., 2022; Battistello et al., 2023), as both articles found cBAF important to reach the terminally exhausted stage. Abbreviations: Teff, T effector cell; Tmem, Memory T cell; WT, wildtype; KO, Knockout.

activation, B cells can form memory cells or plasma cells (Laumont et al., 2022). Plasma cells typically infiltrate the TME, whereas memory B cells typically stay in lymph tissue or tertiary lymphoid structures. Activated B cells have antibodies designed for epitopes expressed on cancer cells, and thus can contribute to the clearing of these cells with antibody-dependent cellular cytotoxicity (ADCC) and antibody-dependent cellular phagocytosis (Laumont et al., 2022). In PCa, B cells can play a negative role by releasing factors that encourage PCa castration resistance and attenuate the T cell response (Kwon, Bryant, and Parkes, 2021). Exhausted B cells and B "regulatory" cells also exist in the microenvironment, though they are currently not well-studied (Laumont et al., 2022). Similar to T cells, B cells also have SWI/SNF dependencies during development (Morshead et al., 2003; Gao et al., 2009; Osipovich et al., 2009; Choi et al., 2012; Bossen et al., 2015). Despite these findings, little has been studied on SWI/SNF's role in plasma B cells of the prostate TME.

Many studies have been published about the role SWI/SNF subunits in B cells of germinal centers during activation and differentiation into antibody-producing plasma cells (Holley and Beezly, 2014; Choi et al., 2015; Tartey et al., 2015; Schmiedel et al., 2021). Whether this has an effect in the prostate TME is unknown; although, germinal centers have been implicated as an important part of tertiary lymphoid structures and associated with longer survival in other cancers (Siliņa et al., 2018; Gunderson et al., 2021). Many areas of B cell differentiation are still unexplored. As referenced, memory versus effector formation and exhaustion are currently not studied. How the individual SWI/SNF complexes may be involved is also unanswered.

### 5.2.5 NK cells

Natural killer (NK) cells are innate cells of lymphoid origin that exhibit cytotoxicity, making them an active area of investigation for anti-cancer immunity (Palano et al., 2022). Upon activation by ligands on cancer cells and through T cell interaction, they release molecules that encourage cancer cell death, including IFNγ, perforin, and granzymes (Palano et al., 2022). Furthermore, they can also eliminate cells tagged with antibodies through ADCC. Similar to T and B cells, NK cells can also become exhausted, reducing anti-cancer efficacy (Palano et al., 2022).

There is little information about SWI/SNF in NK cells. Using murine NK cell lysates, Rautela et al. performed an IP-MS experiment of Inhibitor of DNA-binding 2 (Id2), a protein important for NK cell development by repressing genes that promote T and B cell development, and identified many core SWI/SNF subunits, including SMARCC1, SMARCC2, SMARCA4, ARID1B, SMARCB1, and SMARCD2 (Rautela et al., 2019). Outside of development, a recent study showed exhausted NK cells from oral squamous cell carcinoma downregulated ARID2 in comparison to control splenic NK cells (Li et al., 2023). Knockdown of ARID2 in NK cells reduced pro-inflammatory genes and increased exhaustion markers in comparison to control when injected *in vivo;* overexpression of ARID2 had the opposite effect. However, there was no effect on tumor growth (Li et al., 2023), which may reflect a cancer-dependent role for NK cells. Based on current evidence, it may be possible that PBAF is preventing NK cell exhaustion; however, the role cBAF and GBAF play in this pathway is still unknown, as is SWI/SNF's role in NK cells on PCa progression and therapy resistance.

### 5.3 Effects of SWI/SNF in cancer cells on the tumor microenvironment

Not only does SWI/SNF affect the function of immune cells in the microenvironment, but its expression within the tumor can affect interaction with the TME. In other cancers, SWI/SNF subunits and subunit mutations/aberrations have been shown to change the composition of the TME and the response to immune therapies (Pan et al., 2018; Li et al., 2020; Miao et al., 2018; Liu et al., 2020). Here we will outline the current knowledge of how SWI/SNF complexes in PCa cells control how the TME is shaped (Hagiwara et al., 2022; Li et al., 2022).

Using data available in the TCGA database and histological analysis of murine PCa tumors, it was discovered that *ARID1A* expression is inversely correlated with tumor aggressiveness in PCa (Li et al., 2022). *ARID1A* loss in *in vitro* organoids of PCa cells did not give a notable growth advantage; however, in an immunocompetent mouse model, PCa cells with *ARID1A* knockout did exhibit a growth advantage due to increased PMN-MDSC recruitment, decreased $CD8^+$ T cell infiltration, and decreased IFN-γ expression from the $CD8^+$ T cells (Li et al., 2022) (Figure 7). Mechanistically, *ARID1A* deletion reduced accessibility at *A20*, a deubiquitinase that negatively regulates NF-κB signaling, resulting in NF-κB mediated upregulation of *Cxcl2* and *Cxcl3*, cytokines that encourage MDSC recruitment and an immunosuppressive pro-tumor TME. ARID1A is very rarely mutated in PCa but is often downregulated through phosphorylation and proteosomal degradation, representing potential therapeutic strategies to increase the levels of ARID1A to promote an anti-immunogenic immune microenvironment (Li et al., 2022). In a separate study, the interplay between SWI/SNF complexes and MUC1-C and the wound healing response (Kufe, 2020) revealed a role for SWI/SNF in activating IFN- γ signaling in PCa, which is conducive for cancer growth. cBAF (ARID1A) is required to facilitate the transcription of *IFNGR1* (interferon gamma receptor 1) by MUC1-C. MUC1-C, which also activates the expression of PBAF subunits (Hagiwara et al., 2021), cooperates with PBAF to facilitate the expression of IRF1, a downstream transcription factor in the IFN-γ pathway. IRF1 further increases the expression of IDO1, WARS, PTGES, ISG15, and SERPINB9, all of which contribute to immune suppression in the TME (Hagiwara et al., 2022). In summary, this work implicates both cBAF and PBAF to the upregulation of an immune suppressive state.

Many unknowns still exist about whether other effects of SWI/SNF can contribute to PCa to shape the TME. SWI/SNF expression in cancer cells may be controlling pathways that contribute to a more favorable environment for the cancer, such as fibroblast recruitment and blood vessel development. Through increased analysis of patient data and immune competent mice it would be possible to elucidate these effects that may otherwise be hidden in monoculture or immunocompromised mouse models.

## 6 Discussion

PCa is the most frequent cancer in men in the US, with an increasing number of patients eventually becoming resistant to available treatments. Genetic aberrations have been clearly defined depending on the stage of the disease, with mutations or deletions of common tumor suppressors such as *TP53* and *RB1* frequently observed, while transcription factors such as AR, MYC, and FOXA1 are amplified or overexpressed. Due to the highly transcriptional nature of PCa, chromatin regulators such as the SWI/SNF chromatin remodelers are just starting to be explored as therapeutic targets for advanced and therapy-resistant subtypes. In this review we have covered the multiple functions for SWI/SNF in PCa, including different aspects of AR signaling, the relationship between SWI/SNF and other genetic drivers, how SWI/SNF facilitates metastasis and therapy resistance, and finally the role of SWI/SNF in the tumor microenvironment (TME), which plays important roles in disease progression and therapy resistance. Different types of inhibitors and degraders of SWI/SNF subunits have been developed, although very few have been tested in PCa. Degraders of the ATPase subunits are effective in xenograft models; however, it is undetermined whether targeting other subunits may also be an effective and potentially less toxic strategy. Targeting cBAF seems to be most critical for inhibiting AR and transcription factor drivers of PCa, such as TMPRSS2::ERG and FOXA1; however cBAF-selective inhibitors are limited and have not yet been tested in PCa. Meanwhile, GBAF and PBAF inhibitors, while less effective against the core transcriptional circuit in PCa, may be associated with fewer toxic side effects and more useful in resistant and advanced subtypes of PCa, such as the increasingly common TE-NEPC. With additional knowledge regarding the most critical SWI/SNF subunits for viability, resistance, and progression of PCa, SWI/SNF inhibitors may be successfully utilized in combination therapies to increase efficacy and decrease resistance to more conventional therapies. Importantly, by understanding the role of SWI/SNF subunits on both the tumor and the immune microenvironment, SWI/SNF inhibition could be a much-needed mechanism for turning the immunologically 'cold' PCa tumors into a "hot" ones, which can improve response to immune checkpoint inhibitor immune checkpoint inhibitor therapy or other immunotherapies. In addition, SWI/SNF inhibition may be effective in targeting immunosuppressive cell types, such as MDSCs and Tregs that

are involved in resistance to AR-targeted therapies. Through new genetic studies and the development of novel SWI/SNF inhibitors, the specific SWI/SNF subunits required for different stages of PCa progression and therapy resistance can start to be defined in the appropriate disease-relevant settings.

## Author contributions

SO-R: Conceptualization, Writing–original draft, Writing–review and editing. BS: Writing–original draft, Writing–review and editing. SS: Writing–original draft, Writing–review and editing. ED: Conceptualization, Writing–original draft, Writing–review and editing.

## Funding

The author(s) declare financial support was received for the research, authorship, and/or publication of this article. For ED, U01CA207532 from the NIH-NCI, PC210004 from the DoD-PCRP, and RSG DMC133996 from the ACS. For SO-R, the SIRG Graduate Research Assistantship Award from the Purdue University Institute for Cancer Research (P30CA023168) and the Lilly Endowment Gift Graduate Research Award from the Purdue College of Pharmacy. For BS, The Purdue Drug Discovery Training Grant (T32 GM125620) from NIH-NIGMS and the Ross-Lynn Fellowship from the Purdue Research Foundation. For SS, the Bilsland Dissertation Fellowship from the Purdue University Interdisciplinary Life Sciences-PULSe program and the Yeshwant A. Gore Graduate Fellowship from the Purdue University Institute for Cancer Research.

## Acknowledgments

We thank Dr. Diana Hargreaves (The Salk Institute for Biological Studies), Dr. Alisha Dhiman (Purdue University) and Guanming Jiao (Purdue University) for their insights and comments on the manuscript. Figures created with BioRender.com.

## Conflict of interest

The authors declare that the research was conducted in the absence of any commercial or financial relationships that could be construed as a potential conflict of interest.

## Publisher's note



## References

Abeshouse, A., Ahn, J., Akbani, R., Ally, A., Amin, S., Andry, C. D., et al. (2015). The molecular taxonomy of primary prostate cancer. *Cell* 163 (4), 1011–1025. doi:10.1016/j.cell.2015.10.025

Abida, W., Cyrta, J., Heller, G., Prandi, D., Armenia, J., Coleman, I., et al. (2019). Genomic correlates of clinical outcome in advanced prostate cancer. *Proc. Natl. Acad. Sci.* 116 (23), 11428–11436. doi:10.1073/pnas.1902651116

Adamo, P., and Ladomery, M. R. (2016). The oncogene ERG: a key factor in prostate cancer. *Oncogene* 35 (4), 403–414. doi:10.1038/onc.2015.109

Aggarwal, R., Huang, J., Alumkal, J. J., Zhang, Li, Feng, F. Y., Thomas, G. V., et al. (2018). Clinical and genomic characterization of treatment-emergent small-cell neuroendocrine prostate cancer: a multi-institutional prospective study. *J. Clin. Oncol.* 36 (24), 2492–2503. doi:10.1200/JCO.2017.77.6880

Aggarwal, R., Zhang, T., Small, E. J., and Armstrong, A. J. (2014). Neuroendocrine prostate cancer: subtypes, biology, and clinical outcomes. *J. Natl. Compr. Cancer Netw.* 12 (5), 719–726. doi:10.6004/jnccn.2014.0073

Ahmed, N. S., Gatchalian, J., Ho, J., Burns, M. J., Hah, N., Wei, Z., et al. (2022). BRD9 regulates interferon-stimulated genes during macrophage activation via cooperation with BET protein BRD4. *Proc. Natl. Acad. Sci. U. S. A.* 119 (1), e2110812119. doi:10.1073/pnas.2110812119

Alimirah, F., Chen, J., Basrawala, Z., Xin, H., and Choubey, D. (2006). DU-145 and PC-3 human prostate cancer cell lines express androgen receptor: implications for the androgen receptor functions and regulation. *FEBS Lett.* 580 (9), 2294–2300. doi:10.1016/j.febslet.2006.03.041

Alpsoy, A., and Dykhuizen, E. C. (2018). Glioma tumor suppressor candidate region gene 1 (GLTSCR1) and its paralog GLTSCR1-like form SWI/SNF chromatin remodeling subcomplexes. *J. Biol. Chem.* 293 (11), 3892–3903. doi:10.1074/jbc.RA117.001065

Alpsoy, A., Utturkar, S. M., Carter, B. C., Currie, M. P., Elzey, B. D., Dykhuizen, E. C., et al. (2021). BRD9 is a critical regulator of androgen receptor signaling and prostate cancer progression. *Cancer Res.* 81 (4), 820–833. doi:10.1158/0008-5472.CAN-20-1417

Antuamwine, B. B., Bosnjakovic, R., Hofmann-Vega, F., Wang, X., Theodosiou, T., Iliopoulos, I., et al. (2023). N1 versus N2 and PMN-MDSC: a critical appraisal of current concepts on tumor-associated neutrophils and new directions for human oncology. *Immunol. Rev.* 314 (1), 250–279. doi:10.1111/imr.13176

Balasubramaniam, S., Comstock, C. E. S., Ertel, A., Jeong, K. W., Stallcup, M. R., Addya, S., et al. (2013). Aberrant BAF57 signaling facilitates prometastatic phenotypes. *Clin. Cancer Res.* 19 (10), 2657–2667. doi:10.1158/1078-0432.CCR-12-3049

Ban, F., Leblanc, E., Cavga, A. D., Huang, C. C. F., Flory, M. R., Zhang, F., et al. (2021). Development of an androgen receptor inhibitor targeting the N-terminal domain of androgen receptor for treatment of castration resistant prostate cancer. *Cancers* 13 (14), 3488. doi:10.3390/cancers13143488

Barbieri, C. E., Baca, S. C., Lawrence, M. S., Demichelis, F., Blattner, M., Theurillat, J.-P., et al. (2012). Exome sequencing identifies recurrent SPOP, FOXA1 and MED12 mutations in prostate cancer. *Nat. Genet.* 44 (6), 685–689. doi:10.1038/ng.2279

Battistello, E., Hixon, K. A., Comstock, D. E., Collings, C. K., Chen, X., Rodriguez Hernaez, J., et al. (2023). Stepwise activities of mSWI/SNF family chromatin remodeling complexes direct T cell activation and exhaustion. *Mol. Cell* 83 (8), 1216–1236.e12. doi:10.1016/j.molcel.2023.02.026

Baxter, A. E., Huang, H., Giles, J. R., Chen, Z., Wu, J. E., Drury, S., et al. (2023). The SWI/SNF Chromatin Remodeling Complexes BAF and PBAF Differentially Regulate Epigenetic Transitions in Exhausted CD8+ T Cells. *Immunity* 56 (6), 1320–1340.e10. doi:10.1016/j.immuni.2023.05.008

Belk, J. A., Yao, W., Ly, N., Freitas, K. A., Chen, Y.-T., Shi, Q., et al. (2022). Genome-wide CRISPR screens of T cell exhaustion identify chromatin remodeling factors that limit T cell persistence. *Cancer Cell* 40 (7), 768–786.e7. doi:10.1016/j.ccell.2022.06.001

Bello, D., Webber, M. M., Kleinman, H. K., Wartinger, D. D., and Rhim, J. S. (1997). Androgen responsive adult human prostatic epithelial cell lines immortalized by human papillomavirus 18. *Carcinogenesis* 18 (6), 1215–1223. doi:10.1093/carcin/18.6.1215

Beltran, H., Prandi, D., Mosquera, J. M., Benelli, M., Puca, L., Cyrta, J., et al. (2016). Divergent clonal evolution of castration-resistant neuroendocrine prostate cancer. *Nat. Med.* 22 (3), 298–305. doi:10.1038/nm.4045

Biffi, G., Oni, T. E., Spielman, B., Hao, Y., Elyada, E., Park, Y., et al. (2019). IL1-Induced JAK/STAT signaling is antagonized by TGFβ to shape CAF heterogeneity in pancreatic ductal adenocarcinoma. *Cancer Discov.* 9 (2), 282–301. doi:10.1158/2159-8290.CD-18-0710

Bossen, C., Murre, C. S., Chang, A. N., Mansson, R., Rodewald, H.-R., and Murre, C. (2015). The chromatin remodeler Brg1 activates enhancer repertoires to establish B cell identity and modulate cell growth. *Nat. Immunol.* 16 (7), 775–784. doi:10.1038/ni.3170

Brechka, H., Bhanvadia, R. R., VanOpstall, C., and Vander Griend, D. J. (2017). HOXB13 mutations and binding partners in prostate development and cancer: function, clinical significance, and future directions. *Genes and Dis.* 4 (2), 75–87. doi:10.1016/j.gendis.2017.01.003

Carney, D. N., Gazdar, A. F., Bepler, G., Guccion, J. G., Marangos, P. J., Moody, T. W., et al. (1985). Establishment and identification of small cell lung cancer cell lines having classic and variant features. *Cancer Res.* 45 (6), 2913–2923.

Cenik, B. K., and Shilatifard, A. (2020). COMPASS and SWI/SNF complexes in development and disease. *Nat. Rev. Genet.* 22, 38–58. doi:10.1038/s41576-020-0278-0

Chaiyachati, B. H., Jani, A., Wan, Y., Huang, H., Flavell, R., and Chi, T. (2013). BRG1-Mediated immune tolerance: facilitation of Treg activation and partial independence of chromatin remodelling. *EMBO J.* 32 (3), 395–408. doi:10.1038/emboj.2012.350

Chen, J., Xu, D., Wang, T., Yang, Z., Yang, Y., He, K., et al. (2022). HMGB1 promotes the development of castration-resistant prostate cancer by regulating androgen receptor activation. *Oncol. Rep.* 48 (5), 197. doi:10.3892/or.2022.8412

Chen, Z., Wu, D., Thomas-Ahner, J. M., Lu, C., Zhao, P., Zhang, Q., et al. (2018). Diverse AR-V7 cistromes in castration-resistant prostate cancer are governed by HoxB13. *Proc. Natl. Acad. Sci.* 115 (26), 6810–6815. doi:10.1073/pnas.1718811115

Chen, Z., Zhou, L., Liu, L., Hou, Y., Xiong, M., Yang, Yu, et al. (2020). Single-cell RNA sequencing highlights the role of inflammatory cancer-associated fibroblasts in bladder urothelial carcinoma. *Nat. Commun.* 11 (1), 5077. doi:10.1038/s41467-020-18916-5

Choi, J., Jeon, S., Choi, S., Park, K., and Seong, R. H. (2015). The SWI/SNF chromatin remodeling complex regulates germinal center formation by repressing blimp-1 expression. *Proc. Natl. Acad. Sci. U. S. A.* 112 (7), E718–E727. doi:10.1073/pnas.1418592112

Choi, J., Ko, M., Jeon, S., Jeon, Y., Park, K., Lee, C., et al. (2012). The SWI/SNF-like BAF complex is essential for early B cell development. *J. Immunol.* 188 (8), 3791–3803. doi:10.4049/jimmunol.1103390

Chou, Y.-E., Yang, P.-J., Lin, C.-Y., Chen, Y.-Yu, Chiang, W.-L., Lin, P.-X., et al. (2020). The impact of HMGB1 polymorphisms on prostate cancer progression and clinicopathological characteristics. *Int. J. Environ. Res. Public Health* 17 (19), 7247. doi:10.3390/ijerph17197247

Clapier, C. R., Iwasa, J., Cairns, B. R., and Peterson, C. L. (2017). Mechanisms of action and regulation of ATP-dependent chromatin-remodelling complexes. *Nat. Rev. Mol. Cell Biol.* 18 (7), 407–422. doi:10.1038/nrm.2017.26

Cyrta, J., Augspach, A., De Filippo, M. R., Prandi, D., Thienger, P., Benelli, M., et al. (2020). Role of specialized composition of SWI/SNF complexes in prostate cancer lineage plasticity. *Nat. Commun.* 11 (1), 5549. doi:10.1038/s41467-020-19328-1

Dai, C., Dehm, S. M., and Sharifi, N. (2023). Targeting the androgen signaling Axis in prostate cancer. *J. Clin. Oncol.* 41, 4267–4278. doi:10.1200/JCO.23.00433

Dai, C., Heemers, H., and Sharifi, N. (2017). Androgen signaling in prostate cancer. *Cold Spring Harb. Perspect. Med.* 7 (9), a030452. doi:10.1101/cshperspect.a030452

Dai, Y., Ngo, D., Jacob, J., Forman, L. W., and Faller, D. V. (2008). Prohibitin and the SWI/SNF ATPase subunit BRG1 are required for effective androgen antagonist-mediated transcriptional repression of androgen receptor-regulated genes. *Carcinogenesis* 29 (9), 1725–1733. doi:10.1093/carcin/bgn117

Damaschke, N. A., Gawdzik, J., Avilla, M., Yang, B., Svaren, J., Roopra, A., et al. (2020). CTCF loss mediates unique DNA hypermethylation landscapes in human cancers. *Clin. Epigenetics* 12 (1), 80. doi:10.1186/s13148-020-00869-7

Davies, A., Zoubeidi, A., Beltran, H., and Selth, L. A. (2023). The transcriptional and epigenetic landscape of cancer cell lineage plasticity. *Cancer Discov.* 13 (8), 1771–1788. doi:10.1158/2159-8290.CD-23-0225

Davies, A. H., Beltran, H., and Zoubeidi., A. (2018). Cellular plasticity and the neuroendocrine phenotype in prostate cancer. *Nat. Rev. Urol.* 15 (5), 271–286. doi:10.1038/nrurol.2018.22

Davis, R. B., Supakar, A., Ranganath, A. K., Moosa, M. M., and Banerjee, P. R. (2023). Heterotypic interactions in the dilute phase can drive Co-condensation of prion-like low-complexity domains of FET proteins and mammalian SWI/SNF complex. *bioRxiv*, 2023.04.12.536623. doi:10.1101/2023.04.12.536623

De, S., Wurster, A. L., Precht, P., Wood, W. H., Becker, K. G., and Pazin, M. J. (2011). Dynamic BRG1 recruitment during T helper differentiation and activation reveals distal regulatory elements. *Mol. Cell. Biol.* 31 (7), 1512–1527. doi:10.1128/MCB.00920-10

Deng, X., Shao, G., Zhang, H.-T., Li, C., Zhang, D., Cheng, L., et al. (2017). Protein arginine methyltransferase 5 functions as an epigenetic activator of the androgen receptor to promote prostate cancer cell growth. *Oncogene* 36 (9), 1223–1231. doi:10.1038/onc.2016.287

Desai, K., McManus, J. M., and Sharifi, N. (2021). Hormonal therapy for prostate cancer. *Endocr. Rev.* 42 (3), 354–373. doi:10.1210/endrev/bnab002

Dietrich, N., Trotter, K., Ward, J. M., and Archer, T. K. (2023). BRG1 HSA domain interactions with BCL7 proteins are critical for remodeling and gene expression. *Life Sci. Alliance* 6 (5), e202201770. doi:10.26508/lsa.202201770

Ding, Y., Li, N., Dong, B., Guo, W., Wei, H., Chen, Q., et al. (2019). Chromatin remodeling ATPase BRG1 and PTEN are synthetic lethal in prostate cancer. *J. Clin. Investigation* 129 (2), 759–773. doi:10.1172/JCI123557

Elyada, E., Bolisetty, M., Laise, P., Flynn, W. F., Courtois, E. T., Burkhart, R. A., et al. (2019). Cross-species single-cell analysis of pancreatic ductal adenocarcinoma reveals antigen-presenting cancer-associated fibroblasts. *Cancer Discov.* 9 (8), 1102–1123. doi:10.1158/2159-8290.CD-19-0094

Ertl, I. E., Brettner, R., Kronabitter, H., Mohr, T., Derdak, S., Jeitler, M., et al. (2022). The SMARCD family of SWI/SNF accessory proteins is involved in the transcriptional regulation of androgen receptor-driven genes and plays a role in various essential processes of prostate cancer. *Cells* 12 (1), 124. doi:10.3390/cells12010124

Fraser, M., Sabelnykova, V. Y., Yamaguchi, T. N., Heisler, L. E., Livingstone, J., Huang, V., et al. (2017). Genomic hallmarks of localized, non-indolent prostate cancer. *Nature* 541 (7637), 359–364. doi:10.1038/nature20788

Fu, X., Zhao, J., Yu, G., Zhang, X., Sun, J., Li, L., et al. (2022). OTUD6A promotes prostate tumorigenesis via deubiquitinating Brg1 and AR. *Commun. Biol.* 5 (1), 182. doi:10.1038/s42003-022-03133-1

Fu, Z., Rais, Y., Bismar, T. A., Hyndman, M. E., Le, X. C., and Drabovich, A. P. (2021). Mapping isoform abundance and interactome of the endogenous TMPRSS2-ERG fusion protein by orthogonal immunoprecipitation–mass spectrometry assays. *Mol. Cell. Proteomics* 20 (January), 100075. doi:10.1016/j.mcpro.2021.100075

Fujita, K., and Nonomura, N. (2018). Urinary biomarkers of prostate cancer. *Int. J. Urology* 25 (9), 770–779. doi:10.1111/iju.13734

Gao, H., Lukin, K., Ramírez, J., Fields, S., Lopez, D., and Hagman, J. (2009). Opposing effects of SWI/SNF and mi-2/NuRD chromatin remodeling complexes on epigenetic reprogramming by EBF and Pax5. *Proc. Natl. Acad. Sci.* 106 (27), 11258–11263. doi:10.1073/pnas.0809485106

Gatchalian, J., Liao, J., Maxwell, M. B., and Hargreaves, D. C. (2020). Control of stimulus-dependent responses in macrophages by SWI/SNF chromatin remodeling complexes. *Trends Immunol.* 41 (2), 126–140. doi:10.1016/j.it.2019.12.002

Gatchalian, J., Malik, S., Ho, J., Lee, D.-S., Kelso, T. W. R., Shokhirev, M. N., et al. (2018). A non-canonical BRD9-containing BAF chromatin remodeling complex regulates naive pluripotency in mouse embryonic stem cells. *Nat. Commun.* 9 (1), 5139. doi:10.1038/s41467-018-07528-9

Gaughan, L., Logan, I. R., Neal, D. E., and Robson, C. N. (2005). Regulation of androgen receptor and histone deacetylase 1 by mdm2-mediated ubiquitylation. *Nucleic Acids Res.* 33 (1), 13–26. doi:10.1093/nar/gki141

Gerhardt, J., Montani, M., Wild, P., Beer, M., Huber, F., Hermanns, T., et al. (2012). FOXA1 promotes tumor progression in prostate cancer and represents a novel hallmark of castration-resistant prostate cancer. *Am. J. Pathology* 180 (2), 848–861. doi:10.1016/j.ajpath.2011.10.021

Giles, K. A., Gould, C. M., Clark, S. J., Taberlay, P. C., Achinger-Kawecka, J., Page, S. G., et al. (2021). BRG1 knockdown inhibits proliferation through multiple cellular pathways in prostate cancer. *Clin. Epigenetics* 13 (1), 37. doi:10.1186/s13148-021-01023-7

Giles, K. A., Gould, C. M., Du, Q., Skvortsova, K., Song, J. Z., Maddugoda, M. P., et al. (2019). Integrated epigenomic analysis stratifies chromatin remodellers into distinct functional groups. *Epigenetics Chromatin* 12 (1), 12. doi:10.1186/s13072-019-0258-9

Glabman, R. A., Choyke, P. L., and Sato., N. (2022). Cancer-associated fibroblasts: tumorigenicity and targeting for cancer therapy. *Cancers* 14 (16), 3906. doi:10.3390/cancers14163906

Gleason, D. F., and Mellinger, G. T. (1974). Prediction of prognosis for prostatic adenocarcinoma by combined histological grading and clinical staging. *J. Urology* 111 (1), 58–64. doi:10.1016/S0022-5347(17)59889-4

Groner, A. C., Cato, L., de Tribolet-Hardy, J., Bernasocchi, T., Janouskova, H., Melchers, D., et al. (2016). TRIM24 is an oncogenic transcriptional activator in prostate cancer. *Cancer Cell* 29 (6), 846–858. doi:10.1016/j.ccell.2016.04.012

Guo, Ao, Huang, H., Zhu, Z., Chen, M. J., Shi, H., Yuan, S., et al. (2022). cBAF complex components and MYC cooperate early in CD8+ T cell fate. *Nature* 607 (7917), 135–141. doi:10.1038/s41586-022-04849-0

Guo, Yu, Perez, A. A., Hazelett, D. J., Coetzee, G. A., Rhie, S. K., and Farnham, P. J. (2018). CRISPR-mediated deletion of prostate cancer risk-associated CTCF loop anchors identifies repressive chromatin loops. *Genome Biol.* 19 (1), 160. doi:10.1186/s13059-018-1531-0

Hagiwara, M., Fushimi, A., Bhattacharya, A., Yamashita, N., Morimoto, Y., Oya, M., et al. (2022). MUC1-C integrates type II interferon and chromatin remodeling pathways in immunosuppression of prostate cancer. *OncoImmunology* 11 (1), 2029298. doi:10.1080/2162402X.2022.2029298

Hagiwara, M., Fushimi, A., Yamashita, N., Bhattacharya, A., Rajabi, H., Long, M. D., et al. (2021). MUC1-C activates the PBAF chromatin remodeling complex in integrating redox balance with progression of human prostate cancer stem cells. *Oncogene* 40 (30), 4930–4940. doi:10.1038/s41388-021-01899-y

Hagiwara, M., Yasumizu, Y., Yamashita, N., Rajabi, H., Fushimi, A., Long, M. D., et al. (2021). MUC1-C activates the BAF (mSWI/SNF) complex in prostate cancer stem cells. *Cancer Res.* 81 (4), 1111–1122. doi:10.1158/0008-5472.CAN-20-2588

Han, C., Deng, Y., Xu, W., Liu, Z., Wang, T., Wang, S., et al. (2022). The roles of tumor-associated macrophages in prostate cancer. *J. Oncol.* 2022, 1–20. doi:10.1155/2022/8580043

Han, L., Madan, V., Mayakonda, A., Dakle, P., Woon, T. W., Shyamsunder, P., et al. (2019). Chromatin remodeling mediated by ARID1A is indispensable for normal hematopoiesis in mice. *Leukemia* 33 (9), 2291–2305. doi:10.1038/s41375-019-0438-4

He, Y., Mi, J., Olson, A., Aldahl, J., Hooker, E., Yu, E.-J., et al. (2020). Androgen receptor with short polyglutamine tract preferably enhances wnt/β-catenin-mediated prostatic tumorigenesis. *Oncogene* 39 (16), 3276–3291. doi:10.1038/s41388-020-1214-7

He, Y., Xu, W., Xiao, Y.-T., Huang, H., Gu, Di, and Ren, S. (2022). Targeting signaling pathways in prostate cancer: mechanisms and clinical trials. *Signal Transduct. Target. Ther.* 7 (1), 198. doi:10.1038/s41392-022-01042-7

He, Z., Chen, K., Ye, Y., and Chen, Z. (2021). Structure of the SWI/SNF complex bound to the nucleosome and insights into the functional modularity. *Cell Discov.* 7 (1), 28. doi:10.1038/s41421-021-00262-5

Heemers, H. V., and Tindall, D. J. (2007). Androgen receptor (AR) coregulators: a diversity of functions converging on and regulating the AR transcriptional complex. *Endocr. Rev.* 28 (7), 778–808. doi:10.1210/er.2007-0019

Ho, L., Jothi, R., Ronan, J. L., Cui, K., Zhao, K., and Crabtree, G. R. (2009). An embryonic stem cell chromatin remodeling complex, esBAF, is an essential component of the core pluripotency transcriptional network. *Proc. Natl. Acad. Sci.* 106 (13), 5187–5191. doi:10.1073/pnas.0812888106

Höflmayer, D., Steinhoff, A., Hube-Magg, C., Kluth, M., Simon, R., Burandt, E., et al. (2020). Expression of CCCTC-binding factor (CTCF) is linked to poor prognosis in prostate cancer. *Mol. Oncol.* 14 (1), 129–138. doi:10.1002/1878-0261.12597

Holley, D. W., Groh, B. S., Wozniak, G., Donohoe, D. R., Sun, W., Godfrey, V., et al. (2014). The BRG1 chromatin remodeler regulates widespread changes in gene expression and cell proliferation during B cell activation. *J. Cell. Physiology* 229 (1), 44–52. doi:10.1002/jcp.24414

Hong, C.Yi, Suh, Ji Ho, Kim, K., Gong, E.-Y., Jeon, S.Ho, Ko, M., et al. (2005). Modulation of androgen receptor transactivation by the SWI3-related gene product (SRG3) in multiple ways. *Mol. Cell. Biol.* 25 (12), 4841–4852. doi:10.1128/MCB.25.12.4841-4852.2005

Horoszewicz, J. S., Leong, S. S., Chu, T. M., Wajsman, Z. L., Friedman, M., Papsidero, L., et al. (1980). The LNCaP cell line--a new model for studies on human prostatic carcinoma. *Prog. Clin. Biol. Res.* 37, 115–132.

Hu, G., Gong, A.-Yu, Wang, Y., Ma, S., Chen, X., Chen, J., et al. (2016). LincRNA-Cox2 promotes late inflammatory gene transcription in macrophages through modulating SWI/SNF-mediated chromatin remodeling. *J. Immunol.* 196 (6), 2799–2808. doi:10.4049/jimmunol.1502146

Huang, C.-Y., Beliakoff, J., Li, X., Lee, J., Li, X., Sharma, M., et al. (2005). hZimp7, a novel PIAS-like protein, enhances androgen receptor-mediated transcription and interacts with SWI/SNF-like BAF complexes. *Mol. Endocrinol.* 19 (12), 2915–2929. doi:10.1210/me.2005-0097

Huang, Z. Q., Li, J., Sachs, L. M., Cole, P. A., and Wong, J. (2003). A role for cofactor–cofactor and cofactor–histone interactions in targeting P300, SWI/SNF and mediator for transcription. *EMBO J.* 22 (9), 2146–2155. doi:10.1093/emboj/cdg219

Inoue, H., Furukawa, T., Giannakopoulos, S., Zhou, S., King, D. S., and Tanese, N. (2002). Largest subunits of the human SWI/SNF chromatin-remodeling complex promote transcriptional activation by steroid hormone receptors. *J. Biol. Chem.* 277 (44), 41674–41685. doi:10.1074/jbc.M205961200

Jancewicz, I., Szarkowska, J., Konopinski, R., Stachowiak, M., Swiatek, M., Blachnio, K., et al. (2021). PD-L1 overexpression, SWI/SNF complex deregulation, and profound transcriptomic changes characterize cancer-dependent exhaustion of persistently activated CD4+ T cells. *Cancers* 13 (16), 4148. doi:10.3390/cancers13164148

J Gunderson, A., Rajamanickam, V., Bui, C., Bernard, B., Pucilowska, J., Ballesteros-Merino, C., et al. (2021). Germinal center reactions in tertiary lymphoid structures associate with neoantigen burden, humoral immunity and long-term survivorship in pancreatic cancer. *Oncoimmunology* 10 (1), 1900635. doi:10.1080/2162402X.2021.1900635

Ji, Y., Zhang, R., Han, X., and Zhou, J. (2023). Targeting the N-terminal domain of the androgen receptor: the effective approach in therapy of CRPC. *Eur. J. Med. Chem.* 247 (February), 115077. doi:10.1016/j.ejmech.2022.115077

Jin, M.Li, Kim, Y. W., and Jeong, K. W. (2018). BAF53A regulates androgen receptor-mediated gene expression and proliferation in LNCaP cells. *Biochem. Biophysical Res. Commun.* 505 (2), 618–623. doi:10.1016/j.bbrc.2018.09.149

Johnson, B. E., Whang-Peng, J., Naylor, S. L., Zbar, B., Brauch, H., Lee, E., et al. (1989). Retention of chromosome 3 in extrapulmonary small cell cancer shown by molecular and cytogenetic studies. *JNCI J. Natl. Cancer Inst.* 81 (16), 1223–1228. doi:10.1093/jnci/81.16.1223

Kadoch, C., Hargreaves, D. C., Hodges, C., Elias, L., Ho, L., Ranish, J., et al. (2013). Proteomic and bioinformatic analysis of mammalian SWI/SNF complexes identifies extensive roles in human malignancy. *Nat. Genet.* 45 (6), 592–601. doi:10.1038/ng.2628

Kaighn, M. E., Narayan, K. S., Ohnuki, Y., Lechner, J. F., and Jones, L. W. (1979). Establishment and characterization of a human prostatic carcinoma cell line (PC-3). *Investig. Urol.* 17 (1), 16–23.

Kharel, A., Shen, J., Brown, R., Chen, Y., Nguyen, C., Alson, D., et al. (2023). Loss of PBAF promotes expansion and effector differentiation of CD8+ T cells during chronic viral infection and cancer. *Cell Rep.* 42 (6), 112649. doi:10.1016/j.celrep.2023.112649

Khoury, A., Achinger-Kawecka, J., Bert, S. A., Smith, G. C., French, H. J., Luu, P. L., et al. (2020). Constitutively bound CTCF sites maintain 3D chromatin architecture and long-range epigenetically regulated domains. *Nat. Commun.* 11 (1), 54. doi:10.1038/s41467-019-13753-7

Kikuchi, M., Okumura, F., Tsukiyama, T., Watanabe, M., Miyajima, N., Tanaka, J., et al. (2009). TRIM24 mediates ligand-dependent activation of androgen receptor and is repressed by a bromodomain-containing protein, BRD7, in prostate cancer cells. *Biochimica Biophysica Acta (BBA) - Mol. Cell Res.* 1793 (12), 1828–1836. doi:10.1016/j.bbamcr.2009.11.001

Kim, E. H., Cao, D., Mahajan, N. P., Andriole, G. L., and Mahajan, K. (2020). ACK1–AR and AR–HOXB13 signaling axes: epigenetic regulation of lethal prostate cancers. *Nar. Cancer* 2 (3), zcaa018. doi:10.1093/narcan/zcaa018

Kim, Y.-R., Oh, K.-J., Park, R.-Y., Xuan, N. T., Kang, T. W., Kwon, D. D., et al. (2010). HOXB13 promotes androgen independent growth of LNCaP prostate cancer cells by the activation of E2F signaling. *Mol. Cancer* 9 (1), 124. doi:10.1186/1476-4598-9-124

Klokk, T. I., Kurys, P., Elbi, C., Nagaich, A. K., Hendarwanto, A., Slagsvold, T., et al. (2007). Ligand-specific dynamics of the androgen receptor at its response element in living cells. *Mol. Cell. Biol.* 27 (5), 1823–1843. doi:10.1128/MCB.01297-06

Korenchuk, S., Lehr, J. E., Mclean, L., Lee, Y. G., Whitney, S., Vessella, R., et al. (2001). VCaP, a cell-based model system of human prostate cancer. *vivo (Athens, Greece)* 15 (2), 163–168.

Kuang, J., Zhai, Z., Li, P., Shi, R., Guo, W., Yao, Y., et al. (2021). SS18 regulates pluripotent-somatic transition through phase separation. *Nat. Commun.* 12 (1), 4090. doi:10.1038/s41467-021-24373-5

Kufe, D. (2023). Dependence on MUC1-C in progression of neuroendocrine prostate cancer. *Int. J. Mol. Sci.* 24 (4), 3719. doi:10.3390/ijms24043719

Kufe, D. W. (2020). MUC1-C in chronic inflammation and carcinogenesis; emergence as a target for cancer treatment. *Carcinogenesis* 41 (9), 1173–1183. doi:10.1093/carcin/bgaa082

Kwon, J. T. W., Bryant, R. J., and Parkes, E. E. (2021). The tumor microenvironment and immune responses in prostate cancer patients. *Endocrine-Related Cancer* 28 (8), T95–T107. doi:10.1530/ERC-21-0149

Laumont, C. M., Banville, A. C., Gilardi, M., Hollern, D. P., and Nelson, B. H. (2022). Tumour-infiltrating B cells: immunological mechanisms, clinical impact and therapeutic opportunities. *Nat. Rev. Cancer* 22 (7), 414–430. doi:10.1038/s41568-022-00466-1

Launonen, K., Visakorpi, T., Krijgsveld, J., Niskanen, E. A., Palvimo, J. J., Paakinaho, V., et al. (2021). Chromatin-directed proteomics-identified network of endogenous androgen receptor in prostate cancer cells. *Oncogene* 40 (27), 4567–4579. doi:10.1038/s41388-021-01887-2

Laxman, B., Tomlins, S. A., Mehra, R., Morris, D. S., Wang, L., Helgeson, B. E., et al. (2006). Noninvasive detection of TMPRSS2:ERG fusion transcripts in the urine of men with prostate cancer. *Neoplasia* 8 (10), 885–888. doi:10.1593/neo.06625

Leach, D. A., Fernandes, R. C., and Bevan, C. L. (2022). Cellular specificity of androgen receptor, coregulators, and pioneer factors in prostate cancer. *Endocr. Oncol.* 2 (1), R112–R131. doi:10.1530/EO-22-0065

Lee, S., Kim, J., Min, H., and Seong, R. H. (2020). RORγt-driven TH17 cell differentiation requires epigenetic control by the swi/snf chromatin remodeling complex. *iScience* 23 (5), 101106. doi:10.1016/j.isci.2020.101106

Lempiäinen, J. K., Niskanen, E. A., Vuoti, K. M., Lampinen, R. E., Göös, H., Varjosalo, M., et al. (2017). Agonist-specific protein interactomes of glucocorticoid and androgen receptor as revealed by proximity mapping. *Mol. Cell. Proteomics* 16 (8), 1462–1474. doi:10.1074/mcp.M117.067488

Lessard, J., Wu, J. I., Ranish, J. A., Wan, M., Winslow, M. M., Staahl, B. T., et al. (2007). An essential switch in subunit composition of a chromatin remodeling complex during neural development. *Neuron* 55 (2), 201–215. doi:10.1016/j.neuron.2007.06.019

Letimier, F. A., Passini, N., Gasparian, S., Bianchi, E., and Rogge, L. (2007). Chromatin remodeling by the SWI/SNF-like BAF complex and STAT4 activation synergistically induce IL-12Rβ2 expression during human Th1 cell differentiation. *EMBO J.* 26 (5), 1292–1302. doi:10.1038/sj.emboj.7601586

Li, J., Fu, J., Toumazou, C., Yoon, H.-G., and Wong, J. (2006). A role of the amino-terminal (N) and carboxyl-terminal (C) interaction in binding of androgen receptor to chromatin. *Mol. Endocrinol.* 20 (4), 776–785. doi:10.1210/me.2005-0298

Li, J., Wang, W., Zhang, Y., Cieślik, M., Guo, J., Tan, M., et al. (2020). Epigenetic driver mutations in ARID1A shape cancer immune phenotype and immunotherapy. *J. Clin. Investigation* 130 (5), 2712–2726. doi:10.1172/JCI134402

Li, Ni, Liu, Q., Han, Y., Pei, S., Cheng, B., Xu, J., et al. (2022). ARID1A loss induces polymorphonuclear myeloid-derived suppressor cell chemotaxis and promotes prostate cancer progression. *Nat. Commun.* 13 (1), 7281. doi:10.1038/s41467-022-34871-9

Li, W., An, N., Wang, M., Liu, X., and Mei, Z. (2023). Downregulation of AT-rich interaction domain 2 underlies natural killer cell dysfunction in oral squamous cell carcinoma. *Immunol. Cell Biol.* 101 (1), 78–90. doi:10.1111/imcb.12602

Li, X., Zhu, C., Tu, W. H., Yang, N., Qin, H., and Sun, Z. (2011). ZMIZ1 preferably enhances the transcriptional activity of androgen receptor with short polyglutamine tract. *PLOS ONE* 6 (9), e25040. doi:10.1371/journal.pone.0025040

Li, Y., SiuChan, C. L. J. B., Silverstein, K. A., Dehm, S. M., Brand, L. J., Hwang, T. H., et al. (2013). Androgen receptor splice variants mediate enzalutamide resistance in castration-resistant prostate cancer cell lines. *Cancer Res.* 73 (2), 483–489. doi:10.1158/0008-5472.CAN-12-3630

Liang, Y., Dong, B., Shen, J., Ma, C., and Ma, Z. (2019). Clinical significance of bromodomain-containing protein 7 and its association with tumor progression in prostate cancer. *Oncol. Lett.* 17 (1), 849–856. doi:10.3892/ol.2018.9665

Lin, C., Jan, Y., Kuo, L., Wang, B., Huo, C., Jiang, S. S., et al. (2018). Elevation of androgen receptor promotes prostate cancer metastasis by induction of epithelial-mesenchymal transition and reduction of KAT5. *Cancer Sci.* 109 (11), 3564–3574. doi:10.1111/cas.13776

Link, K. A., Balasubramaniam, S., Sharma, A., Comstock, C. E., Godoy-Tundidor, S., Powers, N., et al. (2008). Targeting the BAF57 SWI/SNF subunit in prostate cancer: a novel platform to control androgen receptor activity. *Cancer Res.* 68 (12), 4551–4558. doi:10.1158/0008-5472.CAN-07-6392

Link, K. A., Burd, C. J., Williams, E., Marshall, T., Rosson, G., Henry, E., et al. (2005). BAF57 governs androgen receptor action and androgen-dependent proliferation through SWI/SNF. *Mol. Cell. Biol.* 25 (6), 2200–2215. doi:10.1128/MCB.25.6.2200-2215.2005

Litwin, M. S., and Tan, H.-J. (2017). The diagnosis and treatment of prostate cancer: a review. *JAMA* 317 (24), 2532–2542. doi:10.1001/jama.2017.7248

Liu, Q., Sun, Z., and Chen, L. (2020). Memory T cells: strategies for optimizing tumor immunotherapy. *Protein and Cell* 11 (8), 549–564. doi:10.1007/s13238-020-00707-9

Liu, S., Kumari, S., Hu, Q., Senapati, D., Venkadakrishnan, V. B., Wang, D., et al. (2017). A comprehensive analysis of coregulator recruitment, androgen receptor function and gene expression in prostate cancer. *eLife* 6 (August), e28482. doi:10.7554/eLife.28482

Liu, W., Wang, Z., Liu, S., Zhang, X., Cao, X., and Jiang, M. (2023). RNF138 inhibits late inflammatory gene transcription through degradation of SMARCC1 of the SWI/SNF complex. *Cell Rep.* 42 (2), 112097. doi:10.1016/j.celrep.2023.112097

Liu, X.-De, Kong, W., Peterson, C. B., McGrail, D. J., Hoang, A., Zhang, X., et al. (2020). PBRM1 loss defines a nonimmunogenic tumor phenotype associated with checkpoint inhibitor resistance in renal carcinoma. *Nat. Commun.* 11 (1), 2135. doi:10.1038/s41467-020-15959-6

Lomelí, H. (2022). ZMIZ proteins: partners in transcriptional regulation and risk factors for human disease. *J. Mol. Med.* 100 (7), 973–983. doi:10.1007/s00109-022-02216-0

Loo, C.-S., Gatchalian, J., Liang, Y., Leblanc, M., Xie, M., Ho, J., et al. (2020). A genome-wide CRISPR screen reveals a role for the non-canonical nucleosome-remodeling BAF complex in Foxp3 expression and regulatory T cell function. *Immunity* 53 (1), 143–157.e8. doi:10.1016/j.immuni.2020.06.011

Lorenzin, F., and Demichelis, F. (2022). Past, current, and future strategies to target ERG fusion-positive prostate cancer. *Cancers* 14 (5), 1118. doi:10.3390/cancers14051118

Lupien, M., Eeckhoute, J., Meyer, C. A., Wang, Q., Zhang, Y., Li, W., et al. (2008). FoxA1 translates epigenetic signatures into enhancer-driven lineage-specific transcription. *Cell* 132 (6), 958–970. doi:10.1016/j.cell.2008.01.018

Lv, D.-J., Song, X.-Lu, Huang, B., Yu, Y. Z., Shu, F.-P., Wang, C., et al. (2019). HMGB1 promotes prostate cancer development and metastasis by interacting with brahma-related gene 1 and activating the akt signaling pathway. *Theranostics* 9 (18), 5166–5182. doi:10.7150/thno.33972

Makkonen, H., Kauhanen, M., Paakinaho, V., Jääskeläinen, T., and Palvimo, J. J. (2009). Long-range activation of FKBP51 transcription by the androgen receptor via distal intronic enhancers. *Nucleic Acids Res.* 37 (12), 4135–4148. doi:10.1093/nar/gkp352

Marshall, T. W., Link, K. A., Petre-Draviam, C. E., and Knudsen, K. E. (2003). Differential requirement of SWI/SNF for androgen receptor activity. *J. Biol. Chem.* 278 (33), 30605–30613. doi:10.1074/jbc.M304582200

Mashtalir, N., D'Avino, A. R., Michel, B. C., Luo, J., Pan, J., Otto, J. E., et al. (2018). Modular organization and assembly of SWI/SNF family chromatin remodeling complexes. *Cell* 175 (5), 1272–1288.e20. doi:10.1016/j.cell.2018.09.032

McAndrew, M. J., Gjidoda, A., Tagore, M., Miksanek, T., and Floer, M. (2016). Chromatin remodeler recruitment during macrophage differentiation facilitates transcription factor binding to enhancers in mature cells. *J. Biol. Chem.* 291 (35), 18058–18071. doi:10.1074/jbc.M116.734186

McDonald, B., Chick, B. Y., Ahmed, N. S., Burns, M., Ma, S., Casillas, E., et al. (2023). Canonical BAF complex activity shapes the enhancer landscape that licenses CD8+ T cell effector and memory fates. *Immunity* 56 (6), 1303–1319.e5. doi:10.1016/j.immuni.2023.05.005

Metzger, E., Wissmann, M., Yin, Na, Müller, J. M., Schneider, R., Peters, A. H. F. M., et al. (2005). LSD1 demethylates repressive histone marks to promote androgen-receptor-dependent transcription. *Nature* 437 (7057), 436–439. doi:10.1038/nature04020

Miao, D., Margolis, C. A., Gao, W., Voss, M. H., Li, W., Martini, D. J., et al. (2018). Genomic correlates of response to immune checkpoint therapies in clear cell renal cell carcinoma. *Sci. (New York, N.Y.)* 359 (6377), 801–806. doi:10.1126/science.aan5951

Mirzaei, S., Paskeh, M. D. A., Saghari, Y., Zarrabi, A., Hamblin, M. R., Entezari, M., et al. (2022). Transforming growth factor-beta (TGF-β) in prostate cancer: a dual function mediator? *Int. J. Biol. Macromol.* 206 (May), 435–452. doi:10.1016/j.ijbiomac.2022.02.094

Mittal, P., and Roberts, C. W. M. (2020). The SWI/SNF complex in cancer — biology, biomarkers and therapy. *Nat. Rev. Clin. Oncol.* 17 (7), 435–448. doi:10.1038/s41571-020-0357-3

Mohler, J. L., Armstrong, A. J., Bahnson, R. R., D'Amico, A. V., Davis, B. J., Eastham, J. A., et al. (2016). Prostate cancer, version 1.2016. *J. Natl. Compr. Cancer Netw.* 14 (1), 19–30. doi:10.6004/jnccn.2016.0004

Morshead, K. B., Ciccone, D. N., Taverna, S. D., Allis, C. D., and Oettinger, M. A. (2003). Antigen receptor loci poised for V(D)J rearrangement are broadly associated with BRG1 and flanked by peaks of histone H3 dimethylated at lysine 4. *Proc. Natl. Acad. Sci.* 100 (20), 11577–11582. doi:10.1073/pnas.1932643100

Mota, S. T. S., Vecchi, L., Zóia, M. A. P., Oliveira, F. M., Alves, D. A., Dornelas, B. C., et al. (2019). New insights into the role of polybromo-1 in prostate cancer. *Int. J. Mol. Sci.* 20 (12), 2852. doi:10.3390/ijms20122852

Muthuswami, R., Bailey, L. A., Rakesh, R., Imbalzano, A. N., Nickerson, J. A., and Hockensmith, J. W. (2019). BRG1 is a prognostic indicator and a potential therapeutic target for prostate cancer. *J. Cell. Physiology* 234 (9), 15194–15205. doi:10.1002/jcp.28161

Nyquist, M. D., Li, Y., Hwang, T. H., Manlove, L. S., Vessella, R. L., Silverstein, K. A. T., et al. (2013). TALEN-engineered AR gene rearrangements reveal endocrine uncoupling of androgen receptor in prostate cancer. *Proc. Natl. Acad. Sci.* 110 (43), 17492–17497. doi:10.1073/pnas.1308587110

Öhlund, D., Handly-Santana, A., Biffi, G., Elyada, E., Almeida, A. S., Ponz-Sarvise, M., et al. (2017). Distinct populations of inflammatory fibroblasts and myofibroblasts in pancreatic cancer. *J. Exp. Med.* 214 (3), 579–596. doi:10.1084/jem.20162024

Olave, I., Wang, W., Xue, Y., Kuo, A., and Crabtree, G. R. (2002). Identification of a polymorphic, neuron-specific chromatin remodeling complex. *Genes and Dev.* 16 (19), 2509–2517. doi:10.1101/gad.992102

Ordonez-Rubiano, S. C., Maschinot, C. A., Wang, S., Sood, S., Baracaldo-Lancheros, L. F., Strohmier, B. P., et al. (2023). Rational Design and Development of Selective BRD7 Bromodomain Inhibitors and Their Activity in Prostate Cancer. *J. Med. Chem.* 66 (16), 11250–11270. doi:10.1021/acs.jmedchem.3c00671

Osipovich, O. A., Subrahmanyam, R., Pierce, S., Sen, R., and Oltz, E. M. (2009). Cutting edge: SWI/SNF mediates antisense igh transcription and locus-wide accessibility in B cell precursors. *J. Immunol.* 183 (3), 1509–1513. doi:10.4049/jimmunol.0900896

Palano, M. T., Gallazzi, M., Cucchiara, M., Dehò, F., Capogrosso, P., Bruno, A., et al. (2022). The tumor innate immune microenvironment in prostate cancer: an overview of soluble factors and cellular effectors. *Explor. Target. Anti-Tumor Ther.* 3 (5), 694–718. doi:10.37349/etat.2022.00108

Paltoglou, S., Das, R., Townley, S. L., Hickey, T. E., Tarulli, G. A., Coutinho, I., et al. (2017). Novel androgen receptor coregulator GRHL2 exerts both oncogenic and antimetastatic functions in prostate cancer. *Cancer Res.* 77 (13), 3417–3430. doi:10.1158/0008-5472.CAN-16-1616

Pan, D., Kobayashi, A., Jiang, P., Ferrari de Andrade, L., Tay, R. E., Luoma, A. M., et al. (2018). A major chromatin regulator determines resistance of tumor cells to T cell-mediated killing. *Sci. (New York, N.Y.)* 359 (6377), 770–775. doi:10.1126/science.aao1710

Park, Su H., Fong, K.-W., Mong, E., Martin, M. C., Schiltz, G. E., and Yu, J. (2021). Going beyond polycomb: EZH2 functions in prostate cancer. *Oncogene* 40 (39), 5788–5798. doi:10.1038/s41388-021-01982-4

Patil, A., Strom, A. R., Paulo, J. A., Collings, C. K., Ruff, K. M., Shinn, M. K., et al. (2023). A disordered region controls cBAF activity via condensation and partner recruitment. *Cell* 186 (22), 4936–4955.e26. doi:10.1016/j.cell.2023.08.032

Pietrzak, J., Płoszaj, T., Pułaski, Ł., and Robaszkiewicz, A. (2019). EP300-HDAC1-SWI/SNF functional unit defines transcription of some DNA repair enzymes during differentiation of human macrophages. *Biochimica Biophysica Acta (BBA) - Gene Regul. Mech.* 1862 (2), 198–208. doi:10.1016/j.bbagrm.2018.10.019

Priam, P., Krasteva, V., Rousseau, P., D'Angelo, G., Gaboury, L., Sauvageau, G., et al. (2017). SMARCD2 subunit of SWI/SNF chromatin-remodeling complexes mediates granulopoiesis through a CEBPε dependent mechanism. *Nat. Genet.* 49 (5), 753–764. doi:10.1038/ng.3812

Quigley, D. A., Dang, Ha X., Zhao, S. G., Lloyd, P., Aggarwal, R., Alumkal, J. J., et al. (2018). Genomic hallmarks and structural variation in metastatic prostate cancer. *Cell* 174 (3), 758–769.e9. doi:10.1016/j.cell.2018.06.039

Ramanand, S. G., Chen, Y., Yuan, J., Daescu, K., Lambros, M. B. K., Houlahan, K. E., et al. (2020). The landscape of RNA polymerase II–associated chromatin interactions in prostate cancer. *J. Clin. investigation* 130 (8), 3987–4005. doi:10.1172/JCI134260

Ramirez-Carrozzi, V. R., Nazarian, A. A., Li, C. C., Gore, S. L., Sridharan, R., Imbalzano, A. N., et al. (2006). Selective and antagonistic functions of SWI/SNF and Mi-2β nucleosome remodeling complexes during an inflammatory response. *Genes and Dev.* 20 (3), 282–296. doi:10.1101/gad.1383206

Rautela, J., Dagley, L. F., Kratina, T., Anthony, A., Goh, W., Surgenor, E., et al. (2019). Generation of novel Id2 and E2-2, E2A and HEB antibodies reveals novel Id2 binding partners and species-specific expression of E-proteins in NK cells. *Mol. Immunol.* 115 (November), 56–63. doi:10.1016/j.molimm.2018.08.017

Rhie, S. K., Perez, A. A., Lay, F. D., Schreiner, S., Shi, J., Polin, J., et al. (2019). A high-resolution 3D epigenomic map reveals insights into the creation of the prostate cancer transcriptome. *Nat. Commun.* 10 (1), 4154. doi:10.1038/s41467-019-12079-8

Robinson, D., Van Allen, E., Wu, Y.-Mi, Schultz, N., Lonigro, R., Mosquera, J.-M., et al. (2015). Integrative clinical genomics of advanced prostate cancer. *Cell* 161 (5), 1215–1228. doi:10.1016/j.cell.2015.05.001

Sanda, M. G., Feng, Z., Sokoll, L. J., Chan, D. W., Regan, M. M., Groskopf, J., et al. (2017). Association between combined TMPRSS2:ERG and PCA3 RNA urinary testing and detection of aggressive prostate cancer. *JAMA Oncol.* 3 (8), 1085–1093. doi:10.1001/jamaoncol.2017.0177

Sandoval, G. J., Pulice, J. L., Pakula, H., Schenone, M., Takeda, D. Y., Pop, M., et al. (2018). Binding of TMPRSS2-ERG to BAF Chromatin Remodeling Complexes Mediates Prostate Oncogenesis. *Mol. Cell* 71 (4), 554–566.e7. doi:10.1016/j.molcel.2018.06.040

Saranyutanon, S., Deshmukh, S. K., Dasgupta, S., Pai, S., Singh, S., and Singh, A. P. (2020). Cellular and molecular progression of prostate cancer: models for basic and preclinical research. *Cancers* 12 (9), 2651. doi:10.3390/cancers12092651

Sarkar, S., Brautigan, D. L., Parsons, S. J., and Larner, J. M. (2014). Androgen receptor degradation by the E3 ligase CHIP modulates mitotic arrest in prostate cancer cells. *Oncogene* 33 (1), 26–33. doi:10.1038/onc.2012.561

Schick, S., Rendeiro, A. F., Runggatscher, K., Ringler, A., Boidol, B., Hinkel, M., et al. (2019). Systematic characterization of BAF mutations provides insights into intracomplex synthetic lethalities in human cancers. *Nat. Genet.* 51, 1399–1410. doi:10.1038/s41588-019-0477-9

Schim van der Loeff, I., Sprenkeler, E. G. G., Tool, A. T., Abinun, M., Grainger, A., Engelhardt, K. R., et al. (2021). Defective neutrophil development and specific granule deficiency caused by a homozygous splice-site mutation in SMARCD2. *J. Allergy Clin. Immunol.* 147 (6), 2381–2385.e2. doi:10.1016/j.jaci.2020.11.025

Schmiedel, D., Hezroni, H., Hamburg, A., and Shulman, Z. (2021). Brg1 supports B cell proliferation and germinal center formation through enhancer activation. *Front. Immunol.* 12, 705848. doi:10.3389/fimmu.2021.705848

Sérandour, A. A., Avner, S., Percevault, F., Demay, F., Bizot, M., Lucchetti-Miganeh, C., et al. (2011). Epigenetic switch involved in activation of pioneer factor FOXA1-dependent enhancers. *Genome Res.* 21 (4), 555–565. doi:10.1101/gr.111534.110

Shafi, A. A., Yen, A. E., and Weigel, N. L. (2013). Androgen receptors in hormone-dependent and castration-resistant prostate cancer. *Pharmacol. Ther.* 140 (3), 223–238. doi:10.1016/j.pharmthera.2013.07.003

Shain, A. H., and Pollack, J. R. (2013). The spectrum of SWI/SNF mutations, ubiquitous in human cancers. *PLOS ONE* 8 (1), e55119. doi:10.1371/journal.pone.0055119

Shen, H., Powers, N., Saini, N., Comstock, C. E., Sharma, A., Weaver, K., et al. (2008). The SWI/SNF ATPase brm is a gatekeeper of proliferative control in prostate cancer. *Cancer Res.* 68 (24), 10154–10162. doi:10.1158/0008-5472.CAN-08-1794

Shishodia, S., Nuñez, R., Strohmier, B. P., Bursch, K. L., Goetz, C. J., Olp, M. D., et al. (2022). Selective and cell-active PBRM1 bromodomain inhibitors discovered through NMR fragment screening. *J. Med. Chem.* 65 (20), 13714–13735. doi:10.1021/acs.jmedchem.2c00864

Siegel, R. L., Miller, K. D., Wagle, N. S., and Jemal, A. (2023). Cancer statistics, 2023. *CA A Cancer J. Clin.* 73 (1), 17–48. doi:10.3322/caac.21763

Siliņa, K., Soltermann, A., Attar, F. M., Casanova, R., Uckeley, Z. M., Thut, H., et al. (2018). Germinal centers determine the prognostic relevance of tertiary lymphoid structures and are impaired by corticosteroids in lung squamous cell carcinoma. *Cancer Res.* 78 (5), 1308–1320. doi:10.1158/0008-5472.CAN-17-1987

Small, E. J., Aggarwal, R. R., Huang, J., Sokolov, A., Zhang, Li, Alumkal, J. J., et al. (2016). Clinical and genomic characterization of metastatic small cell/neuroendocrine prostate cancer (SCNC) and intermediate atypical prostate cancer (IAC): results from the SU2C/PCF/AACRWest coast prostate cancer dream team (WCDT). *J. Clin. Oncol.* 34 (15_Suppl. l), 5019. doi:10.1200/JCO.2016.34.15_suppl.5019

Son, E. Y., and Crabtree., G. R. (2014). The role of BAF (mSWI/SNF) complexes in mammalian neural development. *Am. J. Med. Genet. Part C Seminars Med. Genet.* 166 (3), 333–349. doi:10.1002/ajmg.c.31416

Sramkoski, R. M., Pretlow, T. G., Giaconia, J. M., Pretlow, T. P., Schwartz, S., Sy, M. S., et al. (1999). A new human prostate carcinoma cell line, 22Rv1. *Vitro Cell. Dev. Biol. - Animal* 35 (7), 403–409. doi:10.1007/s11626-999-0115-4

Stelloo, S., Nevedomskaya, E., Kim, Y., Hoekman, L., Bleijerveld, O. B., Mirza, T., et al. (2018). Endogenous androgen receptor proteomic profiling reveals genomic subcomplex involved in prostate tumorigenesis. *Oncogene* 37 (3), 313–322. doi:10.1038/onc.2017.330

Stelloo, S., Nevedomskaya, E., Kim, Y., Schuurman, K., Valle-Encinas, E., Lobo, J., et al. (2018). Integrative epigenetic taxonomy of primary prostate cancer. *Nat. Commun.* 9 (1), 4900. doi:10.1038/s41467-018-07270-2

Stelloo, S., Nevedomskaya, E., van der Poel, H. G., de Jong, J., van Leenders, G. J., Jenster, G., et al. (2015). Androgen receptor profiling predicts prostate cancer outcome. *EMBO Mol. Med.* 7 (11), 1450–1464. doi:10.15252/emmm.201505424

Stone, K. R., Mickey, D. D., Wunderli, H., Mickey, G. H., and Paulson, D. F. (1978). Isolation of a human prostate carcinoma cell line (DU 145). *Int. J. Cancer* 21 (3), 274–281. doi:10.1002/ijc.2910210305

Stopsack, K. H., Nandakumar, S., Wibmer, A. G., Haywood, S., Weg, E. S., Barnett, E. S., et al. (2020). Oncogenic genomic alterations, clinical phenotypes, and outcomes in metastatic castration-sensitive prostate cancer. *Clin. Cancer Res.* 26 (13), 3230–3238. doi:10.1158/1078-0432.CCR-20-0168

Stuchbery, R., McCoy, P. J., Hovens, C. M., and Corcoran, N. M. (2017). Androgen synthesis in prostate cancer: do all roads lead to rome? *Nat. Rev. Urol.* 14 (1), 49–58. doi:10.1038/nrurol.2016.221

Su, S., Liu, L., Li, C., Zhang, J., and Li, S. (2019). Prognostic role of pretreatment derived neutrophil to lymphocyte ratio in urological cancers: a systematic review and meta-analysis. *Int. J. Surg. Lond. Engl.* 72 (December), 146–153. doi:10.1016/j.ijsu.2019.10.043

Sugiura, M., Sato, H., Kanesaka, M., Imamura, Y., Sakamoto, S., Ichikawa, T., et al. (2021). Epigenetic modifications in prostate cancer. *Int. J. Urology* 28 (2), 140–149. doi:10.1111/iju.14406

Sun, A., Tawfik, O., Gayed, B., Thrasher, J. B., Hoestje, S., Li, C., et al. (2007). Aberrant expression of SWI/SNF catalytic subunits BRG1/BRM is associated with tumor development and increased invasiveness in prostate cancers. *Prostate* 67 (2), 203–213. doi:10.1002/pros.20521

Sun, D., Lee, Y. S., Malhotra, A., Kim, H. K., Matecic, M., Evans, C., et al. (2011). miR-99 family of MicroRNAs suppresses the expression of prostate-specific antigen and prostate cancer cell proliferation. *Cancer Res.* 71 (4), 1313–1324. doi:10.1158/0008-5472.CAN-10-1031

Sung, H., Ferlay, J., Siegel, R. L., Laversanne, M., Soerjomataram, I., Jemal, A., et al. (2021). Global cancer statistics 2020: GLOBOCAN estimates of incidence and mortality worldwide for 36 cancers in 185 countries. *CA A Cancer J. Clin.* 71 (3), 209–249. doi:10.3322/caac.21660

Takayama, K.-ichi, and Inoue, S. (2013). Transcriptional network of androgen receptor in prostate cancer progression. *Int. J. Urology* 20 (8), 756–768. doi:10.1111/iju.12146

Tartey, S., Matsushita, K., Imamura, T., Wakabayashi, A., Ori, D., Mino, T., et al. (2015). Essential function for the nuclear protein Akirin2 in B cell activation and humoral immune responses. *J. Immunol.* 195 (2), 519–527. doi:10.4049/jimmunol.1500373

Tartey, S., Matsushita, K., Vandenbon, A., Ori, D., Imamura, T., Mino, T., et al. (2014). Akirin2 is critical for inducing inflammatory genes by bridging iκb-ζ and the SWI/SNF complex. *EMBO J.* 33 (20), 2332–2348. doi:10.15252/embj.201488447

Teo, M. Y., Rathkopf, D. E., and Kantoff, P. (2019). Treatment of advanced prostate cancer. *Annu. Rev. Med.* 70 (January), 479–499. doi:10.1146/annurev-med-051517-011947

Thalmann, G. N., Anezinis, P. E., Chang, S. M., Zhau, H. E., Kim, E. E., Hopwood, V. L., et al. (1994). Androgen-independent cancer progression and bone metastasis in the LNCaP model of human prostate cancer. *Cancer Res.* 54 (10), 2577–2581.

Tian, Y., Dong, D., Wang, Z., Wu, L., Park, J. Y., Wei, G.-H., et al., and PRACTICAL/ELLIPSE consortium (2023). Combined CRISPRi and proteomics screening reveal a cohesin-CTCF-bound allele contributing to increased expression of RUVBL1 and prostate cancer progression. *bioRxiv*, 2023.01.18.524405. doi:10.1101/2023.01.18.524405

Tomlins, S. A., Rhodes, D. R., Perner, S., Dhanasekaran, S. M., Mehra, R., Sun, X.-W., et al. (2005). Recurrent fusion of TMPRSS2 and ETS transcription factor genes in prostate cancer. *Science* 310 (5748), 644–648. doi:10.1126/science.1117679

Urbanucci, A., and Mills, I. G. (2018). Bromodomain-containing proteins in prostate cancer. *Mol. Cell. Endocrinol.* 462 (February), 31–40. doi:10.1016/j.mce.2017.06.007

Valletta, M., Russo, R., Baglivo, I., Russo, V., Ragucci, S., Sandomenico, A., et al. (2020). Exploring the interaction between the SWI/SNF chromatin remodeling complex and the zinc finger factor CTCF. *Int. J. Mol. Sci.* 21 (23), 8950. doi:10.3390/ijms21238950

van Bokhoven, A., Varella-Garcia, M., Korch, C., Johannes, W. U., Smith, E. E., Miller, H. L., et al. (2003). Molecular characterization of human prostate carcinoma cell lines. *Prostate* 57 (3), 205–225. doi:10.1002/pros.10290

van de Wijngaart, D. J., Dubbink, H. J., Molier, M., de Vos, C., Trapman, J., and Jenster, G. (2009). Functional screening of FxxLF-like peptide motifs identifies SMARCD1/BAF60a as an androgen receptor cofactor that modulates TMPRSS2 expression. *Mol. Endocrinol.* 23 (11), 1776–1786. doi:10.1210/me.2008-0280

van Royen, M. E., van Cappellen, W. A., de Vos, C., Houtsmuller, A. B., and Trapman, J. (2012). Stepwise androgen receptor dimerization. *J. Cell Sci.* 125 (8), 1970–1979. doi:10.1242/jcs.096792

Viryasova, G. M., Tatarskiy, V. V., Sheynov, A. A., Tatarskiy, E. V., Sud'ina, G. F., Georgieva, S. G., et al. (2019). PBAF lacking PHD domains maintains transcription in

human neutrophils. *Biochimica Biophysica Acta (BBA) - Mol. Cell Res.* 1866 (12), 118525. doi:10.1016/j.bbamcr.2019.118525

Vummidi Giridhar, P., Williams, K., VonHandorf, A. P., Deford, P. L., and Kasper, S. (2019). Constant degradation of the androgen receptor by MDM2 conserves prostate cancer stem cell integrity. *Cancer Res.* 79 (6), 1124–1137. doi:10.1158/0008-5472.CAN-18-1753

Wang, C., Zhang, Y., and Gao, W.-Q. (2022). The evolving role of immune cells in prostate cancer. *Cancer Lett.* 525 (January), 9–21. doi:10.1016/j.canlet.2021.10.027

Wang, G., Zhao, Di, Spring, D. J., and DePinho, R. A. (2018). Genetics and biology of prostate cancer. *Genes and Dev.* 32 (17–18), 1105–1140. doi:10.1101/gad.315739.118

Wang, H., Ni, Li, Liu, Q., Guo, J., Pan, Q., Cheng, B., et al. (2023). Antiandrogen treatment induces stromal cell reprogramming to promote castration resistance in prostate cancer. *Cancer Cell* S1535-6108, 00183–00186. doi:10.1016/j.ccell.2023.05.016

Wang, H. J., and Cheng, W. C. (2021). Current advances of targeting epigenetic modifications in neuroendocrine prostate cancer. *Tzu-Chi Med. J.* 33 (3), 224–232. doi:10.4103/tcmj.tcmj_220_20

Wang, L., Oh, T. G., Magida, J., Estepa, G., Obayomi, S. M. B., Chong, L.-Wa, et al. (2021). Bromodomain containing 9 (BRD9) regulates macrophage inflammatory responses by potentiating glucocorticoid receptor activity. *Proc. Natl. Acad. Sci. U. S. A.* 118 (35), e2109517118. doi:10.1073/pnas.2109517118

Wang, Q., Carroll, J. S., and Brown, M. (2005). Spatial and temporal recruitment of androgen receptor and its coactivators involves chromosomal looping and polymerase tracking. *Mol. Cell* 19 (5), 631–642. doi:10.1016/j.molcel.2005.07.018

Wang, Q., Udayakumar, T. S., Vasaitis, T. S., Brodie, A. M., and Fondell, J. D. (2004). Mechanistic relationship between androgen receptor polyglutamine tract truncation and androgen-dependent transcriptional hyperactivity in prostate cancer cells. *J. Biol. Chem.* 279 (17), 17319–17328. doi:10.1074/jbc.M400970200

Wang, Xu, Qiu, L., Li, Z., Wang, X.-Y., and Yi, H. (2018). Understanding the multifaceted role of neutrophils in cancer and autoimmune diseases. *Front. Immunol.* 9 (November), 2456. doi:10.3389/fimmu.2018.02456

Wang, X., Wang, Su, Troisi, E. C., Howard, T. P., Haswell, J. R., Wolf, B. K., et al. (2019). BRD9 defines a SWI/SNF sub-complex and constitutes a specific vulnerability in malignant rhabdoid tumors. *Nat. Commun.* 10 (1), 1881. doi:10.1038/s41467-019-09891-7

Wang, Z., Wang, Y., Zhang, J., Hu, Q., Zhi, F., Zhang, S., et al. (2017). Significance of the TMPRSS2:ERG gene fusion in prostate cancer. *Mol. Med. Rep.* 16 (4), 5450–5458. doi:10.3892/mmr.2017.7281

Weichert, W., Röske, A., Gekeler, V., Beckers, T., Stephan, C., Jung, K., et al. (2008). Histone deacetylases 1, 2 and 3 are highly expressed in prostate cancer and HDAC2 expression is associated with shorter PSA relapse time after radical prostatectomy. *Br. J. Cancer* 98 (3), 604–610. doi:10.1038/sj.bjc.6604199

Westerberg, R., Tvrdik, P., Undén, A. B., Månsson, J.-E., Norlén, L., Jakobsson, A., et al. (2004). Role for ELOVL3 and fatty acid chain length in development of hair and skin function. *J. Biol. Chem.* 279 (7), 5621–5629. doi:10.1074/jbc.M310529200

Witzel, M., Petersheim, D., Fan, Y., Bahrami, E., Racek, T., Rohlfs, M., et al. (2017). Chromatin-remodeling factor SMARCD2 regulates transcriptional networks controlling differentiation of neutrophil granulocytes. *Nat. Genet.* 49 (5), 742–752. doi:10.1038/ng.3833

Wu, J. I., Lessard, J., Olave, I. A., Qiu, Z., Ghosh, A., Graef, I. A., et al. (2007). Regulation of dendritic development by neuron-specific chromatin remodeling complexes. *Neuron* 56 (1), 94–108. doi:10.1016/j.neuron.2007.08.021

Wu, S. Z., Roden, D. L., Wang, C., Holliday, H., Harvey, K., Cazet, A. S., et al. (2020). Stromal cell diversity associated with immune evasion in human triple-negative breast cancer. *EMBO J.* 39 (19), e104063. doi:10.15252/embj.2019104063

Wurster, A. L., and Pazin, M. J. (2008). BRG1-Mediated chromatin remodeling regulates differentiation and gene expression of T helper cells. *Mol. Cell. Biol.* 28 (24), 7274–7285. doi:10.1128/MCB.00835-08

Wurster, A. L., and Pazin, M. J. (2012). ATP-dependent chromatin remodeling in T cells[1]This article is part of Special Issue entitled Asilomar Chromatin and has undergone the Journal's usual peer review process. *Biochem. Cell Biol.* 90 (1), 1–13. doi:10.1139/o11-042

Xiao, L., Parolia, A., Qiao, Y., Bawa, P., Eyunni, S., Mannan, R., et al. (2022). Targeting SWI/SNF ATPases in enhancer-addicted prostate cancer. *Nature* 601 (7893), 434–439. doi:10.1038/s41586-021-04246-z

Xue, J., Suarez, J. S., Minaai, M., Li, S., Gaudino, G., Pass, H. I., et al. (2021). HMGB1 as a therapeutic target in disease. *J. Cell. Physiology* 236 (5), 3406–3419. doi:10.1002/jcp.30125

Yasumizu, Y., Rajabi, H., Jin, C., Hata, T., Pitroda, S., Long, M. D., et al. (2020). MUC1-C regulates lineage plasticity driving progression to neuroendocrine prostate cancer. *Nat. Commun.* 11 (1), 338. doi:10.1038/s41467-019-14219-6

Zhang, B., Zhang, M., Shen, C., Liu, G., Zhang, F., Hou, J., et al. (2021). LncRNA PCBP1-AS1-mediated AR/AR-V7 deubiquitination enhances prostate cancer enzalutamide resistance. *Cell Death Dis.* 12 (10), 856. doi:10.1038/s41419-021-04144-2

Zhang, F., and Boothby, M. (2006). T helper type 1-specific Brg1 recruitment and remodeling of nucleosomes positioned at the IFN-gamma promoter are Stat4 dependent. *J. Exp. Med.* 203 (6), 1493–1505. doi:10.1084/jem.20060066

Zhao, C.-B., Bao, J.-M., Lu, Y.-J., Zhao, T., Zhou, X.-H., Zheng, D.-Y., et al. (2014). Co-expression of RAGE and HMGB1 is associated with cancer progression and poor patient outcome of prostate cancer. *Am. J. Cancer Res.* 4 (4), 369–377.

Zhao, S. G., Chen, W. S., Li, H., Foye, A., Zhang, M., Sjöström, M., et al. (2020). The DNA methylation landscape of advanced prostate cancer. *Nat. Genet.* 52 (8), 778–789. doi:10.1038/s41588-020-0648-8

Zhou, Q., Zhang, Y., Wang, Bo, Zhou, W., Bi, Y., Huai, W., et al. (2020). KDM2B promotes IL-6 production and inflammatory responses through brg1-mediated chromatin remodeling. *Cell. Mol. Immunol.* 17 (8), 834–842. doi:10.1038/s41423-019-0251-z

Zou, H., Yang, N., Zhang, X., and Chen, H.-Wu (2022). RORγ is a context-specific master regulator of cholesterol biosynthesis and an emerging therapeutic target in cancer and autoimmune diseases. *Biochem. Pharmacol.* 196 (February), 114725. doi:10.1016/j.bcp.2021.114725

frontiers | Frontiers in Epigenetics and Epigenomics

TYPE Mini Review
PUBLISHED 26 April 2024
DOI 10.3389/freae.2024.1409355



OPEN ACCESS

EDITED BY
Andre J. van Wijnen,
University of Vermont, United States

REVIEWED BY
Hu Wang,
Hangzhou Normal University, China

*CORRESPONDENCE
Luisa Cimmino,
luisa.cimmino@med.miami.edu

RECEIVED 29 March 2024
ACCEPTED 15 April 2024
PUBLISHED 26 April 2024

CITATION
Leesang T, Lyon P, Pinzone J and Cimmino L (2024), Micronutrient regulation of the DNA methylome.
*Front. Epigenet. Epigenom.* 2:1409355.
doi: 10.3389/freae.2024.1409355



# Micronutrient regulation of the DNA methylome

Tiffany Leesang[1,2], Peter Lyon[1,2], Joey Pinzone[1,2] and Luisa Cimmino[1,2]*

[1]Department of Biochemistry and Molecular Biology, Miller School of Medicine, University of Miami, Miami, FL, United States, [2]Sylvester Comprehensive Cancer Center, Miller School of Medicine, University of Miami, Miami, FL, United States

The formation, inheritance, and removal of DNA methylation in the genome of mammalian cells is directly regulated by two families of enzymes–DNA methyltransferases (DNMTs) and Ten-Eleven Translocation proteins (TETs). DNMTs generate and maintain the inheritance of 5-methylcytosine (5mC), which is the substrate targeted by the TET enzymes for conversion to 5-hydroxymethylcytosine (5hmC) and its downstream oxidized derivatives. The activity of DNMT and TET is dependent on the availability of micronutrients and metabolite co-factors, including essential vitamins, amino acids, and trace metals, highlighting how DNA methylation levels can be directly enhanced, suppressed, or remodeled via metabolic and nutritional perturbations. Dynamic changes in DNA methylation are required during embryonic development, lineage specification, and maintenance of somatic cell function that can be fine-tuned based on the influence of essential micronutrients. As we age, DNA methylation and hydroxymethylation levels drift in patterning, leading to epigenetic dysregulation and genomic instability that underlies the formation and progression of multiple diseases including cancer. Understanding how DNA methylation can be regulated by micronutrients will have important implications for the maintenance of normal tissue function upon aging, and in the prevention and treatment of diseases for improved health and lifespan.

KEYWORDS

**DNA methylation, Ten-eleven translocation (TET) enzymes, 5-hydroxymethylation, vitamin A, vitamin B, vitamin C**

## Introduction

DNA methylation in the form of 5-methylcytosine (5mC) can be found in ~80% of CpGs in the genome and is primarily enriched in heterochromatin, working in positive feedback with silencing histone marks to maintain lineage identity (Lister et al., 2009). 5mC is conventionally known as a repressive epigenetic mark, controlling gene expression and chromatin organization to influence cellular development and differentiation (Guo et al., 2014). During development and in response to environmental stimuli, many 5mC marks are dynamic, including at shores of CpG islands, promoters, enhancers, and across gene bodies of differentially expressed genes (Deaton and Bird, 2011; Nguyen et al., 2022). DNA methyltransferases (DNMTs) catalyze the transfer of a methyl group to the 5' position of cytosine residues to regulate *de novo* 5mC formation (DNMT3A and DNMT3B) independently of the cell cycle, or during DNA replication to ensure faithful DNA methylation inheritance (DNMT1) (Okano et al., 1999; Pradhan et al., 1999).

The Ten-eleven translocation (TET1-3) enzymes are considered to have an opposing role to the DNMTs due to their ability to oxidize 5mC to generate 5-hydroxymethylcytosine

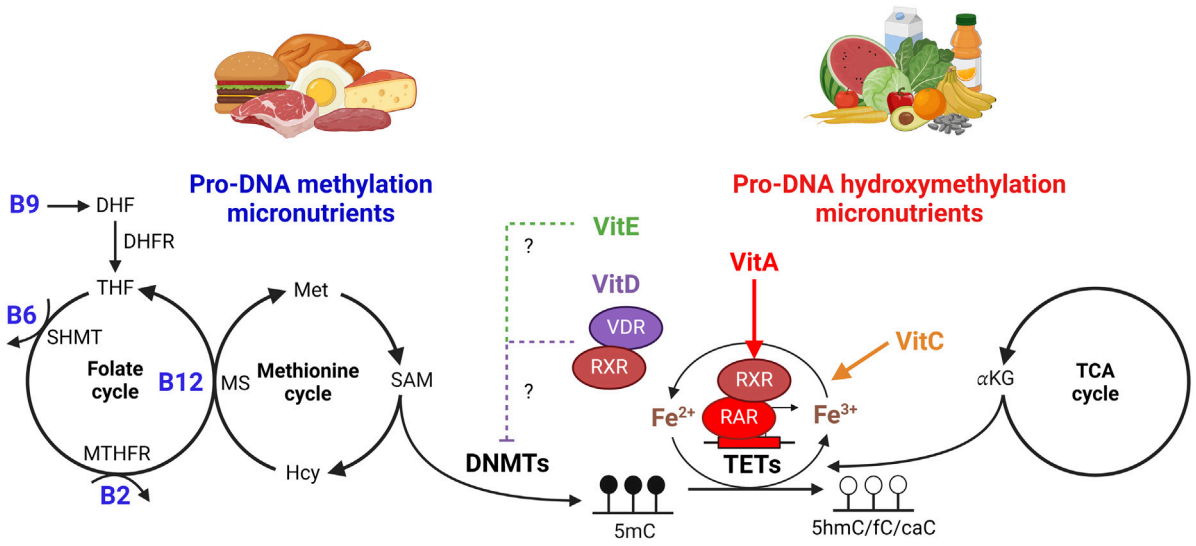


FIGURE 1
Role of micronutrients on DNA (hydroxy) methylation. One-carbon metabolism is comprised of the folate and methionine cycles that coordinate both nucleotide synthesis and the generation of S-adenosylmethionine (SAM), the sole methyl donor used by DNA methyltransferases to generate 5-methylcytosine (5mC) in the genome. Folate (vitamin B9) is converted to dihydrofolate (DHF) then to tetrahydrofolate (THF) by dihydrofolate reductase (DHFR). Serine hydroxymethyltransferase (SHMT) utilizes vitamin B6 as a cofactor to generate the metabolite 5,10-methyleneTHF, which can then be reduced by methylenetetrahydrofolate reductase (MTHFR) into 5-methyltetrahydrofolate (5-mTHF) using B2 as a cofactor. In conjunction with the methionine cycle, vitamin B12 is a cofactor for methionine synthase (MS), which uses 5-mTHF to transfer a methyl group to homocysteine (Hcy) in the recycling of methionine. Methionine, when converted to S-adenosylmethionine (SAM), provides DNA methyltransferases (DNMTs) with the methyl group needed to generate 5mC. Ten-Eleven Translocation (TET) enzymes hydroxylate 5mC to form 5hmC, 5fC, and/or 5caC using $Fe^{2+}$ and α-ketoglutarate (αKG) as cofactors. Vitamin C (VitC) enhances TET function by recycling ferric ($Fe^{3+}$) to ferrous ($Fe^{2+}$) iron, while αKG is supplied by the tricarboxylic acid (TCA) cycle. Vitamin A (VitA) can directly upregulate TET gene expression via retinoid receptor (RAR/RXR) signaling. Vitamin D (VitD) acts as a ligand for the vitamin D receptor (VDR), which can also form a heterodimer with RXR, and both VitD or vitamin E (VitE) treatment have been shown to inhibit DNMT expression to influence DNA methylation maintenance. Figure created with BioRender.com.

(5hmC), 5-formylcytosine (5fC), and 5-carboxylcytosine (5caC) (Tahiliani et al., 2009; Ito et al., 2010; He et al., 2011). TET proteins belong to a superfamily of dioxygenases that utilize $Fe^{2+}$ and α-ketoglutarate (αKG) as essential cofactors (Lorsbach et al., 2003) [reviewed in (Lu et al., 2015a; Rasmussen and Helin, 2016; Wu and Zhang, 2017; Lio et al., 2020)]. The oxidized methylcytosines generated by TETs can be stable modifications in the genome or transient modifications that promote active or passive DNA demethylation (Tahiliani et al., 2009; Zhang et al., 2010; Bachman et al., 2014). DNMT1 preferentially recognizes hemi-methylated DNA to establish inheritance of methylation at palindromic CpG dinucleotides upon DNA replication (Bashtrykov et al., 2012) however, the inability of DNMT1 to recognize 5hmC causes a passive, cell-cycle dependent loss of DNA methylation (Otani et al., 2013). Unlike 5hmC that does not interfere with RNA or DNA polymerase extension, the iterative oxidation products 5fC and 5caC can slow RNA elongation (Wang L. et al., 2015), cause DNA polymerase pausing (Shibutani et al., 2014), and mimic a T:G mismatch leading to active removal and replacement with an unmethylated cytosine via base excision repair (BER) independently of DNA replication (Cortellino et al., 2011; He et al., 2011).

Essential micronutrients can directly or indirectly influence DNMT and/or TET activity that in turn impact DNA methylation levels (Figure 1). B vitamins can be regarded as pro-methylating micronutrients given their role in one-carbon metabolism that generates both nucleotides for DNA synthesis and the transfer of methyl groups required for the maintenance of DNA methylation (Tong et al., 2009; Lyon et al., 2020). The methyl group used in the formation of 5mC by DNMTs is derived from the coordinated effort of B2, B6, B9, B12, and the essential amino acid methionine. Together, these micronutrients regulate the folate and methionine cycles of one-carbon metabolism to generate S-adenosylmethionine (SAM), the sole methyl donor used by all methyltransferases to methylate proteins, RNA and DNA. TET catalytic activity is also dependent on metabolites and micronutrients whose abundance can be directly regulated by dietary supplementation. More recently it has been shown that vitamin C can act as a direct cofactor of TET enzymes to enhance 5hmC formation (Cimmino et al., 2017; Cimmino et al., 2018) by reducing ferric iron ($Fe^{3+}$) to ferrous iron ($Fe^{2+}$). Alterations in iron homeostasis may influence TET activity, as shown in the brain, liver, gut, lymphocytes, and cord blood cells (Jiang et al., 2021; Barks et al., 2022; Gao et al., 2022; Taeubert et al., 2022) and additional micronutrients, such as vitamin A, D, and E, have also been implicated as direct or indirect regulators of DNA methylation (Doig et al., 2013; Hore et al., 2016; Remely et al., 2017). Given that aberrant DNA methylation profiles are associated with aging (Sedivy et al., 2008; Salameh et al., 2020; He et al., 2021; Wilkinson et al., 2021; Lu et al., 2023) and that loss of function mutations in DNMT and TET enzymes are a hallmark of cancer (Delhommeau et al., 2009; Figueroa et al., 2010a; Li et al., 2011;

Buscarlet et al., 2017; Ostrander et al., 2020), understanding the connection between DNA methylation maintenance and micronutrient availability may uncover liabilities associated with diseases upon aging (Patel et al., 2023) and reveal novel metabolic interventions that can be implemented to retain faithful DNA methylation patterns and function for disease prevention and longevity.

## Micronutrient regulation of 5-methylcytosine formation and maintenance (pro-methylating micronutrients)

The role of several B vitamins in the direct regulation of one-carbon metabolism places these essential micronutrients as DNA methylation guardians of the epigenome. One-carbon metabolism is comprised of the folate and methionine cycles that coordinate both pyrimidine synthesis and the generation of S-adenosylmethionine (SAM), the sole methyl donor used by DNA methyltransferases to generate 5mC in the genome. The coordinated regulation of nucleotide synthesis and methylation by one-carbon metabolism ensures that DNA replication is coupled with DNA methylation inheritance (Ducker and Rabinowitz, 2017). A connection between the folate cycle and DNA methylation maintenance has been known for decades. Nutritional vitamin B9 or B12 deficiencies during gestation or polymorphisms in folate cycle enzymes of pregnant women are associated with neural tube defects (NTDs) (Smithells et al., 1976; Prevention of neural tube defects, 1991; Crider et al., 2011). The process of neurulation in embryos requires increased global methylation to promote neural tube fusion (Greene et al., 2011), and NTDs potentially form due to the lack of silencing of *Notch1* and *Sox2* (Alata Jimenez and Strobl-Mazzulla, 2022). Loss of serine hydroxymethyltransferase 1 (SHMT1) activity, which utilizes B6 as a cofactor, can impair neural tube closure (Beaudin et al., 2011; Beaudin et al., 2012). Moreover, polymorphisms that decrease the activity of methylenetetrahydrofolate reductase (MTHFR) (Prevention of neural tube defects, 1991), which depends on B2 as a cofactor, or methionine synthase (MS) that utilizes B12 as a cofactor (Tong et al., 2009; Guéant et al., 2020), and methionine synthase reductase that regenerates methylated B12 levels from its oxidized form have all been associated with NTDs (Botto and Yang, 2000; Imbard et al., 2013). One-carbon metabolism inhibitors such as the anti-folate methotrexate (MTX) that blocks the activity of dihydrofolate reductase (DHFR) promotes DNA hypomethylation in embryonic tissues and leads to NTDs (Greene et al., 2011; Wang X. et al., 2015). DNA methylation generated by DNMTs is required for closure of the neural tube, therefore as per one-carbon metabolic enzyme gene polymorphisms and B vitamin deficiencies, disruption of DNA methylation caused by *Dnmt3b* knockout, and DNMT or methylation cycle inhibitors also result in NTDs (Okano et al., 1999; Afman et al., 2005; Dunlevy et al., 2006).

The role of B vitamins in DNA methylation maintenance in other diseases and cell types have also been described. Clinical studies have shown that lower B9 intake leads to DNA hypomethylation in colonic tissue (Pufulete et al., 2003) and an increased risk of colorectal cancer (CRC) (Kim, 2007). A B9-deficient diet in post-menopausal women also causes DNA hypomethylation in lymphocytes (Jacob et al., 1998). Low dose therapy with MTX used in the treatment of rheumatoid arthritis demethylates the *FOXP3* locus in developing regulatory T cells, resulting in their enhanced differentiation and suppression of inflammation (Cribbs et al., 2015; Rossetti et al., 2015). Furthermore, higher global DNA methylation in leukocytes is associated with decreased responsiveness to MTX in rheumatoid arthritis patients (Gosselt et al., 2019), indicating the importance of MTX's hypomethylating activity.

Elevated levels of B9 or B12 supplementation are positively correlated with increased DNA methylation through increased methyl-donor availability. Combined B9 and B12 supplementation leads to increased DNA methylation in leukocytes (Kok DE. et al., 2015; Kok DEG. et al., 2015), and B12 supplementation alone increases DNA methylation in disease-free children (Yadav et al., 2018) and mouse models of depression and meningitis (de Queiroz et al., 2020; Trautmann et al., 2020). Supplementation with B9 increases sperm DNA methylation levels in a mouse model of the *MTHFR* polymorphism, and supplementation with B2 has also been shown to increase DNA methylation in peripheral leukocytes of healthy individuals or cardiovascular disease patients with an *MTHFR* polymorphism (Amenyah et al., 2020; Amenyah et al., 2021). Amongst the healthy population, there have been no reports of toxicity for excess B vitamin consumption; however, given that one-carbon metabolism promotes DNA methylation, caution may be warranted for high B vitamin supplementation in disease states driven by DNA hypermethylation phenotypes (Ehrlich, 2019).

## Hydroxymethylation formation and DNA methylation removal via micronutrient mediated activation of the TET enzymes (pro-hydroxymethylation micronutrients)

Epigenetic plasticity, including the ability to remodel DNA methylation patterns in the genome, is integral to maintaining stem cell potency, lineage specification, and gene regulation in response to changes in the environment. The TET enzymes (TET1-3) are the only known mammalian DNA demethylases that can trigger the passive or active removal of 5mC in the genome (Tahiliani et al., 2009; Ito et al., 2010; He et al., 2011). TET1 is most highly expressed in embryonic stem cells, primordial germ cells, and neural tissues, whereas TET2 and TET3 are most highly expressed in stem, progenitor, and other differentiated adult cell populations (Lu et al., 2015a; Rasmussen and Helin, 2016; Wu and Zhang, 2017; Lio et al., 2020). While the TET enzymes all exhibit a conserved core C-terminal catalytic domain, they diverge in their N-terminal structure, in which TET2 lacks the CXXC DNA-binding motif found in TET1 and TET3 and therefore relies on protein-binding partners for its recruitment to chromatin (Ko et al., 2013; Rampal et al., 2014). TET activity is primarily associated with gene activation, given the enrichment of 5hmC within enhancers and gene bodies of actively expressed genes (Ficz et al., 2011; Rasmussen and Helin, 2016). The role of TET activity is perceived to oppose the gene silencing role of DNMTs; however, 5mC is an essential

requirement for the generation of 5hmC and the iterative oxidized products 5fC and 5caC, thus DNA methylation and hydroxymethylation, as mediated by DNMTs and TETs, must work together to form and remove cytosine methylation in the DNA (Zhang et al., 2016; Gu et al., 2018; Lopez-Moyado et al., 2019; Chao et al., 2022). In addition to the 5mC DNA substrate, TET enzymes require $Fe^{2+}$ and αKG as obligatory cofactors for their catalytic activity (Tahiliani et al., 2009). Perturbations in $Fe^{2+}$ homeostasis can influence TET activity, where iron sufficiency is associated with increased TET activity and maintenance of 5hmC formation in cord blood, hepatocytes, enterocytes, and splenocytes (Jiang et al., 2021; Taeubert et al., 2022) whereas deficiencies in iron lead to reduced activity in the cerebellum of rats evidenced by decreased 5hmC levels and neurodevelopmental defects (Barks et al., 2022). However, in settings of excess iron and iron overloading, in which homeostatic responses may block cellular uptake of redox active iron (Conrad et al., 1963), TET enzymatic activity can also become impaired and promote pathogenic T cell expansion and systemic lupus erythematosus pathogenesis (Gao et al., 2022). These findings suggest that at a physiological level, the role of iron homeostasis and the balance between iron stores or redox active labile iron on TET activity requires further clarification.

Based on its role as a cofactor of αKG-dependent dioxygenases (αKGDDs), vitamin C was tested as an enhancer of TET activity. Acting as a targeted antioxidant, vitamin C can directly bind the C-terminal catalytic domain of Tet enzymes, promoting the reduction and recycling of $Fe^{3+}$ to $Fe^{2+}$ (Yin et al., 2013; Cimmino et al., 2017). Vitamin C has been shown to increase the levels of 5hmC, 5fC, and 5caC anywhere from 4 to 20-fold in a variety of contexts, including ESCs, fibroblasts and leukemia cells, within as little as 24 h (Wang et al., 2011; Minor et al., 2013; Yin et al., 2013; Cimmino et al., 2017; Mingay et al., 2018; Brabson et al., 2021). Increased 5hmC formation and DNA demethylation upon vitamin C treatment leads to improved reprogramming efficiency during iPSC formation, and enhanced pluripotency of ESC cultures (Hore et al., 2016) by reducing methylation normally gained at CpG islands (CGIs) of pluripotency genes during blastocyst to epiblast transition (Blaschke et al., 2013; Hu et al., 2014). Tissue specific studies of vitamin C treatment in lung, breast, bladder, and kidney cultures have also reported similar increases in 5hmC generation and DNA demethylation (Ge et al., 2018; Sant et al., 2018).

Interestingly, an algal homolog of the TET enzymes uses vitamin C directly instead of αKG as the primary cofactor for the generation of glucosyl-methylation marks in the genome to regulate photosynthesis (Xue et al., 2019). Vitamin C is a structural homolog of αKG, but unlike this TCA cycle intermediate, is an essential micronutrient for humans and therefore imparts a dependence for enhancing TET activity in the context of nutritional availability (Myllyla et al., 1978; Majamaa et al., 1986; Yin et al., 2013). One requirement for increased TET activity may be in the regulation of immune responses. In regulatory T (Treg) cells, vitamin C promotes DNA demethylation of a *Foxp3* enhancer, promoting Treg differentiation and immunosuppressive function akin to the role of low-dose MTX in rheumatoid arthritis patients (Yue et al., 2021; Suga et al., 2023). Vitamin C also drives oxidized methylcytosine formation and DNA demethylation within the three enhancers of the *Prdm1* locus that are silenced in naive B cells but require activation for plasma cell differentiation (Qi et al., 2020). The effect of vitamin C on lymphocyte differentiation, including Tregs and plasma cells, has been shown to be both Tet2 and Tet3 dependent, which are the most highly expressed of the three TET enzymes in hematopoietic cells (An et al., 2015; Brabson et al., 2023). Furthermore, vitamin C increases Th1-type chemokines and PD-L1 gene expression in a TET2-dependent manner resulting in enhanced sensitivity to anti-PD-1/PD-L1 therapy (Xu et al., 2019).

Deficiencies in vitamin C mimic loss-of-function mutations in *TET2,* which is the most frequently mutated of the TET enzymes in cancer and primarily in blood cell malignancy causing impaired DNA de-methylation. Aberrant DNA hypermethylation and/or vitamin C deficiency have both been reported in patients with hematological malignancies (Figueroa et al., 2010a; Figueroa et al., 2010b). Oral supplementation with vitamin C can raise plasma levels in patients with hematological malignancies, leading to an overall increase in the 5hmC/5mC ratio in circulating white blood cells (Gillberg et al., 2019) and a reduction in the proportion of hypermethylated loci caused by *TET2* mutation (Taira et al., 2023). Normalization of low vitamin C serum levels via supplementation in murine models also leads to a restoration of 5hmC formation in hematopoietic cells that suppresses *Tet2*-deficient leukemia progression (Agathocleous et al., 2017). These studies provide proof of principle that altering vitamin C supplementation can have a powerful influence on the blood cell DNA methylome.

Recent studies have also implicated vitamin A as a regulator of TET activity and DNA demethylation. Vitamin A comprises multiple active metabolites termed retinoids that play an essential role in growth, development, and differentiation (Gudas, 2013). The active form of vitamin A, retinoic acid (RA), binds to retinoic acid and retinoid X receptors (RAR/RXR) in the nucleus that, in association with other transcriptional coactivators, localize to retinoic acid responsive elements (RAREs) in target genes to activate gene expression (Gudas, 2013; Hore et al., 2016; Coyle et al., 2018). Thymidine DNA glycosylase (TDG) promotes DNA demethylation by forming a complex with acetylated TET2 (Zhang et al., 2017), and RAR/RXR activation upon RA-signaling has been shown to recruit the histone acetyltransferase CBP, TET proteins, and TDG to trigger oxidized methylcytosine formation and DNA demethylation via BER at target gene loci (Leger et al., 2014; Hassan et al., 2017; Hassan et al., 2020). RA-signaling in this manner can initiate TET2-dependent DNA demethylation at the *Hic1* locus, which is often hypermethylated in human cancers, such as colon, breast, and brain cancer (Hassan et al., 2020). RA-signaling in breast cancer cells also induces a RARB-TET2 complex, targeted to the promoters of genes involved in cellular differentiation, such as *miR-200c* (Wu et al., 2017). Defective RARB/TET2 signaling by loss of TET2 and/or deficient *miR-200c* expression is correlated with RA-resistant breast cancer cell growth and aggressiveness (Wu et al., 2017). RA treatment of human embryonic carcinoma stem cells has also described a TET2-dependent 5mC to 5hmC conversion in the *HOXA* gene cluster (Bocker et al., 2012). These studies collectively show that RAR, CBP, TET, and TDG enzymes play an interconnected role in the initiation of gene expression in response to RA-signaling. TET expression can also be directly up-regulated by RA-signaling, and alone or in combination with vitamin C, enhances 5hmC formation in ESCs (Hore et al., 2016). A conserved RARE identified in the first intron of the *TET2* locus

| Micronutrient | Main dietary sources | Biological function | DNA methylation | Mechanism | Citations |
|---|---|---|---|---|---|
| Vitamin B (B2, B6, B9, B12) |  | Energy, metabolism, hormone regulation | 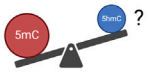 | One carbon metabolism; SAM production for DNMTs ↑5mC ? 5hmC | Lyon 2022 (22), Tong 2009 (23), Kok 2015 (64), Ehrlich 2019 (71) |
| Vitamin C (ascorbate) |  | Immunity, antioxidant, wound healing | 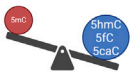 | Cofactor for TET enzymatic activity via iron recycling ↓5mC ↑5hmC, 5fC, 5caC | *Cimmino 2017 (24), *Yin 2013 (80), Mingay 2018 (81), *Brabson 2023 (96), Gillberg 2019 (99) |
| Vitamin A (retinoids) |  | Growth, development, reproduction, vision | 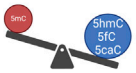 | RA signaling; TET expression upregulation ↓5mC ↑5hmC, 5fC, 5caC | Hore 2016 (30), Leger 2014 (106), *Hassan 2020 (107), Wu 2017 (108), Bocker 2012 (109) |
| Iron ($Fe^{2+}$) |  | Blood oxygen, cellular respiration, energy | 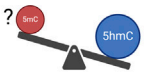 | Direct cofactor for TET enzymatic activity ? 5mC ↑5hmC | Jiang 2021 (26), Barks 2022 (28), Taeubert 2022 (29) |
| Vitamin D (calcitriol) |  | Calcium homeostasis, bone development, growth | 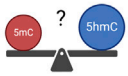 | VDR signaling; inhibit DNMT1 expression ↓5mC ? 5hmC | Doig 2013 (31), Fetahu 2014 (112), Lai 2020 (113), Jiao 2019 (114) |
| Vitamin E (tocopherol) |  | Antioxidant, wound healing, skin & brain protection | 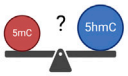 | Oxidative stress protection; inhibit DNMT1 expression ↓5mC ? 5hmC | Remely 2017 (32), Zappe 2018 (115), Huang 2012 (116) |

FIGURE 2
Influence of essential dietary micronutrients on DNA methylation or hydroxymethylation and biological outcome. Summary of biological effects of known micronutrient regulators of DNA methylation and hydroxymethylation. Vitamin A, typically sourced from foods such as carrots, leafy greens, and fish, is essential for development and reproduction, and stimulates TET activity leading to increased 5hmC formation and DNA demethylation. The various B vitamins play a coordinated role in energy production and one-carbon metabolism, are enriched in animal-derived foods, and higher intake can increase SAM production that facilitates DNMT activity and 5mC formation. Vitamin C, a major cellular antioxidant enriched in fruits and vegetables, acts as a cofactor for TET enzymes, driving 5hmC formation and DNA demethylation. Vitamin D is sourced from exposure to sunlight and is enriched in dairy products, whereas vitamin E, sourced from oils and nuts, protects against oxidative stress. Both Vitamin D and E have been shown to inhibit DNMT expression, although the effect on global methylation and hydroxymethylation varies based on cellular context and the mechanism remains unclear. Iron, a trace metal found in legumes, lean meat, and shellfish, is a direct cofactor for TET enzymes and increased supplementation facilitates 5hmC formation. *Studies that quantified micronutrient influence on 5hmC, 5fC, and 5caC levels. Figure created with BioRender.com.

suggests that expression could be mediated via direct RAR binding (Hore et al., 2016). Thus, the ability to directly enhance TET expression and increase the catalytic rate of TET activity via combined treatment with vitamin A and vitamin C suggests that these micronutrients work together to activate gene expression via increased methylcytosine oxidation.

## Indirect micronutrient regulation of DNA methylation

Other essential micronutrients have been reported to play an indirect role in the maintenance of DNA methylation via modulation of chromatin states and the regulation of DNA methyltransferase expression. Similar to RAR, the vitamin D receptor (VDR) forms a heterodimer with RXR at vitamin D responsive elements (VDREs) in the DNA (Doig et al., 2013; Krstic et al., 2022; Mirza et al., 2022). The active form of vitamin D, calcitriol [1,25$(OH)_2D_3$], when bound to VDR-RXR, triggers the recruitment of co-activators, including steroid receptor and p300/CBP (Fetahu et al., 2014). However, in the absence of its ligand, VDR-RXR is bound by co-repressors such as NCOR1 and SMRT that maintain repressive histone modifications at target loci (Doig et al., 2013; Fetahu et al., 2014). Vitamin D signaling may promote DNA hypomethylation via the downregulated expression of *DNMT1* and *DNMT3B* (Jiao et al., 2019; Lai et al., 2020) in this matter. Likewise, vitamin E can influence the expression of *DNMT1;* both a decreased expression in liver cells and an increased level in colon cells have been reported (Remely et al., 2017; Zappe et al., 2018). Prostate cancer models treated with vitamin E exhibit decreased DNMT protein expression and reduced CpG methylation at target loci of genes involved in cellular redox homeostasis such as the *Nrf2* promoter (Huang et al., 2012a). As oxidative stress is often correlated with increased global levels of 5mC (Garcia-Guede et al., 2020; Goncalves et al., 2021), it is possible that vitamin E can reduce DNA methylation indirectly due to its antioxidant activity (Ryan et al., 2010; Zappe et al., 2018).

## Discussion and future directions

The balance of essential micronutrient intake and bioavailability has the potential to significantly alter DNA methylation and hydroxymethylation levels in the body (Figure 2). Research using datasets comprising thousands of samples to track alterations in DNA methylation associated with cellular development, differentiation, aging, and disease progression has led to the identification of DNA methylation biomarkers and epigenetic

clocks that accurately estimate chronological age (Hannum et al., 2013; Horvath, 2013; Horvath and Raj, 2018), healthspan and lifespan (Levine et al., 2018; Lu et al., 2019; Lu et al., 2022), or the pace of aging (Belsky et al., 2022) in both humans and animal models. These same DNA methylation signatures are also being used to investigate the impact of lifestyle factors such as diet and nutritional status on disease risk and aging (Quach et al., 2017; Lu et al., 2019; Fitzgerald et al., 2021) that may reveal potential therapeutic interventions to slow aging phenotypes and age-related diseases, including cancer. Plant-based, Mediterranean, and methylation-supportive diets can rejuvenate DNA methylation aging signatures, decreasing chronological age predictions by 1–10 years in as little as 8 weeks of intervention (Gensous et al., 2020; Dwaraka et al., 2023; Fitzgerald et al., 2023). One study (Dwaraka et al., 2023) using blood samples from paired twins reported that a vegan diet compared to an omnivorous diet led to a significant decrease in overall epigenetic age acceleration measured using multiple DNA methylation biomarkers (Levine et al., 2018; Lu et al., 2019; Belsky et al., 2022; Lu et al., 2022) that correlated with fewer hypermethylated loci in the vegan diet, consistent with the notion that vegan diets contribute to a reduced intake and lower serum levels of B12 (Gilsing et al., 2010; Niklewicz et al., 2023) and methionine (McCarty et al., 2009; Sanderson et al., 2019; Allen and Locasale, 2021), two of the major regulators of methyl-donor (SAM) levels. However, no controlled studies have attempted to address how supplementation with specific micronutrients associates with epigenetic clocks and DNA methylation biomarkers of aging or disease.

An important caveat to consider when interpreting micronutrient influences on DNA methylation status using existing biomarkers is that the gold standard for measuring global DNA methylation in research and clinical diagnostics has historically relied on CpG hybridization array platforms using bisulfite-treated DNA. Unmethylated cytosines, 5fC, and 5caC, are converted to uracil upon bisulfite treatment, while both 5mC and 5hmC remain protected and measured as cytosine, rendering their contribution to DNA methylation signatures indistinguishable (Huang et al., 2010). DNA immunoprecipitation and base-resolution mapping of 5hmC, 5fC and 5caC in the mammalian genome have shown that most reside in a CpG context, enriched within gene bodies, low density CpG regions (CpG island shores), and at distal regulatory elements such as enhancers, where 5mC and 5hmC can be present in nearly equal representation (Williams et al., 2011; Wu et al., 2011; Huang et al., 2012b; Yu et al., 2012; Lu et al., 2015b; Xia et al., 2015). While the contribution of 5hmC, or the rarer modifications 5fC and 5caC, to the major DNA methylation biomarkers currently remains unknown, recent advances in base resolution mapping using alternate chemical and enzymatic conversion strategies (Huang et al., 2010; Booth et al., 2013; Schutsky et al., 2018) [reviewed in (Berney and McGouran, 2018)] should allow the contribution of nutritional interventions and micronutrient levels on DNMT vs. TET-mediated DNA methylation maintenance, epigenetic clocks, and other predictive disease biomarkers to be determined.

## Author contributions

TL: Writing–original draft, Writing–review and editing. PL: Writing–original draft. JP: Writing–original draft. LC: Writing–review and editing.

## Funding

The author(s) declare that financial support was received for the research, authorship, and/or publication of this article. This research was supported by the NIH (NCI 1R01CA282453-01), Leukemia & Lymphoma Society (7028-22), and Castaways Against Cancer Foundation.

## Conflict of interest

The authors declare that the research was conducted in the absence of any commercial or financial relationships that could be construed as a potential conflict of interest.

## Publisher's note



## References

Afman, L. A., Blom, H. J., Drittij, M. J., Brouns, M. R., and van Straaten, H. W. (2005). Inhibition of transmethylation disturbs neurulation in chick embryos. *Dev. Brain Res.* 158 (1-2), 59–65. doi:10.1016/j.devbrainres.2005.06.002

Agathocleous, M., Meacham, C. E., Burgess, R. J., Piskounova, E., Zhao, Z., Crane, G. M., et al. (2017). Ascorbate regulates haematopoietic stem cell function and leukaemogenesis. *Nature* 549 (7673), 476–481. doi:10.1038/nature23876

Alata Jimenez, N., and Strobl-Mazzulla, P. H. (2022). Folate carrier deficiency drives differential methylation and enhanced cellular potency in the neural plate border. *Front. Cell Dev. Biol.* 10, 834625. doi:10.3389/fcell.2022.834625

Allen, A. E., and Locasale, J. W. (2021). Metabolomics: insights into plant-based diets. *EMBO Mol. Med.* 13 (2), e13568. doi:10.15252/emmm.202013568

Amenyah, S. D., McMahon, A., Ward, M., Deane, J., McNulty, H., Hughes, C. F., et al. (2020). Riboflavin supplementation alters global and gene-specific DNA methylation in adults with the MTHFR 677 TT genotype. *Biochimie* 173, 17–26. doi:10.1016/j.biochi.2020.04.007

Amenyah, S. D., Ward, M., McMahon, A., Deane, J., McNulty, H., Hughes, C., et al. (2021). DNA methylation of hypertension-related genes and effect of riboflavin supplementation in adults stratified by genotype for the MTHFR C677T polymorphism. *Int. J. Cardiol.* 322, 233–239. doi:10.1016/j.ijcard.2020.09.011

An, J., Gonzalez-Avalos, E., Chawla, A., Jeong, M., Lopez-Moyado, I. F., Li, W., et al. (2015). Acute loss of TET function results in aggressive myeloid cancer in mice. *Nat. Commun.* 6, 10071. doi:10.1038/ncomms10071

Bachman, M., Uribe-Lewis, S., Yang, X., Williams, M., Murrell, A., and Balasubramanian, S. (2014). 5-Hydroxymethylcytosine is a predominantly stable DNA modification. *Nat. Chem.* 6 (12), 1049–1055. doi:10.1038/nchem.2064

Barks, A., Beeson, M. M., Hallstrom, T. C., Georgieff, M. K., and Tran, P. V. (2022). Developmental iron deficiency dysregulates TET activity and DNA hydroxymethylation in the rat Hippocampus and cerebellum. *Dev. Neurosci.* 44 (2), 80–90. doi:10.1159/000521704

Bashtrykov, P., Jankevicius, G., Smarandache, A., Jurkowska, R. Z., Ragozin, S., and Jeltsch, A. (2012). Specificity of Dnmt1 for methylation of hemimethylated CpG sites resides in its catalytic domain. *Chem. Biol.* 19 (5), 572–578. doi:10.1016/j.chembiol.2012.03.010

Beaudin, A. E., Abarinov, E. V., Malysheva, O., Perry, C. A., Caudill, M., and Stover, P. J. (2012). Dietary folate, but not choline, modifies neural tube defect risk in Shmt1 knockout mice. *Am. J. Clin. Nutr.* 95 (1), 109–114. doi:10.3945/ajcn.111.020305

Beaudin, A. E., Abarinov, E. V., Noden, D. M., Perry, C. A., Chu, S., Stabler, S. P., et al. (2011). Shmt1 and *de novo* thymidylate biosynthesis underlie folate-responsive neural tube defects in mice. *Am. J. Clin. Nutr.* 93 (4), 789–798. doi:10.3945/ajcn.110.002766

Belsky, D. W., Caspi, A., Corcoran, D. L., Sugden, K., Poulton, R., Arseneault, L., et al. (2022). DunedinPACE, a DNA methylation biomarker of the pace of aging. *Elife* 11, e73420. doi:10.7554/elife.73420

Berney, M., and McGouran, J. F. (2018). Methods for detection of cytosine and thymine modifications in DNA. *Nat. Rev. Chem.* 2 (11), 332–348. doi:10.1038/s41570-018-0044-4

Blaschke, K., Ebata, K. T., Karimi, M. M., Zepeda-Martinez, J. A., Goyal, P., Mahapatra, S., et al. (2013). Vitamin C induces Tet-dependent DNA demethylation and a blastocyst-like state in ES cells. *Nature* 500 (7461), 222–226. doi:10.1038/nature12362

Bocker, M. T., Tuorto, F., Raddatz, G., Musch, T., Yang, F. C., Xu, M., et al. (2012). Hydroxylation of 5-methylcytosine by TET2 maintains the active state of the mammalian HOXA cluster. *Nat. Commun.* 3, 818. doi:10.1038/ncomms1826

Booth, M. J., Ost, T. W., Beraldi, D., Bell, N. M., Branco, M. R., Reik, W., et al. (2013). Oxidative bisulfite sequencing of 5-methylcytosine and 5-hydroxymethylcytosine. *Nat. Protoc.* 8 (10), 1841–1851. doi:10.1038/nprot.2013.115

Botto, L. D., and Yang, Q. (2000). 5,10-Methylenetetrahydrofolate reductase gene variants and congenital anomalies: a HuGE review. *Am. J. Epidemiol.* 151 (9), 862–877. doi:10.1093/oxfordjournals.aje.a010290

Brabson, J. P., Leesang, T., Mohammad, S., and Cimmino, L. (2021). Epigenetic regulation of genomic stability by vitamin C. *Front. Genet.* 12, 675780. doi:10.3389/fgene.2021.675780

Brabson, J. P., Leesang, T., Yap, Y. S., Wang, J., Lam, M. Q., Fang, B., et al. (2023). Oxidized mC modulates synthetic lethality to PARP inhibitors for the treatment of leukemia. *Cell Rep.* 42 (1), 112027. doi:10.1016/j.celrep.2023.112027

Buscarlet, M., Provost, S., Zada, Y. F., Barhdadi, A., Bourgoin, V., Lepine, G., et al. (2017). DNMT3A and TET2 dominate clonal hematopoiesis and demonstrate benign phenotypes and different genetic predispositions. *Blood* 130 (6), 753–762. doi:10.1182/blood-2017-04-777029

Chao, L., Yang, S., Li, H., Long, C., Xi, Q., and Zuo, Y. (2022). Competitive binding of TET1 and DNMT3A/B cooperates the DNA methylation pattern in human embryonic stem cells. *Biochimica Biophysica Acta (BBA) - Gene Regul. Mech.* 1865 (7), 194861. doi:10.1016/j.bbagrm.2022.194861

Cimmino, L., Dolgalev, I., Wang, Y., Yoshimi, A., Martin, G. H., Wang, J., et al. (2017). Restoration of TET2 function blocks aberrant self-renewal and leukemia progression. *Cell* 170 (6), 1079–1095.e20. doi:10.1016/j.cell.2017.07.032

Cimmino, L., Neel, B. G., and Aifantis, I. (2018). Vitamin C in stem cell reprogramming and cancer. *Trends Cell Biol.* 28 (9), 698–708. doi:10.1016/j.tcb.2018.04.001

Conrad, M. E., Jr., Crosby, W. H., and Merrill, B. (1963). Intestinal mucosal mechanisms controlling iron absorption. *Blood* 22, 406–415. doi:10.1182/blood.v22.4.406.406

Cortellino, S., Xu, J., Sannai, M., Moore, R., Caretti, E., Cigliano, A., et al. (2011). Thymine DNA glycosylase is essential for active DNA demethylation by linked deamination-base excision repair. *Cell* 146 (1), 67–79. doi:10.1016/j.cell.2011.06.020

Coyle, K. M., Dean, C. A., Thomas, M. L., Vidovic, D., Giacomantonio, C. A., Helyer, L., et al. (2018). DNA methylation predicts the response of triple-negative breast cancers to all-trans retinoic acid. *Cancers (Basel)* 10 (11), 397. doi:10.3390/cancers10110397

Cribbs, A. P., Kennedy, A., Penn, H., Amjadi, P., Green, P., Read, J. E., et al. (2015). Methotrexate restores regulatory T cell function through demethylation of the FoxP3 upstream enhancer in patients with rheumatoid arthritis. *Arthritis & Rheumatology* 67 (5), 1182–1192. doi:10.1002/art.39031

Crider, K. S., Bailey, L. B., and Berry, R. J. (2011). Folic acid food fortification-its history, effect, concerns, and future directions. *Nutrients* 3 (3), 370–384. doi:10.3390/nu3030370

Deaton, A. M., and Bird, A. (2011). CpG islands and the regulation of transcription. *Genes Dev.* 25 (10), 1010–1022. doi:10.1101/gad.2037511

Delhommeau, F., Dupont, S., Valle, V. D., James, C., Trannoy, S., Masse, A., et al. (2009). Mutation in TET2 in myeloid cancers. *N. Engl. J. Med.* 360 (22), 2289–2301. doi:10.1056/nejmoa0810069

de Queiroz, K. B., Cavalcante-Silva, V., Lopes, F. L., Rocha, G. A., D'Almeida, V., and Coimbra, R. S. (2020). Vitamin B(12) is neuroprotective in experimental pneumococcal meningitis through modulation of hippocampal DNA methylation. *J. neuroinflammation* 17 (1), 96. doi:10.1186/s12974-020-01763-y

Doig, C. L., Singh, P. K., Dhiman, V. K., Thorne, J. L., Battaglia, S., Sobolewski, M., et al. (2013). Recruitment of NCOR1 to VDR target genes is enhanced in prostate cancer cells and associates with altered DNA methylation patterns. *Carcinogenesis* 34 (2), 248–256. doi:10.1093/carcin/bgs331

Ducker, G. S., and Rabinowitz, J. D. (2017). One-carbon metabolism in health and disease. *Cell Metab.* 25 (1), 27–42. doi:10.1016/j.cmet.2016.08.009

Dunlevy, L. P., Burren, K. A., Chitty, L. S., Copp, A. J., and Greene, N. D. (2006). Excess methionine suppresses the methylation cycle and inhibits neural tube closure in mouse embryos. *FEBS Lett.* 580 (11), 2803–2807. doi:10.1016/j.febslet.2006.04.020

Dwaraka, V. B., Aronica, L., Carreras-Gallo, N., Robinson, J. L., Hennings, T., Lin, A., et al. (2023). Unveiling the epigenetic impact of vegan vs. Omnivorous diets on aging: insights from the twins nutrition study (TwiNS). medRxiv.

Ehrlich, M. (2019). DNA hypermethylation in disease: mechanisms and clinical relevance. *Epigenetics* 14 (12), 1141–1163. doi:10.1080/15592294.2019.1638701

Fetahu, I. S., Höbaus, J., and Kállay, E. (2014). Vitamin D and the epigenome. *Front. Physiol.* 5, 164. doi:10.3389/fphys.2014.00164

Ficz, G., Branco, M. R., Seisenberger, S., Santos, F., Krueger, F., Hore, T. A., et al. (2011). Dynamic regulation of 5-hydroxymethylcytosine in mouse ES cells and during differentiation. *Nature* 473 (7347), 398–402. doi:10.1038/nature10008

Figueroa, M. E., Abdel-Wahab, O., Lu, C., Ward, P. S., Patel, J., Shih, A., et al. (2010b). Leukemic IDH1 and IDH2 mutations result in a hypermethylation phenotype, disrupt TET2 function, and impair hematopoietic differentiation. *Cancer Cell* 18 (6), 553–567. doi:10.1016/j.ccr.2010.11.015

Figueroa, M. E., Lugthart, S., Li, Y., Erpelinck-Verschueren, C., Deng, X., Christos, P. J., et al. (2010a). DNA methylation signatures identify biologically distinct subtypes in acute myeloid leukemia. *Cancer Cell* 17 (1), 13–27. doi:10.1016/j.ccr.2009.11.020

Fitzgerald, K. N., Campbell, T., Makarem, S., and Hodges, R. (2023). Potential reversal of biological age in women following an 8-week methylation-supportive diet and lifestyle program: a case series. *Aging (Albany NY)* 15 (6), 1833–1839. doi:10.18632/aging.204602

Fitzgerald, K. N., Hodges, R., Hanes, D., Stack, E., Cheishvili, D., Szyf, M., et al. (2021). Potential reversal of epigenetic age using a diet and lifestyle intervention: a pilot randomized clinical trial. *Aging (Albany NY)* 13 (7), 9419–9432. doi:10.18632/aging.202913

Gao, X., Song, Y., Wu, J., Lu, S., Min, X., Liu, L., et al. (2022). Iron-dependent epigenetic modulation promotes pathogenic T cell differentiation in lupus. *J. Clin. investigation* 132 (9), e152345. doi:10.1172/jci152345

Garcia-Guede, A., Vera, O., and Ibanez-de-Caceres, I. (2020). When oxidative stress meets epigenetics: implications in cancer development. *Antioxidants (Basel)* 9 (6), 468. doi:10.3390/antiox9060468

Ge, G., Peng, D., Xu, Z., Guan, B., Xin, Z., He, Q., et al. (2018). Restoration of 5-hydroxymethylcytosine by ascorbate blocks kidney tumour growth. *EMBO Rep.* 19 (8), e45401. doi:10.15252/embr.201745401

Gensous, N., Garagnani, P., Santoro, A., Giuliani, C., Ostan, R., Fabbri, C., et al. (2020). One-year Mediterranean diet promotes epigenetic rejuvenation with country- and sex-specific effects: a pilot study from the NU-AGE project. *Geroscience* 42 (2), 687–701. doi:10.1007/s11357-019-00149-0

Gillberg, L., Orskov, A. D., Nasif, A., Ohtani, H., Madaj, Z., Hansen, J. W., et al. (2019). Oral vitamin C supplementation to patients with myeloid cancer on azacitidine treatment: normalization of plasma vitamin C induces epigenetic changes. *Clin. Epigenetics* 11 (1), 143. doi:10.1186/s13148-019-0739-5

Gilsing, A. M., Crowe, F. L., Lloyd-Wright, Z., Sanders, T. A., Appleby, P. N., Allen, N. E., et al. (2010). Serum concentrations of vitamin B12 and folate in British male omnivores, vegetarians and vegans: results from a cross-sectional analysis of the EPIC-Oxford cohort study. *Eur. J. Clin. Nutr.* 64 (9), 933–939. doi:10.1038/ejcn.2010.142

Goncalves, A. C., Alves, R., Baldeiras, I., Marques, B., Oliveiros, B., Pereira, A., et al. (2021). DNA methylation is correlated with oxidative stress in myelodysplastic syndrome-relevance as complementary prognostic biomarkers. *Cancers (Basel)* 13 (13), 3138. doi:10.3390/cancers13133138

Gosselt, H. R., van Zelst, B. D., de Rotte, M., Hazes, J. M. W., de Jonge, R., and Heil, S. G. (2019). Higher baseline global leukocyte DNA methylation is associated with MTX non-response in early RA patients. *Arthritis Res. Ther.* 21 (1), 157. doi:10.1186/s13075-019-1936-5

Greene, N. D., Stanier, P., and Moore, G. E. (2011). The emerging role of epigenetic mechanisms in the etiology of neural tube defects. *Epigenetics* 6 (7), 875–883. doi:10.4161/epi.6.7.16400

Gu, T., Lin, X., Cullen, S. M., Luo, M., Jeong, M., Estecio, M., et al. (2018). DNMT3A and TET1 cooperate to regulate promoter epigenetic landscapes in mouse embryonic stem cells. *Genome Biol.* 19 (1), 88. doi:10.1186/s13059-018-1464-7

Gudas, L. J. (2013). Retinoids induce stem cell differentiation via epigenetic changes. *Seminars Cell & Dev. Biol.* 24 (10-12), 701–705. doi:10.1016/j.semcdb.2013.08.002

Guéant, J.-L., Oussalah, A., Zgheib, R., Siblini, Y., Hsu, S. B., and Namour, F. (2020). Genetic, epigenetic and genomic mechanisms of methionine dependency of cancer and

tumor-initiating cells: what could we learn from folate and methionine cycles. *Biochimie* 173, 123–128. doi:10.1016/j.biochi.2020.03.015

Guo, H., Zhu, P., Yan, L., Li, R., Hu, B., Lian, Y., et al. (2014). The DNA methylation landscape of human early embryos. *Nature* 511 (7511), 606–610. doi:10.1038/nature13544

Hannum, G., Guinney, J., Zhao, L., Zhang, L., Hughes, G., Sadda, S., et al. (2013). Genome-wide methylation profiles reveal quantitative views of human aging rates. *Mol. Cell* 49 (2), 359–367. doi:10.1016/j.molcel.2012.10.016

Hassan, H. M., Isovic, M., Kolendowski, B., Bauer-Maison, N., Onabote, O., Cecchini, M., et al. (2020). Loss of thymine DNA glycosylase causes dysregulation of bile acid homeostasis and hepatocellular carcinoma. *Cell Rep.* 31 (1), 107475. doi:10.1016/j.celrep.2020.03.039

Hassan, H. M., Kolendowski, B., Isovic, M., Bose, K., Dranse, H. J., Sampaio, A. V., et al. (2017). Regulation of active DNA demethylation through RAR-mediated recruitment of a TET/TDG complex. *Cell Rep.* 19 (8), 1685–1697. doi:10.1016/j.celrep.2017.05.007

He, X., Liu, J., Liu, B., and Shi, J. (2021). The use of DNA methylation clock in aging research. *Exp. Biol. Med. (Maywood)* 246 (4), 436–446. doi:10.1177/1535370220968802

He, Y. F., Li, B. Z., Li, Z., Liu, P., Wang, Y., Tang, Q., et al. (2011). Tet-mediated formation of 5-carboxylcytosine and its excision by TDG in mammalian DNA. *Science* 333 (6047), 1303–1307. doi:10.1126/science.1210944

Hore, T. A., von Meyenn, F., Ravichandran, M., Bachman, M., Ficz, G., Oxley, D., et al. (2016). Retinol and ascorbate drive erasure of epigenetic memory and enhance reprogramming to naive pluripotency by complementary mechanisms. *Proc. Natl. Acad. Sci. U. S. A.* 113 (43), 12202–12207. doi:10.1073/pnas.1608679113

Horvath, S. (2013). DNA methylation age of human tissues and cell types. *Genome Biol.* 14 (10), R115. doi:10.1186/gb-2013-14-10-r115

Horvath, S., and Raj, K. (2018). DNA methylation-based biomarkers and the epigenetic clock theory of ageing. *Nat. Rev. Genet.* 19 (6), 371–384. doi:10.1038/s41576-018-0004-3

Hu, X., Zhang, L., Mao, S. Q., Li, Z., Chen, J., Zhang, R. R., et al. (2014). Tet and TDG mediate DNA demethylation essential for mesenchymal-to-epithelial transition in somatic cell reprogramming. *Cell Stem Cell* 14 (4), 512–522. doi:10.1016/j.stem.2014.01.001

Huang, Y., Khor, T. O., Shu, L., Saw, C. L., Wu, T. Y., Suh, N., et al. (2012a). A gamma-tocopherol-rich mixture of tocopherols maintains Nrf2 expression in prostate tumors of TRAMP mice via epigenetic inhibition of CpG methylation. *J. Nutr.* 142 (5), 818–823. doi:10.3945/jn.111.153114

Huang, Y., Pastor, W. A., Shen, Y., Tahiliani, M., Liu, D. R., and Rao, A. (2010). The behaviour of 5-hydroxymethylcytosine in bisulfite sequencing. *PLoS One* 5 (1), e8888. doi:10.1371/journal.pone.0008888

Huang, Y., Pastor, W. A., Zepeda-Martinez, J. A., and Rao, A. (2012b). The anti-CMS technique for genome-wide mapping of 5-hydroxymethylcytosine. *Nat. Protoc.* 7 (10), 1897–1908. doi:10.1038/nprot.2012.103

Imbard, A., Benoist, J.-F., and Blom, H. J. (2013). Neural tube defects, folic acid and methylation. *Int. J. Environ. Res. Public Health* 10 (9), 4352–4389. doi:10.3390/ijerph10094352

Ito, S., D'Alessio, A. C., Taranova, O. V., Hong, K., Sowers, L. C., and Zhang, Y. (2010). Role of Tet proteins in 5mC to 5hmC conversion, ES-cell self-renewal and inner cell mass specification. *Nature* 466 (7310), 1129–1133. doi:10.1038/nature09303

Jacob, R. A., Gretz, D. M., Taylor, P. C., James, S. J., Pogribny, I. P., Miller, B. J., et al. (1998). Moderate folate depletion increases plasma homocysteine and decreases lymphocyte DNA methylation in postmenopausal women. *J. Nutr.* 128 (7), 1204–1212. doi:10.1093/jn/128.7.1204

Jiang, L., Wang, J., Wang, K., Wang, H., Wu, Q., Yang, C., et al. (2021). RNF217 regulates iron homeostasis through its E3 ubiquitin ligase activity by modulating ferroportin degradation. *Blood* 138 (8), 689–705. doi:10.1182/blood.2020008986

Jiao, X., Wang, L., Wei, Z., Liu, B., Liu, X., and Yu, X. (2019). Vitamin D deficiency during pregnancy affects the function of Th1/Th2 cells and methylation of IFN-gamma gene in offspring rats. *Immunol. Lett.* 212, 98–105. doi:10.1016/j.imlet.2019.06.012

Kim, Y. I. (2007). Folate and colorectal cancer: an evidence-based critical review. *Mol. Nutr. food Res.* 51 (3), 267–292. doi:10.1002/mnfr.200600191

Ko, M., An, J., Bandukwala, H. S., Chavez, L., Aijo, T., Pastor, W. A., et al. (2013). Modulation of TET2 expression and 5-methylcytosine oxidation by the CXXC domain protein IDAX. *Nature* 497 (7447), 122–126. doi:10.1038/nature12052

Kok, D. E., Dhonukshe-Rutten, R. A., Lute, C., Heil, S. G., Uitterlinden, A. G., van der Velde, N., et al. (2015a). The effects of long-term daily folic acid and vitamin B12 supplementation on genome-wide DNA methylation in elderly subjects. *Clin. Epigenetics* 7, 121. doi:10.1186/s13148-015-0154-5

Kok, D. E. G., Dhonukshe-Rutten, R. A. M., Lute, C., Heil, S. G., Uitterlinden, A. G., van der Velde, N., et al. (2015b). The effects of long-term daily folic acid and vitamin B12 supplementation on genome-wide DNA methylation in elderly subjects. *Clin. Epigenetics* 7, 121. doi:10.1186/s13148-015-0154-5

Krstic, N., Bishop, N., Curtis, B., Cooper, C., Harvey, N., Lilycrop, K., et al. (2022). Early life vitamin D depletion and mechanical loading determine methylation changes in the RUNX2, RXRA, and osterix promoters in mice. *Genes Nutr.* 17 (1), 7. doi:10.1186/s12263-022-00711-0

Lai, G. R., Lee, Y. F., Yan, S. J., and Ting, H. J. (2020). Active vitamin D induces gene-specific hypomethylation in prostate cancer cells developing vitamin D resistance. *Am. J. Physiology-Cell Physiology* 318 (5), C836–C847. doi:10.1152/ajpcell.00522.2019

Leger, H., Smet-Nocca, C., Attmane-Elakeb, A., Morley-Fletcher, S., Benecke, A. G., and Eilebrecht, S. (2014). A TDG/CBP/RARα ternary complex mediates the retinoic acid-dependent expression of DNA methylation-sensitive genes. *Genomics Proteomics Bioinforma.* 12 (1), 8–18. doi:10.1016/j.gpb.2013.11.001

Levine, M. E., Lu, A. T., Quach, A., Chen, B. H., Assimes, T. L., Bandinelli, S., et al. (2018). An epigenetic biomarker of aging for lifespan and healthspan. *Aging (Albany NY)* 10 (4), 573–591. doi:10.18632/aging.101414

Li, Z., Cai, X., Cai, C. L., Wang, J., Zhang, W., Petersen, B. E., et al. (2011). Deletion of Tet2 in mice leads to dysregulated hematopoietic stem cells and subsequent development of myeloid malignancies. *Blood* 118 (17), 4509–4518. doi:10.1182/blood-2010-12-325241

Lio, C. W. J., Yue, X., Lopez-Moyado, I. F., Tahiliani, M., Aravind, L., and Rao, A. (2020). TET methylcytosine oxidases: new insights from a decade of research. *J. Biosci.* 45, 21. doi:10.1007/s12038-019-9973-4

Lister, R., Pelizzola, M., Dowen, R. H., Hawkins, R. D., Hon, G., Tonti-Filippini, J., et al. (2009). Human DNA methylomes at base resolution show widespread epigenomic differences. *Nature* 462 (7271), 315–322. doi:10.1038/nature08514

Lopez-Moyado, I. F., Tsagaratou, A., Yuita, H., Seo, H., Delatte, B., Heinz, S., et al. (2019). Paradoxical association of TET loss of function with genome-wide DNA hypomethylation. *Proc. Natl. Acad. Sci. U. S. A.* 116 (34), 16933–16942. doi:10.1073/pnas.1903059116

Lorsbach, R. B., Moore, J., Mathew, S., Raimondi, S. C., Mukatira, S. T., and Downing, J. R. (2003). TET1, a member of a novel protein family, is fused to MLL in acute myeloid leukemia containing the t(10;11)(q22;q23). *Leukemia* 17 (3), 637–641. doi:10.1038/sj.leu.2402834

Lu, A. T., Binder, A. M., Zhang, J., Yan, Q., Reiner, A. P., Cox, S. R., et al. (2022). DNA methylation GrimAge version 2. *Aging (Albany NY)* 14 (23), 9484–9549. doi:10.18632/aging.204434

Lu, A. T., Fei, Z., Haghani, A., Robeck, T. R., Zoller, J. A., Li, C. Z., et al. (2023). Universal DNA methylation age across mammalian tissues. *Nat. Aging* 3 (9), 1144–1166. doi:10.1038/s43587-023-00462-6

Lu, A. T., Quach, A., Wilson, J. G., Reiner, A. P., Aviv, A., Raj, K., et al. (2019). DNA methylation GrimAge strongly predicts lifespan and healthspan. *Aging (Albany NY)* 11 (2), 303–327. doi:10.18632/aging.101684

Lu, X., Han, D., Zhao, B. S., Song, C. X., Zhang, L. S., Dore, L. C., et al. (2015b). Base-resolution maps of 5-formylcytosine and 5-carboxylcytosine reveal genome-wide DNA demethylation dynamics. *Cell Res.* 25 (3), 386–389. doi:10.1038/cr.2015.5

Lu, X., Zhao, B. S., and He, C. (2015a). TET family proteins: oxidation activity, interacting molecules, and functions in diseases. *Chem. Rev.* 115 (6), 2225–2239. doi:10.1021/cr500470n

Lyon, P., Strippoli, V., Fang, B., and Cimmino, L. (2020). B vitamins and one-carbon metabolism: implications in human health and disease. *Nutrients* 12 (9), 2867. doi:10.3390/nu12092867

Majamaa, K., Gunzler, V., Hanauske-Abel, H. M., Myllyla, R., and Kivirikko, K. I. (1986). Partial identity of the 2-oxoglutarate and ascorbate binding sites of prolyl 4-hydroxylase. *J. Biol. Chem.* 261 (17), 7819–7823. doi:10.1016/s0021-9258(19)57475-0

McCarty, M. F., Barroso-Aranda, J., and Contreras, F. (2009). The low-methionine content of vegan diets may make methionine restriction feasible as a life extension strategy. *Med. Hypotheses* 72 (2), 125–128. doi:10.1016/j.mehy.2008.07.044

Mingay, M., Chaturvedi, A., Bilenky, M., Cao, Q., Jackson, L., Hui, T., et al. (2018). Vitamin C-induced epigenomic remodelling in IDH1 mutant acute myeloid leukaemia. *Leukemia* 32 (1), 11–20. doi:10.1038/leu.2017.171

Minor, E. A., Court, B. L., Young, J. I., and Wang, G. (2013). Ascorbate induces ten-eleven translocation (Tet) methylcytosine dioxygenase-mediated generation of 5-hydroxymethylcytosine. *J. Biol. Chem.* 288 (19), 13669–13674. doi:10.1074/jbc.c113.464800

Mirza, I., Mohamed, A., Deen, H., Balaji, S., Elsabbahi, D., Munasser, A., et al. (2022). Obesity-associated vitamin D deficiency correlates with adipose tissue DNA hypomethylation, inflammation, and vascular dysfunction. *Int. J. Mol. Sci.* 23 (22), 14377. doi:10.3390/ijms232214377

Myllyla, R., Kuutti-Savolainen, E. R., and Kivirikko, K. I. (1978). The role of ascorbate in the prolyl hydroxylase reaction. *Biochem. Biophysical Res. Commun.* 83 (2), 441–448. doi:10.1016/0006-291x(78)91010-0

Nguyen, T. T., Tran, T. A., Le, N. Q., Pham, D. M., and Ou, Y. Y. (2022). An extensive examination of discovering 5-methylcytosine sites in genome-wide DNA promoters using machine learning based approaches. *IEEE/ACM Trans. Comput. Biol. Bioinforma.* 19 (1), 87–94. doi:10.1109/tcbb.2021.3082184

Niklewicz, A., Smith, A. D., Smith, A., Holzer, A., Klein, A., McCaddon, A., et al. (2023). The importance of vitamin B(12) for individuals choosing plant-based diets. *Eur. J. Nutr.* 62 (3), 1551–1559. doi:10.1007/s00394-022-03025-4

Okano, M., Bell, D. W., Haber, D. A., and Li, E. (1999). DNA methyltransferases Dnmt3a and Dnmt3b are essential for *de novo* methylation and mammalian development. *Cell* 99 (3), 247–257. doi:10.1016/s0092-8674(00)81656-6

Ostrander, E. L., Kramer, A. C., Mallaney, C., Celik, H., Koh, W. K., Fairchild, J., et al. (2020). Divergent effects of Dnmt3a and Tet2 mutations on hematopoietic progenitor cell fitness. *Stem Cell Rep.* 14 (4), 551–560. doi:10.1016/j.stemcr.2020.02.011

Otani, J., Arita, K., Kato, T., Kinoshita, M., Kimura, H., Suetake, I., et al. (2013). Structural basis of the versatile DNA recognition ability of the methyl-CpG binding domain of methyl-CpG binding domain protein 4. *J. Biol. Chem.* 288 (9), 6351–6362. doi:10.1074/jbc.m112.431098

Patel, P., Selvaraju, V., Babu, J. R., and Geetha, T. (2023). Association of the DNA methylation of obesity-related genes with the dietary nutrient intake in children. *Nutrients* 15 (13), 2840. doi:10.3390/nu15132840

Pradhan, S., Bacolla, A., Wells, R. D., and Roberts, R. J. (1999). Recombinant human DNA (Cytosine-5) methyltransferase. *J. Biol. Chem.* 274 (46), 33002–33010. doi:10.1074/jbc.274.46.33002

Prevention of Neural Tube Defects. (1991). Prevention of neural tube defects: results of the medical research council vitamin study. MRC vitamin study research group. *Lancet.* 338 (8760), 131–137. doi:10.1016/0140-6736(91)90133-A

Pufulete, M., Al-Ghnaniem, R., Leather, A. J., Appleby, P., Gout, S., Terry, C., et al. (2003). Folate status, genomic DNA hypomethylation, and risk of colorectal adenoma and cancer: a case control study. *Gastroenterology* 124 (5), 1240–1248. doi:10.1016/s0016-5085(03)00279-8

Qi, T., Sun, M., Zhang, C., Chen, P., Xiao, C., and Chang, X. (2020). Ascorbic acid promotes plasma cell differentiation through enhancing TET2/3-mediated DNA demethylation. *Cell Rep.* 33 (9), 108452. doi:10.1016/j.celrep.2020.108452

Quach, A., Levine, M. E., Tanaka, T., Lu, A. T., Chen, B. H., Ferrucci, L., et al. (2017). Epigenetic clock analysis of diet, exercise, education, and lifestyle factors. *Aging (Albany NY)* 9 (2), 419–446. doi:10.18632/aging.101168

Rampal, R., Alkalin, A., Madzo, J., Vasanthakumar, A., Pronier, E., Patel, J., et al. (2014). DNA hydroxymethylation profiling reveals that WT1 mutations result in loss of TET2 function in acute myeloid leukemia. *Cell Rep.* 9 (5), 1841–1855. doi:10.1016/j.celrep.2014.11.004

Rasmussen, K. D., and Helin, K. (2016). Role of TET enzymes in DNA methylation, development, and cancer. *Genes Dev.* 30 (7), 733–750. doi:10.1101/gad.276568.115

Remely, M., Ferk, F., Sterneder, S., Setayesh, T., Kepcija, T., Roth, S., et al. (2017). Vitamin E modifies high-fat diet-induced increase of DNA strand breaks, and changes in expression and DNA methylation of Dnmt1 and MLH1 in C57bl/6J male mice. *Nutrients* 9 (6), 607. doi:10.3390/nu9060607

Rossetti, M., Spreafico, R., Saidin, S., Chua, C., Moshref, M., Leong, J. Y., et al. (2015). *Ex vivo*-expanded but not *in vitro*-induced human regulatory T cells are candidates for cell therapy in autoimmune diseases thanks to stable demethylation of the FOXP3 regulatory T cell-specific demethylated region. *J. Immunol.* 194 (1), 113–124. doi:10.4049/jimmunol.1401145

Ryan, M. J., Dudash, H. J., Docherty, M., Geronilla, K. B., Baker, B. A., Haff, G. G., et al. (2010). Vitamin E and C supplementation reduces oxidative stress, improves antioxidant enzymes and positive muscle work in chronically loaded muscles of aged rats. *Exp. Gerontol.* 45 (11), 882–895. doi:10.1016/j.exger.2010.08.002

Salameh, Y., Bejaoui, Y., and El Hajj, N. (2020). DNA methylation biomarkers in aging and age-related diseases. *Front. Genet.* 11, 171. doi:10.3389/fgene.2020.00171

Sanderson, S. M., Gao, X., Dai, Z., and Locasale, J. W. (2019). Methionine metabolism in health and cancer: a nexus of diet and precision medicine. *Nat. Rev. Cancer* 19 (11), 625–637. doi:10.1038/s41568-019-0187-8

Sant, D. W., Camarena, V., Mustafi, S., Li, Y., Wilkes, Z., Van Booven, D., et al. (2018). Ascorbate suppresses VEGF expression in retinal pigment epithelial cells. *Invest. Ophthalmol. Vis. Sci.* 59 (8), 3608–3618. doi:10.1167/iovs.18-24101

Schutsky, E. K., DeNizio, J. E., Hu, P., Liu, M. Y., Nabel, C. S., Fabyanic, E. B., et al. (2018). Nondestructive, base-resolution sequencing of 5-hydroxymethylcytosine using a DNA deaminase. *Nat. Biotechnol.* 36, 1083–1090. doi:10.1038/nbt.4204

Sedivy, J. M., Banumathy, G., and Adams, P. D. (2008). Aging by epigenetics--a consequence of chromatin damage? *Exp. Cell Res.* 314 (9), 1909–1917. doi:10.1016/j.yexcr.2008.02.023

Shibutani, T., Ito, S., Toda, M., Kanao, R., Collins, L. B., Shibata, M., et al. (2014). Guanine- 5-carboxylcytosine base pairs mimic mismatches during DNA replication. *Sci. Rep.* 4, 5220. doi:10.1038/srep05220

Smithells, R. W., Sheppard, S., and Schorah, C. J. (1976). Vitamin dificiencies and neural tube defects. *Archives Dis. Child.* 51 (12), 944–950. doi:10.1136/adc.51.12.944

Suga, K., Suto, A., Tanaka, S., Sugawara, Y., Kageyama, T., Ishikawa, J., et al. (2023). TAp63, a methotrexate target in CD4+ T cells, suppresses Foxp3 expression and exacerbates autoimmune arthritis. *JCI Insight.* 8 (10), e164778. doi:10.1172/jci.insight.164778

Taeubert, M. J., de Prado-Bert, P., Geurtsen, M. L., Mancano, G., Vermeulen, M. J., Reiss, I. K. M., et al. (2022). Maternal iron status in early pregnancy and DNA methylation in offspring: an epigenome-wide meta-analysis. *Clin. Epigenetics* 14 (1), 59. doi:10.1186/s13148-022-01276-w

Tahiliani, M., Koh, K. P., Shen, Y., Pastor, W. A., Bandukwala, H., Brudno, Y., et al. (2009). Conversion of 5-methylcytosine to 5-hydroxymethylcytosine in mammalian DNA by MLL partner TET1. *Science* 324 (5929), 930–935. doi:10.1126/science.1170116

Taira, A., Palin, K., Kuosmanen, A., Valimaki, N., Kuittinen, O., Kuismin, O., et al. (2023). Vitamin C boosts DNA demethylation in TET2 germline mutation carriers. *Clin. Epigenetics* 15 (1), 7. doi:10.1186/s13148-022-01404-6

Tong, X., Zhao, F., and Thompson, C. B. (2009). The molecular determinants of *de novo* nucleotide biosynthesis in cancer cells. *Curr. Opin. Genet. Dev.* 19 (1), 32–37. doi:10.1016/j.gde.2009.01.002

Trautmann, C., Bock, A., Urbach, A., Hübner, C. A., and Engmann, O. (2020). Acute vitamin B12 supplementation evokes antidepressant response and alters Ntrk-2. *Neuropharmacology* 171, 108112. doi:10.1016/j.neuropharm.2020.108112

Wang, L., Zhou, Y., Xu, L., Xiao, R., Lu, X., Chen, L., et al. (2015a). Molecular basis for 5-carboxycytosine recognition by RNA polymerase II elongation complex. *Nature* 523 (7562), 621–625. doi:10.1038/nature14482

Wang, T., Chen, K., Zeng, X., Yang, J., Wu, Y., Shi, X., et al. (2011). The histone demethylases Jhdm1a/1b enhance somatic cell reprogramming in a vitamin-C-dependent manner. *Cell Stem Cell* 9 (6), 575–587. doi:10.1016/j.stem.2011.10.005

Wang, X., Guan, Z., Chen, Y., Dong, Y., Niu, Y., Wang, J., et al. (2015b). Genomic DNA hypomethylation is associated with neural tube defects induced by methotrexate inhibition of folate metabolism. *PloS one* 10 (3), e0121869. doi:10.1371/journal.pone.0121869

Wilkinson, G. S., Adams, D. M., Haghani, A., Lu, A. T., Zoller, J., Breeze, C. E., et al. (2021). DNA methylation predicts age and provides insight into exceptional longevity of bats. *Nat. Commun.* 12 (1), 1615. doi:10.1038/s41467-021-21900-2

Williams, K., Christensen, J., Pedersen, M. T., Johansen, J. V., Cloos, P. A., Rappsilber, J., et al. (2011). TET1 and hydroxymethylcytosine in transcription and DNA methylation fidelity. *Nature* 473 (7347), 343–348. doi:10.1038/nature10066

Wu, H., D'Alessio, A. C., Ito, S., Wang, Z., Cui, K., Zhao, K., et al. (2011). Genome-wide analysis of 5-hydroxymethylcytosine distribution reveals its dual function in transcriptional regulation in mouse embryonic stem cells. *Genes Dev.* 25 (7), 679–684. doi:10.1101/gad.2036011

Wu, M. J., Kim, M. R., Chen, Y. S., Yang, J. Y., and Chang, C. J. (2017). Retinoic acid directs breast cancer cell state changes through regulation of TET2-PKCζ pathway. *Oncogene* 36 (22), 3193–3206. doi:10.1038/onc.2016.467

Wu, X., and Zhang, Y. (2017). TET-mediated active DNA demethylation: mechanism, function and beyond. *Nat. Rev. Genet.* 18 (9), 517–534. doi:10.1038/nrg.2017.33

Xia, B., Han, D., Lu, X., Sun, Z., Zhou, A., Yin, Q., et al. (2015). Bisulfite-free, base-resolution analysis of 5-formylcytosine at the genome scale. *Nat. Methods* 12 (11), 1047–1050. doi:10.1038/nmeth.3569

Xu, Y. P., Lv, L., Liu, Y., Smith, M. D., Li, W. C., Tan, X. M., et al. (2019). Tumor suppressor TET2 promotes cancer immunity and immunotherapy efficacy. *J. Clin. Investigation* 129 (10), 4316–4331. doi:10.1172/jci129317

Xue, J. H., Chen, G. D., Hao, F., Chen, H., Fang, Z., Chen, F. F., et al. (2019). A vitamin-C-derived DNA modification catalysed by an algal TET homologue. *Nature* 569 (7757), 581–585. doi:10.1038/s41586-019-1160-0

Yadav, D. K., Shrestha, S., Lillycrop, K. A., Joglekar, C. V., Pan, H., Holbrook, J. D., et al. (2018). Vitamin B(12) supplementation influences methylation of genes associated with Type 2 diabetes and its intermediate traits. *Epigenomics* 10 (1), 71–90. doi:10.2217/epi-2017-0102

Yin, R., Mao, S. Q., Zhao, B., Chong, Z., Yang, Y., Zhao, C., et al. (2013). Ascorbic acid enhances Tet-mediated 5-methylcytosine oxidation and promotes DNA demethylation in mammals. *J. Am. Chem. Soc.* 135 (28), 10396–10403. doi:10.1021/ja4028346

Yu, M., Hon, G. C., Szulwach, K. E., Song, C. X., Zhang, L., Kim, A., et al. (2012). Base-resolution analysis of 5-hydroxymethylcytosine in the mammalian genome. *Cell* 149 (6), 1368–1380. doi:10.1016/j.cell.2012.04.027

Yue, X., Samaniego-Castruita, D., Gonzalez-Avalos, E., Li, X., Barwick, B. G., and Rao, A. (2021). Whole-genome analysis of TET dioxygenase function in regulatory T cells. *EMBO Rep.* 22 (8), e52716. doi:10.15252/embr.202152716

Zappe, K., Pointner, A., Switzeny, O. J., Magnet, U., Tomeva, E., Heller, J., et al. (2018). Counteraction of oxidative stress by vitamin E affects epigenetic regulation by increasing global methylation and gene expression of MLH1 and DNMT1 dose dependently in caco-2 cells. *Oxidative Med. Cell. Longev.* 2018, 1–13. doi:10.1155/2018/3734250

Zhang, H., Zhang, X., Clark, E., Mulcahey, M., Huang, S., and Shi, Y. G. (2010). TET1 is a DNA-binding protein that modulates DNA methylation and gene transcription via hydroxylation of 5-methylcytosine. *Cell Res.* 20 (12), 1390–1393. doi:10.1038/cr.2010.156

Zhang, X., Su, J., Jeong, M., Ko, M., Huang, Y., Park, H. J., et al. (2016). DNMT3A and TET2 compete and cooperate to repress lineage-specific transcription factors in hematopoietic stem cells. *Nat. Genet.* 48 (9), 1014–1023. doi:10.1038/ng.3610

Zhang, Y. W., Wang, Z., Xie, W., Cai, Y., Xia, L., Easwaran, H., et al. (2017). Acetylation enhances TET2 function in protecting against abnormal DNA methylation during oxidative stress. *Mol. Cell* 65 (2), 323–335. doi:10.1016/j.molcel.2016.12.013

frontiers | Frontiers in Epigenetics and Epigenomics

TYPE Mini Review
PUBLISHED 16 May 2024
DOI 10.3389/freae.2024.1404958



OPEN ACCESS

EDITED BY
Raul Mostoslavsky,
Massachusetts General Hospital Cancer Center, United States

REVIEWED BY
Jordi Moreno-Romero,
Autonomous University of Barcelona, Spain

*CORRESPONDENCE
Mark Zander,
mzander@waksman.rutgers.edu

†These authors have contributed equally to this work

RECEIVED 22 March 2024
ACCEPTED 30 April 2024
PUBLISHED 16 May 2024

CITATION
Ammari M, Maseh K and Zander M (2024), PIF transcription factors-versatile plant epigenome landscapers.
*Front. Epigenet. Epigenom.* 2:1404958.
doi: 10.3389/freae.2024.1404958



# PIF transcription factors-versatile plant epigenome landscapers

Moonia Ammari†, Kashif Maseh† and Mark Zander*

Department of Plant Biology, Waksman Institute of Microbiology, Rutgers, The State University of New Jersey, Piscataway, NJ, United States

Plants are exquisitely responsive to their local light and temperature environment utilizing these environmental cues to modulate their developmental pathways and adjust growth patterns. This responsiveness is primarily achieved by the intricate interplay between the photoreceptor phyB (phytochrome B) and PIF (PHYTOCHROME INTERACTING FACTORs) transcription factors (TFs), forming a pivotal signaling nexus. phyB and PIFs co-associate in photobodies (PBs) and depending on environmental conditions, PIFs can dissociate from PBs to orchestrate gene expression. Until recently, the mechanisms governing epigenome modifications subsequent to PIF binding to target genes remained elusive. This mini review sheds light on the emerging role of PIFs in mediating epigenome reprogramming by recruiting chromatin regulators (CRs). The formation of numerous different PIF-CR complexes enables precise temporal and spatial control over the gene regulatory networks (GRNs) governing plant-environment interactions. We refer to PIFs as epigenome landscapers, as while they do not directly reprogram the epigenome, they act as critical sequence-specific recruitment platforms for CRs. Intriguingly, in the absence of PIFs, the efficacy of epigenome reprogramming is largely compromised in light and temperature-controlled processes. We have thoroughly examined the composition and function of known PIF-CR complexes and will explore also unanswered questions regarding the precise of locations PIF-mediated epigenome reprogramming within genes, nuclei, and plants.

KEYWORDS

**plant epigenomics, chromatin dynamics, transcription factors, chromatin remodeling complexes, light and temperature signaling**

## Introduction

The major sensor of red (R), far-red (FR) light as well temperature in *Arabidopsis* is the photoreceptor phyB (Quail et al., 1995; Rockwell et al., 2006; Jung et al., 2016; Legris et al., 2016). After photoactivation, phyB translocates from the cytosol to the nucleus where it compartmentalizes into PBs through liquid-liquid phase separation (LLPS) (Sakamoto and Nagatani, 1996; Kircher et al., 1999; Chen et al., 2003; Chen et al., 2022). PBs function as regulatory light and temperature modules, housing a variety of signaling components that interact directly or indirectly with phyB (Van Buskirk et al., 2012; Jung et al., 2016; Legris et al., 2016; Hahm et al., 2020; Pardi and Nusinow, 2021; Kim et al., 2023; Kwon et al., 2024; Willige et al., 2024). One of the most critical PB component are the PIFs, a family of basic helix-loop-helix (bHLH) TFs which acts a transcriptional activators or repressors (Ni et al., 1998; Huq and Quail, 2002; Huq et al., 2004; Oh et al., 2004; Castillon et al., 2007; Leivar et al., 2008; Shen et al., 2008; Leivar and Quail, 2011; Leivar and Monte, 2014). The *Arabidopsis* genome encodes eight *PIFs* (*PIF1-PIF8*), which integrate phyB's environmental input into GRNs underlying light and temperature responses (Leivar and Quail, 2011; Jeong

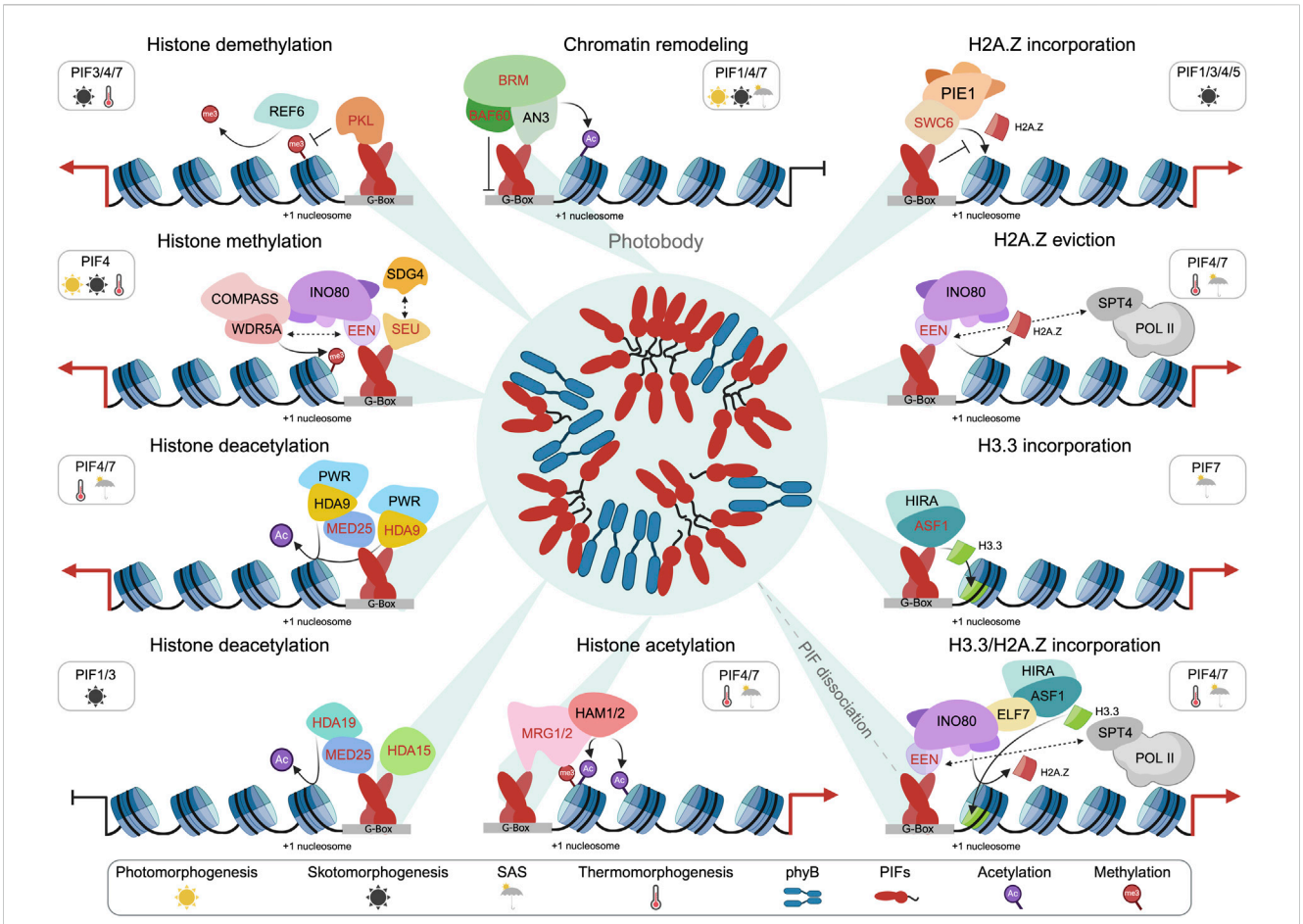


FIGURE 1
The illustration provides an overview of the current understanding of different PIF-CR complexes. The PBs containing phyB-PIF act as a reservoir for PIFs, enabling their dissociation based on environmental cues. Various PIF-controlled features are depicted. While the complexes are presented separately for clarity, they likely function concurrently. The respective PIFs implicated in specific epigenomic features are highlighted, along with symbols denoting the four major processes (SM, PM, SAS, and TM) where the PIF-CR complexes act. EEN-SPT4 and EEN-WDR5A interactions are shown as dashed double arrows for better visualization. Abbreviations: AN3 (ANGUSTIFOLIA3), ASF1 (ANTI-SILENCING FUNCTION 1A/B), BAF60 (BRG1/BRM associated factor 60), BRM (BRAHMA), COMPASS (Complex Proteins Associated with Set1), EEN (EIN6 ENHANCER), ELF7 (EARLY FLOWERING 7), HAM1/2 (HISTONE ACETYLTRANSFERASE OF THE MYST FAMILY 1 and 2), HDA9 (HISTONE DEACETYLASE 9), HDA15 (HISTONE DEACETYLASE 15), HDA19 (HISTONE DEACETYLASE 19), HDA9 (HISTONE DEACETYLASE 9), HIRA (HISTONE REGULATORY HOMOLOG A), INO80 (INOSITOL REQUIRING 80), MED25 (MEDIATOR 25), MRG1/2 (MORF-RELATED GENE 1/2), PIE1 (PHOTOPERIOD-INDEPENDENT EARLY FLOWERING 1), PKL (PICKLE), POL II (RNA Polymerase II), PWR (POWERDRESS), REF6 (RELATIVE OF EARLY FLOWERING 6), SDG4 (SET DOMAIN GROUP 4), SEU (SEUSS), SPT4 (Suppressor of Ty 4), SWC6 (SWR1 complex subunit 6), and WDR5A (WD40 REPEAT 5).

and Choi, 2013; Leivar and Monte, 2014; Pham et al., 2018; Bian et al., 2022; Han et al., 2023). PIF1/3/4/5 control the transition from skotomorphogenesis (SM) to photomorphogenesis (PM) by repressing light-responsive gene expression in the dark until light exposure initiates their phytochrome-mediated phosphorylation, ubiquitination and subsequent proteasomal degradation (Leivar and Quail, 2011; Leivar and Monte, 2014; Pham et al., 2018). Furthermore, PIF7 functions as the major regulator alongside PIF1/3/4/5 in orchestrating the shade avoidance syndrome (SAS) (Willige et al., 2021). This syndrome is induced by low R:FR light ratios (referred to as shade) resulting from nearby vegetation, prompting elongation of hypocotyls and petioles, early flowering, and upward leaf positioning (Franklin and Whitelam, 2005; Franklin, 2008; Casal, 2012; Sessa et al., 2018; Casal and Fankhauser, 2023). A phenotypically similar response to SAS is thermomorphogenesis (TM) which refers to the profound effect of elevated ambient temperature (EAT) (up to 28°C, below the heat stress range) on plant growth, development, and immunity (Casal and Balasubramanian, 2019; Burko et al., 2022). In *Arabidopsis*, TM regulation primarily involves PIF4 and PIF7 (Koini et al., 2009; Kumar et al., 2012; Gangappa et al., 2017; Chung et al., 2020; Fiorucci et al., 2020) whereas TM under shade (low R:FR light) conditions is mainly regulated by PIF7 alone (Burko et al., 2022).

The detailed complex mechanisms governing PIFs at both the transcriptional and protein levels along the crosstalk with other signaling pathways have been extensively discussed in several excellent reviews (Leivar and Quail, 2011; Jeong and Choi, 2013; Shin et al., 2013; Leivar and Monte, 2014; Paik et al., 2017; Pham et al., 2018; Favero, 2020). Additionally, readers are encouraged to explore superb reviews that delve into the exciting connection between light/temperature signaling and chromatin dynamics (Perrella and Kaiserli, 2016; Bourbousse et al., 2019; Jing and Lin,

2020; Perrella et al., 2020). We aim to provide a brief introduction to PIF7, which serves as a partial representation of other PIFs and highlights crucial regulatory aspects such as posttranslational modifications (PTMs), condensate formation, and DNA binding among PIF proteins. In white light (WL) PIF7 is phosphorylated and unlike other PIFs relatively light-stable (Leivar et al., 2008; Huang et al., 2018; Willige et al., 2021; Zhou et al., 2021). PIF7 undergoes LLPS to form biocondensates under WL conditions which subsequently associate with phyB condensates in photobodies (PBs) (Leivar et al., 2008; Willige et al., 2021; Chen et al., 2022; Xie et al., 2023). Upon exposure to shade, PIF7 gets rapidly dephosphorylated and dissociates from PBs to bind to G-boxes (CACGTG) within *cis*-regulatory elements (CREs) of its targets (Chung et al., 2020; Willige et al., 2021; Xie et al., 2023). PIF7 regulates an extensive GRN encompassing multiple biosynthesis genes for the growth-promoting plant hormone auxin, along with numerous transcription factors (TFs) such as *ATHB2* (*ARABIDOPSIS THALIANA HOMEOBOX PROTEIN 2)* (Chung et al., 2020; Willige et al., 2021). A similar signaling mechanism operates during TM (Chung et al., 2020; Fiorucci et al., 2020; Burko et al., 2022), where PIF7 mRNA also serves as a direct thermosensor (Chung et al., 2020).

Here, we will discuss the emerging role of PIFs as epigenome landscapers by recruiting various chromatin regulators (CRs) to shape the epigenome at their target genes (Figure 1). The plant epigenome plays a crucial role as a regulatory framework, integrating both developmental signals and environmental cues into spatiotemporal-specific GRNs (Lloyd and Lister, 2022). In a broad sense, the epigenome encompasses not only all chemical modifications of DNA and histone proteins but also other features that control gene expression, including DNA binding of TFs and CRs, chromatin accessibility, 3D chromatin conformation, nucleosome positioning, and long non-coding RNAs (Rivera and Ren, 2013). We utilize the term CR to encompass all regulatory factors capable of modifying the epigenome, chromatin remodeling complexes (CRCs), histone acetyltransferases/deacetylases (HATs/HDACs), histone methyltransferases/demethylases (KMTs/KDMs), and many others. To enhance comprehension, we discuss various epigenome feature dynamics separately, although it is crucial to recognize their intricate interconnections. Finally, we outline some unresolved questions for further exploration.

## H2A.Z and H3.3 dynamics

Histone variants are histone proteins that differ from canonical histones in their amino acid sequence, structure, and functions (Yi et al., 2006; Borg et al., 2021). One of the best studied histone variants in *Arabidopsis* is H2A.Z that confers gene responsiveness to environmentally-responsive genes (Coleman-Derr and Zilberman, 2012). The *Arabidopsis* genome encodes three functionally redundant H2A.Z genes (*HTA8*, *HTA9*, *HTA11*) whose mutations leads to pleiotropic effects such as early flowering, enhanced disease resistance and DNA hypermethylation (Choi et al., 2007; March-Diaz et al., 2008; Coleman-Derr and Zilberman, 2012; Nie et al., 2019). H2A.Z exerts a repressive influence on transcription, and its eviction is a common characteristic of transcriptional activation in plant-environment interactions (Kumar and Wigge, 2010; Kumar et al., 2012; Boden et al., 2013; Cortijo et al., 2017; Sura et al., 2017; Zander et al., 2019; Willige et al., 2021; Xue et al., 2021).

The discovery of H2A.Z's involvement in PIF-regulated processes occurred with a forward genetic screen aiming to identify temperature sensors in *Arabidopsis* (Kumar and Wigge, 2010). This screen revealed ARP6 (ACTIN-RELATED PROTEIN 6), a subunit of the SWR1 (SWI2/SNF2 (SWITCH/SUCROSE NONFERMENTABLE)-related 1) chromatin remodeler (Choi et al., 2005; Martin-Trillo et al., 2006; Choi et al., 2007), as a negative TM regulator (Kumar and Wigge, 2010). Other key components of the multi-subunit plant SWR1 complex (SWR1-C) are the ATPase PIE1 (PHOTOPERIOD-INDEPENDENT EARLY FLOWERING 1) and accessory units such as SWC6 (SWR1 COMPLEX 6) and SEF (SERRATED LEAVES AND EARLY FLOWERING) (Noh and Amasino, 2003; Choi et al., 2007; March-Di et al., 2007; Luo et al., 2020). Consistent with SWR1-C's role in incorporating H2A.Z into chromatin (Deal et al., 2007), *arp6* mutants have reduced H2A.Z levels resulting in the elevation of thermo-responsive gene expression and longer hypocotyls and petioles even without an EAT stimulus (Kumar and Wigge, 2010). As PIF4 governs the expression of EAT-induced genes (Koini et al., 2009), it was suggested that H2A.Z-containing nucleosomes occlude PIF4 from binding to its target genes. This hindrance is lifted in *arp6* mutants, thereby facilitating higher thermo-responsive gene expression (Kumar and Wigge, 2010).

The first direct connection between H2A.Z and PIFs was shown for PIF4-dependent EAT-induced flowering in *Arabidopsis* (Kumar et al., 2012). EAT-induced expression of *FT* (*FLOWERING LOCUS T*) requires direct PIF4 binding at *FT* which is facilitated by EAT-induced eviction of H2A.Z nucleosomes (Kumar et al., 2012). To elucidate the PIF-H2A.Z interplay in more detail, PIF7 DNA binding as well as H2A.Z occupancy in wildtype and *pif457* mutants were tracked simultaneously during SAS over time using ChIP-seq (Chromatin immunoprecipitation followed by sequencing) (Willige et al., 2021). PIF7 initiates shade-induced H2A.Z eviction at its target genes through the association with the INO80 (INOSITOL REQUIRING 80) chromatin remodeling complex (INO80-C) via direct interaction with its essential subunit EEN (EIN6 ENHANCER) (Zander et al., 2019; Willige et al., 2021). Strikingly, this PIF-INO80-C regulatory module is also operational with PIF4 during TM (Figure 1) (Sureshkumar and Balasubramanian, 2021; Xue et al., 2021).

INO80-C belongs to the INO80-type subfamily of SWI2/SNF2 chromatin remodeler (Clapier and Cairns, 2009; Han et al., 2015) and it was shown in various species that INO80-C can facilitate H2A.Z eviction to regulate gene expression (Papamichos-Chronakis et al., 2011; Alatwi and Downs, 2015; Brahma et al., 2017; Zhao et al., 2022). In plants, INO80-C's role in H2A.Z eviction was shown for ethylene-, low R:FR light-, and EAT-induced genes (Zander et al., 2019; Willige et al., 2021; Xue et al., 2021). INO80-C additionally acts as a platform for recruiting other CRs, thereby potentially expanding the functional capabilities of the PIF-INO80-C regulatory module (Shang et al., 2021; Xue et al., 2021; Zhao et al., 2023). Its subunit EEN interacts with WDR5a (WD40 REPEAT 5), an integral component of the COMPASS (Complex Proteins Associated with Set1) histone H3K4 methyltransferase complex, to facilitate trimethylation of histone 3 lysine 4 (H3K4me3) at PIF4 target genes (Figure 1)

(Xue et al., 2021). The association of INO80-C with other major COMPASS histone H3K4 methyltransferase complex components was independently shown (Shang et al., 2021). In addition, EEN interacts with the transcription elongation factors (TEFs) SPT4 (Suppressor of Ty 4)-1 and SPT4-2 to mediate RNA Polymerase II (RNAPII) elongation during TM (Figure 1) (Xue et al., 2021). Interestingly, PIF1/3/4/5 can also associate with SWR1-C via SWC6 during PM to inhibit H2A.Z deposition (Figure 1) (Chen H. et al., 2023). Under this scenario, PIFs inhibit SWR1-C activity at auxin-responsive genes in the dark through an unknown mechanism (Chen H. et al., 2023). All these findings indicate that PIFs can use multiple strategies to alter the H2A.Z landscape at their target genes thereby fine-tuning their expression in an environmental stimulus-dependent manner.

The histone variant H3.3 forms together with the replicative H3.1/H3.2, and the centromeric CenH3 the H3 (Histone 3) family (Henikoff and Ahmad, 2005; Borg et al., 2021). H3.3 is incorporated during transcription and rapid upregulation of environmentally-responsive genes is compromised in *h3.3* knockdown mutants (Wollmann et al., 2017). The deposition of H3.3 is in part mediated by the histone chaperones ASF1A (ANTI-SILENCING FUNCTION 1A) and ASF1B in conjunction with the histone chaperone HIRA (HISTONE REGULATORY HOMOLOG A) (Tagami et al., 2004; Zhu et al., 2011; Nie et al., 2014; Duc et al., 2015; Zhong et al., 2022). During SAS, PIF7 recruits ASF1A/B and HIRA to facilitate H3.3 deposition at shade-responsive genes (Figure 1) (Yang et al., 2023). In addition, *asf1ab* and *hira* mutants show also reduced hypocotyl elongation under EAT (Yang et al., 2023; Zhao et al., 2023) which suggest that the PIF-ASF1A/B-HIRA module is also operational during TM. Although a PIF4-ASF1A/B interaction has not been confirmed, ASF1A/B could also be indirectly recruited by PIF4 through the INO80 ATPase that associates with ASF1A/B through the TEF PAF1c (Polymerase-Associated Factor 1 complex) subunit ELF7 (EARLY FLOWERING 7) (Figure 1) (Zhao et al., 2023). These findings highlight again the prominent role of PIFs in initiating epigenomic reprogramming through the recruitment of functionally diverse CRs.

## Histone acetylation dynamics

One of the most extensively studied PTM of histones is acetylation, which plays a crucial role in numerous gene regulatory processes (Jiang et al., 2020; Shvedunova and Akhtar, 2022; Chen Y. et al., 2023). Acetylation occurring at various lysine residues of histones H3 and H4, such as H3K9ac or H3K27ac, typically corresponds to gene activation, whereas deacetylation is associated with gene repression (Pandey et al., 2002). The balance of histone acetylation is regulated by the interplay between HATs and HDACs (Eberharter and Becker, 2002). The *Arabidopsis* genome encodes for 12 HATs and 18 HDACs (Pandey et al., 2002; Hollender and Liu, 2008), and although no direct interactions between PIFs and HATs have been documented, an active role of HATs in PIF-mediated chromatin reprogramming can be inferred (Martínez-García and Moreno-Romero, 2020). During SAS, H3K9ac levels rapidly increase at gene bodies of shade-responsive genes in a PIF4/5/7-dependent manner (Willige et al., 2021). Furthermore, levels of H4K5ac, H3K9ac, and H3K27ac increase in response to shade and EAT at *YUC8* in a PIF4/7-dependent manner (Peng et al., 2018; Zhou et al., 2024).

PIF4/7 directly associate with MRG1/2 (MORF-RELATED GENE 1/2) which are histone methylation readers that bind to H3K4/H3K36 trimethylation (H3K4me3/H3K36me3) and can interact with the HATs HAM1/2 (HISTONE ACETYLTRANSFERASE OF THE MYST FAMILY 1 and 2) (Xu et al., 2014). The recruitment of HAM1/2 through the PIF4/7-MRG1/2 module is the current model of PIF4/7-driven histone acetylation dynamics during SAS and TM (Figure 1) (Peng et al., 2018; Zhou et al., 2024). However, additional experimental support is needed because no direct association of HAM1/2 with PIF target genes has been shown so far (Latrasse et al., 2008).

HDA9 (HISTONE DEACETYLASE 9) was found to positively regulate hypocotyl elongation during TM and SAS (Tasset et al., 2018; van der Woude et al., 2019; Nguyen et al., 2023). HDA9's positive role is still puzzling since expression of *PIF4* and *YUC8*, both essential regulators of EAT-induced hypocotyl elongation (Koini et al., 2009; Franklin et al., 2011; Sun et al., 2012; Proveniers and van Zanten, 2013; Bellstaedt et al., 2019), requires HDA9-mediated H3K9ac/14ac deacetylation at its +1 nucleosome (van der Woude et al., 2019). Interestingly, mutation of the HDA9-interacting SANT-domain containing protein PWR (POWERDRESS), phenocopies *hda9* mutants regarding reduced *PIF4/YUC8* expression due to higher H3K9ac levels (Tasset et al., 2018). EAT-induced H2A.Z eviction was also compromised in *hda9* mutants (van der Woude et al., 2019), however, the mechanism of how HDA9 regulates H2A.Z eviction is still unclear. Although PIF4 was not found to interact with HDA9 (van der Woude et al., 2019), PIF7 was recently identified as an interactor of HDA9 (Nguyen et al., 2023). Given PIF7's critical role in TM and its capacity to heterodimerize with PIF4 (Kidokoro et al., 2009; Fiorucci et al., 2020), it's possible that a PIF7/PIF4 heterodimer recruits the HDA9-PWR module to its target genes (Figure 1). The hypothesis of HDA9 recruitment to shade-induced genes via PIF7 has also been proposed for SAS (Nguyen et al., 2023).

During SM, HDA15 (HISTONE DEACETYLASE 15) is recruited by PIF3 to repress the expression of photosynthesis genes through H4 deacetylation (Liu et al., 2013). In addition, PIF1 also interacts with HDA15 to repress genes via histone deacetylation (H3ac) during seed germination in the dark (Figure 1) (Gu et al., 2017). In contrast to HDA9's positive role, HDA15 is a negative TM regulator directly associating at thermo-responsive genes potentially through HFR1 (LONG HYPOCOTYL IN FAR-RED) (Shen et al., 2019). A current hypothesis that elucidates the contradictory functions of HDA9 and HDA15 proposes that at higher temperatures, the HFR1-HDA15 complex is displaced by PIF4, possibly forming a complex with HDA9 and PWR (Shen et al., 2019). HDA19 is an additional PIF1/3-interacting HDAC that represses PM via H3 deacetylation at the PM genes *BBX21* (*B-BOX CONTAINING PROTEIN 21*) and *GLK1* (*GOLDEN2-LIKE1*) (Guo et al., 2023). Another possible route of connecting PIFs with HDACs is HOS1 (HIGH EXPRESSION OF OSMOTICALLY RESPONSIVE GENE 1), a RING E3 ligase which can directly interact with PIF4 but also with HDA6 (HISTONE DEACETYLASE 6) and HDA15 (Jung et al., 2013; Kim et al., 2017).

An additional functional link between PIFs and HDACs are the subunits MED25 (MEDIATOR 25) and MED14 (MEDIATOR 14) of the Mediator complex (Bajracharya et al., 2022; Guo et al., 2023; Shapulatov et al., 2023), which is an evolutionary conserved large multi-subunit protein complex regulating RNAPII function on various levels (Allen and Taatjes, 2015; Soutourina, 2018). MED25 or PFT1 (PHYTOCHROME AND FLOWERING TIME 1) was first discovered as a SAS regulator and can interact with PIF4 in *Arabidopsis* and tomato to recruit RNAPII (Sun et al., 2020; Shapulatov et al., 2023). During TM, MED25 can associate with HDA9, thereby potentially facilitating the PIF4-mediated recruitment of HDA9 for histone deacetylation at the *PIF4* and *YUC8* gene (Figure 1) (Shapulatov et al., 2023). Moreover, PIF1 and PIF3 also interact with MED25 and HDA19 to down-regulate the expression of positive the positive PM regulators *BBX21* and *GLK1* via histone deacetylation and reducing chromatin accessibility (Figure 1) (Guo et al., 2023). Intriguingly, MED25 also undergoes LLPS to form biomolecular condensates with PIF1/3 and HDA19 (Guo et al., 2023). Moreover, PIF4 as well as its coactivator HMR (HEMERA) interact with MED14 to positively regulate thermo-responsive genes (Bajracharya et al., 2022).

Also noteworthy is the recently resolved protein composition of PBs, which has identified the Groucho/Tup1-type co-repressors TPL (TOPLESS) and TPR1 (TOPLESS-RELATED 1) as PB components (Kim et al., 2023). TPL and TPRs putatively exert their repressive function through the direct association with various HDACs such HDA6 and HDA19 (Long et al., 2006; Krogan et al., 2012; Wang et al., 2013; Plant et al., 2021). The confirmation of whether PIFs indeed interact with TPL/TPRs at their target genes remains uncertain at this point. However, the spatial proximity of PIFs and TPL/TPRs in PBs implies a potential functional connection (Kim et al., 2023). In addition, an interaction of PIF1 with LUH (LEUNIG_HOMOLOG), another member of the Groucho/Tup1-type co-repressor family, was shown to regulate expression of PIF1 target genes during seed germination through an unknown mechanism (Lee et al., 2015; Kim et al., 2023).

## Histone methylation dynamics

Methylation of various lysine (K) residues of histones H3 and H4 can occur in plants and depending on the modified lysine residue and degree of methylation (mono-, di-, and/or tri), gene expression is instructed differently (Liu et al., 2010; Xiao et al., 2016; Cheng et al., 2020). H3K4me3 on the +1 nucleosome is a critical epigenome feature indicating active genes, and assessing H3K4me3 occupancy is commonly employed as an indicator of an active chromatin state (Bernstein et al., 2002). Mutants in PIF-interacting CRs frequently exhibit altered levels of H3K4me3 at PIF target genes (Huai et al., 2018) However, whether this alteration is regulatory in nature or merely a consequence of transcriptional changes remains unclear. Until very recently, the exact function of H3K4me3 remained elusive. Using an elegant acute depletion method, all SET1/COMPASS complexes were eliminated from mouse embryonic stem cells, unveiling the critical involvement of H3K4me3 in regulating RNAPII pausing, elongation, and eviction (Wang et al., 2023).

The dark-to-light transition at the beginning of PM leads to a PIF-dependent rapid upregulation of gene expression and H3K4me3 levels (Calderon et al., 2022). How this achieved in a PIF-dependent manner is not clear but the PIF4 interacting transcriptional co-regulator SEU (SEUSS) might provide a link between PIFs and active H3K4me3 regulation (Figure 1) (Huai et al., 2018). SEU is a negative PM regulator under red, far-red, and blue light conditions, but interestingly a positive TM regulator (Huai et al., 2018). It has been demonstrated for SEUSS that it controls H3K4me3 deposition at *WOX5* (*WUSCHEL-RELATED HOMEOBOX 5*) targets genes by associating with the H3K4 methyltransferase SDG4 (SET DOMAIN GROUP 4) (Zhai et al., 2020). Therefore, it is plausible to hypothesize the existence of an operational PIF-SEU-SDG4 complex. Additionally, PIFs regulate the local H3K4me3 environment at their target genes by associating with INO80-C/COMPASS complexes during TM (Figure 1) (Shang et al., 2021; Xue et al., 2021).

Removal of histone methylation marks is facilitated by jumonji domain-containing histone demethylases (Lu et al., 2008; Mosammaparast and Shi, 2010). The primary demethylase in *Arabidopsis* is REF6 (RELATIVE OF EARLY FLOWERING 6) whose mutation causes ectopic gain of H3K27me3 at thousands of genes (Lu et al., 2011; Zander et al., 2019). REF6 was found to cooperatively regulate EAT-induced gene expression with PIF4 via H3K27me3 demethylation (Figure 1) (He et al., 2022). Whether REF6 can interact with PIFs is unknown but it can interact with INO80-C (Smaczniak et al., 2012), suggesting a potential regulatory pathway through which PIFs could influence the H3K27me3 landscape. During SM, PIF3 interacts with the SWI/SWF chromatin-remodeler (PKL/EPP1) (PICKLE/ENHANCED PHOTOMORPHOGENIC1) to repress H3K27me3 deposition at PIF3 target sites (Figure 1) (Zhang et al., 2014). How PKL inhibits the H3K27me3 deposition is not understood since PKL acts cooperatively with the SWR1-C ATPase PIE1 and the H3K27 methyltransferase CLF (CURLY LEAF) to establish and maintain the H3K27me3 landscape in *Arabidopsis* (Carter et al., 2018).

## Chromatin remodeling

Chromatin remodeling is a key process in genome organization, transcriptional regulation, DNA repair and replication (Clapier and Cairns, 2009). Of particular importance for gene expression is the accessibility of *cis*-regulatory elements and incorporation/eviction of histone variants which is regulated by multi-subunit ATP-dependent SWI2/SNF2 CRCs (Clapier and Cairns, 2009). Besides the interaction of PIFs with the INO80-type remodelers SWR1-C and INO80-C (Willige et al., 2021; Xue et al., 2021; Chen H. et al., 2023), PIFs also interact with various SWI/SNF-type remodelers (Zhang et al., 2017; Hussain et al., 2022). The SWI/SNF-type family consists of the BRM (BRAHMA)-, SYD (SPLAYED)-, and MINU1/2 (MINUSCULE1/2)-associated SWI/SNF (BAS, SASc (to avoid confusion with SAS), and MAS) complexes (Guo et al., 2022). PIF1 recruits BRM to photosynthesis genes in the dark to repress their expression though mechanism that remains unidentified (Zhang et al., 2017). Moreover, PIF7 interacts with AN3 (ANGUSTIFOLIA3), a subunit of either the BAS or SASc complex (Guo et al., 2022) to regulate leaf cell proliferation during shade (Hussain et al., 2022). Shade-stabilized

PIF7 outcompetes AN3 at it target genes and represses their expression (Hussain et al., 2022). An additional antagonism between PIFs and a SWI/SNF subunit was shown for PIF4 and BAF60 (BRG1/BRM associated factor 60) (Jegu et al., 2017). BAF60 can be a subunit of the BAS, SASc, and MAS complex but because of a reported direct interaction between PIF4 and BRM, an association within the BAS complex is likely (Zhang et al., 2017; Guo et al., 2022). BAF60 target sites overlap with PIF4 DNA binding sites and strikingly BAF60 antagonizes PIF4 binding through the diurnal regulation of DNA accessibility at PIF4 binding sites (Figure 1) (Jegu et al., 2017).

## Discussion

Where in the gene, where in the nucleus, and where in the plant do the PIF-CR complexes act? For PIFs and their respective CRs to interact, they must be brought into proximity. Unlike CRs, which typically occupy gene bodies, PIFs span a wide spectrum, ranging from proximal to distal, intronic, and 3′ CRE binding (Chung et al., 2020; Willige et al., 2021). Most CRE-promoter communications are established by chromatin loops where TF-bound distal CREs or enhancers make direct physical with the proximal promoter/gene body region (Panigrahi and O'Malley, 2021). Indeed, a COP1 (CONSTITUTIVELY PHOTOMORPHOGENIC 1)-controlled phyB-PRC2 (POLYCOMB REPRESSIVE COMPLEX 2)-mediated chromatin loop has been identified at the positive SAS regulator *ATHB2* (Steindler et al., 1999; Kim et al., 2021; Wang et al., 2024), which is one of the most prominent shade and EAT-induced PIF7 targets, possessing an unusually large CRE with five PIF7 binding peaks 3–9 kb (kilobase) upstream of its transcription start site (Chung et al., 2020; Willige et al., 2021; Burko et al., 2022). Notably, the PIF interactor MED25 facilitates chromatin looping during active jasmonic acid (JA) signaling through interaction with the JA master TF MYC2 (Wang et al., 2019). Like MYC2 which can form tetramers to support loop formation (Lian et al., 2017), PIF4 can also form tetramers suggesting the potential of PIF4 to form loops (Gao et al., 2022).

This leads us to the nuclear 3D space and our second question: where precisely within the nucleus do the PIF-CR complexes act? We pose this question due to the rapid nature of shade-induced PIF7 DNA binding, which occurs at a few hundred genes within 5 min of shade exposure (Willige et al., 2021), potentially even earlier. Since we lack information regarding the DNA scanning speed of PIF7, we cannot ascertain whether the swift DNA targeting of PIF7 is attributable to PIF7's search throughout the entire nucleus, or as previously speculated, solely in proximity to PBs (Van Buskirk et al., 2012). Various nuclear bodies in mammals are known to directly regulate chromatin activities (Shan et al., 2023), and intriguingly, a temperature-dependent chromatin association has been demonstrated for phyB (Jung et al., 2016). Moreover, recent findings have unveiled an active role of phyB in chromatin loop formation at the PIF target *ATHB2* (Kim et al., 2021; Wang et al., 2024). To further explore this exciting scenario of PB-associated chromatin structures, future research necessitates 3D chromatin conformation analyses as well as single locus imaging technologies.

All findings presented here stem from bulk-level analyses, which may obscure crucial spatial information (Cole et al., 2021). It has been demonstrated that for EAT-induced hypocotyl elongation, it is crucial for PIF4 to function within the epidermis (Kim et al., 2020), in conjunction with the DOF TF CDF2 (CYCLING DOF FACTOR 2) (Gao et al., 2022). Similarly, epidermal phyB plays a pivotal role in regulating most light responses, including SAS (Kim et al., 2016). Recent advancements in single-cell (sc) technologies, such as single-cell RNA sequencing (scRNA-seq), now facilitate the capturing of gene expression profiles at the single-cell level (Han et al., 2023). Thus far, only one scRNA-seq study has been reported for a *pif* mutant revealing that expression levels of *PIF1/3/4/5* remain relatively uniformly across cells in wildtype aerial tissues, but interestingly, the expression of PIF target genes varies among different cell types in *pifq* mutants (Han et al., 2023). This suggests that the cell-type specificity of PIF signaling may stem from cell type-specific epigenome disparities at PIF target genes (Han et al., 2023). Considering that PIFs initiate epigenome reprogramming at their target genes by recruiting various CR complexes, we hypothesize the existence of cell type-specific PIF-CR complexes to establish gene expression patterns unique to each cell type.

Highlighting these discoveries underscores the pivotal role of PIFs as epigenome landscapers. From our viewpoint, three key elements of PIFs' epigenome landscaping abilities are particularly noteworthy. Firstly, binding of PIFs to CREs at their target genes is the starting point of stimulus-induced epigenome reprogramming. Secondly, most epigenome features can be directly and simultaneously governed by functionally diverse PIF-CR complexes. Thirdly, several PIF-CR modules, such as PIF-INO80-C, PIF-MRG1/2, and PIF-ASF1-HIRA are operational in multiple response pathways like SAS and TM (Shang et al., 2021; Willige et al., 2021; Yang et al., 2023; Zhao et al., 2023; Zhou et al., 2024), indicating that these complexes belong to the general repertoire of PIF-mediated transcriptional regulation.

## Author contributions

MA: Conceptualization, Data curation, Visualization, Writing–original draft. KM: Conceptualization, Data curation, Writing–original draft. MZ: Conceptualization, Data curation, Funding acquisition, Visualization, Writing–original draft, Writing–review and editing.

## Funding

The author(s) declare that financial support was received for the research, authorship, and/or publication of this article. MZ is supported by a National Science Foundation (NSF) CAREER grant IOS-2339927. KM is supported by a Fulbright Foreign Student Program (PS00316055).

## Conflict of interest

The authors declare that the research was conducted in the absence of any commercial or financial relationships that could be construed as a potential conflict of interest.

## Publisher's note



## References

Alatwi, H. E., and Downs, J. A. (2015). Removal of H2A.Z by INO80 promotes homologous recombination. *EMBO Rep.* 16 (8), 986–994. doi:10.15252/embr.201540330

Allen, B. L., and Taatjes, D. J. (2015). The Mediator complex: a central integrator of transcription. *Nat. Rev. Mol. Cell Biol.* 16 (3), 155–166. doi:10.1038/nrm3951

Bajracharya, A., Xi, J., Grace, K. F., Bayer, E. E., Grant, C. A., Clutton, C. H., et al. (2022). PHYTOCHROME-INTERACTING FACTOR 4/HEMERA-mediated thermosensory growth requires the Mediator subunit MED14. *Plant Physiol.* 190 (4), 2706–2721. doi:10.1093/plphys/kiac412

Bellstaedt, J., Trenner, J., Lippmann, R., Poeschl, Y., Zhang, X. X., Friml, J., et al. (2019). A mobile auxin signal connects temperature sensing in cotyledons with growth responses in hypocotyls. *Plant Physiol.* 180 (2), 757–766. doi:10.1104/pp.18.01377

Bernstein, B. E., Humphrey, E. L., Erlich, R. L., Schneider, R., Bouman, P., Liu, J. S., et al. (2002). Methylation of histone H3 Lys 4 in coding regions of active genes. *Proc. Natl. Acad. Sci. U. S. A.* 99 (13), 8695–8700. doi:10.1073/pnas.082249499

Bian, Y., Chu, L., Lin, H., Qi, Y., Fang, Z., and Xu, D. (2022). PIFs- and COP1-HY5-mediated temperature signaling in higher plants. *Stress Biol.* 2 (1), 35. doi:10.1007/s44154-022-00059-w

Boden, S. A., Kavanova, M., Finnegan, E. J., and Wigge, P. A. (2013). Thermal stress effects on grain yield in Brachypodium distachyon occur via H2A.Z-nucleosomes. *Genome Biol.* 14 (6), R65. doi:10.1186/gb-2013-14-6-r65

Borg, M., Jiang, D., and Berger, F. (2021). Histone variants take center stage in shaping the epigenome. *Curr. Opin. Plant Biol.* 61, 101991. doi:10.1016/j.pbi.2020.101991

Bourbousse, C., Barneche, F., and Laloi, C. (2019). Plant chromatin catches the Sun. *Front. Plant Sci.* 10, 1728. doi:10.3389/fpls.2019.01728

Brahma, S., Udugama, M. I., Kim, J., Hada, A., Bhardwaj, S. K., Hailu, S. G., et al. (2017). INO80 exchanges H2A.Z for H2A by translocating on DNA proximal to histone dimers. *Nat. Commun.* 8, 15616. doi:10.1038/ncomms15616

Burko, Y., Willige, B. C., Seluzicki, A., Novak, O., Ljung, K., and Chory, J. (2022). PIF7 is a master regulator of thermomorphogenesis in shade. *Nat. Commun.* 13 (1), 4942. doi:10.1038/s41467-022-32585-6

Calderon, R. H., Dalton, J., Zhang, Y., and Quail, P. H. (2022). Shade triggers posttranscriptional PHYTOCHROME-INTERACTING FACTOR-dependent increases in H3K4 trimethylation. *Plant Physiol.* 190 (3), 1915–1926. doi:10.1093/plphys/kiac282

Carter, B., Bishop, B., Ho, K. K., Huang, R., Jia, W., Zhang, H., et al. (2018). The chromatin remodelers PKL and PIE1 act in an epigenetic pathway that determines H3K27me3 homeostasis in Arabidopsis. *Plant Cell* 30 (6), 1337–1352. doi:10.1105/tpc.17.00867

Casal, J. J. (2012). Shade avoidance. *Arabidopsis Book* 10, e0157. doi:10.1199/tab.0157

Casal, J. J., and Balasubramanian, S. (2019). Thermomorphogenesis. *Annu. Rev. Plant Biol.* 70, 321–346. doi:10.1146/annurev-arplant-050718-095919

Casal, J. J., and Fankhauser, C. (2023). Shade avoidance in the context of climate change. *Plant Physiol.* 191 (3), 1475–1491. doi:10.1093/plphys/kiad004

Castillon, A., Shen, H., and Huq, E. (2007). Phytochrome Interacting Factors: central players in phytochrome-mediated light signaling networks. *Trends Plant Sci.* 12 (11), 514–521. doi:10.1016/j.tplants.2007.10.001

Chen, D., Lyu, M., Kou, X., Li, J., Yang, Z., Gao, L., et al. (2022). Integration of light and temperature sensing by liquid-liquid phase separation of phytochrome B. *Mol. Cell* 82 (16), 3015–3029.e6. doi:10.1016/j.molcel.2022.05.026

Chen, H., Wang, W., Chen, X., Niu, Y., Qi, Y., Yu, Z., et al. (2023a). PIFs interact with SWI2/SNF2-related 1 complex subunit 6 to regulate H2A.Z deposition and photomorphogenesis in Arabidopsis. *J. Genet. Genomics* 50 (12), 983–992. doi:10.1016/j.jgg.2023.04.008

Chen, M., Schwab, R., and Chory, J. (2003). Characterization of the requirements for localization of phytochrome B to nuclear bodies. *Proc. Natl. Acad. Sci. U. S. A.* 100 (24), 14493–14498. doi:10.1073/pnas.1935989100

Chen, Y., Guo, P. G., and Dong, Z. C. (2023b). The role of histone acetylation in transcriptional regulation and seed development. *Plant Physiol.* 194, 1962–1979. doi:10.1093/plphys/kiad614

Cheng, K., Xu, Y., Yang, C., Ouellette, L., Niu, L., Zhou, X., et al. (2020). Histone tales: lysine methylation, a protagonist in Arabidopsis development. *J. Exp. Bot.* 71 (3), 793–807. doi:10.1093/jxb/erz435

Choi, K., Kim, S., Kim, S. Y., Kim, M., Hyun, Y., Lee, H., et al. (2005). *SUPPRESSOR of FRIGIDA3*Encodes a nuclear ACTIN-RELATED PROTEIN6 required for floral repression in*Arabidopsis* 🅜. *Plant Cell* 17 (10), 2647–2660. doi:10.1105/tpc.105.035485

Choi, K., Park, C., Lee, J., Oh, M., Noh, B., and Lee, I. (2007). Arabidopsis homologs of components of the SWR1 complex regulate flowering and plant development. *Development* 134 (10), 1931–1941. doi:10.1242/dev.001891

Chung, B. Y. W., Balcerowicz, M., Di Antonio, M., Jaeger, K. E., Geng, F., Franaszek, K., et al. (2020). An RNA thermoswitch regulates daytime growth in Arabidopsis. *Nat. Plants* 6 (5), 522–532. doi:10.1038/s41477-020-0633-3

Clapier, C. R., and Cairns, B. R. (2009). The biology of chromatin remodeling complexes. *Annu. Rev. Biochem.* 78, 273–304. doi:10.1146/annurev.biochem.77.062706.153223

Cole, B., Bergmann, D., Blaby-Haas, C. E., Blaby, I. K., Bouchard, K. E., Brady, S. M., et al. (2021). Plant single-cell solutions for energy and the environment. *Commun. Biol.* 4 (1), 962. doi:10.1038/s42003-021-02477-4

Coleman-Derr, D., and Zilberman, D. (2012). Deposition of histone variant H2A.Z within gene bodies regulates responsive genes. *PLoS Genet.* 8 (10), e1002988. doi:10.1371/journal.pgen.1002988

Cortijo, S., Charoensawan, V., Brestovitsky, A., Buning, R., Ravarani, C., Rhodes, D., et al. (2017). Transcriptional regulation of the ambient temperature response by H2A.Z nucleosomes and HSF1 transcription factors in Arabidopsis. *Mol. Plant* 10 (10), 1258–1273. doi:10.1016/j.molp.2017.08.014

Deal, R. B., Topp, C. N., McKinney, E. C., and Meagher, R. B. (2007). Repression of flowering in*Arabidopsis*Requires activation of*FLOWERING LOCUS C*Expression by the histone variant H2A.Z. *Plant Cell* 19 (1), 74–83. doi:10.1105/tpc.106.048447

Duc, C., Benoit, M., Le Goff, S., Simon, L., Poulet, A., Cotterell, S., et al. (2015). The histone chaperone complex HIR maintains nucleosome occupancy and counterbalances impaired histone deposition in CAF-1 complex mutants. *Plant J.* 81 (5), 707–722. doi:10.1111/tpj.12758

Eberharter, A., and Becker, P. B. (2002). Histone acetylation: a switch between repressive and permissive chromatin - second in review series on chromatin dynamics. *Embo Rep.* 3 (3), 224–229. doi:10.1093/embo-reports/kvf053

Favero, D. S. (2020). Mechanisms regulating PIF transcription factor activity at the protein level. *Physiol. Plant.* 169 (3), 325–335. doi:10.1111/ppl.13075

Fiorucci, A. S., Galvao, V. C., Ince, Y. C., Boccaccini, A., Goyal, A., Allenbach Petrolati, L., et al. (2020). PHYTOCHROME INTERACTING FACTOR 7 is important for early responses to elevated temperature in Arabidopsis seedlings. *New Phytol.* 226 (1), 50–58. doi:10.1111/nph.16316

Franklin, K. A. (2008). Shade avoidance. *New Phytol.* 179 (4), 930–944. doi:10.1111/j.1469-8137.2008.02507.x

Franklin, K. A., Lee, S. H., Patel, D., Kumar, S. V., Spartz, A. K., Gu, C., et al. (2011). PHYTOCHROME-INTERACTING FACTOR 4 (PIF4) regulates auxin biosynthesis at high temperature. *Proc. Natl. Acad. Sci.* 108 (50), 20231–20235. doi:10.1073/pnas.1110682108

Franklin, K. A., and Whitelam, G. C. (2005). Phytochromes and shade-avoidance responses in plants. *Ann. Bot.* 96 (2), 169–175. doi:10.1093/aob/mci165

Gangappa, S. N., Berriri, S., and Kumar, S. V. (2017). PIF4 coordinates thermosensory growth and immunity in Arabidopsis. *Curr. Biol.* 27 (2), 243–249. doi:10.1016/j.cub.2016.11.012

Gao, H., Song, W., Severing, E., Vayssieres, A., Huettel, B., Franzen, R., et al. (2022). PIF4 enhances DNA binding of CDF2 to co-regulate target gene expression and promote Arabidopsis hypocotyl cell elongation. *Nat. Plants* 8 (9), 1082–1093. doi:10.1038/s41477-022-01213-y

Gu, D. C., Chen, C. Y., Zhao, M. L., Zhao, L. M., Duan, X. W., Duan, J., et al. (2017). Identification of HDA15-PIF1 as a key repression module directing the transcriptional network of seed germination in the dark. *Nucleic Acids Res.* 45 (12), 7137–7150. doi:10.1093/nar/gkx283

Guo, J., Cai, G., Li, Y. Q., Zhang, Y. X., Su, Y. N., Yuan, D. Y., et al. (2022). Comprehensive characterization of three classes of Arabidopsis SWI/SNF chromatin remodelling complexes. *Nat. Plants* 8 (12), 1423–1439. doi:10.1038/s41477-022-01282-z

Guo, Q., Jing, Y. J., Gao, Y., Liu, Y. T., Fang, X. F., and Lin, R. C. (2023). The PIF1/PIF3-MED25-HDA19 transcriptional repression complex regulates phytochrome signaling in Arabidopsis. *New Phytol.* 240 (3), 1097–1115. doi:10.1111/nph.19205

Hahm, J., Kim, K., Qiu, Y., and Chen, M. (2020). Increasing ambient temperature progressively disassembles Arabidopsis phytochrome B from individual photobodies with distinct thermostabilities. *Nat. Commun.* 11 (1), 1660. doi:10.1038/s41467-020-15526-z

Han, S. K., Wu, M. F., Cui, S., and Wagner, D. (2015). Roles and activities of chromatin remodeling ATPases in plants. *Plant J.* 83 (1), 62–77. doi:10.1111/tpj.12877

Han, X., Zhang, Y., Lou, Z., Li, J., Wang, Z., Gao, C., et al. (2023). Time series single-cell transcriptional atlases reveal cell fate differentiation driven by light in Arabidopsis seedlings. *Nat. Plants* 9 (12), 2095–2109. doi:10.1038/s41477-023-01544-4

He, K. X., Mei, H. L., Zhu, J. P., Qiu, Q., Cao, X. F., and Deng, X. (2022). The histone H3K27 demethylase REF6/JMJ12 promotes thermomorphogenesis in *Arabidopsis*. *Natl. Sci. Rev.* 9 (5), nwab213. doi:10.1093/nsr/nwab213

Henikoff, S., and Ahmad, K. (2005). Assembly of variant histones into chromatin. *Annu. Rev. Cell Dev. Biol.* 21, 133–153. doi:10.1146/annurev.cellbio.21.012704.133518

Hollender, C., and Liu, Z. (2008). Histone deacetylase genes in Arabidopsis development. *J. Integr. Plant Biol.* 50 (7), 875–885. doi:10.1111/j.1744-7909.2008.00704.x

Huai, J., Zhang, X., Li, J., Ma, T., Zha, P., Jing, Y., et al. (2018). SEUSS and PIF4 coordinately regulate light and temperature signaling pathways to control plant growth. *Mol. Plant* 11 (7), 928–942. doi:10.1016/j.molp.2018.04.005

Huang, X., Zhang, Q., Jiang, Y. P., Yang, C. W., Wang, Q. Y., and Li, L. (2018). Shade-induced nuclear localization of PIF7 is regulated by phosphorylation and 14-3-3 proteins in Arabidopsis. *Elife* 7, e31636. doi:10.7554/elife.31636

Huq, E., Al-Sady, B., Hudson, M., Kim, C. H., Apel, K., and Quail, P. H. (2004). PHYTOCHROME-INTERACTING FACTOR 1 is a critical bHLH regulator of chlorophyll biosynthesis. *Science* 305 (5692), 1937–1941. doi:10.1126/science.1099728

Huq, E., and Quail, P. H. (2002). PIF4, a phytochrome-interacting bHLH factor, functions as a negative regulator of phytochrome B signaling in Arabidopsis. *EMBO J.* 21 (10), 2441–2450. doi:10.1093/emboj/21.10.2441

Hussain, E., Romanowski, A., and Halliday, K. J. (2022). PIF7 controls leaf cell proliferation through an AN3 substitution repression mechanism. *Proc. Natl. Acad. Sci. U. S. A.* 119 (5), e2115682119. doi:10.1073/pnas.2115682119

Jegu, T., Veluchamy, A., Ramirez-Prado, J. S., Rizzi-Paillet, C., Perez, M., Lhomme, A., et al. (2017). The Arabidopsis SWI/SNF protein BAF60 mediates seedling growth control by modulating DNA accessibility. *Genome Biol.* 18 (1), 114. doi:10.1186/s13059-017-1246-7

Jeong, J., and Choi, G. (2013). Phytochrome-interacting factors have both shared and distinct biological roles. *Mol. Cells* 35 (5), 371–380. doi:10.1007/s10059-013-0135-5

Jiang, J. J., Ding, A. B., Liu, F. Q., and Zhong, X. H. (2020). Linking signaling pathways to histone acetylation dynamics in plants. *J. Exp. Bot.* 71 (17), 5179–5190. doi:10.1093/jxb/eraa202

Jing, Y., and Lin, R. (2020). Transcriptional regulatory network of the light signaling pathways. *New Phytol.* 227 (3), 683–697. doi:10.1111/nph.16602

Jung, J. H., Domijan, M., Klose, C., Biswas, S., Ezer, D., Gao, M., et al. (2016). Phytochromes function as thermosensors in Arabidopsis. *Science* 354 (6314), 886–889. doi:10.1126/science.aaf6005

Jung, J. H., Park, J. H., Lee, S., To, T. K., Kim, J. M., Seki, M., et al. (2013). The cold signaling attenuator HIGH EXPRESSION OF OSMOTICALLY RESPONSIVE GENE1 activates FLOWERING LOCUS C transcription via chromatin remodeling under short-term cold stress in Arabidopsis. *Plant Cell* 25 (11), 4378–4390. doi:10.1105/tpc.113.118364

Kidokoro, S., Maruyama, K., Nakashima, K., Imura, Y., Narusaka, Y., Shinwari, Z. K., et al. (2009). The phytochrome-interacting factor PIF7 negatively regulates DREB1 expression under circadian control in Arabidopsis. *Plant Physiol.* 151 (4), 2046–2057. doi:10.1104/pp.109.147033

Kim, C., Kwon, Y., Jeong, J., Kang, M., Lee, G. S., Moon, J. H., et al. (2023). Phytochrome B photobodies are comprised of phytochrome B and its primary and secondary interacting proteins. *Nat. Commun.* 14 (1), 1708. doi:10.1038/s41467-023-37421-z

Kim, J., Bordiya, Y., Kathare, P. K., Zhao, B., Zong, W., Huq, E., et al. (2021). Phytochrome B triggers light-dependent chromatin remodelling through the PRC2-associated PHD finger protein VIL1. *Nat. Plants* 7 (9), 1213–1219. doi:10.1038/s41477-021-00986-y

Kim, J., Song, K., Park, E., Kim, K., Bae, G., and Choi, G. (2016). Epidermal phytochrome B inhibits hypocotyl negative gravitropism non-cell-autonomously. *Plant Cell* 28 (11), 2770–2785. doi:10.1105/tpc.16.00487

Kim, J. H., Lee, H. J., Jung, J. H., Lee, S., and Park, C. M. (2017). HOS1 facilitates the phytochrome B-mediated inhibition of PIF4 function during hypocotyl growth in Arabidopsis. *Mol. Plant* 10 (2), 274–284. doi:10.1016/j.molp.2016.11.009

Kim, S., Hwang, G., Kim, S., Thi, T. N., Kim, H., Jeong, J., et al. (2020). The epidermis coordinates thermoresponsive growth through the phyB-PIF4-auxin pathway. *Nat. Commun.* 11 (1), 1053. doi:10.1038/s41467-020-14905-w

Kircher, S., Kozma-Bognar, L., Kim, L., Adam, E., Harter, K., Schafer, E., et al. (1999). Light quality-dependent nuclear import of the plant photoreceptors phytochrome A and B. *Plant Cell* 11 (8), 1445–1456. doi:10.2307/3870974

Koini, M. A., Alvey, L., Allen, T., Tilley, C. A., Harberd, N. P., Whitelam, G. C., et al. (2009). High temperature-mediated adaptations in plant architecture require the bHLH transcription factor PIF4. *Curr. Biol.* 19 (5), 408–413. doi:10.1016/j.cub.2009.01.046

Krogan, N. T., Hogan, K., and Long, J. A. (2012). APETALA2 negatively regulates multiple floral organ identity genes in Arabidopsis by recruiting the co-repressor TOPLESS and the histone deacetylase HDA19. *Development* 139 (22), 4180–4190. doi:10.1242/dev.085407

Kumar, S. V., Lucyshyn, D., Jaeger, K. E., Alos, E., Alvey, E., Harberd, N. P., et al. (2012). Transcription factor PIF4 controls the thermosensory activation of flowering. *Nature* 484 (7393), 242–245. doi:10.1038/nature10928

Kumar, S. V., and Wigge, P. A. (2010). H2A.Z-containing nucleosomes mediate the thermosensory response in Arabidopsis. *Cell* 140 (1), 136–147. doi:10.1016/j.cell.2009.11.006

Kwon, Y., Kim, C., and Choi, G. (2024). Phytochrome B photobody components. *New Phytol.* 242, 909–915. doi:10.1111/nph.19675

Latrasse, D., Benhamed, M., Henry, Y., Domenichini, S., Kim, W., Zhou, D. X., et al. (2008). The MYST histone acetyltransferases are essential for gametophyte development in Arabidopsis. *BMC Plant Biol.* 8, 121. doi:10.1186/1471-2229-8-121

Lee, N., Park, J., Kim, K., and Choi, G. (2015). The transcriptional coregulator LEUNIG_HOMOLOG inhibits light-dependent seed germination in Arabidopsis. *Plant Cell* 27 (8), 2301–2313. doi:10.1105/tpc.15.00444

Legris, M., Klose, C., Burgie, E. S., Rojas, C. C., Neme, M., Hiltbrunner, A., et al. (2016). Phytochrome B integrates light and temperature signals in Arabidopsis. *Science* 354 (6314), 897–900. doi:10.1126/science.aaf5656

Leivar, P., and Monte, E. (2014). PIFs: systems integrators in plant development. *Plant Cell* 26 (1), 56–78. doi:10.1105/tpc.113.120857

Leivar, P., Monte, E., Al-Sady, B., Carle, C., Storer, A., Alonso, J. M., et al. (2008). The Arabidopsis phytochrome-interacting factor PIF7, together with PIF3 and PIF4, regulates responses to prolonged red light by modulating phyB levels. *Plant Cell* 20 (2), 337–352. doi:10.1105/tpc.107.052142

Leivar, P., and Quail, P. H. (2011). PIFs: pivotal components in a cellular signaling hub. *Trends Plant Sci.* 16 (1), 19–28. doi:10.1016/j.tplants.2010.08.003

Lian, T. F., Xu, Y. P., Li, L. F., and Su, X. D. (2017). Crystal structure of tetrameric Arabidopsis MYC2 reveals the mechanism of enhanced interaction with DNA. *Cell Rep.* 19 (7), 1334–1342. doi:10.1016/j.celrep.2017.04.057

Liu, C., Lu, F., Cui, X., and Cao, X. (2010). Histone methylation in higher plants. *Annu. Rev. Plant Biol.* 61, 395–420. doi:10.1146/annurev.arplant.043008.091939

Liu, X., Chen, C. Y., Wang, K. C., Luo, M., Tai, R., Yuan, L., et al. (2013). PHYTOCHROME INTERACTING FACTOR3 associates with the histone deacetylase HDA15 in repression of chlorophyll biosynthesis and photosynthesis in etiolated Arabidopsis seedlings. *Plant Cell* 25 (4), 1258–1273. doi:10.1105/tpc.113.109710

Lloyd, J. P. B., and Lister, R. (2022). Epigenome plasticity in plants. *Nat. Rev. Genet.* 23 (1), 55–68. doi:10.1038/s41576-021-00407-y

Long, J. A., Ohno, C., Smith, Z. R., and Meyerowitz, E. M. (2006). TOPLESS regulates apical embryonic fate in Arabidopsis. *Science* 312 (5779), 1520–1523. doi:10.1126/science.1123841

Lu, F., Cui, X., Zhang, S., Jenuwein, T., and Cao, X. (2011). Arabidopsis REF6 is a histone H3 lysine 27 demethylase. *Nat. Genet.* 43 (7), 715–719. doi:10.1038/ng.854

Lu, F., Li, G., Cui, X., Liu, C., Wang, X. J., and Cao, X. (2008). Comparative analysis of JmjC domain-containing proteins reveals the potential histone demethylases in Arabidopsis and rice. *J. Integr. Plant Biol.* 50 (7), 886–896. doi:10.1111/j.1744-7909.2008.00692.x

Luo, Y. X., Hou, X. M., Zhang, C. J., Tan, L. M., Shao, C. R., Lin, R. N., et al. (2020). A plant-specific SWR1 chromatin-remodeling complex couples histone H2A.Z deposition with nucleosome sliding. *EMBO J.* 39 (7), e102008. doi:10.15252/embj.2019102008

March-Diaz, R., Garcia-Dominguez, M., Florencio, F. J., and Reyes, J. C. (2007). SEF, a new protein required for flowering repression in Arabidopsis, interacts with PIE1 and ARP6. *Plant Physiol.* 143 (2), 893–901. doi:10.1104/pp.106.092270

March-Diaz, R., Garcia-Dominguez, M., Lozano-Juste, J., Leon, J., Florencio, F. J., and Reyes, J. C. (2008). Histone H2A.Z and homologues of components of the SWR1 complex are required to control immunity in Arabidopsis. *Plant J.* 53 (3), 475–487. doi:10.1111/j.1365-313x.2007.03361.x

Martínez-García, J. F., and Moreno-Romero, J. (2020). Shedding light on the chromatin changes that modulate shade responses. *Physiol. Plant.* 169 (3), 407–417. doi:10.1111/ppl.13101

Martin-Trillo, M., Lazaro, A., Poethig, R. S., Gomez-Mena, C., Pineiro, M. A., Martinez-Zapater, J. M., et al. (2006). EARLY IN SHORT DAYS 1 (ESD1) encodes ACTIN-RELATED PROTEIN 6 (AtARP6), a putative component of chromatin remodelling complexes that positively regulates FLC accumulation in Arabidopsis. *Development* 133 (7), 1241–1252. doi:10.1242/dev.02301

Mosammaparast, N., and Shi, Y. (2010). Reversal of histone methylation: biochemical and molecular mechanisms of histone demethylases. *Annu. Rev. Biochem.* 79, 155–179. doi:10.1146/annurev.biochem.78.070907.103946

Nguyen, N. H., Sng, B. J. R., Chin, H. J., Choi, I. K. Y., Yeo, H. C., and Jang, I. C. (2023). HISTONE DEACETYLASE 9 promotes hypocotyl-specific auxin response under shade. *Plant J.* 116 (3), 804–822. doi:10.1111/tpj.16410

Ni, M., Tepperman, J. M., and Quail, P. H. (1998). PIF3, a phytochrome-interacting factor necessary for normal photoinduced signal transduction, is a novel basic helix-loop-helix protein. *Cell* 95 (5), 657–667. doi:10.1016/s0092-8674(00)81636-0

Nie, W. F., Lei, M., Zhang, M., Tang, K., Huang, H., Zhang, C., et al. (2019). Histone acetylation recruits the SWR1 complex to regulate active DNA demethylation in Arabidopsis. *Proc. Natl. Acad. Sci. U. S. A.* 116 (33), 16641–16650. doi:10.1073/pnas.1906023116

Nie, X., Wang, H., Li, J., Holec, S., and Berger, F. (2014). The HIRA complex that deposits the histone H3.3 is conserved in Arabidopsis and facilitates transcriptional dynamics. *Biol. Open* 3 (9), 794–802. doi:10.1242/bio.20148680

Noh, Y. S., and Amasino, R. M. (2003). PIE1, an ISWI family gene, is required for FLC activation and floral repression in Arabidopsis. *Plant Cell* 15 (7), 1671–1682. doi:10.1105/tpc.012161

Oh, E., Kim, J., Park, E., Kim, J. I., Kang, C., and Choi, G. (2004). PIL5, a phytochrome-interacting basic helix-loop-helix protein, is a key negative regulator of seed germination in *Arabidopsis thaliana*. *Plant Cell* 16 (11), 3045–3058. doi:10.1105/tpc.104.025163

Paik, I., Kathare, P. K., Kim, J. I., and Huq, E. (2017). Expanding roles of PIFs in signal integration from multiple processes. *Mol. Plant* 10 (8), 1035–1046. doi:10.1016/j.molp.2017.07.002

Pandey, R., Muller, A., Napoli, C. A., Selinger, D. A., Pikaard, C. S., Richards, E. J., et al. (2002). Analysis of histone acetyltransferase and histone deacetylase families of *Arabidopsis thaliana* suggests functional diversification of chromatin modification among multicellular eukaryotes. *Nucleic Acids Res.* 30 (23), 5036–5055. doi:10.1093/nar/gkf660

Panigrahi, A., and O'Malley, B. W. (2021). Mechanisms of enhancer action: the known and the unknown. *Genome Biol.* 22 (1), 108. doi:10.1186/s13059-021-02322-1

Papamichos-Chronakis, M., Watanabe, S., Rando, O. J., and Peterson, C. L. (2011). Global regulation of H2A.Z localization by the INO80 chromatin-remodeling enzyme is essential for genome integrity. *Cell* 144 (2), 200–213. doi:10.1016/j.cell.2010.12.021

Pardi, S. A., and Nusinow, D. A. (2021). Out of the dark and into the light: a new view of phytochrome photobodies. *Front. Plant Sci.* 12, 732947. doi:10.3389/fpls.2021.732947

Peng, M., Li, Z., Zhou, N., Ma, M., Jiang, Y., Dong, A., et al. (2018). Linking PHYTOCHROME-INTERACTING FACTOR to histone modification in plant shade avoidance. *Plant Physiol.* 176 (2), 1341–1351. doi:10.1104/pp.17.01189

Perrella, G., and Kaiserli, E. (2016). Light behind the curtain: photoregulation of nuclear architecture and chromatin dynamics in plants. *New Phytol.* 212 (4), 908–919. doi:10.1111/nph.14269

Perrella, G., Zioutopoulou, A., Headland, L. R., and Kaiserli, E. (2020). The impact of light and temperature on chromatin organization and plant adaptation. *J. Exp. Bot.* 71 (17), 5247–5255. doi:10.1093/jxb/eraa154

Pham, V. N., Kathare, P. K., and Huq, E. (2018). Phytochromes and phytochrome interacting factors. *Plant Physiol.* 176 (2), 1025–1038. doi:10.1104/pp.17.01384

Plant, A. R., Larrieu, A., and Causier, B. (2021). Repressor for hire! The vital roles of TOPLESS-mediated transcriptional repression in plants. *New Phytol.* 231 (3), 963–973. doi:10.1111/nph.17428

Proveniers, M. C. G., and van Zanten, M. (2013). High temperature acclimation through PIF4 signaling. *Trends Plant Sci.* 18 (2), 59–64. doi:10.1016/j.tplants.2012.09.002

Quail, P. H., Boylan, M. T., Parks, B. M., Short, T. W., Xu, Y., and Wagner, D. (1995). Phytochromes: photosensory perception and signal transduction. *Science.* 268 (5211), 675–680. doi:10.1126/science.7732376

Rivera, C. M., and Ren, B. (2013). Mapping human epigenomes. *Cell* 155 (1), 39–55. doi:10.1016/j.cell.2013.09.011

Rockwell, N. C., Su, Y. S., and Lagarias, J. C. (2006). Phytochrome structure and signaling mechanisms. *Annu. Rev. Plant Biol.* 57, 837–858. doi:10.1146/annurev.arplant.56.032604.144208

Sakamoto, K., and Nagatani, A. (1996). Nuclear localization activity of phytochrome B. *Plant J.* 10 (5), 859–868. doi:10.1046/j.1365-313x.1996.10050859.x

Sessa, G., Carabelli, M., Possenti, M., Morelli, G., and Ruberti, I. (2018). Multiple pathways in the control of the shade avoidance response. *Plants (Basel)* 7 (4), 102. doi:10.3390/plants7040102

Shan, L., Li, P., Yu, H., and Chen, L. L. (2023). Emerging roles of nuclear bodies in genome spatial organization. *Trends Cell Biol.* doi:10.1016/j.tcb.2023.10.012

Shang, J. Y., Lu, Y. J., Cai, X. W., Su, Y. N., Feng, C., Li, L., et al. (2021). COMPASS functions as a module of the INO80 chromatin remodeling complex to mediate histone H3K4 methylation in Arabidopsis. *Plant Cell* 33 (10), 3250–3271. doi:10.1093/plcell/koab187

Shapulatov, U., van Zanten, M., van Hoogdalem, M., Meisenburg, M., van Hall, A., Kappers, I., et al. (2023). The Mediator complex subunit MED25 interacts with HDA9 and PIF4 to regulate thermomorphogenesis. *Plant Physiol.* 192 (1), 582–600. doi:10.1093/plphys/kiac581

Shen, H., Zhu, L., Castillon, A., Majee, M., Downie, B., and Huq, E. (2008). Light-induced phosphorylation and degradation of the negative regulator PHYTOCHROME-INTERACTING FACTOR1 from Arabidopsis depend upon its direct physical interactions with photoactivated phytochromes. *Plant Cell* 20 (6), 1586–1602. doi:10.1105/tpc.108.060020

Shen, Y., Lei, T. T., Cui, X. Y., Liu, X. Y., Zhou, S. L., Zheng, Y., et al. (2019). Arabidopsis histone deacetylase HDA15 directly represses plant response to elevated ambient temperature. *Plant J.* 100 (5), 991–1006. doi:10.1111/tpj.14492

Shin, J., Anwer, M. U., and Davis, S. J. (2013). Phytochrome-interacting factors (PIFs) as bridges between environmental signals and the circadian clock: diurnal regulation of growth and development. *Mol. Plant* 6 (3), 592–595. doi:10.1093/mp/sst060

Shvedunova, M., and Akhtar, A. (2022). Modulation of cellular processes by histone and non-histone protein acetylation. *Nat. Rev. Mol. Cell Biol.* 23 (5), 329–349. doi:10.1038/s41580-021-00441-y

Smaczniak, C., Li, N., Boeren, S., America, T., van Dongen, W., Goerdayal, S. S., et al. (2012). Proteomics-based identification of low-abundance signaling and regulatory protein complexes in native plant tissues. *Nat. Protoc.* 7 (12), 2144–2158. doi:10.1038/nprot.2012.129

Soutourina, J. (2018). Transcription regulation by the Mediator complex. *Nat. Rev. Mol. Cell Biol.* 19 (4), 262–274. doi:10.1038/nrm.2017.115

Steindler, C., Matteucci, A., Sessa, G., Weimar, T., Ohgishi, M., Aoyama, T., et al. (1999). Shade avoidance responses are mediated by the ATHB-2 HD-zip protein, a negative regulator of gene expression. *Development* 126 (19), 4235–4245. doi:10.1242/dev.126.19.4235

Sun, J. Q., Qi, L. L., Li, Y. N., Chu, J. F., and Li, C. Y. (2012). PIF4–Mediated activation of YUCCA8 expression integrates temperature into the auxin pathway in regulating Arabidopsis hypocotyl growth. *Plos Genet.* 8 (3), e1002594. doi:10.1371/journal.pgen.1002594

Sun, W., Han, H., Deng, L., Sun, C., Xu, Y., Lin, L., et al. (2020). Mediator subunit MED25 physically interacts with PHYTOCHROME INTERACTING FACTOR4 to regulate shade-induced hypocotyl elongation in tomato. *Plant Physiol.* 184 (3), 1549–1562. doi:10.1104/pp.20.00587

Sura, W., Kabza, M., Karlowski, W. M., Bieluszewski, T., Kus-Slowinska, M., Paweloszek, L., et al. (2017). Dual role of the histone variant H2A.Z in transcriptional regulation of stress-response genes. *Plant Cell* 29 (4), 791–807. doi:10.1105/tpc.16.00573

Sureshkumar, S., and Balasubramanian, S. (2021). Complexes and complexities: INO80 takes center stage. *Mol. Plant* 14 (11), 1776–1778. doi:10.1016/j.molp.2021.08.012

Tagami, H., Ray-Gallet, D., Almouzni, G., and Nakatani, Y. (2004). Histone H3.1 and H3.3 complexes mediate nucleosome assembly pathways dependent or independent of DNA synthesis. *Cell* 116 (1), 51–61. doi:10.1016/s0092-8674(03)01064-x

Tasset, C., Singh Yadav, A., Sureshkumar, S., Singh, R., van der Woude, L., Nekrasov, M., et al. (2018). POWERDRESS-mediated histone deacetylation is essential for thermomorphogenesis in *Arabidopsis thaliana*. *PLoS Genet.* 14 (3), e1007280. doi:10.1371/journal.pgen.1007280

Van Buskirk, E. K., Decker, P. V., and Chen, M. (2012). Photobodies in light signaling. *Plant Physiol.* 158 (1), 52–60. doi:10.1104/pp.111.186411

van der Woude, L. C., Perrella, G., Snoek, B. L., van Hoogdalem, M., Novak, O., van Verk, M. C., et al. (2019). HISTONE DEACETYLASE 9 stimulates auxin-dependent thermomorphogenesis in *Arabidopsis thaliana* by mediating H2A.Z depletion. *Proc. Natl. Acad. Sci.* 116 (50), 25343–25354. doi:10.1073/pnas.1911694116

Wang, H., Fan, Z., Shliaha, P. V., Miele, M., Hendrickson, R. C., Jiang, X. J., et al. (2023). H3K4me3 regulates RNA polymerase II promoter-proximal pause-release. *Nature* 615 (7951), 339–348. doi:10.1038/s41586-023-05780-8

Wang, H., Li, S., Li, Y., Xu, Y., Wang, Y., Zhang, R., et al. (2019). MED25 connects enhancer-promoter looping and MYC2-dependent activation of jasmonate signalling. *Nat. plants* 5 (6), 616–625. doi:10.1038/s41477-019-0441-9

Wang, L., Kim, J., and Somers, D. E. (2013). Transcriptional corepressor TOPLESS complexes with pseudoresponse regulator proteins and histone deacetylases to regulate circadian transcription. *Proc. Natl. Acad. Sci. U. S. A.* 110 (2), 761–766. doi:10.1073/pnas.1215010110

Wang, W., Kim, J., Martinez, T. S., Huq, E., and Sung, S. (2024). COP1 controls light-dependent chromatin remodeling. *Proc. Natl. Acad. Sci. U. S. A.* 121 (8), e2312853121. doi:10.1073/pnas.2312853121

Willige, B. C., Yoo, C. Y., and Saldierna Guzman, J. P. (2024). What is going on inside of phytochrome B photobodies? *Plant Cell*, koae084. doi:10.1093/plcell/koae084

Willige, B. C., Zander, M., Yoo, C. Y., Phan, A., Garza, R. M., Wanamaker, S. A., et al. (2021). PHYTOCHROME-INTERACTING FACTORs trigger environmentally responsive chromatin dynamics in plants. *Nat. Genet.* 53 (7), 955–961. doi:10.1038/s41588-021-00882-3

Wollmann, H., Stroud, H., Yelagandula, R., Tarutani, Y., Jiang, D., Jing, L., et al. (2017). The histone H3 variant H3.3 regulates gene body DNA methylation in *Arabidopsis thaliana*. *Genome Biol.* 18 (1), 94. doi:10.1186/s13059-017-1221-3

Xiao, J., Lee, U. S., and Wagner, D. (2016). Tug of war: adding and removing histone lysine methylation in Arabidopsis. *Curr. Opin. Plant Biol.* 34, 41–53. doi:10.1016/j.pbi.2016.08.002

Xie, Y., Liu, W., Liang, W., Ling, X., Ma, J., Yang, C., et al. (2023). Phytochrome B inhibits the activity of phytochrome-interacting factor 7 involving phase separation. *Cell Rep.* 42 (12), 113562. doi:10.1016/j.celrep.2023.113562

Xu, Y. F., Gan, E. S., Zhou, J., Wee, W. Y., Zhang, X. Y., and Ito, T. (2014). Arabidopsis MRG domain proteins bridge two histone modifications to elevate expression of flowering genes. *Nucleic Acids Res.* 42 (17), 10960–10974. doi:10.1093/nar/gku781

Xue, M., Zhang, H., Zhao, F., Zhao, T., Li, H., and Jiang, D. (2021). The INO80 chromatin remodeling complex promotes thermomorphogenesis by connecting H2A.Z eviction and active transcription in Arabidopsis. *Mol. Plant* 14 (11), 1799–1813. doi:10.1016/j.molp.2021.07.001

Yang, C., Zhu, T., Zhou, N., Huang, S., Zeng, Y., Jiang, W., et al. (2023). PIF7-mediated epigenetic reprogramming promotes the transcriptional response to shade in Arabidopsis. *EMBO J.* 42 (8), e111472. doi:10.15252/embj.2022111472

Yi, H., Sardesai, N., Fujinuma, T., Chan, C. W., Veena, G. S. B., and Gelvin, S. B. (2006). Constitutive expression exposes functional redundancy between the Arabidopsis histone H2A gene HTA1 and other H2A gene family members. *Plant Cell* 18 (7), 1575–1589. doi:10.1105/tpc.105.039719

Zander, M., Willige, B. C., He, Y., Nguyen, T. A., Langford, A. E., Nehring, R., et al. (2019). Epigenetic silencing of a multifunctional plant stress regulator. *eLife* 8, e47835. doi:10.7554/elife.47835

Zhai, H., Zhang, X., You, Y., Lin, L., Zhou, W., and Li, C. (2020). SEUSS integrates transcriptional and epigenetic control of root stem cell organizer specification. *EMBO J.* 39 (20), e105047. doi:10.15252/embj.2020105047

Zhang, D., Jing, Y., Jiang, Z., and Lin, R. (2014). The chromatin-remodeling factor PICKLE integrates brassinosteroid and gibberellin signaling during skotomorphogenic growth in Arabidopsis. *Plant Cell* 26 (6), 2472–2485. doi:10.1105/tpc.113.121848

Zhang, D., Li, Y., Zhang, X., Zha, P., and Lin, R. (2017). The SWI2/SNF2 chromatin-remodeling ATPase BRAHMA regulates chlorophyll biosynthesis in Arabidopsis. *Mol. Plant* 10 (1), 155–167. doi:10.1016/j.molp.2016.11.003

Zhao, F., Xue, M., Zhang, H., Li, H., Zhao, T., and Jiang, D. (2023). Coordinated histone variant H2A.Z eviction and H3.3 deposition control plant thermomorphogenesis. *New Phytol.* 238 (2), 750–764. doi:10.1111/nph.18738

Zhao, Q., Dai, B. D., Wu, H. Y., Zhu, W. C., and Chen, J. Y. (2022). Ino80 is required for H2A.Z eviction from hypha-specific promoters and hyphal development of *Candida albicans*. *Mol. Microbiol.* 118 (1-2), 92–104. doi:10.1111/mmi.14954

Zhong, Z., Wang, Y., Wang, M., Yang, F., Thomas, Q. A., Xue, Y., et al. (2022). Histone chaperone ASF1 mediates H3.3-H4 deposition in Arabidopsis. *Nat. Commun.* 13 (1), 6970. doi:10.1038/s41467-022-34648-0

Zhou, N., Li, C., Xie, W., Liang, N., Wang, J., Wang, B., et al. (2024). Histone methylation readers MRG1/2 interact with PIF4 to promote thermomorphogenesis in Arabidopsis. *Cell Rep.* 43 (2), 113726. doi:10.1016/j.celrep.2024.113726

Zhou, Y., Park, S. H., Soh, M. Y., and Chua, N. H. (2021). Ubiquitin-specific proteases UBP12 and UBP13 promote shade avoidance response by enhancing PIF7 stability. *Proc. Natl. Acad. Sci. U. S. A.* 118 (45), e2103633118. doi:10.1073/pnas.2103633118

Zhu, Y., Weng, M., Yang, Y., Zhang, C., Li, Z., Shen, W. H., et al. (2011). Arabidopsis homologues of the histone chaperone ASF1 are crucial for chromatin replication and cell proliferation in plant development. *Plant J.* 66 (3), 443–455. doi:10.1111/j.1365-313x.2011.04504.x

frontiers | Frontiers in Epigenetics and Epigenomics

TYPE Original Research
PUBLISHED 15 July 2024
DOI 10.3389/freae.2024.1423454



OPEN ACCESS

EDITED BY
Sharon Y. R. Dent,
University of Texas MD Anderson Cancer Center, United States

REVIEWED BY
Ying-Jiun Chen,
University of Texas MD Anderson Cancer Center, United States
Katherine Williams,
Genentech Inc., United States

*CORRESPONDENCE
Ricardo Iván Martínez-Zamudio,
ricardo.martinezzamudio@rutgers.edu

RECEIVED 25 April 2024
ACCEPTED 17 June 2024
PUBLISHED 15 July 2024

CITATION
Vasilopoulos T and Martínez-Zamudio RI (2024), Transcription factor network dynamics during the commitment to oncogene-induced senescence.
*Front. Epigenet. Epigenom.* 2:1423454.
doi: 10.3389/freae.2024.1423454



# Transcription factor network dynamics during the commitment to oncogene-induced senescence

Themistoklis Vasilopoulos and Ricardo Iván Martínez-Zamudio*

Robert Wood Johnson Medical School, Department of Pharmacology, Rutgers University, Piscataway, NJ, United States

Aberrant oncogenic signaling causes cells to transition into oncogene-induced senescence (OIS) to limit uncontrolled proliferation. Despite being a potent tumor suppressor mechanism, OIS is an unstable cell state susceptible to reprogramming that can promote tumorigenesis. Therefore, elucidating the underlying gene regulatory mechanisms that commit cells to OIS is critical to identifying actionable targets to modulate the senescence state. We previously showed that timely execution of the OIS program is governed by hierarchical transcription factor (TF) networks. However, the gene regulatory mechanisms that prime cells to commit to the OIS fate early upon oncogene hyperactivation are currently not known. Here, we leveraged our time-resolved multi-omic profiling approach to generate TF networks during the first 24 h of oncogenic $HRAS^{G12V}$ activation. Using this approach, we demonstrate that the commitment to OIS requires the rearrangement of the TF network on a pre-established epigenomic landscape, priming the cells for the substantial chromatin remodeling that underpins the transition to OIS. Our results provide a detailed map of the chromatin landscape before cells transition to OIS thus offering a platform for manipulation of senescence outcomes of potentially therapeutic value.

KEYWORDS

**transcription factor networks, cell fate transition, OIS, multiomics, epigenome, highthroughput sequencing**

## Introduction

Loss of cell identity (i.e., the differentiated phenotype) by oncogene hyperactivation, one of the earliest events during oncogenic transformation, occurs due to the destabilization of the transcription factor networks (Ji et al., 2021) that control cell type-specific gene expression (Wilkinson et al., 2017; Ferreiros et al., 2019). Aberrant oncogenic signaling can force cells with perturbed identities into oncogene-induced senescence (OIS), a potent tumor suppressor mechanism defined by a stable proliferative arrest and a pleiotropic senescence-associated secretory phenotype (SASP) (Braig et al., 2005; Bartkova et al., 2006; Campisi, 2013; Martinez-Zamudio et al., 2017). Despite the loss of proliferative capacity, cells in OIS remain highly dynamic entities which can reprogram themselves as well as destabilize the identity of cells within their surrounding tissue environment through cell autonomous and cell non-autonomous mechanisms (Lee and Schmitt, 2019). This functional heterogeneity of cells in OIS can lead to multiple, and sometimes paradoxical, outcomes, including reinforcement and destabilization of the proliferative

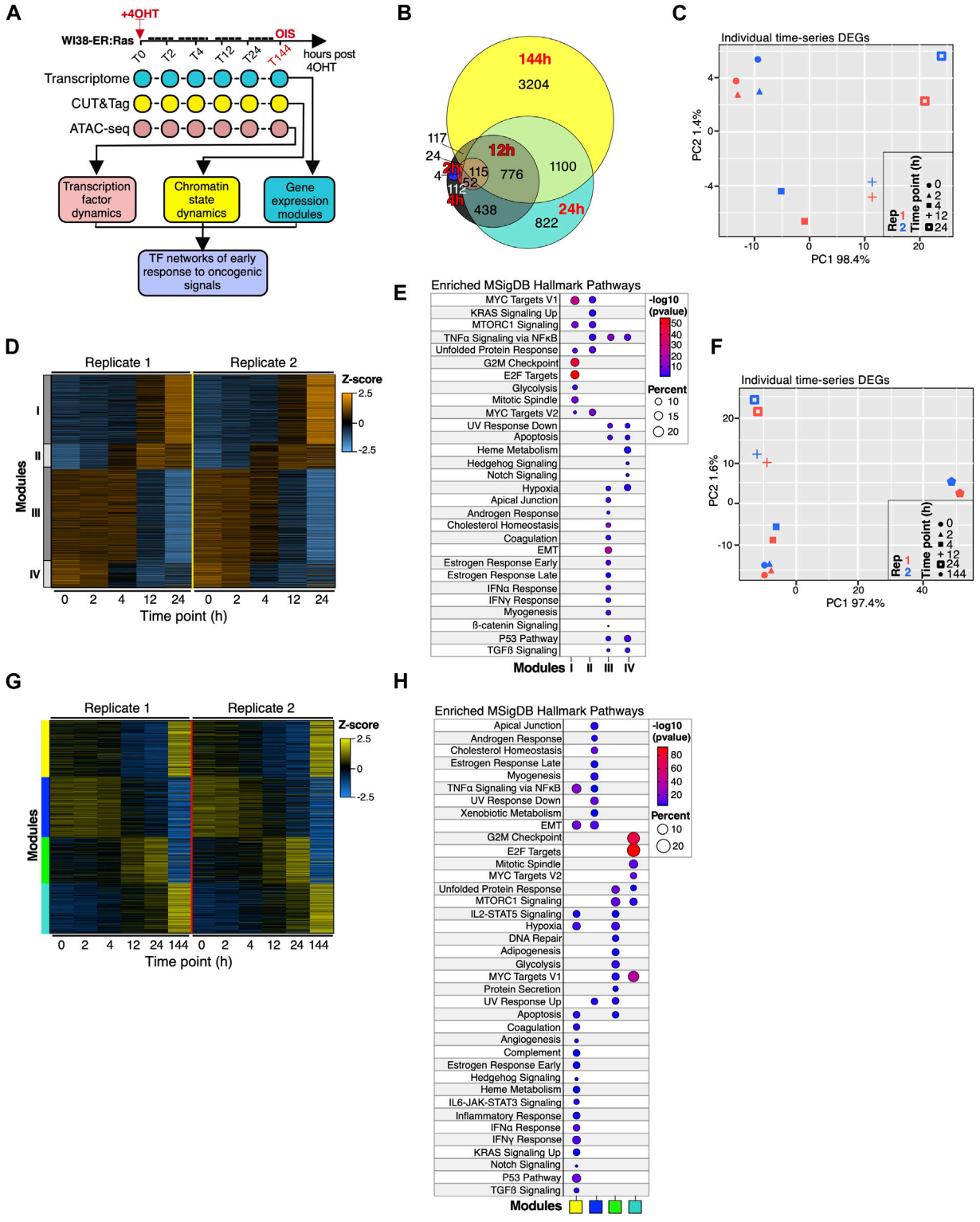


FIGURE 1
Transcriptional landscape of WI38 fibroblasts during the first 24 h of oncogenic HRAS$^{G12V}$ overexpression. **(A)** Diagram describing the experimental approach for the time-resolved multi-omic profiling used to define the early gene-regulatory networks preceding OIS commitment. **(B)** Euler diagrams showing overlaps of differentially expressed genes (DEGs) for each time point in the time series relative to proliferating cells (0 h). **(C)** PCA projection plots showing the individual transcriptional trajectories of DEGs identified within 24 h of RAS induction. Two biologically independent time series are shown. **(D)** Heatmap showing the number-coded modules (I-IV) of DEGs identified within 24 h of RAS overexpression. Two biologically independent time series experiments are shown. **(E)** Functional over-representation analysis map showing significant associations of the Molecular Signatures Database (MSigDB) Hallmark gene sets for each module described in **(D)**. Circle fill is color-coded according to the FDR-corrected *p-value* from a hypergeometric distribution test. Circle size is proportional to the percentage of genes in each MSigDB gene set found within each gene module. $N > 200$ genes per module. **(F)** PCA projection plots showing the trajectories of DEGs identified through the entire time series (up to 144 h after RAS overexpression). **(G)**
(*Continued*)

FIGURE 1 (Continued)
Heatmap showing the color-coded modules (yellow, blue, green and turquoise) of DEGs identified throughout the entire time series (up to 144 h after RAS overexpression). Two biologically independent time series experiments are shown. **(H)** Functional over-representation analysis map showing significant associations of the Molecular Signatures Database (MSigDB) Hallmark gene sets for each module described in **(G)**. Circle fill is color-coded according to the FDR-corrected *p-value* from a hypergeometric distribution test. Circle size is proportional to the percentage of genes in each MSigDB gene set found within each gene module. *N* > 200 genes per module.

arrest (Acosta et al., 2008; Martinez-Zamudio et al., 2023), reprogramming into a stem cell-like state (Milanovic et al., 2018) and transformation of non-malignant cells (Krtolica et al., 2001). Given their considerable impact on the outcome of carcinogenesis (Haugstetter et al., 2010; Eggert et al., 2016; Yu et al., 2018; Martinez-Zamudio et al., 2020; Martinez-Zamudio et al., 2023), understanding the mechanisms that commit cells to the OIS state early upon oncogene hyperactivation can lead to new therapeutic interventions of premalignant lesions.

Timing and duration of the oncogenic stimulus is critical for the commitment to the OIS phenotype (Wilson et al., 2017; Khaliq and Fallahi-Sichani, 2019). For instance, SASP from OIS fibroblasts has been shown to dynamically change its composition based on a NOTCH1-controlled switch that divides the secretome in two distinct phases post-induction of oncogenic RAS (Hoare et al., 2016). Additionally, it has been shown that the proliferative output of cells upon induction of $BRAF^{V600E}$ can create population wide heterogeneity on the senescence outcome within the first 72 h (Chen et al., 2023). The transition to OIS is a highly organized, epigenetically precoded and reversible program that is mediated by hierarchical TF networks (Martinez-Zamudio et al., 2020). Yet, although the MAPK/ERK signaling cascade is activated within hours after RAS/BRAF activation (Chen et al., 2023), the duration of the oncogenic signal input and the time point at which cells commit to transition to OIS are unknown. Revealing the gene regulatory mechanisms that prime cells to commit to OIS can provide a detailed platform for manipulation of senescent cells with potentially therapeutic implications.

In this study, we defined the gene regulatory networks formed within the first 24 h of oncogenic $HRAS^{G12V}$ activation that lead up to OIS commitment. We measured and integrated bulk transcriptome, epigenome and TF network dynamics at the early stages (0–24 h) upon oncogenic activation in the WI38 human lung fibroblasts undergoing HRAS-mediated OIS. This approach revealed that the TF network leverages a pre-established epigenomic landscape to promote the transcriptional changes required to transition to OIS within 24 h of oncogenic signaling.

# Results

## Dynamic multi-omic profiling to define the commitment to OIS

We performed time series experiments on human lung fibroblasts (strain WI38) undergoing OIS using the well characterized 4-hydroxytamoxifen (4-OHT)-inducible ER:$RAS^{G12V}$ system (Young et al., 2009). We determined global transcriptomic, epigenomic and chromatin accessibility profiles using bulk RNA-seq, Cleavage Under Targets and Tagmentation (CUT&Tag) (Kaya-Okur et al., 2019) against H3K4me1 (putative enhancers), H3K27ac (activation) and H3K27me3 (facultative heterochromatin), and ATAC-seq at six time points (0, 2, 4, 12, 24, and 144 h after ER:RAS induction; Figure 1A). We verified the OIS state by monitoring morphological changes through light microscopy at each time point (Supplementary Figure S1A), RT-qPCR profiling of a panel of OIS-associated genes at 144 h post-induction as an end-point control (Supplementary Figure S1B), which we further confirmed by plotting their normalized counts at each time point (Supplementary Figure S1C). We confirmed activation of the RAS-MAPK pathway by immunoblotting against phosphorylated ERK1/2, which showed activation as early as 2 h after induction with 4-OHT. Levels of pERK1/2 peaked at 24 h post-induction and were maintained until the last time point at 144 h post-induction (see below).

## Early transcriptome dynamics precede commitment to OIS

To examine early gene expression dynamics occurring upon activation of the OIS program (up to 24 h post-induction), we applied principal component analysis and a machine learning self-organizing map (SOM) algorithm (Loffler-Wirth et al., 2015) to the transcriptomes of WI38 fibroblasts expressing $HRAS^{G12V}$. These approaches revealed that cells rapidly activate a transcriptional response to $HRAS^{G12V}$ expression, with detectable changes to the transcriptional trajectory as well as the SOM portraits as early as 4 h after $HRAS^{G12V}$ induction, which continued to evolve until 24 h (Supplementary Figures S2A–D). Importantly, the transcriptional trajectories were remarkably reproducible across independent experiments. We identified ~3,500 differentially expressed genes (DEGs) within 24 h upon $HRAS^{G12V}$ activation (Figure 1B; Supplementary Table S1), whose transcriptional trajectory was virtually identical to that identified at the global transcriptome level (Figure 1C; Supplementary Figure S2A). We characterized the DEGs using weighted correlated gene network analysis (WGCNA) (Langfelder and Horvath, 2008), which identified 4 distinct modules (Figure 1D; Supplementary Table S1). Pathway analysis revealed upregulation of genes involved in RAS signaling, MYC targets, as well as TNF signaling (module II) all of which are associated with the activation of the MAPK/ERK pathway (Sabio and Davis, 2014), within 4 h of $HRAS^{G12V}$ activation (Figure 1E). By 12 h, cells upregulate genes associated with mTORC1 signaling as well as G2M checkpoints (module I), indicating the cells are processing the aberrant oncogenic signal that perturbs the regulation of the cell cycle (Figure 1E) (Hsieh et al., 2018). Interestingly, genes in modules III and IV representing pathways playing major roles in senescence outcomes, such as the p53 pathway as well as SASP-associated pathways (interferon

responses (IFNα/γ), transforming growth factor β (TGFβ) signaling and Notch signaling), are expressed in proliferating fibroblasts but become repressed by 24 h, indicating that a basal activity of these pathways is required to maintain cell identity which, upon $HRAS^{G12V}$ induction, become repressed as the cells transition into OIS (see modules III, IV; Figure 1D). We then evaluated whether the transcriptional dynamics observed within 24 h of $HRAS^{G12V}$ induction manifest in cells in OIS by reanalyzing the time series including the reference OIS time point of 144 h. To our surprise, inclusion of the 144 h time point resulted in the detection of an additional 3,204 DEGs (Figure 1B), which drove a drastic shift in the transcriptional trajectory of both DEGs and global transcriptomes between 24 h and 144 h (Figure 1F; Supplementary Figure S2E), consistent with our previous results (Martinez-Zamudio et al., 2020). WGCNA clustering identified 4 distinct modules (Figure 1G). Genes in the blue module, which enriched for pathways such as EMT, myogenesis and cholesterol homeostasis, were highly expressed in proliferating fibroblasts and early after $HRAS^{G12V}$ induction, steadily decreasing until cells reached OIS (Figures 1G,H; Supplementary Table S1). Genes in the turquoise module, which steadily increased as the cells committed to OIS, were representative of cell cycle control and the metabolic sensor mTORC1 pathways, likely reflecting implementation of the cell cycle arrest and increased metabolic rates that are typical of senescent cells (Wiley and Campisi, 2021). Interestingly, genes in the yellow and green modules exhibited linear expression kinetics, decreasing and increasing, respectively, until 24 h after $HRAS^{G12V}$ induction, then suddenly switching direction of expression, achieving maximal expression and repression, respectively, by 144 h (see yellow and green modules Figure 1G). Genes in the yellow module enriched for pathways characteristic of senescent cells, including inflammatory response, p53 pathway and various cytokine signaling pathways, while genes in the green module represented pathways characteristic of response to cell damage including DNA repair, apoptosis and UV response (Figure 1H). We confirmed the effect of the transcriptome at 144 h on the overall transcriptional trajectory as well as the switch in expression for a subset of gene clusters by SOM analysis (Supplementary Figures S2F–H; clusters D-I). To provide additional validation of the gene expression behavior during the first 24 h of oncogenic activation on a different cell line, we performed RT-qPCR profiling of a panel of OIS-associated gene in GM21-ER:RAS skin fibroblasts undergoing OIS. The pattern of expression of this OIS gene panel was comparable across two independent time series (Supplementary Figures S2I,J) and was also remarkably similar to normalized read counts for the same gene set in WI38-ER:RAS fibroblasts (compare to Supplementary Figure S1C). Together, these results highlight the highly organized nature of the early transcriptional events leading up to the commitment to OIS.

## Early gene regulatory events leading to the commitment to OIS take place in a pre-established chromatin landscape

Previous studies have shown a critical role of enhancers in the timely execution of the OIS program (Tasdemir et al., 2016; Guan et al., 2020; Martinez-Zamudio et al., 2020; Martinez-Zamudio et al., 2023). We therefore asked whether enhancer dynamics underpin the early transcriptional changes during the commitment to OIS. To this end, we initially focused on chromatin accessibility dynamics at H3K4me1-defined putative enhancers (Natoli, 2010; Heinz et al., 2015). PCA analysis of differentially accessible regions (DARs) (Figure 2A) matched those of DEGs and global transcriptomes. Surprisingly, despite the strong correlation between chromatin accessibility and transcriptional trajectories, only a modest amount of DARs was identified within 24 h of $HRAS^{G12V}$ induction (244 DARs), with most chromatin accessibility changes occurring between 24h and 144 h (21,301 DARs) (Figure 2B; Supplementary Table S2). Clustering with WGCNA identified four modules (1–4) (Figure 2C; Supplementary Table S2). Modules 2 and 3 exhibited linear accessibility dynamics, closing and opening, respectively. Reminiscent of transcriptional modules, DAR modules 1 and 4 exhibited dynamic behavior, with increasing and decreasing accessibility up until 24 h, respectively, followed by a reversal of their accessibility by 144 h (Figure 2C). Similar results were obtained when chromatin accessibility datasets were analyzed in their totality (i.e., irrespective of histone modification-defined regulatory regions), with most chromatin accessibility changes occurring between 24 h and 144 h (Supplementary Figures S3A–C). Importantly, DARs, irrespective of the presence of H3K4me1, were prominently bound by AP1 family TFs prior to the induction of OIS (Figures 2D–F; Supplementary Figures S3D–F), confirming the critical role of these TFs in the execution of the OIS program (Han et al., 2018; Martinez-Zamudio et al., 2020). The limited chromatin accessibility changes occurring within 24 h of $HRAS^{G12V}$ induction despite significant transcriptional dynamics within this time frame prompted us to evaluate the activation state of enhancers. We quantified the signal intensities of H3K4me1, H3K27ac and TF binding (ATAC) at opening, closing and dynamic enhancers throughout all timepoints. H3K4me1 levels remained stable for the duration of the experiment across all enhancer classes, as expected (Figures 2G–I, top panels). Surprisingly, basal levels of H3K27ac were detectable at all enhancer classes prior to RAS induction (Figures 2G–I, middle panels). The activation state of these enhancers varied modestly through the time series, reaching levels concordant with the accessibility state of each enhancer class once cells had achieved the OIS state (i.e., opening enhancers gained H3K27ac; closing lost H3K27ac; dynamic enhancers remained constant) (Figures 2G–I). This behavior was also observed for ATAC signals, which were readily detectable prior to RAS induction, remaining stable up until 24 h and followed by measurable gains or losses of chromatin binding by 144 h (Figures 2G–I, bottom panels).

To gain further insight into the chromatin-based mechanisms leading to commitment to OIS, we performed a chromatin state transition analysis on our chromatin accessibility and histone modification datasets using the chromstaR algorithm. This approach maximizes detection of chromatin regions undergoing transitions through segmentation and quantification of non-overlapping featured-enriched regions at each time point (Hanna et al., 2018). Sixteen distinct chromatin states were identified, which were correctly annotated to their respective genomic regulatory regions in ENCODE project-defined chromatin states in normal human lung fibroblasts (NHLF) at each time point (i.e., H3K4me1 enriched at enhancers; H3K27me3 enriched at

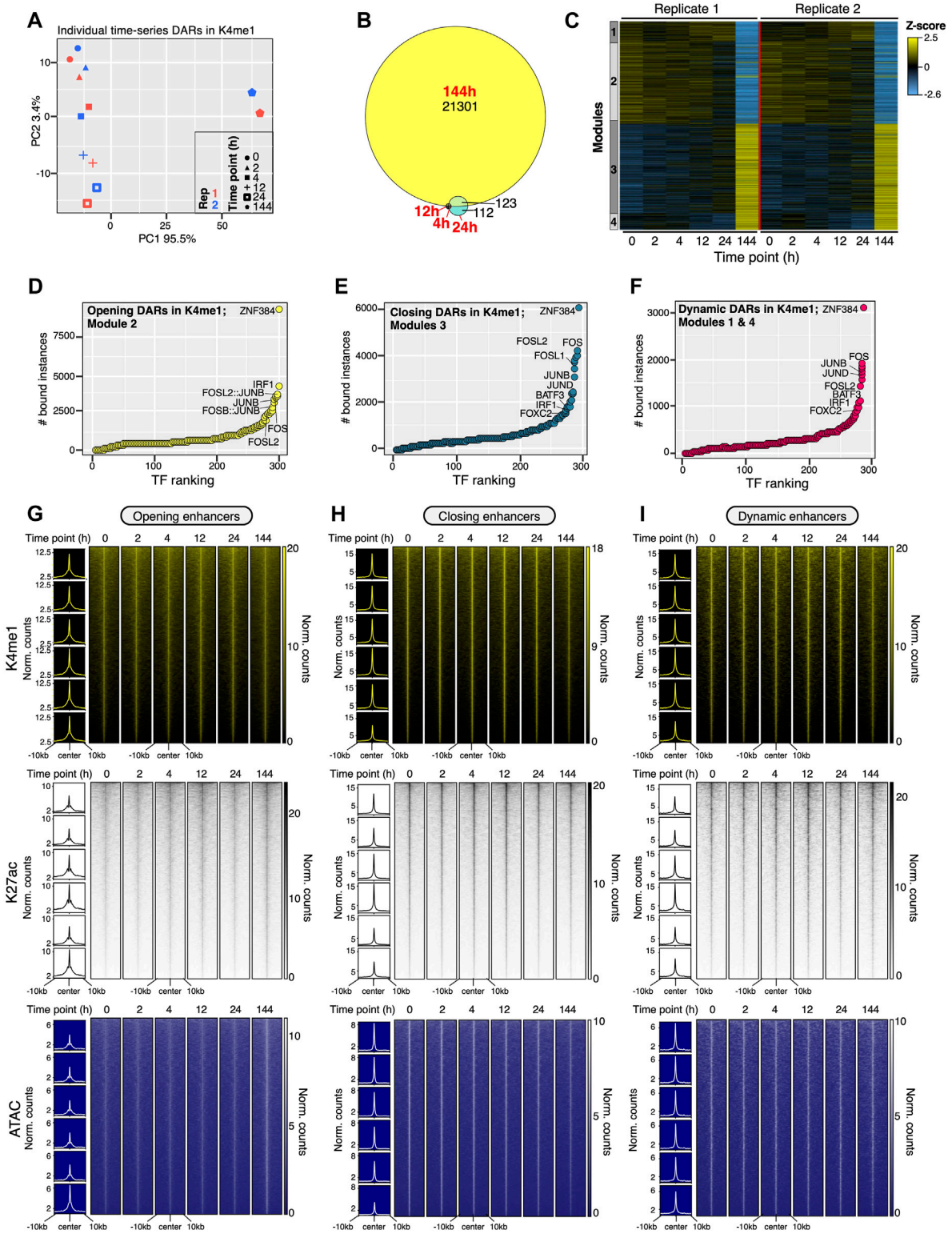


FIGURE 2
Gene regulatory events leading to commitment to OIS occur on a pre-established enhancer landscape. **(A)** PCA projection plots showing the individual trajectories of the differentially accessible regions (DARs) within putative enhancer regions (H3K4me1-defined enhancers). Two biologically independent time series are shown. **(B)** Euler diagram showing overlaps of DARs within putative enhancers regions for all time-points of the experiment up to 144 h. **(C)** Heatmap showing the number-coded modules (1–4) of DARs within putative enhancers per time-point as cells commit to OIS. The average of two biologically independent time series is shown. Modules represent DARs that are opening (Module 3), closing (Module 2) or demonstrate a more dynamic behavior (Modules 1, 4) throughout the time series. **(D–F)** Rank plots showing the summed binding instances of TFs at DARs within putative enhancers at each module defined in **(C)**. **(G–I)** Genome-wide signal intensity evolution heatmaps of H3K4me1, H3K27ac and ATAC-Seq signals in opening **(G)**, closing **(H)** and dynamic **(I)** putative enhancers as cells commit to OIS. The average of two independent time series is shown **(D–I)**. Insets to

(*Continued*)

FIGURE 2 (Continued)
the left of heatmaps show the signal metaprofile of each respective histone modification and ATAC-seq signal in consecutive time points from top to bottom.

repressed regions; Supplementary Data). Consistent with our previous observations (Martinez-Zamudio et al., 2020; Martinez-Zamudio et al., 2023), the majority of the genome was devoid of histone modification or ATAC-seq signals (~65%) (unmarked chromatin) followed by facultative heterochromatin (~15%). Chromatin states linked to gene regulatory regions (enhancers and promoters) represented ~20% collectively (Supplementary Figure S4A). Intriguingly, we did not find major chromatin state transitions within the first 24 h of $HRAS^{G12V}$ induction. Most of the chromatin state transitions occurred between 24 h and 144 h, which largely involved activation of poised enhancers, commissioning of putative enhancers from unmarked chromatin and gains in TF binding at bivalent enhancers (defined as regions possessing H3K4me1, H3K27me3 and in some instances H3K27ac) (Blanco et al., 2020) (Figure 3A; Supplementary Figure S4B; Supplementary Table S3). Quantification of signal intensities of histone modifications and TF binding at each time point confirmed the results from the chromatin state transition analysis (Supplementary Figures S4C–E). The stability of the epigenome during the first 24 h upon induction of OIS seemed at odds with the measurable changes in gene expression during the same timeframe. To address this apparent incongruency, we integrated the top eight chromatin state transitions with the expression distribution dynamics of their nearby DEGs (Figure 3B). This analysis yielded several unexpected observations: I) the expression levels of DEGs near the top eight chromatin state transitions exhibited a relatively tight unimodal distribution during the first 12 h upon $HRAS^{G12V}$ induction, II) as cells approach the transition point at 24 h, this unimodal distribution flattens, reflecting increased transcriptional noise (Tsuchiya et al., 2015) before III) committing to OIS by 144 h, at which time the distribution of DEG expression becomes bimodal, with gene expression reflecting its respective chromatin state transition (i.e., most genes near enhancers activated from a poised state become highly expressed in OIS cells) (Figure 3B; Supplementary Table S3). Correspondence analysis (CA) confirmed the coherence between chromatin state transitions and expression dynamics of DEG modules defined in Figure 1G (i.e., highly expressed genes in the turquoise module are closely associated with enhancer activation from the unmarked state upon commitment to OIS; Figure 3C). The early transcriptional dynamics in the absence of major chromatin remodeling suggests that early upon $HRAS^{G12V}$ induction, gene expression is primarily controlled by TFs binding already accessible regions. This is consistent with the minor fraction of DARs observed within the first 24hrs in contrast to when the cells acquire OIS (Figure 2B; Supplementary Figure S3B). To identify potential TFs regulating chromatin state transitions during commitment to OIS, we performed footprinting analysis of unmarked, poised and bivalent enhancers prior to induction of $HRAS^{G12V}$ (0 h) (Supplementary Table S3). We identified potential new players including IRF1, SOX15 and KLF family TFs as well as TFs involved in the regulation of OIS such as FOX family TFs and POU2F2 (Han et al., 2018; Martinez-Zamudio et al., 2023) (Figures 3D–F and see below). Overall, our comprehensive epigenomic analyses demonstrate that the early gene regulatory events leading to the commitment to OIS (within 24 h) occur within a pre-established chromatin landscape.

## Widespread transcription factor network dynamics precede commitment to OIS

Given the limited changes to chromatin accessibility and chromatin states early upon $HRAS^{G12V}$ induction, we explored the possibility that TF network activity may underlie the gene expression dynamics required for the commitment to OIS. To this end, we leveraged our TF footprinting datasets and initially determined TF co-binding interactions at DAR modules (Figure 4). We quantified TF binding instances identified at each point at closing, dynamic and opening DARs and subsequently projected them onto a co-binding matrix (Figures 4A–C). We identified AP1 family TFs as major mediators of TF interactions at all DAR classes, consistent with our previous findings (Martinez-Zamudio et al., 2023). In addition, we also detected additional co-binding clusters involving KLF, EGR and HOX family TFs. This was particularly notable at opening DARs, where widespread dynamic TF connectivity was observed (Figure 4C). Focusing the analysis on putative enhancers revealed similar results, albeit to a lesser degree (Supplementary Figures S5A–C). These data indicated that major TF network rearrangements are required during the early stages prior to the commitment to OIS. To address this possibility, we determined TF binding activity at all DAR classes (Li et al., 2019). Of note, widespread differential TF binding activity was readily detectable as early as 2 h upon induction of $HRAS^{G12V}$ across all DAR classes and at putative enhancers (Figures 4D–F; Supplementary Figures S5D–F). Consistent with our transcriptome and epigenome analyses, the TF binding activity profile of cells in OIS was most dissimilar relative to those at earlier time points, particularly at opening DARs (and DARs at putative enhancers) where most of the TF network rearrangements were observed (Figures 4C, F; Supplementary Figures S5C, F). We observed similar TF binding activity dynamics at poised enhancers, unmarked chromatin and bivalent enhancers which underwent major transitions between 24 h and 144 h after $HRAS^{G12V}$ induction (Supplementary Figure S6). Incorporating the transcriptional status of the TFs in the network revealed that, although the TF network dynamics can be attributed to differentially expressed TFs (see annotations on Figures 4D–F, Supplementary Figures S5D–F, S6), most of these TFs are already expressed prior to the induction of OIS (i.e., TFs in the yellow and blue modules), consistent with the notion that the commitment to OIS leverages a pre-established epigenomic landscape.

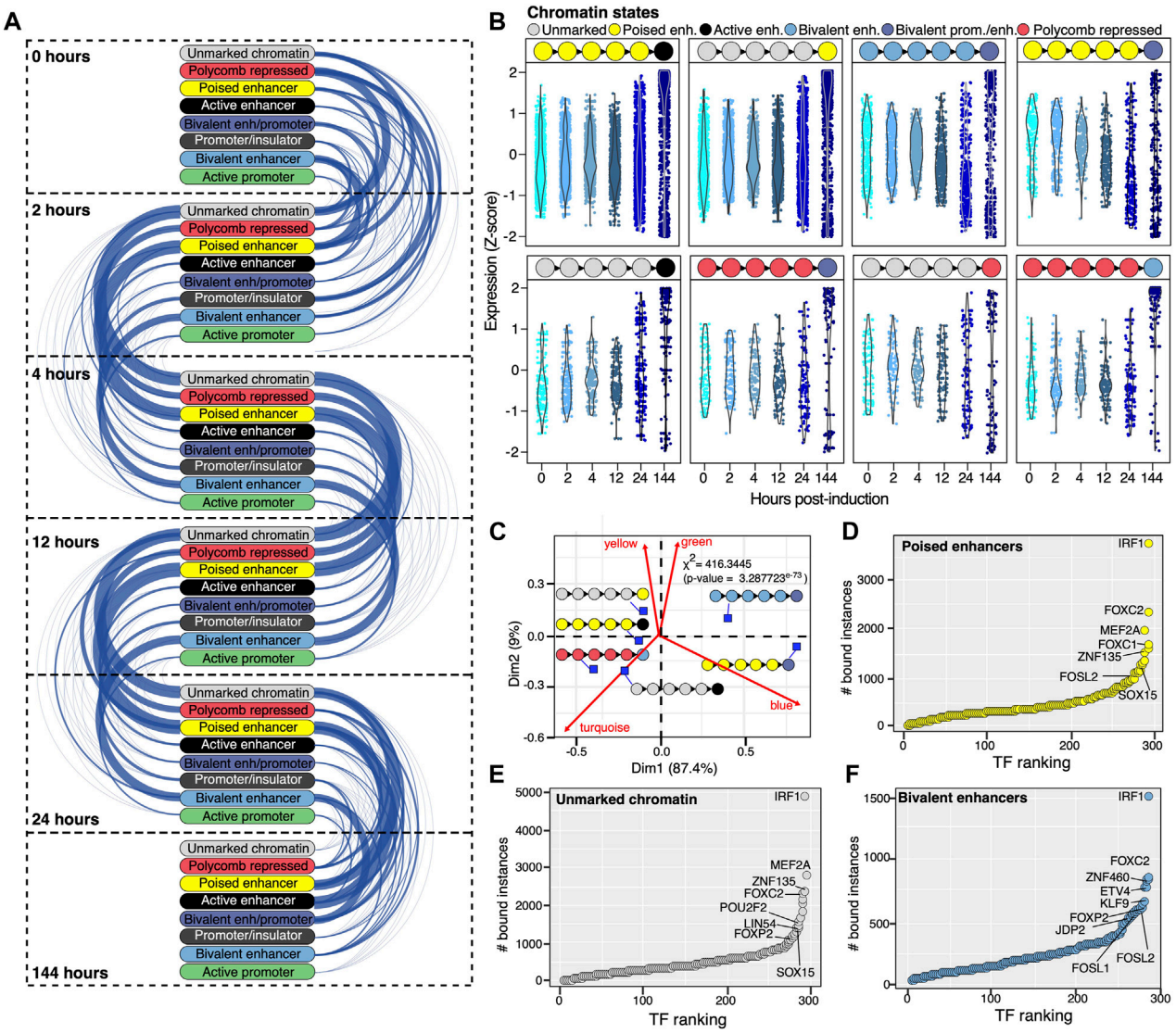


FIGURE 3
A stable epigenomic landscape precedes commitment to OIS. **(A)** Arc-plot visualization of eight select chromatin state transitions (each colored differently) at each indicated time-point during the first 24hrs post 4-OHT treatment and until OIS (144 h). The width of the edge is proportional to the number of 200 bp bins undergoing a given chromatin transition. **(B)** Integration of the top eight chromatin state transitions (top pictograms; 0 h–144 h from left to right) with nearby expression output of DEGs (Z score; violin plots; each dot represents a DEG). **(C)** Asymmetric biplot of the correspondence analysis (CA) showing the association between the top six, best-projected (squared cosine > 0.5), chromatin state transitions and DEG modules as defined in Figure 1G (blue, green, turquoise and yellow). The statistical significance of the association was calculated using a chi-squared test and shown as an inset. **(D–F)** Rank plots showing the summed binding instances of TFs at poised enhancers **(D)**, unmarked chromatin **(E)** and bivalent enhancers **(F)** prior to the induction of OIS (0 h). Chromatin state transitions, footprinting and expression data are the average of two independent time series.

To visualize the dynamicity and structure of the TF interactome as cells transition to the OIS fate, we constructed TF networks focusing on the co-binding interactions at opening, dynamic and closing DARs (Figure 5; Supplementary Figure S7; Supplementary Table S4). In line with our previous work, the TF networks had a hierarchical structure composed of top, core and bottom layers (Figure 5; Supplementary Figure S7; Supplementary Table S4). However, and in contrast to our previous work at later time points during the commitment to and escape from OIS, the top layers of TF networks at opening and dynamic DARs were composed of numerous constitutively as well as differentially expressed TFs (202 TFs at opening DARs; 185 TFs at dynamic DARs) comprising multiple TF families including HOX, FOX, KLF, IRF, EGR as well as various ZNF TFs in addition to master regulators AP1 TFs (Figures 5A,B; Supplementary Table S4). In contrast, the top layer of the TF network at closing DARs featured exclusively AP1 TFs (Supplementary Figure S7; Supplementary Table S4). The increased complexity at the top layers at opening and dynamic DARs is reminiscent of the TF binding dynamics during embryonic stem (ES) cell differentiation, which, similar to findings presented here, precede the widespread chromatin remodeling upon germ layer commitment (Tsankov et al., 2015). To validate the observations from TF co-binding and activity studies, we

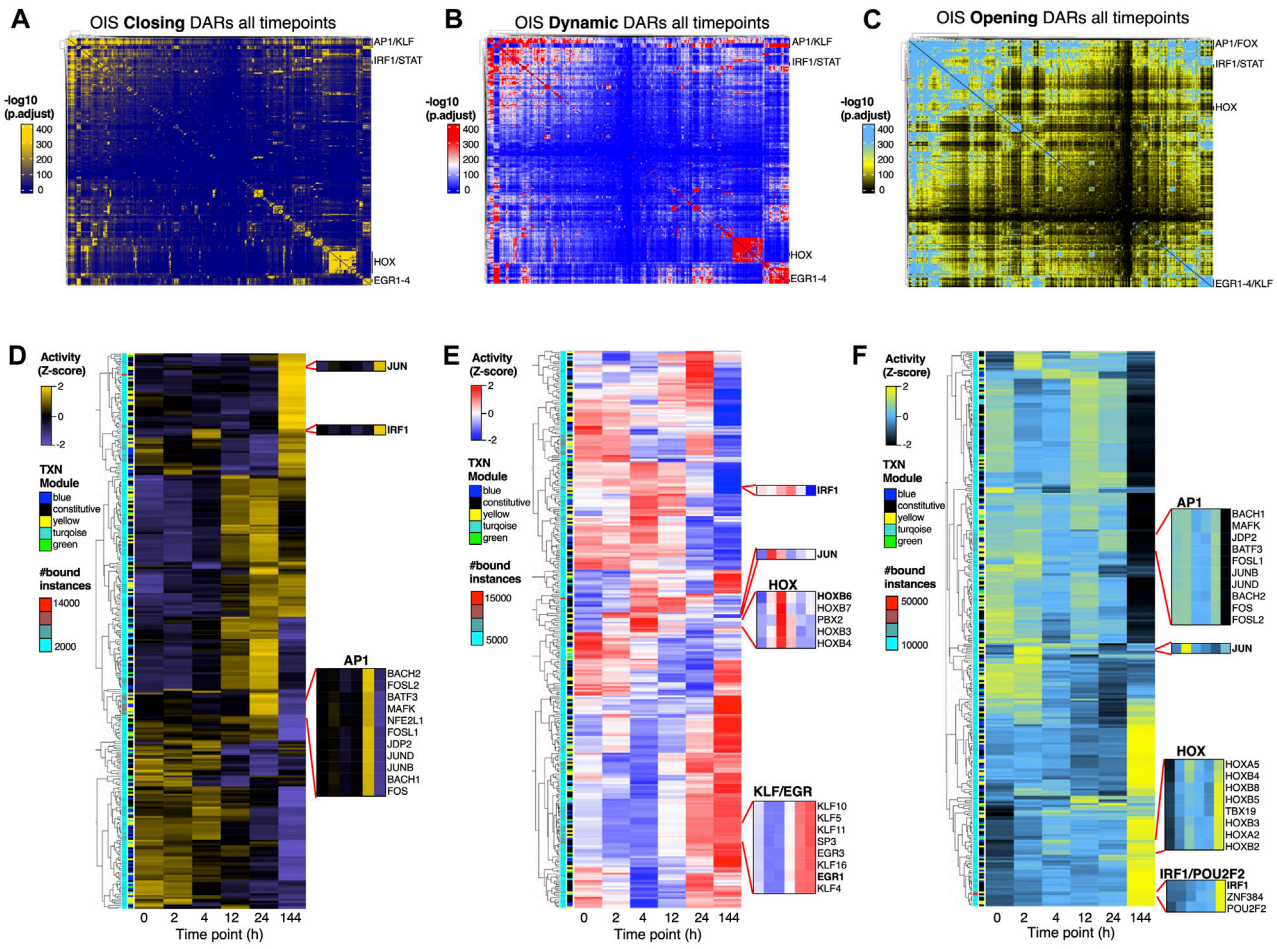


FIGURE 4
Widespread TF network rearrangements precede commitment to OIS. **(A–C)** Transcription factor co-binding matrices at closing **(A)**, dynamic **(B)** and opening **(C)** DARs (as defined in Supplementary Figure S3C modules) during the first 24 h and as cells enter OIS (144hrs). All binding instances across time points were collapsed onto the matrix and clustered using Ward's aggregation criterion. The corresponding *q* values were projected onto the clustering and are color-coded based on significance calculated using a hypergeometric distribution test. **(D–F)** Heatmaps showing the differential TF chromatin binding activity (row Z-score) at closing **(D)**, dynamic **(E)** and opening **(F)** DARs for each time point. Only expressed TFs were considered in the analysis. The annotations on the left show the number of bound instances per TF and their gene expression (TXN) category (i.e., constitutively expressed [black] or differentially regulated according to the module color code shown in Figure 1G). Insets show the chromatin binding activity of representative TFs. TF footprinting **(A–F)** and differential chromatin binding activity were performed on ATAC-seq datasets from two biologically independent time series.

monitored the protein levels of a subset of top layer, differentially expressed TFs; Interferon response factor 1 (IRF1), Early growth response 1 (EGR1) and Homeobox B6 (HOXB6) (Figure 5C; insets), which exhibited dynamic binding activity at DARs, putative enhancers, and at the top three most frequent chromatin state transitions (Figures 4D–F, Supplementary Figures S5, S6). As a reference, we also included the AP1 TF c-JUN. Immunoblot analysis showed strong basal expression for all TFs across independent experiments (Figure 5D). Upon induction of HRAS$^{G12V}$, levels of EGR1, one of the early sensors of growth and stress signaling (Wang et al., 2021), were drastically reduced within 4 h–12 h, and remained at similar levels until the last time point at 144 h. Interestingly, EGR1 activity at DARs and putative enhancers was variable through the duration of the experiments (Figures 4D–F). Similarly, protein expression of IRF1, master regulator of the interferon response (Feng et al., 2021), exhibited cycles of down- and up-regulation, which generally matched its activity at genomic regulatory regions (Figures 4D–F; Figure 5D). Expression of HOXB6, a member of the developmental regulators HOX TFs (Smith et al., 2019; Steens and Klein, 2022), gradually increased until reaching maximal levels at 24 h post HRAS$^{G12V}$ induction. Expectedly, the protein levels of c-JUN were essentially stable throughout the duration of the experiments (Figure 5D). The readily detectable basal expression of these and other TFs in our network highlight a widespread role for the TF network in the maintenance of the fibroblast cell identity (Wilkinson et al., 2017). Additionally, the ability of the cell to rapidly control both the expression and activity of nodes within the network in response to HRAS$^{G12V}$ induction emphasizes its sensitivity to cell identity-perturbing stimuli. Collectively, our analyses of TF network dynamics confirm that a high degree of responsiveness of the pre-existing TF network to oncogenic stress induced by HRAS$^{G12V}$ overexpression precedes the commitment to OIS.

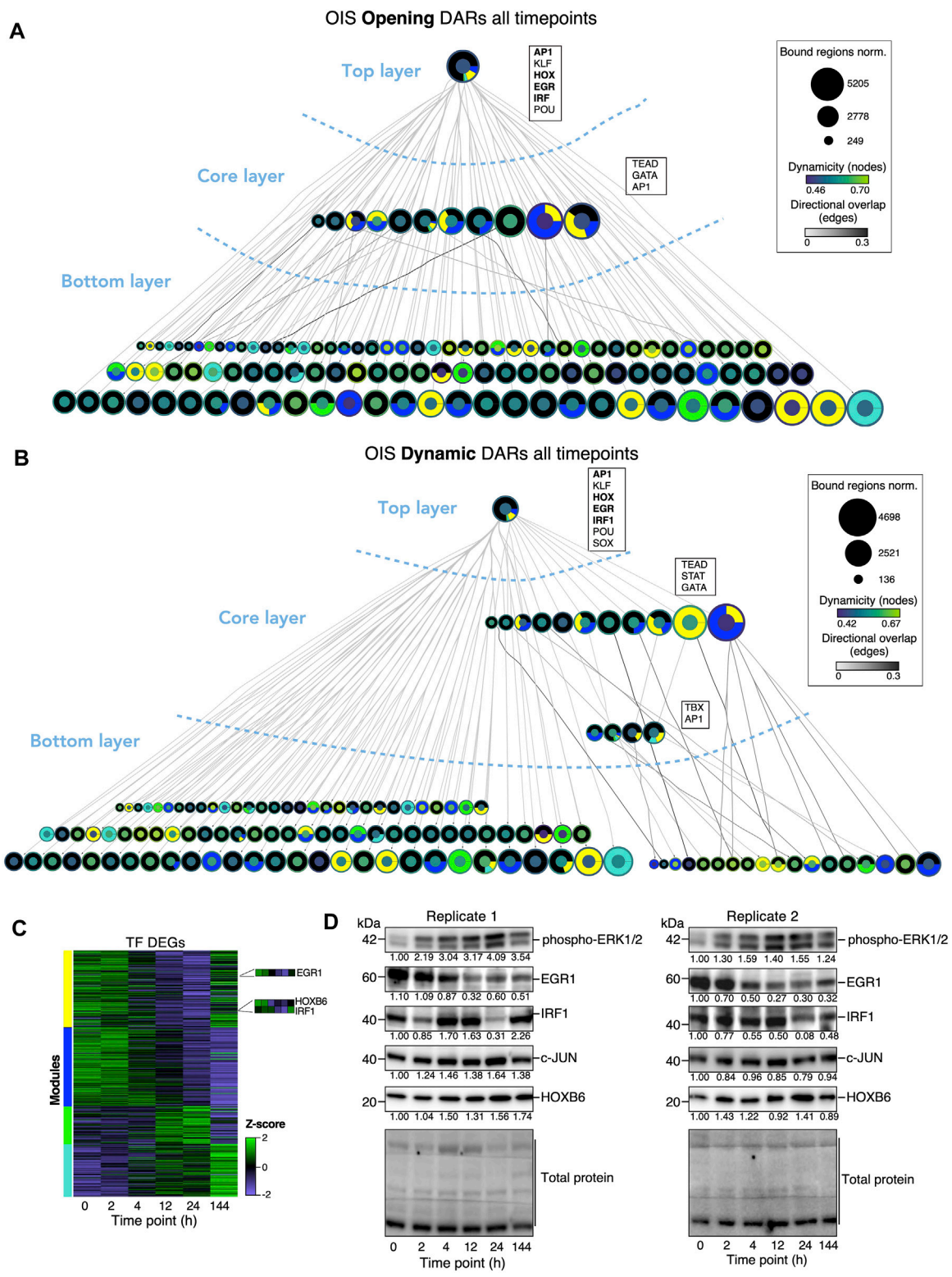


FIGURE 5
TF networks dynamics define the commitment to OIS. **(A, B)** TF networks at opening **(A)** and dynamic **(B)** DARs. TFs (nodes) are represented as circles. Oriented edges (arrows) connecting nodes indicate that at least 15% of the regions bound by a given TF in the bottom and core layers were bound by the interacting TF in the core and top layers, respectively, at the same or previous time points. Strongly connected components (SCCs) are represented as a single node to facilitate visualization. The fill color of the node's inner circle is based on the normalized dynamicity of TFs. The fill color of the outer ring indicates whether the TF is constitutively expressed or belongs to a transcriptomic module (yellow, blue, green, turquoise). The node's size is proportional to the bound regions by a given TF. Each network has three layers: i) the top layer with no incoming edges, ii) the core layer with incoming and outgoing edges, and iii) the bottom layer with no outgoing edges. Representative TF families at the top and core layers are shown (see text). Networks were generated from pooled ATAC-seq data sets from two biologically independent time series. **(C)** Heatmap showing the expression levels of genes
(*Continued*)

FIGURE 5 (Continued)
encoding TFs at each DEG modules as defined in Figure 1G throughout the time series. **(D)** Western blot analysis of representative top layer, dynamic TFs (EGR1, IRF1, cJUN, HOXB6) as well as phorphorylated ERK at the indicated timepoints after induction of OIS. Relative quantification values of band density relative to T0 are shown below bands. Total protein staining of the blot was used as a loading control. Two biologically independent time series are shown. Data in **(C)** are averaged from two independent time series.

## Discussion

Although the tumor suppressive role of OIS has been well established, recent evidence shows that OIS can play a determinant role on the outcome of carcinogenesis via cell autonomous and cell non-autonomous mechanisms. For instance, the SASP generated by hepatocytes in OIS can promote the immune clearance of pre-malignant hepatocytes while simultaneously fueling growth of carcinoma cells through inhibition of the natural killer cell function (Eggert et al., 2016). Also, cells which have remained in OIS or therapy-induced senescence (TIS) for prolonged periods can undergo epigenetic reprogramming, resulting in TF network rearrangements and stemness reprogramming that facilitate senescence escape (Milanovic et al., 2018; Zampetidis et al., 2021; Martinez-Zamudio et al., 2023). Furthermore, the heterogeneity of OIS, which is dependent on the nature and duration of the oncogenic trigger as well as the tissue of origin, manifests at the single cell level and can impact cancer development at the subpopulation level (Chatsirisupachai et al., 2021). Thus, the continuous evolution of the OIS state determines the functional outcome in the progression of premalignant lesions. This heterogeneity of the OIS state has an outsized negative impact on the development of therapies that target senescent cells, which is reflected by an underwhelming efficacy of senotherapies (Dolgin, 2020). Under this light, understanding the gene regulatory mechanisms that commit cells to OIS may open new opportunities to develop more effective therapies to prevent cancer development by preventing the transition to this metastable cell state susceptible to reprogramming.

Here we defined the gene regulatory networks during the early time points prior to the commitment to OIS. By integrating gene expression, epigenome and TF binding dynamics we identified the time point at which cells under oncogenic stress due to $HRAS^{G12V}$ overexpression prepare to commit to OIS. Based on our findings, we hypothesize this event occurs at 24 h post RAS induction, at which the transcriptional and chromatin accessibility trajectories of these cells undergo a drastic shift. From a gene expression point of view, this shift in trajectory coincides with the repression of DNA repair and metabolic genes and the upregulation of cell cycle control and SASP-associated genes between 24 h and 144 h after RAS induction. These events likely reflect an initial attempt of the cell to overcome the DNA damage incurred by $HRAS^{G12V}$ overexpression, including replication stress (Fumagalli et al., 2014). As the cell's machinery becomes insufficient to deal with the damage, the transition to OIS occurs, as reflected by the detection of an additional 3,204 DEGs exclusive to senescent cells.

In contrast, despite being virtually identical to transcriptional trajectories, only a small fraction of the accessible chromatin globally and at putative enhancers underwent detectable changes within 24 h, with the bulk of the chromatin accessibility changes occurring between 24 h and 144 h. Of note, putative enhancers were already bound by AP1 prior to the induction of oncogenic hyperactivity and basally activated, which subsequently underwent subtle but detectable (de)activation and gain/loss of TF binding as cells commit to OIS. Consistent with the stability of putative enhancers early upon induction of OIS, genomic regions undergoing chromatin state transitions were also remarkably stable within 24 h of $HRAS^{G12V}$ induction. The most abundant transitions involved unmarked chromatin, poised and bivalent enhancers gaining substantial chromatin binding and acetylation between 24 h and 144 h, which coincided with the resolution of the directionality of expression of nearby genes. Thus, cells leverage and modulate their existing epigenomic landscape to prepare for the commitment to OIS. In the absence of a requirement of major chromatin remodeling, we identified extensive TF network rewiring occurring early upon $HRAS^{G12V}$ overexpression. Indeed, in addition to the master regulators AP1, the cell modulates the expression and activity of various top layer, previously bound TFs, which subsequently drive the transcriptional and chromatin state changes required for commitment to OIS. Among these TFs, we validated the dynamic regulation of IRF1, EGR1 and HOXB6. Interestingly, IRF1 and EGR1 have been recently implicated with cellular senescence (Sadangi et al., 2022; Moiseeva et al., 2023). IRF1, a master regulator of the interferon pathway, has been reported to induce proliferative arrest and regulate SASP-mediated inflammatory responses (Moiseeva et al., 2023; Recchia Luciani et al., 2024). Given the dynamic regulation of IRF1 expression, with downregulation at 24 h and upregulation in senescent cells, we hypothesize that the interferon response may be required to commit cells to OIS, similar to cells undergoing replicative senescence (De Cecco et al., 2019). In contrast, EGR1, an early response TF, has been shown to act in a context-dependent manner playing roles both as a tumor suppressor and as an oncogene through direct regulation of p53 and TGFβ1 (Baron et al., 2006; Wang et al., 2021). Here, we show that EGR1 gets rapidly downregulated within 4 h post oncogenic induction and then stays stably expressed at low levels as cells become senescent (Figure 5C). Given its established role as a regulator of the MAPK pathway, the downregulation of EGR1 is surprising and suggests that its downregulation reflects an insult to cell identity. In line with this observation, it has been recently demonstrated that perturbance of EGR1 levels delayed the onset of B-RAF senescence in human skin fibroblasts (Carvalho et al., 2019). This highly organized response of the TF network to a cell identity disrupting stimulus, previously described during the differentiation of ES cells (Tsankov et al., 2015), provides further evidence that OIS-associated cell fate transitions are the result of epigenetically precoded programs and not simple stress responses. Future work on the role of new TF network nodes in the commitment to OIS is required to identify actionable targets to manipulate this highly relevant cell state. In summary, this work provides further evidence of the dynamic yet highly organized nature of OIS and provides a logical framework for the modulation of senescence-associated cell fate transitions through manipulation of TF networks.

## Limitations of the study

While we provided a comprehensive description of the gene regulatory networks during the commitment to OIS, our data and particularly the lack of chromatin state transitions linked to transcriptional changes early upon induction of OIS, highlights the possibility of additional chromatin-based mechanisms that contribute to this process. For instance, we cannot exclude the possibility of modulation of the three-dimensional structure of chromatin, which has been recently shown to play a critical role in the differentiation of myeloid progenitors into neutrophils (Patta et al., 2024). Similarly, while we detected widespread rearrangements of the TF network early upon the induction of OIS, this activity did not result in any detectable changes to enhancer-linked histone modifications. One possibility that could potentially link TF network rearrangements to transcriptional changes during the early stages of OIS is the ability of TFs to recruit DNA demethylation machinery to prospective OIS enhancers, as has been previously described during the reprogramming of B cells into induced pluripotent stem cells (iPSCs) (Sardina et al., 2018). Incorporation of time resolved high-throughput chromosome conformation capture methods such as Hi-C, ChIA-PET and (oxidative)bisulphite-sequencing ([ox]BS-seq) will address these possibilities in future work.

# Methods

## Cell culture

WI38 normal human lung fibroblasts (CCL-75, ATCC -American Type Culture Collection) and GM21808 normal human skin fibroblasts (Coriell Institute) were cultured in a DMEM (D6429, Millipore-Sigma) medium supplemented with 10% fetal bovine serum, (#25–514, GenClone) at 37°C in a 5% $CO_2$ and 2% $O_2$ atmosphere. WI38-ER:RAS$^{G12V}$ & GM21-ER:RAS$^{G12V}$ cells have been generated via retroviral transduction as described in (Benhamed et al., 2012) using retroviral plasmid pLNCX2 ER:RAS (Young et al., 2009) (Addgene: 67844) and Platinum-A (Plat-A, Cell Biolabs) as the retroviral packaging cell line cultured in the same medium as WI38 cells. Once generated, WI38-ER:RAS$^{G12V}$ fibroblasts were cultured as above and stimulated with 400 nM 4-hydroxytamoxifen (4-OHT)(H7904, Millipore-Sigma); samples were collected and processed at the time points indicated in the main text post treatment with 4-OHT. The 0 h uninduced control sample was treated with the same volume of EtOH (4-OHT vehicle) for 2 h. Cell images for phenotypic validation of OIS induction were obtained using an EVOS M5000 digital inverted microscope (Thermo Fisher Scientific).

## Western blotting

Protein extracts from samples from each timepoint were prepared in 1x CHAPS Lysis buffer (S7705, Millipore-Sigma) containing protease and phosphatase inhibitor cocktail (#78440, Thermo Fisher Scientific). Protein concentration was measured using Qubit™ Protein and Protein Broad Range (BR) Assay Kit (Q33212, Thermo Fisher Scientific) on a Qubit™ 4 Fluorometer (Thermo Fisher Scientific) according to manufacturer's instructions. A total of 15 μgs of whole-cell lysates were resolved on 4% –12% Bis-Tris Plus precast gels (NW4125, Thermo Fisher Scientific) in 1X MOPS SDS running buffer (Thermo Fisher Scientific), and proteins were transferred to PVDF membranes via the iBlot 3 Western blot transfer system (Invitrogen/Thermo Fisher Scientific) according to manufacturer's instructions. Total protein staining in post transfer membranes was done using No-Stain™ Protein Labeling Reagent (A44449, Thermo Fisher Scientific) according to manufacturer's instructions. Membranes were blocked in 5% non-fat dry milk in 1x TBST (150 mM NaCl, 10 mM Tris–HCl, pH 8.0, 0.05% Tween 20) at room temperature for 1 h, then incubated with primary antibodies for 2 h at room temperature or at 4°C overnight with gentle agitation. Membranes were washed three times in 1 × TBST for 10 min with shaking, then incubated with secondary antibodies for 1 h shaking, washed three times in 1 × TBST for 10 min with shaking. All blots were imaged using Amersham™ Imager 680 (GE Life Sciences). The following primary antibodies and dilutions were used: pERK (Cell Signaling Technologies; Cat no. #4370; 1:1000 dilution), EGR-1 (Santa Cruz Biotechnology; Cat no. sc-101033; 1:500 dilution), IRF-1 (Santa Cruz Biotechnology; Cat no. sc-74530; 1:500 dilution), c-Jun (Santa Cruz Biotechnology; Cat no. sc-1694; 1:1000 dilution), HoxB6 (Santa Cruz Biotechnology; Cat no. sc-166950; 1:1000 dilution). The following antibodies were used as secondary: HRP-conjugated goat anti-rabbit (PerkinElmer; Cat no. NEF812001EA; 1:6000 dilution) or anti-mouse (Cell Signaling Technologies; Cat no. #70765; 1:3000 dilution). Relative quantification of band intensity for each blot was performed with background subtraction and normalized to total protein for each lane (most prominent band of the total protein was used) using Fiji (ImageJ) software Version: 2.14.0/1.54f.

## Real-time quantitative polymerase chain reaction for molecular validation of OIS induction

WI38-ER:Ras$^{G12V}$ were induced with 4-OHT as described above and collected 144 h post treatment. Total RNA was isolated from cells with RNeasy Mini kit (Qiagen, Germantown, MD) according to the manufacturer's instructions. As per the manufacturer's instructions, reverse transcription of 500–1000 ng of total RNA was carried out using the iScript cDNA synthesis kit (Bio-rad). Quantitative real-time PCR (qPCR) was performed using primers (listed below) with the iTaq Universal SYBR Green Supermix (Bio-rad) on a CFX Opus 96 Real-Time PCR detection system (Bio-rad). Samples were analyzed in technical triplicates, and GADPH levels were used for normalization. The following Qiagen QuantiTect Primers were used: GADPH (QT00079247), (QT00008799), IL1B (QT00021385), IL8 (QT00000322), CDKN2A (QT00089964), CDKN1A (QT00062090), CCNA2 (QT00014798).

## CUT&Tag

We performed CUT&Tag on 100,000–200,000 cells per target per timepoint using the CUTANA CUT&Tag kit (Epicypher: 14–1102) using the following antibodies: Epicypher: H3K4me1 (Epicypher: 13–0057), H3K27me3 (Epicypher: 13–005), H3K27ac

(Active Motif: 39,133) and rabbit IgG as a negative control (Epicypher: 13–0042), according to the manufacturer's instructions. Libraries were amplified for 16 cycles and quality assessed using a TapeStation 4200 instrument. Libraries were paired-end sequenced on a Novaseq-X instrument. 10–20 million reads per library were used for downstream analyses.

## ATAC-seq

The transposition reaction and library construction were performed as previously described in the original publication (Buenrostro et al., 2013) using 50,000–100,000 cells from each time point of the OIS escape time series (two biological replicates). DNA fragments were extracted using a Qiagen MinElute kit (Qiagen) and libraries were produced by PCR amplification (7 cycles) of tagmented DNA using an NEB Next High-Fidelity 2× PCR Master Mix (New England Biolabs). Library quality was assessed using an TapeStation 4200 instrument (Applied Biosystems). Paired-end sequencing was performed in an Illumina Novaseq-X instrument. Typically, 30–50 million reads per library were required for downstream analyses.

## RNA-seq

RNA from 50,000–100,000 cells per time point was purified using a Macherey-Nagel RNA XS Plus kit according to the manufacturer's instructions (Macherey-Nagel, Duren, Germany). RNA integrity was evaluated in a TapeStation 4200 instrument system and only RNA with an integrity number >= 9 was used for library preparation. Libraries were constructed using the SMARTer Stranded V2 (TakaraBio) according to the manufacturer's instructions (TakaraBio). Paired-end sequencing was performed on an Illumina Novaseq-X instrument. At least 40 million reads per sample (20 million per strand) were obtained and used for downstream analyses.

## Preprocessing of high-throughput sequencing data

Paired-end (RNA-seq, CUT&Tag and ATAC-seq) reads were processed as we previously described (Martinez-Zamudio et al., 2023) aligned to the GRCh38.d1.v1 version of the human genome using bowtie2 (Langmead and Salzberg, 2012) using the local mode. Low-quality reads and adapters were removed using fastq-mcf v.1.0.5 and cutadapt. Alignments were further processed using samtools v.1.1.1, and PCR and optical duplicates were removed with PicardTools v.2.2.2. Enriched regions for histone modifications and ATAC-seq were identified using MACS v.3.0 (Liu, 2014) (macs3 callpeak—nomodel—shiftsize—shift-control—gsize hs -p 1e-3). The identified peaks were subsequently processed using the irreproducibility discovery rate (IDR) pipeline (Landt et al., 2012), generating time point-specific reproducible peak sets for histone modifications and ATAC-seq at each time point. A master peak set was constructed using a custom bedops script that merges common peaks between samples. For RNA-seq samples, reads were counted using summarized overlaps and normalized with DESeq2 for visualization.

## Chromatin state transitions

We analyzed the genome-wide combinations of H3K4me1, H3K27ac, H3K27me3 and ATAC-seq signals on IDR-controlled reproducible peaks of each time point using the chromstaR package. The algorithm was run on differential mode and configured to partition the genome in 200 bp non-overlapping bins and count the number of reads of histone modification/ATAC-seq mapping into each bin at the time points indicated in the main text and modeled using a univariate HMM based on a two-component mixture, the zero-inflated binomial distribution. Subsequently, a multivariate HMM assigns every bin in the genome to one of the multivariate components considering 2(6-time points x4 genomic enrichment variables [histone modifications and ATAC-seq]) possible states. We focused on robust transitions of an enrichment score of >= 1 for further analysis. Integration with gene expression data was achieved by annotating the nearest DEGs with ChIPSeeker (Yu et al., 2015) to the 8 most frequent chromatin state transitions and monitoring their expression using violin plots. The association between chromatin state transitions and DEG modules was performed through Correspondence analysis (CA) and visualized on an asymmetric biplot after filtering for the top contributing chromatin state transitions (square cosine >0.5).

## Heatmap and metaprofile visualizations of ATAC-seq and CUT&Tag datasets

ATAC-seq and CUT&Tag alignments were normalized using deeptools v3.3.1100103 (Ramirez et al., 2016) using the RPGC approach to obtain 1X coverage (bamCoverage -b–normalizeUsing RPGC–effectiveGenomeSize 2864785220 –ignoreDuplicates–binSize 10 –verbose -o).

## Differential expression and accessibility

Differentially accessible regions (DARs) and differentially expressed genes (DEGs) throughout the time course were identified from ATAC-seq and RNA-seq data, respectively using DESeq2. Raw reads are internally normalized by DESeq2 using the median of ratios method (Anders and Huber, 2010). Reads per peak (ATAC-seq, using a custom master peak list as feature input) or exon (RNA-seq, using the GRCh38.107 genome model) were quantified using the *summarizeOverlaps* package and peaks/genes with at least 10 reads in at least 10 libraries were kept. Correction of batch effects was performed with limma (Ritchie et al., 2015) using "replicate" as the surrogate variable. Data transformation (regularized-log [rld] transformation), exploratory visualization (PCA and hierarchical clustering) and differential expression analysis were performed with DESeq2 using the default parameters as previously described (Love et al., 2014) and base R functions. We focused on highly significant DARs and DEGs by using an adjusted $p$-value filter of 0.05.

### WGCNA

Differentially expressed genes (DEGs) and accessible regions (DARs) identified with DESeq2 were used as input for unsupervised clustering using WGCNA. We used the "signed" option with default parameters, with the exception of the soft thresholding power which was set to 12 for RNA-seq data (0 h–24 h), 14 for RNA-seq data (all time points) and 12 for ATAC-seq data (accessible chromatin and H3K4me1-defined regions). The minimum size for the DEG and DAR modules was set to 200 features for the initial set of modules, which were then merged by a dissimilarity threshold of 0.3 for RNA-seq data and 0.08 for ATAC-seq data. For RNA-seq, WGCNA modules were functionally profiled using clusterProfiler (Wu et al., 2021) using the Molecular Signatures Database Hallmark gene sets (Liberzon et al., 2015). Statistical significance was calculated by a hypergeometric test with a cut-off of an adjusted *p*-value of <= 0.1 with Benjamini–Hochberg correction.

### Transcription factor footprinting

Footprinting, TF motif enrichment, and differential binding activity were performed as we previously described with HINT-ATAC (Li et al., 2019) using the JASPAR position weight matrix database for vertebrate TFs (Fornes et al., 2020) on merged ATAC-seq datasets, focusing on enhancer and global DARs as well as the 3 most frequent chromatin state transitions. To investigate TF co-binding, we joined chromatin regions containing TF binding instances less than 500 bp apart, resulting in a set of chromatin regions with variable sizes concentrating TF activity during the entire time course. We performed a hypergeometric test for each pairwise co-binding possibility for each time point and adjusted *p*-values for multiple testing using Bonferroni correction.

### Transcription factor networks

We built TF hierarchical networks as previously described in (Martinez-Zamudio et al., 2023), at opening, closing and dynamic DARs. Each identified TF is represented as a node, connected by directed edges representing co-binding events along the chromatin and during the entire time course. An edge with TF A as the source and TF B as the target indicates that TF A binds to the same chromatin regions as TF B at the same or at a previous time point. For each TF, we computed their normalized total number of bound regions and dynamicity and represented those properties in the networks as node size and node color, respectively. Each edge is associated with a weight in the interval [0, 1], representing the fraction of TF B binding instances previously occupied by TF A. We filtered the networks for edges with a weight higher than 0.15 and performed a transitive reduction to simplify the obtained networks while keeping essential topological features. Nodes included in the same strongly connected component (SCC), i.e., connected both by incoming and outgoing paths, were merged into a single node. We represented the identified transcriptomic module distribution for TFs included in the same SCC as Doughnut Charts.

## Data availability statement

The data presented in the study are deposited in the GEO repository, accession numbers are GSE271459, GSE271460 and GSE271461.

## Ethics statement

Ethical approval was not required for the studies on humans in accordance with the local legislation and institutional requirements because only commercially available established cell lines were used.

## Author contributions

TV: Formal Analysis, Investigation, Methodology, Validation, Writing–original draft, Writing–review and editing. RM-Z: Conceptualization, Data curation, Formal Analysis, Funding acquisition, Investigation, Methodology, Project administration, Resources, Software, Supervision, Validation, Visualization, Writing–original draft, Writing–review and editing.

## Funding

The author(s) declare that financial support was received for the research, authorship, and/or publication of this article. This study was supported by start-up fund provided to RM-Z.

## Conflict of interest

The authors declare that the research was conducted in the absence of any commercial or financial relationships that could be construed as a potential conflict of interest.

## Publisher's note



## Supplementary material

The Supplementary Material for this article can be found online at: https://www.frontiersin.org/articles/10.3389/freae.2024.1423454/full#supplementary-material

**SUPPLEMENTARY FIGURE S1**
Validation of the WI38-ER:RASG12V cell system for induction of OIS. **(A)** Representative micrographs of proliferating (2 h post addition of vehicle [EtOH]) and senescent (144h post addition of 4-OHT) WI38 fibroblasts. Scale bar: 300 μm. **(B)** RT-qPCR profiling of senescence biomarkers for each individual biological replicate of time series (n = 2) comparing WI38-ER:RAS cells 144 h post treatment with EtOH (Proliferating) and 4-OHT (OIS). All

targets were normalized using GAPDH as a reference gene. **(C)** Histogram showing the normalized reads for the indicated senescence biomarkers for each time point in WI38-ER:RAS$^{G12V}$ fibroblasts undergoing OIS. The bars indicated the range of read counts per indicated gene (n = 2 biologically independent time series).

**SUPPLEMENTARY FIGURE S2**
Transcriptional landscape of WI38 fibroblasts during the first 24 h of oncogenic RAS overexpression. **(A)** PCA projection plots showing the individual global transcriptional trajectories of two biologically independent early time series during the first 24 h. **(B)** Averaged self-organizing maps (SOMs) of global transcriptomes of two biologically independent time series of WI38 fibroblasts during the first 24 h upon RAS activation, expressed as logarithmic fold-change. **(C)** D-cluster projection showing regions of SOMs with significant changes in expression during the first 24 h (see regions of SOMs in **(B)** that change color through time). **(D)** Expression of D-cluster metagenes in WI38 fibroblasts for every time point during the first 24hrs post RAS overexpression. The histograms show the change in the expression of metagenes in clusters identified in **(C)** (top of each panel). They are color-coded according to time point (bottom of panels). **(E)** PCA projection plots as in (A) through the entire time series (up to 144 h). **(F–H)** Averaged SOMs like, D-cluster projection and expression of respective metagenes as in (B-D) through the entire time series (up to 144 h). **(I,J)** RT-qPCR profiling of the indicated senescence biomarkers in GM21-ER:RAS$^{G12V}$ skin fibroblasts undergoing OIS (n = 2 biologically independent time series).

**SUPPLEMENTARY FIGURE S3**
Gene regulatory events leading to commitment to OIS occur on a pre-established chromatin accessibility landscape. **(A)** Principal component analysis projection plots showing the individual trajectories of the differentially accessible regions (DARs) as assessed by ATAC-Seq of every time-point of two biologically independent time series. **(B)** Venn diagram showing intersections of DARs in **(A)** for all time-points of the experiment up to 144 h. **(C)** Heatmap showing the letter-coded modules **(A–C)** of DARs of WI38-ERRAS fibroblasts for every time-point through the entire time-course. The average of two biologically independent time series experiments is shown. Modules represent DARs that are opening throughout the duration of the time-course (Module A), closing (Module B) or demonstrate a more dynamic behavior (Modules C). **(D–F)** Rank plots showing the summed binding instances of TFs in chromatin regions of the modules defined in **(C)** of Opening **(D)**, Closing **(E)** and Dynamic **(F)** DARs.

**SUPPLEMENTARY FIGURE S4**
A stable epigenomic landscape precedes commitment to OIS. **(A)** Histograms showing the percentage of the genome enriched in the indicated combinations of H3K4me1, H3K27ac, H3K27me3 from CUT&Tag and ATAC-seq signals at the indicated time points after induction of OIS. **(B)** Quantification of the top 8 most frequent chromatin state transitions occurring through the time series. **(C–E)** Genome-wide signal intensity evolution heatmaps of H3K4me1, H3K27ac, H3K27me3 and ATAC-Seq signals at unmarked chromatin **(C)**, poised **(D)** and bivalent **(E)** enhancers identified prior to the induction of OIS (0 h) during the span of the time series. The average of two independent is shown. Insets to the left of heatmaps show the signal metaprofile of each respective histone modification and ATAC-seq signal in consecutive time points from top to bottom.

**SUPPLEMENTARY FIGURE S5**
Widespread TF network rearrangements precede commitment to OIS. **(A–C)** Transcription factor co-binding matrices at closing **(A)**, dynamic **(B)** and opening **(C)** putative enhancers (as defined in Figure 2C modules) during the first 24 h and as cells enter OIS (144 h). All binding instances across time points were collapsed onto the matrix and clustered using Ward's aggregation criterion. The corresponding *q* values were projected onto the clustering and are color-coded based on significance calculated using a hypergeometric distribution test. **(D–F)** Heatmaps showing the differential TF chromatin binding activity (row Z-score) at closing **(D)**, dynamic **(E)** and opening **(F)** putative enhancers for each time point. Only expressed TFs were considered in the analysis. The annotations on the left show the number of bound instances per TF and their gene expression (TXN) category (i.e., constitutively expressed [black] or differentially regulated according to the module color code shown in Figure 1G). Insets show the chromatin binding activity of representative TFs. TF footprinting (A-F) and differential chromatin binding activity were performed on ATAC-seq/CUT&Tag (H3K4me1) datasets from two biologically independent time series.

**SUPPLEMENTARY FIGURE S6**
Widespread TF network rearrangements precede commitment to OIS. Heatmaps showing the differential TF chromatin binding activity (row Z-score) at poised enhancers **(A)**, unmarked chromatin **(B)** and bivalent enhancers **(C)** (as defined in Figures 3D–F) for each time point. Only expressed TFs were considered in the analysis. The annotations on the left show the number of bound instances per TF and their gene expression (TXN) category (i.e., constitutively expressed [black] or differentially regulated according to the module color code shown in Figure 1G). Insets show the chromatin binding activity of representative TFs. TF footprinting **(A–F)** and differential chromatin binding activity were performed on ATAC-seq/CUT&Tag datasets from two biologically independent time series.

**SUPPLEMENTARY FIGURE S7**
TF networks dynamics define the commitment to OIS. TF networks at closing DARs. TFs (nodes) are represented as circles. Oriented edges (arrows) connecting nodes indicate that at least 15% of the regions bound by a given TF in the bottom and core layers were bound by the interacting TF in the core and top layers, respectively, at the same or previous time points. Strongly connected components (SCCs) are represented as a single node to facilitate visualization. The fill color of the node's inner circle is based on the normalized dynamicity of TFs. The fill color of the outer ring indicates whether the TF is constitutively expressed or belongs to a transcriptomic module (yellow, blue, green, turquoise). The node's size is proportional to the bound regions by a given TF. Each network has three layers: i) the top layer with no incoming edges, ii) the core layer with incoming and outgoing edges, and iii) the bottom layer with no outgoing edges. Representative TF families at the top and core layers are shown (see text). Networks were generated from pooled ATAC-seq data sets from two biologically independent time series.

**SUPPLEMENTARY DATA**
Enrichment heatmap for all time points of two averaged biologically independent time series showing the combinations of H3K4me1, H3K27ac, H3K27me3 CUT&Tag and ATAC-seq signals with reference chromatin states in normal human lung fibroblasts from the ENCODE project. Txn, transcription; CNV, copy number variation.

# References


Acosta, J. C., O'loghlen, A., Banito, A., Guijarro, M. V., Augert, A., Raguz, S., et al. (2008). Chemokine signaling via the CXCR2 receptor reinforces senescence. *Cell* 133, 1006–1018. doi:10.1016/j.cell.2008.03.038

Anders, S., and Huber, W. (2010). Differential expression analysis for sequence count data. *Genome Biol.* 11, R106. doi:10.1186/gb-2010-11-10-r106

Baron, V., Adamson, E. D., Calogero, A., Ragona, G., and Mercola, D. (2006). The transcription factor Egr1 is a direct regulator of multiple tumor suppressors including TGFβ1, PTEN, p53, and fibronectin. *Cancer Gene Ther.* 13, 115–124. doi:10.1038/sj.cgt.7700896

Bartkova, J., Rezaei, N., Liontos, M., Karakaidos, P., Kletsas, D., Issaeva, N., et al. (2006). Oncogene-induced senescence is part of the tumorigenesis barrier imposed by DNA damage checkpoints. *Nature* 444, 633–637. doi:10.1038/nature05268

Benhamed, M., Herbig, U., Ye, T., Dejean, A., and Bischof, O. (2012). Senescence is an endogenous trigger for microRNA-directed transcriptional gene silencing in human cells. *Nat. Cell Biol.* 14, 266–275. doi:10.1038/ncb2443

Blanco, E., Gonzalez-Ramirez, M., Alcaine-Colet, A., Aranda, S., and Di Croce, L. (2020). The bivalent genome: characterization, structure, and regulation. *Trends Genet.* 36, 118–131. doi:10.1016/j.tig.2019.11.004

Braig, M., Lee, S., Loddenkemper, C., Rudolph, C., Peters, A. H., Schlegelberger, B., et al. (2005). Oncogene-induced senescence as an initial barrier in lymphoma development. *Nature* 436, 660–665. doi:10.1038/nature03841

Buenrostro, J. D., Giresi, P. G., Zaba, L. C., Chang, H. Y., and Greenleaf, W. J. (2013). Transposition of native chromatin for fast and sensitive epigenomic profiling of open chromatin, DNA-binding proteins and nucleosome position. *Nat. Methods* 10, 1213–1218. doi:10.1038/nmeth.2688

Campisi, J. (2013). Aging, cellular senescence, and cancer. *Annu. Rev. Physiol.* 75, 685–705. doi:10.1146/annurev-physiol-030212-183653

Carvalho, C., L'hote, V., Courbeyrette, R., Kratassiouk, G., Pinna, G., Cintrat, J. C., et al. (2019). Glucocorticoids delay RAF-induced senescence promoted by EGR1. *J. Cell Sci.* 132, jcs230748. doi:10.1242/jcs.230748

Chatsirisupachai, K., Lesluyes, T., Paraoan, L., Van Loo, P., and De Magalhaes, J. P. (2021). An integrative analysis of the age-associated multi-omic landscape across cancers. *Nat. Commun.* 12, 2345. doi:10.1038/s41467-021-22560-y

Chen, J. Y., Hug, C., Reyes, J., Tian, C., Gerosa, L., Frohlich, F., et al. (2023). Multi-range ERK responses shape the proliferative trajectory of single cells following oncogene induction. *Cell Rep.* 42, 112252. doi:10.1016/j.celrep.2023.112252

De Cecco, M., Ito, T., Petrashen, A. P., Elias, A. E., Skvir, N. J., Criscione, S. W., et al. (2019). L1 drives IFN in senescent cells and promotes age-associated inflammation. *Nature* 566, 73–78. doi:10.1038/s41586-018-0784-9

Dolgin, E. (2020). Send in the senolytics. *Nat. Biotechnol.* 38, 1371–1377. doi:10.1038/s41587-020-00750-1

Eggert, T., Wolter, K., Ji, J., Ma, C., Yevsa, T., Klotz, S., et al. (2016). Distinct functions of senescence-associated immune responses in liver tumor surveillance and tumor progression. *Cancer Cell* 30, 533–547. doi:10.1016/j.ccell.2016.09.003

Feng, H., Zhang, Y. B., Gui, J. F., Lemon, S. M., and Yamane, D. (2021). Interferon regulatory factor 1 (IRF1) and anti-pathogen innate immune responses. *PLoS Pathog.* 17, e1009220. doi:10.1371/journal.ppat.1009220

Ferreiros, A., Pedrosa, P., Da Silva-Alvarez, S., Triana-Martinez, F., Vilas, J. M., Picallos-Rabina, P., et al. (2019). Context-dependent impact of RAS oncogene expression on cellular reprogramming to pluripotency. *Stem Cell Rep.* 12, 1099–1112. doi:10.1016/j.stemcr.2019.04.006

Fornes, O., Castro-Mondragon, J. A., Khan, A., Van Der Lee, R., Zhang, X., Richmond, P. A., et al. (2020). JASPAR 2020: update of the open-access database of transcription factor binding profiles. *Nucleic Acids Res.* 48, D87–D92. doi:10.1093/nar/gkz1001

Fumagalli, M., Rossiello, F., Mondello, C., and D'adda Di Fagagna, F. (2014). Stable cellular senescence is associated with persistent DDR activation. *PLoS One* 9, e110969. doi:10.1371/journal.pone.0110969

Guan, Y., Zhang, C., Lyu, G., Huang, X., Zhang, X., Zhuang, T., et al. (2020). Senescence-activated enhancer landscape orchestrates the senescence-associated secretory phenotype in murine fibroblasts. *Nucleic Acids Res.* 48, 10909–10923. doi:10.1093/nar/gkaa858

Han, R., Li, L., Ugalde, A. P., Tal, A., Manber, Z., Barbera, E. P., et al. (2018). Functional CRISPR screen identifies AP1-associated enhancer regulating FOXF1 to modulate oncogene-induced senescence. *Genome Biol.* 19, 118. doi:10.1186/s13059-018-1494-1

Hanna, C. W., Taudt, A., Huang, J., Gahurova, L., Kranz, A., Andrews, S., et al. (2018). MLL2 conveys transcription-independent H3K4 trimethylation in oocytes. *Nat. Struct. Mol. Biol.* 25, 73–82. doi:10.1038/s41594-017-0013-5

Haugstetter, A. M., Loddenkemper, C., Lenze, D., Grone, J., Standfuß, C., Petersen, I., et al. (2010). Cellular senescence predicts treatment outcome in metastasised colorectal cancer. *Br. J. Cancer* 103, 505–509. doi:10.1038/sj.bjc.6605784

Heinz, S., Romanoski, C. E., Benner, C., and Glass, C. K. (2015). The selection and function of cell type-specific enhancers. *Nat. Rev. Mol. Cell Biol.* 16, 144–154. doi:10.1038/nrm3949

Hoare, M., Ito, Y., Kang, T. W., Weekes, M. P., Matheson, N. J., Patten, D. A., et al. (2016). NOTCH1 mediates a switch between two distinct secretomes during senescence. *Nat. Cell Biol.* 18, 979–992. doi:10.1038/ncb3397

Hsieh, H. J., Zhang, W., Lin, S. H., Yang, W. H., Wang, J. Z., Shen, J., et al. (2018). Systems biology approach reveals a link between mTORC1 and G2/M DNA damage checkpoint recovery. *Nat. Commun.* 9, 3982. doi:10.1038/s41467-018-05639-x

Ji, Y., Lotfollahi, M., Wolf, F. A., and Theis, F. J. (2021). Machine learning for perturbational single-cell omics. *Cell Syst.* 12, 522–537. doi:10.1016/j.cels.2021.05.016

Kaya-Okur, H. S., Wu, S. J., Codomo, C. A., Pledger, E. S., Bryson, T. D., Henikoff, J. G., et al. (2019). CUT&Tag for efficient epigenomic profiling of small samples and single cells. *Nat. Commun.* 10, 1930. doi:10.1038/s41467-019-09982-5

Khaliq, M., and Fallahi-Sichani, M. (2019). Epigenetic mechanisms of escape from BRAF oncogene dependency. *Cancers (Basel)* 11, 1480. doi:10.3390/cancers11101480

Krtolica, A., Parrinello, S., Lockett, S., Desprez, P. Y., and Campisi, J. (2001). Senescent fibroblasts promote epithelial cell growth and tumorigenesis: a link between cancer and aging. *Proc. Natl. Acad. Sci. U. S. A.* 98, 12072–12077. doi:10.1073/pnas.211053698

Landt, S. G., Marinov, G. K., Kundaje, A., Kheradpour, P., Pauli, F., Batzoglou, S., et al. (2012). ChIP-seq guidelines and practices of the ENCODE and modENCODE consortia. *Genome Res.* 22, 1813–1831. doi:10.1101/gr.136184.111

Langfelder, P., and Horvath, S. (2008). WGCNA: an R package for weighted correlation network analysis. *BMC Bioinforma.* 9, 559. doi:10.1186/1471-2105-9-559

Langmead, B., and Salzberg, S. L. (2012). Fast gapped-read alignment with Bowtie 2. *Nat. Methods* 9, 357–359. doi:10.1038/nmeth.1923

Lee, S., and Schmitt, C. A. (2019). The dynamic nature of senescence in cancer. *Nat. Cell Biol.* 21, 94–101. doi:10.1038/s41556-018-0249-2

Li, Z., Schulz, M. H., Look, T., Begemann, M., Zenke, M., and Costa, I. G. (2019). Identification of transcription factor binding sites using ATAC-seq. *Genome Biol.* 20, 45. doi:10.1186/s13059-019-1642-2

Liberzon, A., Birger, C., Thorvaldsdottir, H., Ghandi, M., Mesirov, J. P., and Tamayo, P. (2015). The molecular Signatures database Hallmark gene set collection. *Cell Syst.* 1, 417–425. doi:10.1016/j.cels.2015.12.004

Liu, T. (2014). Use model-based Analysis of ChIP-Seq (MACS) to analyze short reads generated by sequencing protein-DNA interactions in embryonic stem cells. *Methods Mol. Biol.* 1150, 81–95. doi:10.1007/978-1-4939-0512-6_4

Loffler-Wirth, H., Kalcher, M., and Binder, H. (2015). oposSOM: R-package for high-dimensional portraying of genome-wide expression landscapes on bioconductor. *Bioinformatics* 31, 3225–3227. doi:10.1093/bioinformatics/btv342

Love, M. I., Huber, W., and Anders, S. (2014). Moderated estimation of fold change and dispersion for RNA-seq data with DESeq2. *Genome Biol.* 15, 550. doi:10.1186/s13059-014-0550-8

Martinez-Zamudio, R. I., Robinson, L., Roux, P. F., and Bischof, O. (2017). SnapShot: cellular senescence pathways. *Cell* 170, 816–816.e1. doi:10.1016/j.cell.2017.07.049

Martinez-Zamudio, R. I., Roux, P. F., De Freitas, J., Robinson, L., Dore, G., Sun, B., et al. (2020). AP-1 imprints a reversible transcriptional programme of senescent cells. *Nat. Cell Biol.* 22, 842–855. doi:10.1038/s41556-020-0529-5

Martinez-Zamudio, R. I., Stefa, A., Nabuco Leva Ferreira Freitas, J. A., Vasilopoulos, T., Simpson, M., Dore, G., et al. (2023). Escape from oncogene-induced senescence is controlled by POU2F2 and memorized by chromatin scars. *Cell Genomics* 3, 100293. doi:10.1016/j.xgen.2023.100293

Milanovic, M., Fan, D. N. Y., Belenki, D., Dabritz, J. H. M., Zhao, Z., Yu, Y., et al. (2018). Senescence-associated reprogramming promotes cancer stemness. *Nature* 553, 96–100. doi:10.1038/nature25167

Moiseeva, V., Cisneros, A., Sica, V., Deryagin, O., Lai, Y., Jung, S., et al. (2023). Senescence atlas reveals an aged-like inflamed niche that blunts muscle regeneration. *Nature* 613, 169–178. doi:10.1038/s41586-022-05535-x

Natoli, G. (2010). Maintaining cell identity through global control of genomic organization. *Immunity* 33, 12–24. doi:10.1016/j.immuni.2010.07.006

Patta, I., Zand, M., Lee, L., Mishra, S., Bortnick, A., Lu, H., et al. (2024). Nuclear morphology is shaped by loop-extrusion programs. *Nature* 627, 196–203. doi:10.1038/s41586-024-07086-9

Ramirez, F., Ryan, D. P., Gruning, B., Bhardwaj, V., Kilpert, F., Richter, A. S., et al. (2016). deepTools2: a next generation web server for deep-sequencing data analysis. *Nucleic Acids Res.* 44, W160–W165. doi:10.1093/nar/gkw257

Recchia Luciani, G., Barilli, A., Visigalli, R., Sala, R., Dall'asta, V., Rotoli, B. M., et al. (2024). IRF1 mediates growth arrest and the induction of a secretory phenotype in alveolar epithelial cells in response to inflammatory cytokines ifnγ/tnfα. *Int. J. Mol. Sci.* 25, 3463. doi:10.3390/ijms25063463

Ritchie, M. E., Phipson, B., Wu, D., Hu, Y., Law, C. W., Shi, W., et al. (2015). Limma powers differential expression analyses for RNA-sequencing and microarray studies. *Nucleic Acids Res.* 43, e47. doi:10.1093/nar/gkv007

Sabio, G., and Davis, R. J. (2014). TNF and MAP kinase signalling pathways. *Seminars Immunol.* 26, 237–245. doi:10.1016/j.smim.2014.02.009

Sadangi, S., Milosavljevic, K., Castro-Perez, E., Lares, M., Singh, M., Altameemi, S., et al. (2022). Role of the skin microenvironment in melanomagenesis: epidermal keratinocytes and dermal fibroblasts promote BRAF oncogene-induced senescence escape in melanocytes. *Cancers (Basel)* 14, 1233. doi:10.3390/cancers14051233

Sardina, J. L., Collombet, S., Tian, T. V., Gomez, A., Di Stefano, B., Berenguer, C., et al. (2018). Transcription factors drive tet2-mediated enhancer demethylation to reprogram cell fate. *Cell Stem Cell* 23, 905–906. doi:10.1016/j.stem.2018.11.001

Smith, J., Zyoud, A., and Allegrucci, C. (2019). A case of identity: HOX genes in normal and cancer stem cells. *Cancers (Basel)* 11, 512. doi:10.3390/cancers11040512

Steens, J., and Klein, D. (2022). HOX genes in stem cells: maintaining cellular identity and regulation of differentiation. *Front. Cell Dev. Biol.* 10, 1002909. doi:10.3389/fcell.2022.1002909

Tasdemir, N., Banito, A., Roe, J. S., Alonso-Curbelo, D., Camiolo, M., Tschaharganeh, D. F., et al. (2016). BRD4 connects enhancer remodeling to senescence immune surveillance. *Cancer Discov.* 6, 612–629. doi:10.1158/2159-8290.cd-16-0217

Tsankov, A. M., Gu, H., Akopian, V., Ziller, M. J., Donaghey, J., Amit, I., et al. (2015). Transcription factor binding dynamics during human ES cell differentiation. *Nature* 518, 344–349. doi:10.1038/nature14233

Tsuchiya, M., Giuliani, A., Hashimoto, M., Erenpreisa, J., and Yoshikawa, K. (2015). Emergent self-organized criticality in gene expression dynamics: temporal development of global phase transition revealed in a cancer cell line. *PLoS One* 10, e0128565. doi:10.1371/journal.pone.0128565

Wang, B., Guo, H., Yu, H., Chen, Y., Xu, H., and Zhao, G. (2021). The role of the transcription factor EGR1 in cancer. *Front. Oncol.* 11, 642547. doi:10.3389/fonc.2021.642547

Wiley, C. D., and Campisi, J. (2021). The metabolic roots of senescence: mechanisms and opportunities for intervention. *Nat. Metab.* 3, 1290–1301. doi:10.1038/s42255-021-00483-8

Wilkinson, A. C., Nakauchi, H., and Gottgens, B. (2017). Mammalian transcription factor networks: recent advances in interrogating biological complexity. *Cell Syst.* 5, 319–331. doi:10.1016/j.cels.2017.07.004

Wilson, M. Z., Ravindran, P. T., Lim, W. A., and Toettcher, J. E. (2017). Tracing information flow from erk to target gene induction reveals mechanisms of dynamic and combinatorial control. *Mol. Cell* 67, 757–769.e5. doi:10.1016/j.molcel.2017.07.016

Wu, T., Hu, E., Xu, S., Chen, M., Guo, P., Dai, Z., et al. (2021). clusterProfiler 4.0: a universal enrichment tool for interpreting omics data. *Innovation* 2, 100141. doi:10.1016/j.xinn.2021.100141

Young, A. R., Narita, M., Ferreira, M., Kirschner, K., Sadaie, M., Darot, J. F., et al. (2009). Autophagy mediates the mitotic senescence transition. *Genes Dev.* 23, 798–803. doi:10.1101/gad.519709

Yu, G., Wang, L. G., and He, Q. Y. (2015). ChIPseeker: an R/Bioconductor package for ChIP peak annotation, comparison and visualization. *Bioinformatics* 31, 2382–2383. doi:10.1093/bioinformatics/btv145

Yu, Y., Schleich, K., Yue, B., Ji, S., Lohneis, P., Kemper, K., et al. (2018). Targeting the senescence-overriding cooperative activity of structurally unrelated H3K9 demethylases in melanoma. *Cancer Cell* 33, 322–336.e8. doi:10.1016/j.ccell.2018.01.002

Zampetidis, C. P., Galanos, P., Angelopoulou, A., Zhu, Y., Polyzou, A., Karamitros, T., et al. (2021). A recurrent chromosomal inversion suffices for driving escape from oncogene-induced senescence via subTAD reorganization. *Mol. Cell* 81, 4907–4923.e8. doi:10.1016/j.molcel.2021.10.017

frontiers | Frontiers in Epigenetics and Epigenomics

TYPE Mini Review
PUBLISHED 31 July 2024
DOI 10.3389/freae.2024.1451971



OPEN ACCESS

EDITED BY
Yun Nancy Huang,
Texas A and M University, United States

REVIEWED BY
Luisa Cimmino,
University of Miami, United States

*CORRESPONDENCE
Tiziano Bernasocchi,
tbernasocchi@mgh.harvard.edu
Raul Mostoslavsky,
rmostoslavsky@mgh.harvard.edu

RECEIVED 20 June 2024
ACCEPTED 17 July 2024
PUBLISHED 31 July 2024

CITATION
Bernasocchi T and Mostoslavsky R (2024), Subcellular one carbon metabolism in cancer, aging and epigenetics.
*Front. Epigenet. Epigenom.* 2:1451971.
doi: 10.3389/freae.2024.1451971



# Subcellular one carbon metabolism in cancer, aging and epigenetics

Tiziano Bernasocchi[1,2]* and Raul Mostoslavsky[1,2]*

[1]The Krantz Family Center for Cancer Research, The Massachusetts General Hospital Cancer Center and Harvard Medical School, Boston, MA, United States, [2]The Broad Institute of Harvard and MIT, Cambridge, MA, United States

The crosstalk between metabolism and epigenetics is an emerging field that is gaining importance in different areas such as cancer and aging, where changes in metabolism significantly impacts the cellular epigenome, in turn dictating changes in chromatin as an adaptive mechanism to bring back metabolic homeostasis. A key metabolic pathway influencing an organism's epigenetic state is one-carbon metabolism (OCM), which includes the folate and methionine cycles. Together, these cycles generate S-adenosylmethionine (SAM), the universal methyl donor essential for DNA and histone methylation. SAM serves as the sole methyl group donor for DNA and histone methyltransferases, making it a crucial metabolite for chromatin modifications. In this review, we will discuss how SAM and its byproduct, S-adenosylhomocysteine (SAH), along with the enzymes and cofactors involved in OCM, may function in the different cellular compartments, particularly in the nucleus, to directly regulate the epigenome in aging and cancer.

KEYWORDS

**one carbon metabolism, DNA methylation, histone methylation, SAM, subcellular metabolism, cancer, aging**

## Introduction

The connection between metabolic intermediates and epigenetic regulation has become increasingly evident in recent years. Metabolites serve as crucial signaling molecules, orchestrating cellular responses and adaptability based on the broad range of nutrients absorbed from our diet. Previous works have shown that dietary changes can influence an organism's epigenetic landscape, with the potential for these modifications to be inherited by future generations (Padmanabhan et al., 2013; Vaiserman and Lushchak, 2021). A compelling example of this is the devastating famine that occurred at the end of World War II in the Netherlands known as the Dutch famine, where thousands suffered from malnutrition. The children of women who were pregnant during this period exhibited an increased incidence of obesity, schizophrenia, and diabetes. Subsequent studies on this population demonstrated that these children inherited epigenetic marks that significantly impacted their lives (Vaiserman and Lushchak, 2021; González-Rodríguez et al., 2023). One of the key reasons for this effect is due to the fact that all the epigenetic modifications in our chromatin are chemical modifications (metabolites), and thus, their availability directly affects chromatin dynamics. Specifically, changes in an organism's nutrient intake can significantly influence both DNA and histone modifications. For instance, Acetyl-CoA is a pivotal player in acetylation, S-adenosylmethionine (SAM) is the universal donor for methylation reactions, and adenosine triphosphate (ATP) is a fundamental component for phosphorylation (Wei et al., 1999; Rossetto et al., 2012; Etchegaray and Mostoslavsky, 2016;

Mentch and Locasale, 2016; Boon et al., 2020; Guertin and Wellen, 2023). Among these, multiple studies have shown that the availability of Acetyl-CoA is critical for chromatin function. In that context, nuclear acetyl-CoA is derived from multiple pathways, including the (ATP)-citrate lyase (ACLY)-dependent conversion of cytosolic citrate (Wellen et al., 2009), the Acyl-CoA synthetase short-chain member 2 (ACSS2)-dependent conversion of acetate (Bulusu et al., 2017), and the generation of acetyl-CoA from pyruvate by the pyruvate dehydrogenase enzyme. Interestingly, all these enzymes can translocate to the nucleus to generate acetyl-CoA *in situ* to support histone acetylation at specific genes. Such an adaptation was key to drive the expression of lysosomal and autophagy genes to support these metabolic pathways in neurons, as well as to support local repair of DNA damage (Sutendra et al., 2014; Bulusu et al., 2017; Li et al., 2017; Sivanand et al., 2017; Li et al., 2021). Parallel studies have shown that nuclear translocation of ACSS2 in hippocampal neurons was key to allowing histone acetylation locally at neuronal genes, a critical switch to drive long-term spatial memory (Mews et al., 2017). These mechanisms were dependent on phosphorylation reactions initiated by signaling cascades, including activation of the AMPK kinase (Li et al., 2017), suggesting that nuclear metabolic demands were coordinated with nutrient supply. In addition to acetyl-CoA, subcellular availability of the central metabolic coenzyme $NAD^+$ also appears critical to supporting epigenetic reactions. Beyond its key roles as an electron carrier in mitochondrial respiration and other redox reactions (Luengo et al., 2021), $NAD^+$ can also act as a co-factor in deacetylation reactions driven by the sirtuin enzymes, as well as an ADP-ribosylation donor for the PARP enzymes (Finkel et al., 2009). Given their $NAD^+$ dependency, sirtuins can link nutritional states to metabolic reprogramming through sensing of $NAD^+$ levels (Liu et al., 2012; Martinez-Pastor and Mostoslavsky, 2012). For instance, the histone deacetylase SIRT6 modulates glycolytic metabolism as a silencer of glycolytic genes in response to glucose availability, a role that defines it as a strong tumor suppressor, while SIRT1 is a major inducer of PGC1α-dependent mitochondrial biogenesis under conditions of nutrient stress (Rodgers et al., 2005). Notably, metabolic stress was shown to increase nuclear levels of $NAD^+$ specifically through the nuclear localization and activation of the $NAD^+$ synthesis enzyme Nicotinamide Phosphoribosyltransferase (NAMPT) (Svoboda et al., 2019). In addition, SIRT6 was shown to directly activate local NAMPT (Sociali et al., 2019) while in parallel regulating the activity of PARP1 as a sensor of DNA damage (Mao et al., 2011), thus balancing $NAD^+$ consumption and production. Local NAD synthesis and SIRT1 activation were also shown as key to preventing axonal degeneration (Araki et al., 2004). Another strong evidence of subcellular regulation of NAD levels was determined in studies showing a switch in expression from the nuclear NMNAT1 to the cytoplasmic NMNAT2 to shift NAD + production from the nucleus to the cytoplasm to inhibit PARP1-dependent parylation of adipogenic genes, in turn driving activation of these genes during adipogenesis (Ryu et al., 2018).

The recent discovery of novel histone modifications involving other metabolites, such as lactylation (Zhang et al., 2019), homocysteinylation (Zhang et al., 2018), dopaminylation (Lepack et al., 2020), benzoylation (Huang et al., 2018), serotonylation (Farrelly et al., 2019), O-GlcNAcylation (Chen et al., 2013), succinylation (Xie et al., 2012), and ADP-ribosylation (Messner and Hottiger, 2011), underscores the profound connection between metabolic pathways and cellular epigenetics. A striking example is lactate, which was conventionally viewed as a mere metabolic waste product. Recent studies have unveiled its role in various pathways, including redox balance and serving as an intermediary energy store, mirroring glucose (Rabinowitz and Enerbäck, 2020). Specifically, lactate has been found to have a significant influence on embryonic stem cells, which are predominantly glycolytic; lactylation marks in these cells are associated with active enhancers crucial for the development of the neural crest and presomitic mesoderm, highlighting the reevaluation of lactate from a waste product to a key epigenetic regulator (Martinez-Outschoorn et al., 2011; Merkuri et al., 2024).

Despite its central role as a metabolic node and modulator of methylation reactions on chromatin, the roles of one-carbon metabolism in the different cellular compartments have been less explored. This review will delve into the one-carbon pathway and its pivotal role in cellular methylation processes.

## OCM pathway overview

One-carbon metabolism, which includes the folate pathway, the methionine cycles, and the transsulfuration pathway, plays a critical role in generating one-carbon units (methyl groups). These groups are required for several metabolic processes, including DNA synthesis, protein methylation (e.g., of histones and creatine), DNA methylation at heterochromatin regions and CpG islands in promoters and enhancers, and the biosynthesis of polyamines and lipids (Yang and Vousden, 2016) (Figure 1).

Starting with the folate cycle, central to one-carbon metabolism, vitamins, and amino acids are utilized as cofactors and methyl group donors, respectively. The cycle is divided between the cytoplasmic and mitochondrial folate cycles (Petrova et al., 2023) (see Figure 1, Folate cycle). In the cytosol, the amino acids serine, histidine, and the metabolite formate act as methyl group donors, with vitamin B9 (folate) serving as the acceptor. Serine is not an essential amino acid; thus, it can be taken up by the cells through different transporters or produced by the cells from other metabolites (Reid et al., 2018; Tajan et al., 2021; Papalazarou et al., 2023). The serine synthesis pathway (SSP) is the major pathway for serine synthesis. The cycle begins with a glycolytic intermediate, 3-phosphoglycerate (3-PG). Initially, Phosphoglycerate dehydrogenase (PHGDH) catalyzes the oxidation of 3-PG to 3-phosphohydroxypyruvate (3-PHP), simultaneously producing NADH. Subsequently, 3-PHP is transformed into 3-phosphoserine (3-PS) by phosphoserine aminotransferase (PSAT1) in a transamination reaction, with glutamate donating the amino group and concurrently generating α-ketoglutarate. The final step is the dephosphorylation of 3-PS to serine, facilitated by phosphoserine phosphatase (PSPH). This reaction produces serine and generates reducing power in the form of NADH and provides α-ketoglutarate, an important intermediate for the TCA cycle (Yang and Vousden, 2016). To underscore the importance of maintaining appropriate serine levels within cells, serine acts as an activator of the enzyme pyruvate kinase M2 (PKM2). This enzyme catalyzes the transfer of a phosphate group to ADP, producing ATP from phosphoenolpyruvate in the final step of the glycolysis pathway, resulting in the formation of pyruvate. Low levels of serine inhibit this reaction, potentially reversing the pathway toward gluconeogenesis, thereby increasing the availability of 3-

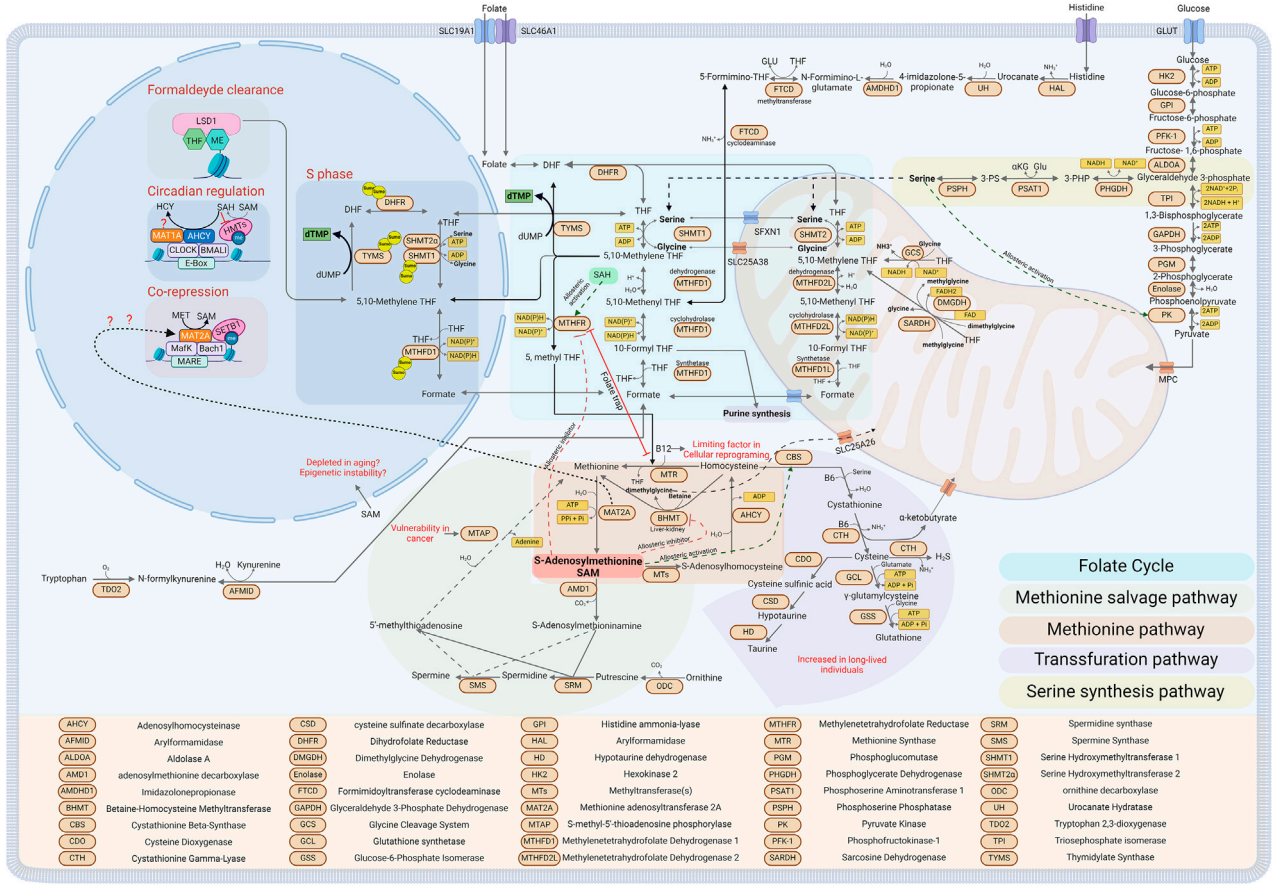


FIGURE 1
Diagram depicting One Carbon Metabolism and its related metabolic pathways in the different sub-cellular compartments (see text for details). Created with BioRender.com.

phosphoglycerate (3-PG) for the serine synthesis pathway (SSP) (Chaneton et al., 2012; Ye et al., 2012) (see Figure 1, Serine synthesis pathway).

Additionally, carbon units for the folate cycle can also be derived from formate, which can donate one carbon directly to tetrahydrofolate in a reversible reaction catalyzed by the tri-enzyme Methylenetetrahydrofolate Dehydrogenase, Cyclohydrolase, and Formyltetrahydrofolate Synthetase 1 (MTHFD1). This reaction consumes an ATP and generates 10-formyl-THF, which can directly enter the *de novo* synthesis of purines or continue through the folate cycle via the cyclohydrolase and dehydrogenase activities of MTHFD1 (Brosnan and Brosnan, 2016) (See Figure 1, Cytoplasmatic Folate cycle). Formate can be generated in cells by tryptophan catabolism or by the activity of aldehyde dehydrogenase class 3 (ADH5), detoxifying formaldehyde from the cells and converting it into the more stable formate (Burgos-Barragan et al., 2017). Moreover, formaldehyde itself can directly condense with THF, driving the formation of 5, 10-methylene THF, the only form of folate that could be combined with homocysteine to generate methionine, which in turn is used by the MAT2 enzymes to synthesize SAM (see Figure 1, Methionine cycle). It has been shown that Lysine-specific demethylase 1 (LSD1) is a folate-binding protein, indicating that while it demethylates and releases the highly reactive metabolite formaldehyde, it could directly recycle it by condensing with THF, thus forming nuclear 5, 10-methylene THF (Luka et al., 2011; Luka et al., 2014; Garcia et al., 2016) (see Figure 1, Formaldehyde clearance). Moreover, histidine catabolism can also generate a carbon unit when it is oxidized to glutamate. The intermediate of the reaction that releases a carbon unit is N-formiminoglutamate (FIGLU) throught the bifunctional enzyme glutamate formiminotransferase (FTCD) that donates one carbon from FIGLU to THF, forming N5-formimino-THF and glutamate. N5-formimino-THF is then further processed to 5, 10-methenyl-THF by formiminotransferase cyclodeaminase (FTCD) (Brosnan and Brosnan, 2020). In this context, histidine catabolism has been suggested as a major consumer of THF, and contributing to the toxicity of the chemotherapeutic antifolate methotrexate (Kanarek et al., 2018). In other organisms but not in humans, the essential amino acid threonine can be converted to Serine in a two-step process: initially, threonine is transformed into 2-amino-3-ketobutyrate by L-threonine dehydrogenase, generating NADH in the process. Subsequently, glycine C-acetyltransferase (GCAT) catalyzes the conversion of 2-amino-3-ketobutyrate to acetyl-CoA and glycine. This pathway has been shown to be essential for mouse Embrionic Stem Cells (mESCs) (Wang et al., 2009; Shyh-Chang et al., 2013).

In the mitochondria, the sources of methyl groups are more diverse. Here, dimethylglycine (DMG), glycine, and sarcosine, along

with serine and formate can be utilized as carbon sources to fuel the cycle. The serine required for the mitochondrial folate cycle is transported into the mitochondria through the sideroflexin 1 (SFXN1) transporter (Kory et al., 2018). Once inside, it enters the folate cycle, where it is converted to glycine by serine hydroxymethyltransferase 2 (SHMT2), and a carbon unit is donated to THF to generate 5, 10-methylene THF (Ducker and Rabinowitz, 2017). As highlighted above, most serine is derived from glucose or cellular intake. However, this is not the case in the liver, where it has been shown that Serine hydroxymethyltransferase 2 (SHMT2), which in most organs converts mitochondrial serine to glycine while donating a carbon unit to Tetrahydrofolate, primarily operates in the reverse direction in the liver. This process helps clear the glycine pool and generates serine, which can then be converted by the enzyme serine dehydratase (SDH) into pyruvate and utilized by the TCA cycle (McBride et al., 2024). In the mitochondria, glycine can further contribute to the folate cycle by donating an additional carbon unit through the Glycine Cleavage System (GCS), generating 5, 10-methylene THF, ammonia, and NADH (Kikuchi et al., 2008). Both DMG and methylglycine, also known as sarcosine, can enter the folate cycle. DMG can release two one-carbon units in subsequent reaction steps. First, the enzyme dimethylglycine dehydrogenase (DMGDH) converts DMG to sarcosine, releasing 5, 10-methylene THF and reductive power in FADH2 (Frisell and Mackenzie, 1962). The subsequent reaction utilizes a second mitochondrial enzyme, sarcosine dehydrogenase (SARDH), that catalyzes the oxidation of sarcosine to glycine, generating formaldehyde, which will react with THF to form 5, 10-methylene THF (Wittwer and Wagner, 1981) (See Figure 1, Mitochondria folate cycle).

The methionine cycle is a crucial component of one-carbon metabolism, which is linked to and dependent on the folate cycle. While the folate cycle is essential for generating most of the methyl groups for purine synthesis and reductive power in the mitochondria in the form of FADH2 and NADPH, the methionine cycle's primary role is generating the universal methyl donor S-adenosylmethionine (SAM), regenerating methionine, and producing polyamines such as spermine and spermidine (Cantoni, 1952; Sanderson et al., 2019) (see, Figure 1, Methionine and salvage cycle). The folate and methionine cycles intersect at the conversion of homocysteine back to methionine by the cytosolic enzyme methionine synthase (MTR), which uses methylcobalamin (methylated vitamin B12) as a cofactor. During this step, a carbon unit generated in the folate cycle and carried by 5-methyl THF is donated to homocysteine, resulting in methionine (Banerjee and Matthews, 1990). This part of the cycle is critical to prevent the accumulation of homocysteine in cells. Dysfunctions led by a polymorphism in MTHFR (the enzyme converting 5, 10-methylene THF to 5-methyl THF) or a lack of vitamin B12 can lead to both hyperhomocysteinemia and folate deficiency. This occurs because 5, 10-methylene THF cannot be recycled in the folate cycle, and homocysteine cannot be recycled in the methionine cycle, thus leading to what is known as the "folate trap" (Scott and Weir, 1981; Gershoni-Baruch et al., 2000; Refsum et al., 2006; Maruti et al., 2009; Hasan et al., 2019) (see Figure 1, Folate trap). The methionine cycle is not the sole pathway that uses homocysteine; the transsulfuration pathway is an alternative route. Here, the enzyme cystathionine β-synthase (CBS) catalyzes the initial reaction, combining serine with homocysteine to generate cystathionine while releasing a molecule of water (Werge et al., 2021). The subsequent reaction, catalyzed by cystathionase, produces cysteine and α-ketobutyrate, releasing ammonia and water. Both reactions require vitamin B6 (pyridoxal phosphate) as a cofactor and can produce hydrogen sulfide as an alternative byproduct. Cysteine then enters the glutathione biosynthesis pathway; initially, it is converted to γ-glutamylcysteine by glutamate-cysteine ligase (GCL), adding glutamate (Chandel, 2021). Subsequently, glutathione synthetase (GSS) adds glycine to form glutathione (GSH), a critical tripeptide that acts as a reducing agent to counteract oxidative stress, to facilitate the detoxification of xenobiotics, and to regulate the cellular redox state (Aquilano et al., 2014) (see Figure 1, Transsulfuration pathway).

The methionine cycle and the transsulfuration pathway are intricately interconnected and regulated by S-adenosylmethionine (SAM) levels. High levels of SAM enhance CBS activity by binding non-covalently to a heme group within CBS, stabilizing the enzyme and increasing the homocysteine flux into the transsulfuration pathway (Prudova et al., 2006). Concurrently, high levels of SAM allosterically inhibit methylenetetrahydrofolate reductase (MTHFR) and betaine-homocysteine S-methyltransferase (BHMT), respectively inhibiting the formation of 5-methyltetrahydrofolate and methionine. Conversely, a low SAM/SAH ratio inhibits CBS due to the lack of SAM and activates MTHFR when bound by S-adenosylhomocysteine (SAH), directing more homocysteine towards the methionine cycle (Kutzbach and Stokstad, 1967; Kutzbach and Stokstad, 1971; Jencks and Mathews, 1987; Ou et al., 2007) (See Figure 1, Allosteric inhibition activation).

Methionine can be regenerated from homocysteine in a folate-independent manner by the enzyme BHMT, which is exclusively expressed in the liver and kidneys. In this pathway, trimethylglycine (known as betaine) donates a methyl group to homocysteine, generating methionine and releasing dimethylglycine (DMG) in an ATP-independent manner (Pajares and Pérez-Sala, 2006). DMG can then enter the mitochondrial folate cycle, as previously mentioned. The subsequent step involves the generation of SAM, facilitated by the methionine adenosyltransferase (MAT) enzyme family. In mammals, there are two MAT enzymes, MAT1A and MAT2A, that encode for two homologous catalytic subunits, α1 and α2, respectively. MAT1A is primarily expressed in the liver and organizes into two isoenzymes, MATIII (a dimer) and MATI (a tetramer) (Kotb et al., 1997; Ramani and Lu, 2017). Conversely, MAT2A is expressed in most tissues and forms the MATII isoenzyme, which can exist as both a dimer and a tetramer (Kotb and Kredich, 1985). MAT enzymes catalyze the reaction between methionine and ATP to generate SAM (also known as AdoMet), releasing phosphate and diphosphate (Niland et al., 2021). At this step, SAM can follow two pathways: it can be used for methylation reactions throughout the cell or enter the polyamine pathway. In the polyamine pathway, SAM is decarboxylated by adenosylmethionine decarboxylase (AMD1) to S-adenosylmethioninamine (dcAdoMet), where it donates a propylamine group to putrescine and spermidine to generate spermidine and subsequently spermine through the enzymes spermidine synthase (SRM) and spermine synthase (SMS), releasing 5-methylthioadenosine (MTA) (Minois et al., 2011). Intriguingly, MTA can reenter the methionine cycle using what is termed the methionine salvage pathway or MTA cycle,

where MTA can be recycled back to methionine by S-methyl-5-thioadenosine phosphorylase (MTAP) (Albers, 2009) (See Figure 1, Methionine salvage pathway). The main pathway for SAM involves donating a methyl group in various methylation reactions catalyzed by several methyltransferases, producing S-adenosylhomocysteine (SAH), a potent allosteric inhibitor of many methyltransferases (Richon et al., 2011; Kung et al., 2015). SAH can continue the cycle where it is converted back to homocysteine by S-adenosylhomocysteinase (AHCY) (Turner et al., 1998; Vizán et al., 2021). Moreover, SAM can refuel the folate cycle too by donating a carbon to glycine in the reaction guided by Glycine N-methyltransferase (GNMT) and generating sarcosine that will feed the mitochondrial folate pathway (Yeo and Wagner, 1992; Luka et al., 2009).

## Nuclear OCM and its epigenetics implications

Histone and DNA methylation are metabolic reactions driven by enzymes that add or remove methyl groups (Xiao and Locasale, 2021). These changes depend directly on two key components: the availability of the substrate, S-adenosylmethionine (SAM), and the presence of enzymes. In the case of histones, these enzymes are histone methyltransferases (HMTs), which belong to two main classes: SET domain-containing and non-SET domain-containing enzymes. Both classes require the metabolite SAM as a methyl donor and release S-adenosylhomocysteine (SAH) after the transmethylation reaction (Dillon et al., 2005; Husmann and Gozani, 2019). Interestingly, SAH itself can act as an inhibitor of both classes of HMTs. Therefore, changes in the SAM/SAH ratio can activate or inhibit several methyltransferases, thereby increasing or decreasing histone methylation (Richon et al., 2011; Mentch and Locasale, 2016). This ratio is referred to as the "Methylation Index" because it is directly proportional to the cell's capacity to methylate (Zhang, 2018) (see Figure 1, Circadian regulation). Mimicking the chemical structure of SAH has led to the development of a new class of drugs targeting methyltransferases (Zhang and Zheng, 2016). A notable example is EZH2, which is highly expressed in several cancers, such as prostate cancer. EZH2 is part of the polycomb repressive complex and represses transcriptional activity through the methylation of H3K27 (Kung et al., 2015; Duan et al., 2020).

As mentioned above, although not strictly related to the subcellular regulation of the OCM, few recent studies have emerged pointing to compartment-specific roles for some enzymes in the cycle (Boon et al., 2020). A significant example is AHCY, which catalyzes the hydrolysis of SAH to homocysteine and has been shown to be associated with CLOCK-BMAL1, the circadian complex that in turn interacts with the SET-dependent MLL family of H3K4 methyl transferases. AHCY's binding was required to mediate an oscillation of H3K4me3 marks that are circadian dependent, suggesting that these daily chromatin changes are AHCY-dependent and that pharmacological inhibition of AHCY in the hypothalamus alters the amplitude of circadian gene expression. Similarly, another one-carbon pathway gene, MAT1A, was shown to be recruited to the same chromatin complex, suggesting a possible role in the transcriptional regulation of one-carbon enzymes, though its role was not fully explained (Greco et al., 2020) (See Figure 1, Circadian regulation).

Furthermore, MAT2A, which catalyzes the conversion of methionine to SAM, has been shown to interact on a chromatin complex with MafK, Swi/Snf, and NuRD complexes, and its catalytic activity was required for the expression of the MafK-dependent HO-1 gene (Katoh et al., 2011). Subsequent work from the Igarashi lab demonstrated that MAT2A represses the expression of cyclooxygenase 2 (COX2) by specifically interacting with the H3K9 methyltransferase SET-dependent SETB1, inducing the repressive mark H3K9me1/3 and specifically repressing COX-2 genes (Kera et al., 2013). These results suggest a possible compartmentalized role of OCM at the nuclear level (See Figure 1, Co-repression), although it remains unclear whether such roles for MAT2A in the nucleus represent a specific function on few loci or a broader, chromatin-wide role.

In addition, methionine restriction has been shown to impair the methylation pattern of histones. Mentch et al., (2015) demonstrated that H3K4me3, a histone mark commonly found near transcription start site (TSS) regions of actively transcribed genes, was depleted upon methionine restriction. Interestingly, the study found that the methylation mark was depleted across the genome, and the breadth of the peak decreased after methionine restriction, suggesting a potential additional role of these markers as a methyl sink that could be reused in case of necessity. Although Bérénice et al., (2014) linked the breadth of H3K4me3 to transcriptional consistency, this could suggest that in times of need, cells could sacrifice consistency to gain access to additional methyl groups. Along these lines, another study suggested a similar pattern in yeast, demonstrating that demethylation of the Protein Phosphatase 2 A complex (PP2A) in response to methionine deprivation activates PP2A, which then phosphorylates Rph1, a histone demethylase that specifically demethylates H3K4 and H3K36, allowing the preservation of SAM (Ye et al., 2019). Haws et al., (2020) further demonstrated that with the depletion of the cellular SAM pool *in vivo*, cells preferentially conserve H3K9 monomethylation at the expense of di- and tri-methylation, suggesting that maintaining H3K9me1 could help retain the heterochromatin region and preserve genome stability.

## OCM in cancer

The concept of altered metabolic changes in cancer cells was first identified by Otto Warburg in the 1920s, as evidenced by his discovery of increased aerobic glycolysis in cancer cells (Vander Heiden et al., 2009). Additionally, cancer cells, in their quest for rapid proliferation, frequently upregulate several other metabolic pathways, such as the OCM, reflecting the increased demand for synthesizing purine and pyrimidine nucleotides. These nucleotides are essential for synthesizing DNA and RNA, underscoring the critical role of OCM in supporting the proliferative needs of cancer cells (Shuvalov et al., 2017; Petrova et al., 2023). Building on these foundations, anti-folates, targeting the one-carbon pathway, were developed following Sydney Farber's observation of leukemia's response to folate-deficient diets (Farber et al., 1948). Despite antifolate's efficacy in cancer treatment, its broad impact on metabolic pathways can lead to severe side effects.

Traditional strategies targeting cancer metabolism often face limitations due to the essential role of these pathways in normal

physiology, leading to limited success. To circumvent these collateral effects, researchers are now exploring the combination of specific diets with targeted therapy. A notable example comes from the work of Gao et al., (2019) who demonstrated that a methionine restriction diet was sufficient to inhibit tumor proliferation *in vivo* in a human PDX model harboring a KRAS mutation. Additionally, the therapeutic effect was enhanced by combining methionine restriction with radiation therapy, which induced a cell-autonomous response dependent on decreased redox and nucleotide metabolism flux. Similarly, a recent study by Li et al., (2024) targeted the one-carbon pathway in liver cancer through the pharmacological inhibition of MAT2A, resulting in increased DNA damage and cell cycle arrest. Further pharmacological screening identified a GSK3 inhibitor that selectively kills MAT2A-inhibited senescent liver cancer cells, suggesting a potential combination therapy between MAT2A and GSK3 inhibitors. Wang et al., (2019) demonstrated that OCM plays a critical role even in tumor-initiating cells (TICs). They performed metabolomic and tracing experiments, specifically identifying an increase in methionine cycle consumption and a high dependency on exogenous methionine in TICs. In this case, pharmacological inhibition of MAT2A was sufficient to cripple the tumor-initiating capability of these cancer cells and alter their epigenetic state. Further highlighting the importance of OCM in cancer, several tumors harbor deletions in the loci containing cyclin-dependent kinase 2A (CDKN2A). Methylthioadenosine (MTAP), as previously discussed, is a gene involved in the methionine salvage pathway and is co-deleted in almost 15% of all cancers with CDKN2A deletion. The deletion of MTAP makes the cells more reliant on the methionine cycle, lacking the ability to recycle methionine from the salvage pathway and, more specifically, depending on MAT2A. Kalev et al., (2021). developed and tested two new inhibitors of MAT2A and demonstrated that cancer cells lacking MTAP were more susceptible to MAT2A inhibitors compared to their wild-type counterparts; they also showed increased sensitivity to taxane therapy *in vivo* when co-treated. Moreover, MAT2A has been identified as a potential target in Diffuse Midline Gliomas (DMGs), a new subclass of high-grade gliomas, over 80% of which are characterized by a hotspot mutation in H3K27 that leads to a global reduction in H3K27me3. Impairment of H3K27me3 spares SAM, increasing its intracellular levels which are used by the RNA methyltransferase METTL16 to methylate the mRNA of MAT2A, causing intron retention and degradation of MAT2A itself. The authors showed that further inhibition of MAT2A activity under these conditions disturbed H3K36me3 methylation and inhibited the oncogenic and developmental transcriptional program of the gliomas, extending survival in multiple models of DMG (Golbourn et al., 2022). The metabolic pathways highlighted above are extremely plastic, exemplified by the carbon units utilized by OCM that can be derived from various sources such as serine, glycine, formate, and others as shown above. For instance, a study by Sullivan et al., (2021) showed that the major source of folate in the cellular environment *in vivo* is 5-methyl-THF, which can sustain the folate cycle *in vivo* instead of folic acid and bypass the efficacy of antifolate therapies such as methotrexate, which inhibit the pathway upstream.

The SSP pathway is tightly regulated in several cancers, underscoring the dependency of cancer cells on serine catabolism. An example is the work by Ding and colleagues, where several cancer cells experiencing serine depletion require the histone 3 lysine 9 (H3K9) methyltransferase G9A to maintain the expression of SSP genes such as PHGDH and SHMT2. Genetic knockdown of G9A inhibited cell proliferation and depleted the serine pool in cancer cells (Ding et al., 2013). Moreover, SHMT2 and GLDC have been shown to antagonize the activity of PKM2 and reduce oxygen consumption in glioblastoma multiforme (GBM), thereby driving a survival advantage by reprogramming the metabolic state of the tumor (Kim et al., 2015). In a similar fashion, cancer cells have been shown to deplete exogenous serine, triggering a p53-dependent activation of the SSP pathway, which suppresses anaerobic glycolysis and increases the flux toward the TCA cycle (Maddocks et al., 2013). The OCM pathway is not only deregulated somatically in cancer. Inherited polymorphisms in the OCM pathway are associated with an increased risk of tumorigenesis. A study exploring the inherited susceptibility to cancer-related epigenetic alterations analyzed 233 patients with colorectal, breast, or lung cancer for germ-line variants in genes critical for methyl group metabolism, including methylenetetrahydrofolate reductase, methionine synthase, and cystathionine β-synthase. This investigation revealed a complex link between genetic predispositions and epigenetic modifications in cancer. Key findings indicated that individuals with the methylenetetrahydrofolate reductase 677 T allele exhibited inherently low genomic 5-methylcytosine levels and less severe global hypomethylation in tumors. Additionally, tumors in patients homozygous for the methionine synthase 2756G allele had fewer hypermethylated CpG islands in tumor suppressor genes, further underscoring the intricate relationship between metabolism and epigenetics in cancer (Paz et al., 2002).

## Impact of OCM on pluripotency and aging

Aging and pluripotency are closely interconnected, albeit in opposing manners. Aging can be described as the gradual exhaustion of an organism's cellular pluripotency (Pal and Tyler, 2016; López-Otín et al., 2023). Similarly, both processes are heavily influenced by epigenetic modifications. Studies pioneered by the Horvath's lab defined changes in the methylation of specific CpGs as one of the best predictors of chronological and biological aging in organisms, a phenomenon termed "epigenetic clock" (Horvath, 2013). Conversely, the maintenance of pluripotency necessitates a distinct epigenetic state, as demonstrated by induced pluripotent stem cells (iPSCs), which are reprogrammed through the Yamanaka factors (Oct4, Sox2, Klf4, and c-Myc), which are characterized by a "rejuvenated" epigenetic landscape (Stadtfeld and Hochedlinger, 2010).

The significance of one-carbon metabolism (OCM) in maintaining the pluripotent state of cells was highlighted by the discovery of a more than 200-fold upregulation of threonine dehydrogenase (TDH) in mouse Embrionic Stem Cells (mESCs) (Alexander et al., 2011). Furthermore, the deprivation of threonine among 20 amino acids tested was found critical for the proliferation and differentiation of these cells (Wang et al., 2009). TDH, an enzyme within the OCM, catalyzes the oxidation of threonine to 2-

amino-acetate, which subsequently contributes to the generation of acetyl-CoA and glycine through Glycine C-acetyltransferase (GCAT). The depletion of threonine was shown to slow growth and increase differentiation in mESCs due to a reduction in the SAM pool and, consequently, decreasing H3K4me3 markers. Only supplementation with both glycine and acetyl-CoA could rescue this phenotype, suggesting that ES cells require both methyl donors from glycine and reductive power from acetyl-CoA (Shyh-Chang et al., 2013). It is important to note, however, that the TDH enzyme is a pseudogene in human cells and is therefore not active (Edgar, 2002). In another study, Shiraki et al., (2014) tested the reliance of both human Embryonic Stem Cells (ESCs) and iPSCs on single amino acid deprivation. They highlighted that deprivation of leucine, lysine, or methionine inhibited cell proliferation, with methionine deprivation causing the most significant decrease. Similar to previous studies, methionine deprivation led to a decrease in the cellular content of SAM, triggering demethylation of H3K4me3 followed by broader global demethylation, which consequently increased p53 signaling and decreased the expression of the pluripotency marker NANOG.

The reprogramming of iPSCs driven by Yamanaka factors requires extensive epigenetic remodeling, necessitating a large supply of methyl donor groups in the form of SAM. Kovatcheva et al., (2023) demonstrated that during reprogramming, cells deplete the essential cofactor vitamin B12, crucial for methionine and, consequently, SAM production. Replenishing the vitamin B12 pool significantly enhanced the efficiency of reprogramming and prevented illegitimate transcription initiation by maintaining the histone mark H3K36me3. Contrary to the works discussed above suggesting the requirement of one-carbon metabolism (OCM) in pluripotency, overall aging, and lifespan have been associated with what seems to be a downregulation of OCM through methionine restriction (MR). Several studies have shown that dietary restriction of methionine alone is sufficient to improve metabolic function and life extension (Orentreich et al., 1993; Miller et al., 2005; Lees et al., 2014). For example, a study using male Fischer 344 rats showed a 30% increase in lifespan. In a subsequent study on the same rats, it was demonstrated that those on a methionine-restricted diet exhibited reduced visceral fat, decreased levels of insulin and glucose, and increased energy expenditure (DEE) (Malloy et al., 2006). It is important to note that DEE is normalized to body weight, and the MR rats weighed almost half as much as the control group. This further suggests that the lifespan extension phenotype could be attributed to the effects of a restricted caloric diet, which is known to extend lifespan and inhibit full development (McCay et al., 1939; Fontana et al., 2010). In a similar study with *Drosophila*, methionine was found to be necessary and sufficient to increase fecundity in the context of dietary restriction (DR), without negating the positive lifespan effects induced by DR. (Grandison et al., 2009). Moreover, alteration in the OCM has been shown to be in part responsible for the increased life span induced by Metformin, an oral antihyperglycemic drug for type 2 diabetes (T2D). Cabreiro et al., (2013) demonstrated that *C. elegans* co-cultured with *Escherichia coli* exhibited impairment in folate and methionine pathways upon metformin treatment, mimicking a methionine-restricted diet. Mechanistically, metformin inhibits methionine synthase in *E. coli*, causing an accumulation of S-adenosylmethionine (SAM) and 5-methyl tetrahydrofolate (5-methyl THF). This accumulation leads to the inhibition of *C. elegans* SAMS-1, decreasing SAM and S-adenosylhomocysteine (SAH) levels, which drives the life extension phenotype. The study suggests an important role of the microbiota in the influence of the OCM and that the beneficial effect of metformin could be mediated through the OCM pathway.

All the studies above suggest that MR and OCM downregulation are possible mechanisms of healthy and extended life. MR and DR have been shown to increase the fluxes towards the transsulfuration pathway responsible for the production of Hydrogen Sulfide and Taurine (Kabil et al., 2011; Kosakamoto et al., 2023). In line with this, several studies have shown that the aging population has a decrease in the levels of taurine, a semi-essential amino acid that can be taken from the diet or generated by a branch of the OCM, the transsulfuration pathway (See Figure 1, Transsulfuration pathway) (Stuerenburg et al., 2006; Wallace and Dawson, 2009; Ripps and Shen, 2012; Yoshimura et al., 2021; Singh et al., 2023). Taurine deficiency in early life is associated with skeletal, central nervous system and vision impairment (Ripps and Shen, 2012). In a recent study, Singh et al., (2023) demonstrated that taurine levels drop by 80% in the elderly population across several species, including mice, monkeys, and humans. This finding suggests that taurine may play a role in aging-related diseases. To explore this further, the researchers administered daily intraperitoneal taurine to middle-aged mice. The results revealed a significant decrease in cellular senescence, DNA damage, mitochondrial dysfunction, and inflammaging. Notably, both monkeys and mice receiving taurine supplementation exhibited increased health span and lifespan. Moreover, the upregulation of enzymes in the transsulfuration pathway, such as cystathionine β-synthase (CBS), has been observed in long-lived *Drosophila* under dietary restriction (DR), further validating the importance of this pathway and possibly suggesting that one-carbon metabolism (OCM) could be one of the main players in the effects of DR on longevity (Kabil et al., 2011). Similarly, in humans, when comparing taurine and one-carbon metabolism (OCM) levels between centenarians and the normal elderly population, centenarians exhibit upregulation of the transsulfuration pathway and taurine levels and of a microbiome supporting sulfate metabolism (Mota-Martorell et al., 2021; Johansen et al., 2023). These findings suggest that OCM may be crucial for maintaining a healthy aging phenotype.

Changes in DNA and histone methylation are hallmarks of aging (López-Otín et al., 2023). Recently, it has been shown that double-stranded DNA breaks induce the recruitment of DNA repair genes, including chromatin remodeling enzymes such as SIRT6, HDAC1, and PARP1, to repair the breaks. This recruitment can lead to the loss of epigenetic marks, resulting in the loss of a youthful epigenome and an increased rate of aging (Mostoslavsky et al., 2006; Toiber et al., 2013; Tian et al., 2019; Kovatcheva et al., 2023; Yang et al., 2023). The addition or removal of epigenetic marks, as discussed above, are driven by enzymatic reactions, as exemplified by the one-carbon metabolism (OCM) pathway with S-adenosylmethionine (SAM) as the universal methyl donor. Impairment in the OCM pathway could lead to a loss of these epigenetic marks and potentially increase the rate of aging. An interesting example comes from the work of Kang et al., (2024) where similar results were observed *in vivo* in a study comparing aged versus young mice, focusing on the quantity of muscle stem

cells (MuSCs). The study revealed that aged MuSCs were associated with decreased levels of heterochromatin, such as H3K9 di- and tri-methylation, and the heterochromatin protein HP1. This reduction was due to the depletion of SAM, which was preferentially utilized for polyamine production at the expense of nuclear methylation. Supplementation with SAM or inhibition of the polyamine pathway greatly enhanced heterochromatin formation, improved the functionality of MuSCs, and reversed the aging phenotype.

## Conclusion

Since the discovery of the double helix and particularly after the Human Genome Project, genetics was hailed as the holy grail for understanding biological processes and curing diseases such as cancer. However, the reality is that while the genome provides the instructions for building cellular components, it does not dictate their use. Often, these decisions are influenced by the environment, which includes metabolites among other factors. Two recent studies challenge this conventional view. The first, by Kong et al., (2024) revisits Knudson's "two-hit" paradigm in cancer, which posits that both copies of an autosomal tumor suppressor gene must be inactivated for carcinogenesis to occur. This study elegantly demonstrates that a single metabolite, Methylglyoxal (MGO)—derived nonenzymatically from glyceraldehyde-3-phosphate mainly during glycolysis—can act as an oncogene by transiently inactivating Breast cancer type 2 (BRCA2). This transient inhibition of BRCA2 is sufficient to trigger single-base substitutions (SBSs) and increase genomic instability. The second significant study, by Parreno et al., (2024) shows for the first time that a transient epigenetic event can induce tumorigenesis in the absence of additional stimuli. The authors transiently downregulated the polycomb complex (PRC) in flies, which is responsible for depositing H3K27me3 repressive marks and H2AK118UB, which is important for repressing developmental genes through cellular memory. This downregulation activates JAK-STAT signaling and zfh1 (ZEB1 in mammals), which alone was sufficient to induce cancer without driver mutations. Notably, the activity of the PRC complex, including the histone methyltransferase EZH2, as previously discussed, depends on the availability of SAM and is inhibited by SAH. This suggests that transient disruptions in one-carbon metabolism (OCM) could lead to enduring changes in chromatin architecture and, subsequently, cancer.

A longstanding question in oncology is why most cancers develop later in life. One possible explanation is metabolic impairment, which may drive epigenetic changes in chromatin that are sufficient to initiate tumorigenesis independently or to induce DNA damage, thereby leading to cancer-driver mutations. Although we lack current data to support this hypothesis, further studies could establish such a connection. In this context, it might be worthwhile to consider integrating metabolic analysis with standard tests such as PSA or PAP tests.

In this review we aimed to highlight the nuclear role of OCM metabolic enzymes not only as agents in oxidative or reductive reactions but also as signaling proteins. As mentioned above, components of the OCM can relocate to the nucleus, bind to nuclear proteins, and perform signaling functions. This suggests that cellular functions, although compartmentalized, are tightly regulated by metabolic processes, and there is a need to adopt a systems biology approach rather than focusing solely on individual genes or metabolic pathways independently. In discussing the role of OCM in cancer and aging, we highlight the fact that genetic manipulation of the genome, without considering the actuating role of metabolites, could yield modest results, whether in activating pluripotency pathways or in attempts to modulate organismal aging. Future research will undoubtedly continue to elucidate this critical interplay between metabolite levels, metabolic enzymes, subcellular localization, and changes in the chromatin landscape.

## Author contributions

TB: Conceptualization, Investigation, Writing–original draft, Writing–review and editing. RM: Conceptualization, Investigation, Writing–original draft, Writing–review and editing.

## Funding

The author(s) declare that financial support was received for the research, authorship, and/or publication of this article. Work in the Mostoslavsky's lab is supported by NIH grants R01GM128448 and R01CA235412, an award from the Waxman Cancer Research Foundation/Israel Cancer Research Foundation (WCRF/ICRF), funds from the Andrew Warshaw M.D. Institute for Pancreatic Cancer Research, a Massachusetts Life Sciences Center Bits to Bytes award and a Breakthrough Award from the Krantz Family Center for Cancer Research. RM is the Laurel Schwarz Endowed Chair of Oncology at Harvard Medical School. TB is a recipient of an EMBO Postdoctoral Fellowship, ALTF 359-2022.

## Conflict of interest

The authors declare that the research was conducted in the absence of any commercial or financial relationships that could be construed as a potential conflict of interest.

The author(s) declared that they were an editorial board member of Frontiers, at the time of submission. This had no impact on the peer review process and the final decision.

## Publisher's note

# References


Albers, E. (2009). Metabolic characteristics and importance of the universal methionine salvage pathway recycling methionine from 5′-methylthioadenosine. *IUBMB Life* 61, 1132–1142. doi:10.1002/iub.278

Alexander, P. B., Wang, J., and McKnight, S. L. (2011). Targeted killing of a mammalian cell based upon its specialized metabolic state. *Proc. Natl. Acad. Sci.* 108, 15828–15833. doi:10.1073/pnas.1111312108

Aquilano, K., Baldelli, S., and Ciriolo, M. R. (2014). Glutathione: new roles in redox signaling for an old antioxidant. *Front. Pharmacol.* 5, 196. doi:10.3389/fphar.2014.00196

Araki, T., Sasaki, Y., and Milbrandt, J. (2004). Increased nuclear NAD biosynthesis and SIRT1 activation prevent axonal degeneration. *Science* 305, 1010–1013. doi:10.1126/science.1098014

Banerjee, R. V., and Matthews, R. G. (1990). Cobalamin-dependent methionine synthase. *FASEB J.* 4, 1450–1459. doi:10.1096/fasebj.4.5.2407589

Bérénice, A. B., Pollina, E., Ucar, D., Mahmoudi, S., Karra, K., Wong, E., et al. (2014). H3K4me3 breadth is linked to cell identity and transcriptional consistency. *Cell* 158, 673–688. doi:10.1016/j.cell.2014.06.027

Boon, R., Silveira, G. G., and Mostoslavsky, R. (2020). Nuclear metabolism and the regulation of the epigenome. *Nat. Metab.* 2, 1190–1203. doi:10.1038/s42255-020-00285-4

Brosnan, M. E., and Brosnan, J. T. (2020). Histidine metabolism and function. *J. Nutr.* 150, 2570S–2575S. doi:10.1093/jn/nxaa079

Brosnan, M. E., and Brosnan, J. T. F. (2016). Formate: the neglected member of one-carbon metabolism. *Annu. Rev. Nutr.* 36, 369–388. doi:10.1146/annurev-nutr-071715-050738

Bulusu, V., Tumanov, S., Michalopoulou, E., van den Broek, N. J., MacKay, G., Nixon, C., et al. (2017). Acetate recapturing by nuclear acetyl-CoA synthetase 2 prevents loss of histone acetylation during oxygen and serum limitation. *Cell Rep.* 18, 647–658. doi:10.1016/j.celrep.2016.12.055

Burgos-Barragan, G., Wit, N., Meiser, J., Dingler, F. A., Pietzke, M., Mulderrig, L., et al. (2017). Mammals divert endogenous genotoxic formaldehyde into one-carbon metabolism. *Nature* 548, 549–554. doi:10.1038/nature23481

Cabreiro, F., Au, C., Leung, K. Y., Vergara-Irigaray, N., Cochemé, H., Noori, T., et al. (2013). Metformin retards aging in *C. elegans* by altering microbial folate and methionine metabolism. *Cell* 153, 228–239. doi:10.1016/j.cell.2013.02.035

Cantoni, G. L. (1952). The nature of the active methyl donor formed enzymatically from l-methionine and adenosinetriphosphate1,2. *J. Am. Chem. Soc.* 74, 2942–2943. doi:10.1021/ja01131a519

Chandel, N. S. (2021). Amino acid metabolism. *Cold Spring Harb. Perspect. Biol.* 13, a040584. doi:10.1101/cshperspect.a040584

Chaneton, B., Hillmann, P., Zheng, L., Martin, A. C. L., Maddocks, O. D. K., Chokkathukalam, A., et al. (2012). Serine is a natural ligand and allosteric activator of pyruvate kinase M2. *Nature* 491, 458–462. doi:10.1038/nature11540

Chen, Q., Chen, Y., Bian, C., Fujiki, R., and Yu, X. (2013). TET2 promotes histone O-GlcNAcylation during gene transcription. *Nature* 493, 561–564. doi:10.1038/nature11742

Dillon, S. C., Zhang, X., Trievel, R. C., and Cheng, X. (2005). The SET-domain protein superfamily: protein lysine methyltransferases. *Genome Biol.* 6, 227. doi:10.1186/gb-2005-6-8-227

Ding, J., Li, T., Wang, X., Zhao, E., Choi, J. H., Yang, L., et al. (2013). The histone H3 methyltransferase G9A epigenetically activates the serine-glycine synthesis pathway to sustain cancer cell survival and proliferation. *Cell Metab.* 18, 896–907. doi:10.1016/j.cmet.2013.11.004

Duan, R., Du, W., and Guo, W. (2020). EZH2: a novel target for cancer treatment. *J. Hematol. Oncol.* 13, 104. doi:10.1186/s13045-020-00937-8

Ducker, G. S., and Rabinowitz, J. D. (2017). One-carbon metabolism in health and disease. *Cell Metab.* 25, 27–42. doi:10.1016/j.cmet.2016.08.009

Edgar, A. J. (2002). The human L-threonine 3-dehydrogenase gene is an expressed pseudogene. *BMC Genet.* 3, 18. doi:10.1186/1471-2156-3-18

Etchegaray, J.-P., and Mostoslavsky, R. (2016). Interplay between metabolism and epigenetics: a nuclear adaptation to environmental changes. *Mol. Cell* 62, 695–711. doi:10.1016/j.molcel.2016.05.029

Farber, S., Diamond, L. K., Mercer, R. D., Sylvester, R. F., and Wolff, J. A. (1948). Temporary remissions in acute leukemia in children produced by folic acid antagonist, 4-aminopteroyl-glutamic acid (aminopterin). *N. Engl. J. Med.* 238, 787–793. doi:10.1056/nejm194806032382301

Farrelly, L. A., Thompson, R. E., Zhao, S., Lepack, A. E., Lyu, Y., Bhanu, N. V., et al. (2019). Histone serotonylation is a permissive modification that enhances TFIID binding to H3K4me3. *Nature* 567, 535–539. doi:10.1038/s41586-019-1024-7

Finkel, T., Deng, C.-X., and Mostoslavsky, R. (2009). Recent progress in the biology and physiology of sirtuins. *Nature* 460, 587–591. doi:10.1038/nature08197

Fontana, L., Partridge, L., and Longo, V. D. (2010). Extending healthy life span—from yeast to humans. *Science* 328, 321–326. doi:10.1126/science.1172539

Frisell, W. R., and Mackenzie, C. G. (1962). Separation and purification of sarcosine dehydrogenase and dimethylglycine dehydrogenase. *J. Biol. Chem.* 237, 94–98. doi:10.1016/s0021-9258(18)81367-9

Gao, X., Sanderson, S. M., Dai, Z., Reid, M. A., Cooper, D. E., Lu, M., et al. (2019). Dietary methionine influences therapy in mouse cancer models and alters human metabolism. *Nature* 572, 397–401. doi:10.1038/s41586-019-1437-3

Garcia, B. A., Luka, Z., Loukachevitch, L. V., Bhanu, N. V., and Wagner, C. (2016). Folate deficiency affects histone methylation. *Med. Hypotheses* 88, 63–67. doi:10.1016/j.mehy.2015.12.027

Gershoni-Baruch, R., Dagan, E., Israeli, D., Kasinetz, L., Kadouri, E., and Friedman, E. (2000). Association of the C677T polymorphism in the MTHFR gene with breast and/or ovarian cancer risk in Jewish women. *Eur. J. Cancer* 36, 2313–2316. doi:10.1016/s0959-8049(00)00306-3

Golbourn, B. J., Halbert, M. E., Halligan, K., Varadharajan, S., Krug, B., Mbah, N. E., et al. (2022). Loss of MAT2A compromises methionine metabolism and represents a vulnerability in H3K27M mutant glioma by modulating the epigenome. *Nat. Cancer* 3, 629–648. doi:10.1038/s43018-022-00348-3

González-Rodríguez, P., Füllgrabe, J., and Joseph, B. (2023). The hunger strikes back: an epigenetic memory for autophagy. *Cell Death Differ.* 30, 1404–1415. doi:10.1038/s41418-023-01159-4

Grandison, R. C., Piper, M. D. W., and Partridge, L. (2009). Amino-acid imbalance explains extension of lifespan by dietary restriction in Drosophila. *Nature* 462, 1061–1064. doi:10.1038/nature08619

Greco, C. M., Cervantes, M., Fustin, J. M., Ito, K., Ceglia, N., Samad, M., et al. (2020). S-adenosyl- l -homocysteine hydrolase links methionine metabolism to the circadian clock and chromatin remodeling. *Sci. Adv.* 6, eabc5629. doi:10.1126/sciadv.abc5629

Guertin, D. A., and Wellen, K. E. (2023). Acetyl-CoA metabolism in cancer. *Nat. Rev. Cancer* 23, 156–172. doi:10.1038/s41568-022-00543-5

Hasan, T., Arora, R., Bansal, A. K., Bhattacharya, R., Sharma, G. S., and Singh, L. R. (2019). Disturbed homocysteine metabolism is associated with cancer. *Exp. Mol. Med.* 51, 1–13. doi:10.1038/s12276-019-0216-4

Haws, S. A., Yu, D., Ye, C., Wille, C. K., Nguyen, L. C., Krautkramer, K. A., et al. (2020). Methyl-metabolite depletion elicits adaptive responses to support heterochromatin stability and epigenetic persistence. *Mol. Cell* 78, 210–223.e8. doi:10.1016/j.molcel.2020.03.004

Horvath, S. (2013). DNA methylation age of human tissues and cell types. *Genome Biol.* 14, R115. doi:10.1186/gb-2013-14-10-r115

Huang, H., Zhang, D., Wang, Y., Perez-Neut, M., Han, Z., Zheng, Y. G., et al. (2018). Lysine benzoylation is a histone mark regulated by SIRT2. *Nat. Commun.* 9, 3374. doi:10.1038/s41467-018-05567-w

Husmann, D., and Gozani, O. (2019). Histone lysine methyltransferases in biology and disease. *Nat. Struct. Mol. Biol.* 26, 880–889. doi:10.1038/s41594-019-0298-7

Jencks, D. A., and Mathews, R. G. (1987). Allosteric inhibition of methylenetetrahydrofolate reductase by adenosylmethionine. Effects of adenosylmethionine and NADPH on the equilibrium between active and inactive forms of the enzyme and on the kinetics of approach to equilibrium. *J. Biol. Chem.* 262, 2485–2493. doi:10.1016/s0021-9258(18)61530-3

Johansen, J., Atarashi, K., Arai, Y., Hirose, N., Sørensen, S. J., Vatanen, T., et al. (2023). Centenarians have a diverse gut virome with the potential to modulate metabolism and promote healthy lifespan. *Nat. Microbiol.* 8, 1064–1078. doi:10.1038/s41564-023-01370-6

Kabil, H., Kabil, O., Banerjee, R., Harshman, L. G., and Pletcher, S. D. (2011). Increased transsulfuration mediates longevity and dietary restriction in Drosophila. *Proc. Natl. Acad. Sci.* 108, 16831–16836. doi:10.1073/pnas.1102008108

Kalev, P., Hyer, M. L., Gross, S., Konteatis, Z., Chen, C. C., Fletcher, M., et al. (2021). MAT2A inhibition blocks the growth of MTAP-deleted cancer cells by reducing PRMT5-dependent mRNA splicing and inducing DNA damage. *Cancer Cell* 39, 209–224.e11. doi:10.1016/j.ccell.2020.12.010

Kanarek, N., Keys, H. R., Cantor, J. R., Lewis, C. A., Chan, S. H., Kunchok, T., et al. (2018). Histidine catabolism is a major determinant of methotrexate sensitivity. *Nature* 559, 632–636. doi:10.1038/s41586-018-0316-7

Kang, J., Benjamin, D. I., Kim, S., Salvi, J. S., Dhaliwal, G., Lam, R., et al. (2024). Depletion of SAM leading to loss of heterochromatin drives muscle stem cell ageing. *Nat. Metab.* 6, 153–168. doi:10.1038/s42255-023-00955-z

Katoh, Y., Ikura, T., Hoshikawa, Y., Tashiro, S., Ito, T., Ohta, M., et al. (2011). Methionine adenosyltransferase II serves as a transcriptional corepressor of maf oncoprotein. *Mol. Cell* 41, 554–566. doi:10.1016/j.molcel.2011.02.018

Kera, Y., Katoh, Y., Ohta, M., Matsumoto, M., Takano-Yamamoto, T., and Igarashi, K. (2013). Methionine adenosyltransferase II-dependent histone H3K9 methylation at the COX-2 gene locus. *J. Biol. Chem.* 288, 13592–13601. doi:10.1074/jbc.m112.429738

Kikuchi, G., Motokawa, Y., Yoshida, T., and Hiraga, K. (2008). Glycine cleavage system: reaction mechanism, physiological significance, and hyperglycinemia. *Proc. Jpn. Acad. Ser. B* 84, 246–263. doi:10.2183/pjab.84.246

Kim, D., Fiske, B. P., Birsoy, K., Freinkman, E., Kami, K., Possemato, R. L., et al. (2015). SHMT2 drives glioma cell survival in ischaemia but imposes a dependence on glycine clearance. *Nature* 520, 363–367. doi:10.1038/nature14363

Kong, L. R., Gupta, K., Wu, A. J., Perera, D., Ivanyi-Nagy, R., Ahmed, S. M., et al. (2024). A glycolytic metabolite bypasses "two-hit" tumor suppression by BRCA2. *Cell* 187, 2269–2287.e16. doi:10.1016/j.cell.2024.03.006

Kory, N., Wyant, G. A., Prakash, G., uit de Bos, J., Bottanelli, F., Pacold, M. E., et al. (2018). SFXN1 is a mitochondrial serine transporter required for one-carbon metabolism. *Science* 362, eaat9528. doi:10.1126/science.aat9528

Kosakamoto, H., Obata, F., Kuraishi, J., Aikawa, H., Okada, R., Johnstone, J. N., et al. (2023). Early-adult methionine restriction reduces methionine sulfoxide and extends lifespan in Drosophila. *Nat. Commun.* 14, 7832. doi:10.1038/s41467-023-43550-2

Kotb, M., and Kredich, N. M. (1985). S-Adenosylmethionine synthetase from human lymphocytes. Purification and characterization. *J. Biol. Chem.* 260, 3923–3930. doi:10.1016/s0021-9258(18)89210-9

Kotb, M., Mudd, S., Mato, J. M., Geller, A. M., Kredich, N. M., Chou, J. Y., et al. (1997). Consensus nomenclature for the mammalian methionine adenosyltransferase genes and gene products. *Trends Genet.* 13, 51–52. doi:10.1016/s0168-9525(97)01013-5

Kovatcheva, M., Melendez, E., Chondronasiou, D., Pietrocola, F., Bernad, R., Caballe, A., et al. (2023). Vitamin B12 is a limiting factor for induced cellular plasticity and tissue repair. *Nat. Metab.* 5, 1911–1930. doi:10.1038/s42255-023-00916-6

Kung, P.-P., Huang, B., Zehnder, L., Tatlock, J., Bingham, P., Krivacic, C., et al. (2015). SAH derived potent and selective EZH2 inhibitors. *Bioorg. Med. Chem. Lett.* 25, 1532–1537. doi:10.1016/j.bmcl.2015.02.017

Kutzbach, C., and Stokstad, E. L. (1967). Feedback inhibition of methylene-tetrahydrofolate reductase in rat liver by S-adenosylmethionine. *Biochimica Biophysica Acta (BBA) - Enzym.* 139, 217–220. doi:10.1016/0005-2744(67)90140-4

Kutzbach, C., and Stokstad, E. L. R. (1971). Mammalian methylenetetrahydrofolate reductase Partial purification, properties, and inhibition by S-adenosylmethionine. *Biochimica Biophysica Acta (BBA) - Enzym.* 250, 459–477. doi:10.1016/0005-2744(71)90247-6

Lees, E. K., Król, E., Grant, L., Shearer, K., Wyse, C., Moncur, E., et al. (2014). Methionine restriction restores a younger metabolic phenotype in adult mice with alterations in fibroblast growth factor 21. *Aging Cell* 13, 817–827. doi:10.1111/acel.12238

Lepack, A. E., Werner, C. T., Stewart, A. F., Fulton, S. L., Zhong, P., Farrelly, L. A., et al. (2020). Dopaminylation of histone H3 in ventral tegmental area regulates cocaine seeking. *Science* 368, 197–201. doi:10.1126/science.aaw8806

Li, F., Liu, P., Mi, W., Li, L., Anderson, N. M., Lesner, N. P., et al. (2024). Blocking methionine catabolism induces senescence and confers vulnerability to GSK3 inhibition in liver cancer. *Nat. Cancer* 5, 131–146. doi:10.1038/s43018-023-00671-3

Li, X., Yu, W., Qian, X., Xia, Y., Zheng, Y., Lee, J. H., et al. (2017). Nucleus-translocated ACSS2 promotes gene transcription for lysosomal biogenesis and autophagy. *Mol. Cell* 66, 684–697.e9. doi:10.1016/j.molcel.2017.04.026

Li, Z., Liu, H., He, J., Wang, Z., Yin, Z., You, G., et al. (2021). NAcetyl-CoA synthetase 2: a critical linkage in obesity-induced tumorigenesis in myeloma. *Cell Metab.* 33, 78–93.e7. doi:10.1016/j.cmet.2020.12.011

Liu, T. F., Vachharajani, V. T., Yoza, B. K., and McCall, C. E. (2012). NAD+-dependent sirtuin 1 and 6 proteins coordinate a switch from glucose to fatty acid oxidation during the acute inflammatory response. *J. Biol. Chem.* 287, 25758–25769. doi:10.1074/jbc.m112.362343

López-Otín, C., Blasco, M. A., Partridge, L., Serrano, M., and Kroemer, G. (2023). Hallmarks of aging: an expanding universe. *Cell* 186, 243–278. doi:10.1016/j.cell.2022.11.001

Luengo, A., Li, Z., Gui, D. Y., Sullivan, L. B., Zagorulya, M., Do, B. T., et al. (2021). Increased demand for NAD+ relative to ATP drives aerobic glycolysis. *Mol. Cell* 81, 691–707.e6. doi:10.1016/j.molcel.2020.12.012

Luka, Z., Moss, F., Loukachevitch, L. V., Bornhop, D. J., and Wagner, C. (2011). Histone demethylase LSD1 is a folate-binding protein. *Biochemistry* 50, 4750–4756. doi:10.1021/bi200247b

Luka, Z., Mudd, S. H., and Wagner, C. (2009). Glycine N-methyltransferase and regulation of S-adenosylmethionine levels. *J. Biol. Chem.* 284, 22507–22511. doi:10.1074/jbc.r109.019273

Luka, Z., Pakhomova, S., Loukachevitch, L. V., Calcutt, M. W., Newcomer, M. E., and Wagner, C. (2014). Crystal structure of the histone lysine specific demethylase LSD1 complexed with tetrahydrofolate. *Protein Sci.* 23, 993–998. doi:10.1002/pro.2469

Maddocks, O. D. K., Berkers, C. R., Mason, S. M., Zheng, L., Blyth, K., Gottlieb, E., et al. (2013). Serine starvation induces stress and p53-dependent metabolic remodelling in cancer cells. *Nature* 493, 542–546. doi:10.1038/nature11743

Malloy, V. L., Krajcik, R. A., Bailey, S. J., Hristopoulos, G., Plummer, J. D., and Orentreich, N. (2006). Methionine restriction decreases visceral fat mass and preserves insulin action in aging male Fischer 344 rats independent of energy restriction. *Aging Cell* 5, 305–314. doi:10.1111/j.1474-9726.2006.00220.x

Mao, Z., Hine, C., Tian, X., Van Meter, M., Au, M., Vaidya, A., et al. (2011). SIRT6 promotes DNA repair under stress by activating PARP1. *Science* 332, 1443–1446. doi:10.1126/science.1202723

Martinez-Outschoorn, U. E., Prisco, M., Ertel, A., Tsirigos, A., Lin, Z., Pavlides, S., et al. (2011). Ketones and lactate increase cancer cell "stemness," driving recurrence, metastasis and poor clinical outcome in breast cancer. *Cell Cycle* 10, 1271–1286. doi:10.4161/cc.10.8.15330

Martinez-Pastor, B., and Mostoslavsky, R. (2012). Sirtuins, metabolism, and cancer. *Front. Pharmacol.* 3, 22. doi:10.3389/fphar.2012.00022

Maruti, S. S., Ulrich, C. M., Jupe, E. R., and White, E. (2009). MTHFR C677T and postmenopausal breast cancer risk by intakes of one-carbon metabolism nutrients: a nested case-control study. *Breast Cancer Res.* 11, R91. doi:10.1186/bcr2462

McBride, M. J., Hunter, C. J., Zhang, Z., TeSlaa, T., Xu, X., Ducker, G. S., et al. (2024). Glycine homeostasis requires reverse SHMT flux. *Cell Metab.* 36, 103–115.e4. doi:10.1016/j.cmet.2023.12.001

McCay, C. M., Maynard, L. A., Sperling, G., and Barnes, L. L. (1939). Retarded growth, life span, ultimate body size and age changes in the albino rat after feeding diets restricted in calories: four figures. *J. Nutr.* 18, 1–13. doi:10.1093/jn/18.1.1

Mentch, S. J., and Locasale, J. W. (2016). One-carbon metabolism and epigenetics: understanding the specificity. *Ann. N. Y. Acad. Sci.* 1363, 91–98. doi:10.1111/nyas.12956

Mentch, S. J., Mehrmohamadi, M., Huang, L., Liu, X., Gupta, D., Mattocks, D., et al. (2015). Histone methylation dynamics and gene regulation occur through the sensing of one-carbon metabolism. *Cell Metab.* 22, 861–873. doi:10.1016/j.cmet.2015.08.024

Merkuri, F., Rothstein, M., and Simoes-Costa, M. (2024). Histone lactylation couples cellular metabolism with developmental gene regulatory networks. *Nat. Commun.* 15, 90. doi:10.1038/s41467-023-44121-1

Messner, S., and Hottiger, M. O. (2011). Histone ADP-ribosylation in DNA repair, replication and transcription. *Trends Cell Biol.* 21, 534–542. doi:10.1016/j.tcb.2011.06.001

Mews, P., Donahue, G., Drake, A. M., Luczak, V., Abel, T., and Berger, S. L. (2017). Acetyl-CoA synthetase regulates histone acetylation and hippocampal memory. *Nature* 546, 381–386. doi:10.1038/nature22405

Miller, R. A., Buehner, G., Chang, Y., Harper, J. M., Sigler, R., and Smith-Wheelock, M. (2005). Methionine-deficient diet extends mouse lifespan, slows immune and lens aging, alters glucose, T4, IGF-I and insulin levels, and increases hepatocyte MIF levels and stress resistance. *Aging Cell* 4, 119–125. doi:10.1111/j.1474-9726.2005.00152.x

Minois, N., Carmona-Gutierrez, D., and Madeo, F. (2011). Polyamines in aging and disease. *Aging (Albany NY)* 3, 716–732. doi:10.18632/aging.100361

Mostoslavsky, R., Chua, K. F., Lombard, D. B., Pang, W. W., Fischer, M. R., Gellon, L., et al. (2006). Genomic instability and aging-like phenotype in the absence of mammalian SIRT6. *Cell* 124, 315–329. doi:10.1016/j.cell.2005.11.044

Mota-Martorell, N., Jové, M., Borrás, C., Berdún, R., Obis, È., Sol, J., et al. (2021). Methionine transsulfuration pathway is upregulated in long-lived humans. *Free Radic. Biol. Med.* 162, 38–52. doi:10.1016/j.freeradbiomed.2020.11.026

Niland, C. N., Ghosh, A., Cahill, S. M., and Schramm, V. L. (2021). Mechanism and inhibition of human methionine adenosyltransferase 2A. *Biochemistry* 60, 791–801. doi:10.1021/acs.biochem.0c00998

Orentreich, N., Matias, J. R., DeFelice, A., and Zimmerman, J. A. (1993). Low methionine ingestion by rats extends life span. *J. Nutr.* 123, 269–274. doi:10.1093/jn/123.2.269

Ou, X., Yang, H., Ramani, K., Ara, A., Chen, H., Mato, J., et al. (2007). Inhibition of human betaine–homocysteine methyltransferase expression by S-adenosylmethionine and methylthioadenosine. *Biochem. J.* 401, 87–96. doi:10.1042/bj20061119

Padmanabhan, N., Jia, D., Geary-Joo, C., Wu, X., Ferguson-Smith, A., Fung, E., et al. (2013). Mutation in folate metabolism causes epigenetic instability and transgenerational effects on development. *Cell* 155, 81–93. doi:10.1016/j.cell.2013.09.002

Pajares, M. A., and Pérez-Sala, D. (2006). Betaine homocysteine S-methyltransferase: just a regulator of homocysteine metabolism? *Cell. Mol. Life Sci.* 63, 2792–2803. doi:10.1007/s00018-006-6249-6

Pal, S., and Tyler, J. K. (2016). Epigenetics and aging. *Sci. Adv.* 2, e1600584. doi:10.1126/sciadv.1600584

Papalazarou, V., Newman, A. C., Huerta-Uribe, A., Legrave, N. M., Falcone, M., Zhang, T., et al. (2023). Phenotypic profiling of solute carriers characterizes serine transport in cancer. *Nat. Metab.* 5, 2148–2168. doi:10.1038/s42255-023-00936-2

Parreno, V., Loubiere, V., Schuettengruber, B., Fritsch, L., Rawal, C. C., Erokhin, M., et al. (2024). Transient loss of Polycomb components induces an epigenetic cancer fate. *Nature* 629, 688–696. doi:10.1038/s41586-024-07328-w

Paz, M. F., Avila, S., Fraga, M. F., Pollan, M., Capella, G., Peinado, M. A., et al. (2002). Germ-line variants in methyl-group metabolism genes and susceptibility to DNA methylation in normal tissues and human primary tumors. *Cancer Res.* 62, 4519–4524.

Petrova, B., Maynard, A. G., Wang, P., and Kanarek, N. (2023). Regulatory mechanisms of one-carbon metabolism enzymes. *J. Biol. Chem.* 299, 105457. doi:10.1016/j.jbc.2023.105457

Prudova, A., Bauman, Z., Braun, A., Vitvitsky, V., Lu, S. C., and Banerjee, R. (2006). *S*-adenosylmethionine stabilizes cystathionine β-synthase and modulates redox capacity. *Proc. Natl. Acad. Sci.* 103, 6489–6494. doi:10.1073/pnas.0509531103

Rabinowitz, J. D., and Enerbäck, S. (2020). Lactate: the ugly duckling of energy metabolism. *Nat. Metab.* 2, 566–571. doi:10.1038/s42255-020-0243-4

Ramani, K., and Lu, S. C. (2017). Methionine adenosyltransferases in liver health and diseases. *Liver Res.* 1, 103–111. doi:10.1016/j.livres.2017.07.002

Refsum, H., Nurk, E., David Smith, A., Ueland, P. M., Gjesdal, C. G., Bjelland, I., et al. (2006). The Hordaland Homocysteine Study: a community-based study of homocysteine, its determinants, and associations with disease. *J. Nutr.* 136, 1731s–1740s. doi:10.1093/jn/136.6.1731S

Reid, M. A., Allen, A. E., Liu, S., Liberti, M. V., Liu, P., Liu, X., et al. (2018). Serine synthesis through PHGDH coordinates nucleotide levels by maintaining central carbon metabolism. *Nat. Commun.* 9, 5442. doi:10.1038/s41467-018-07868-6

Richon, V. M., Johnston, D., Sneeringer, C. J., Jin, L., Majer, C. R., Elliston, K., et al. (2011). Chemogenetic analysis of human protein methyltransferases. *Chem. Biol. Drug Des.* 78, 199–210. doi:10.1111/j.1747-0285.2011.01135.x

Ripps, H., and Shen, W. (2012). Review: taurine: a "very essential" amino acid. *Mol. Vis.* 18, 2673–2686.

Rodgers, J. T., Lerin, C., Haas, W., Gygi, S. P., Spiegelman, B. M., and Puigserver, P. (2005). Nutrient control of glucose homeostasis through a complex of PGC-1α and SIRT1. *Nature* 434, 113–118. doi:10.1038/nature03354

Rossetto, D., Avvakumov, N., and Côté, J. (2012). Histone phosphorylation. *Epigenetics* 7, 1098–1108. doi:10.4161/epi.21975

Ryu, K. W., Nandu, T., Kim, J., Challa, S., DeBerardinis, R. J., and Kraus, W. L. (2018). Metabolic regulation of transcription through compartmentalized NAD $^+$ biosynthesis. *Science* 360, eaan5780. doi:10.1126/science.aan5780

Sanderson, S. M., Gao, X., Dai, Z., and Locasale, J. W. (2019). Methionine metabolism in health and cancer: a nexus of diet and precision medicine. *Nat. Rev. Cancer* 19, 625–637. doi:10.1038/s41568-019-0187-8

Scott, J., and Weir, D. (1981). The methyl folate trap: a physiological response in man to prevent methyl group deficiency in kwashiorkor (methionine deficiency) and an explanation for folic-acid-induced exacerbation of subacute combined degeneration in pernicious anaemia. *Lancet* 318, 337–340. doi:10.1016/S0140-6736(81)90650-4

Shiraki, N., Shiraki, Y., Tsuyama, T., Obata, F., Miura, M., Nagae, G., et al. (2014). Methionine metabolism regulates maintenance and differentiation of human pluripotent stem cells. *Cell Metab.* 19, 780–794. doi:10.1016/j.cmet.2014.03.017

Shuvalov, O., Petukhov, A., Daks, A., Fedorova, O., Vasileva, E., and Barlev, N. A. (2017). One-carbon metabolism and nucleotide biosynthesis as attractive targets for anticancer therapy. *Oncotarget* 8, 23955–23977. doi:10.18632/oncotarget.15053

Shyh-Chang, N., Locasale, J. W., Lyssiotis, C. A., Zheng, Y., Teo, R. Y., Ratanasirintrawoot, S., et al. (2013). Influence of threonine metabolism on S -adenosylmethionine and histone methylation. *Science* 339, 222–226. doi:10.1126/science.1226603

Singh, P., Gollapalli, K., Mangiola, S., Schranner, D., Yusuf, M. A., Chamoli, M., et al. (2023). Taurine deficiency as a driver of aging. *Science* 380, eabn9257. doi:10.1126/science.abn9257

Sivanand, S., Rhoades, S., Jiang, Q., Lee, J. V., Benci, J., Zhang, J., et al. (2017). Nuclear acetyl-CoA production by ACLY promotes homologous recombination. *Mol. Cell* 67, 252–265.e6. doi:10.1016/j.molcel.2017.06.008

Sociali, G., Grozio, A., Caffa, I., Schuster, S., Becherini, P., Damonte, P., et al. (2019). SIRT6 deacetylase activity regulates NAMPT activity and NAD(P)(H) pools in cancer cells. *FASEB J.* 33, 3704–3717. doi:10.1096/fj.201800321R

Stadtfeld, M., and Hochedlinger, K. (2010). Induced pluripotency: history, mechanisms, and applications. *Genes and Dev.* 24, 2239–2263. doi:10.1101/gad.1963910

Stuerenburg, H. J., Stangneth, B., and Schoser, B. G. (2006). Age related profiles of free amino acids in human skeletal muscle. *Neuro Endocrinol. Lett.* 27, 133–136.

Sullivan, M. R., Darnell, A. M., Reilly, M. F., Kunchok, T., Joesch-Cohen, L., Rosenberg, D., et al. (2021). Methionine synthase is essential for cancer cell proliferation in physiological folate environments. *Nat. Metab.* 3, 1500–1511. doi:10.1038/s42255-021-00486-5

Sutendra, G., Kinnaird, A., Dromparis, P., Paulin, R., Stenson, T., Haromy, A., et al. (2014). A nuclear pyruvate dehydrogenase complex is important for the generation of acetyl-CoA and histone acetylation. *Cell* 158, 84–97. doi:10.1016/j.cell.2014.04.046

Svoboda, P., Krizova, E., Sestakova, S., Vapenkova, K., Knejzlik, Z., Rimpelova, S., et al. (2019). Nuclear transport of nicotinamide phosphoribosyltransferase is cell cycle–dependent in mammalian cells, and its inhibition slows cell growth. *J. Biol. Chem.* 294, 8676–8689. doi:10.1074/jbc.ra118.003505

Tajan, M., Hennequart, M., Cheung, E. C., Zani, F., Hock, A. K., Legrave, N., et al. (2021). Serine synthesis pathway inhibition cooperates with dietary serine and glycine limitation for cancer therapy. *Nat. Commun.* 12, 366. doi:10.1038/s41467-020-20223-y

Tian, X., Firsanov, D., Zhang, Z., Cheng, Y., Luo, L., Tombline, G., et al. (2019). SIRT6 is responsible for more efficient DNA double-strand break repair in long-lived species. *Cell* 177, 622–638.e22. doi:10.1016/j.cell.2019.03.043

Toiber, D., Erdel, F., Bouazoune, K., Silberman, D., Zhong, L., Mulligan, P., et al. (2013). SIRT6 recruits SNF2H to DNA break sites, preventing genomic instability through chromatin remodeling. *Mol. Cell* 51, 454–468. doi:10.1016/j.molcel.2013.06.018

Turner, M. A., Yuan, C. S., Borchardt, R. T., Hershfield, M. S., Smith, G. D., and Howell, P. L. (1998). Structure determination of selenomethionyl S-adenosylhomocysteine hydrolase using data at a single wavelength. *Nat. Struct. Biol.* 5, 369–376. doi:10.1038/nsb0598-369

Vaiserman, A., and Lushchak, O. (2021). Prenatal famine exposure and adult health outcomes: an epigenetic link. *Environ. Epigenetics* 7, dvab013. doi:10.1093/eep/dvab013

Vander Heiden, M. G., Cantley, L. C., and Thompson, C. B. (2009). Understanding the Warburg effect: the metabolic requirements of cell proliferation. *Science* 324, 1029–1033. doi:10.1126/science.1160809

Vizán, P., Di Croce, L., and Aranda, S. (2021). Functional and pathological roles of AHCY. *Front. Cell Dev. Biol.* 9, 654344. doi:10.3389/fcell.2021.654344

Wallace, D. R., and Dawson, R. (2009). Decreased plasma taurine in aged rats. *Gerontology* 36, 19–27. doi:10.1159/000213171

Wang, J., Alexander, P., Wu, L., Hammer, R., Cleaver, O., and McKnight, S. L. (2009). Dependence of mouse embryonic stem cells on threonine catabolism. *Science* 325, 435–439. doi:10.1126/science.1173288

Wang, Z., Yip, L. Y., Lee, J. H. J., Wu, Z., Chew, H. Y., Chong, P. K. W., et al. (2019). Methionine is a metabolic dependency of tumor-initiating cells. *Nat. Med.* 25, 825–837. doi:10.1038/s41591-019-0423-5

Wei, Y., Yu, L., Bowen, J., Gorovsky, M. A., and Allis, C. D. (1999). Phosphorylation of histone H3 is required for proper chromosome condensation and segregation. *Cell* 97, 99–109. doi:10.1016/s0092-8674(00)80718-7

Wellen, K. E., Hatzivassiliou, G., Sachdeva, U. M., Bui, T. V., Cross, J. R., and Thompson, C. B. (2009). ATP-citrate lyase links cellular metabolism to histone acetylation. *Science* 324, 1076–1080. doi:10.1126/science.1164097

Werge, M. P., McCann, A., Galsgaard, E. D., Holst, D., Bugge, A., Albrechtsen, N. J. W., et al. (2021). The role of the transsulfuration pathway in non-alcoholic fatty liver disease. *J. Clin. Med.* 10, 1081. doi:10.3390/jcm10051081

Wittwer, A. J., and Wagner, C. (1981). Identification of the folate-binding proteins of rat liver mitochondria as dimethylglycine dehydrogenase and sarcosine dehydrogenase. Flavoprotein nature and enzymatic properties of the purified proteins. *J. Biol. Chem.* 256, 4109–4115. doi:10.1016/s0021-9258(19)69572-4

Xiao, Z., and Locasale, J. W. (2021). Epigenomic links from metabolism—methionine and chromatin architecture. *Curr. Opin. Chem. Biol.* 63, 11–18. doi:10.1016/j.cbpa.2021.01.011

Xie, Z., Dai, J., Dai, L., Tan, M., Cheng, Z., Wu, Y., et al. (2012). Lysine succinylation and lysine malonylation in histones. *Mol. Cell. Proteomics* 11, 100–107. doi:10.1074/mcp.M111.015875

Yang, J. H., Hayano, M., Griffin, P. T., Amorim, J. A., Bonkowski, M. S., Apostolides, J. K., et al. (2023). Loss of epigenetic information as a cause of mammalian aging. *Cell* 186, 305–326.e27. doi:10.1016/j.cell.2022.12.027

Yang, M., and Vousden, K. H. (2016). Serine and one-carbon metabolism in cancer. *Nat. Rev. Cancer* 16, 650–662. doi:10.1038/nrc.2016.81

Ye, C., Sutter, B. M., Wang, Y., Kuang, Z., Zhao, X., Yu, Y., et al. (2019). Demethylation of the protein phosphatase PP2A promotes demethylation of histones to enable their function as a methyl group sink. *Mol. Cell* 73, 1115–1126.e6. doi:10.1016/j.molcel.2019.01.012

Ye, J., Mancuso, A., Tong, X., Ward, P. S., Fan, J., Rabinowitz, J. D., et al. (2012). Pyruvate kinase M2 promotes *de novo* serine synthesis to sustain mTORC1 activity and cell proliferation. *Proc. Natl. Acad. Sci.* 109, 6904–6909. doi:10.1073/pnas.1204176109

Yeo, E. J., and Wagner, C. (1992). Purification and properties of pancreatic glycine N-methyltransferase. *J. Biol. Chem.* 267, 24669–24674. doi:10.1016/S0021-9258(18)35816-2

Yoshimura, T., Inokuchi, Y., Mutou, C., Sakurai, T., Nagahama, T., and Murakami, S. (2021). Age-related decline in the taurine content of the skin in rodents. *Amino Acids* 53, 429–434. doi:10.1007/s00726-021-02956-2

Zhang, D., Tang, Z., Huang, H., Zhou, G., Cui, C., Weng, Y., et al. (2019). Metabolic regulation of gene expression by histone lactylation. *Nature* 574, 575–580. doi:10.1038/s41586-019-1678-1

Zhang, J., and Zheng, Y. G. (2016). SAM/SAH analogs as versatile tools for SAM-dependent methyltransferases. *ACS Chem. Biol.* 11, 583–597. doi:10.1021/acschembio.5b00812

Zhang, N. (2018). Role of methionine on epigenetic modification of DNA methylation and gene expression in animals. *Anim. Nutr.* 4, 11–16. doi:10.1016/j.aninu.2017.08.009

Zhang, Q., Bai, B., Mei, X., Wan, C., Cao, H., Dan Li, , et al. (2018). Elevated H3K79 homocysteinylation causes abnormal gene expression during neural development and subsequent neural tube defects. *Nat. Commun.* 9, 3436. doi:10.1038/s41467-018-05451-7

frontiers | Frontiers in Epigenetics and Epigenomics

TYPE Review
PUBLISHED 22 August 2024
DOI 10.3389/freae.2024.1445765



OPEN ACCESS

EDITED BY
Sharon Y. R. Dent,
University of Texas MD Anderson Cancer Center, United States

REVIEWED BY
Bing Li,
Shanghai Jiao Tong University, China
Yanzhong Yang,
Beckman Research Institute, City of Hope, United States

*CORRESPONDENCE
Jacques Côté,
Jacques.cote@crchudequebec.ulaval.ca
Amélie Fradet-Turcotte,
Amelie.fradet-turcotte@crchudequebec.ulaval.ca

†These authors have contributed equally to this work

RECEIVED 08 June 2024
ACCEPTED 07 August 2024
PUBLISHED 22 August 2024

CITATION
Clerf E, Galloy M, Fradet-Turcotte A and Côté J (2024) Histone H2A variants play a key role at DNA double-strand breaks during repair pathway choice.
*Front. Epigenet. Epigenom.* 2:1445765.
doi: 10.3389/freae.2024.1445765



# Histone H2A variants play a key role at DNA double-strand breaks during repair pathway choice

Emile Clerf†, Maxime Galloy†, Amélie Fradet-Turcotte* and Jacques Côté*

St-Patrick Research Group in Basic Oncology, Oncology Division of Centre Hospitalier Universitaire (CHU) de Québec-Université Laval Research Center, Laval University Cancer Research Center, Department of Molecular Biology, Medical Biochemistry and Pathology, Faculty of Medicine, Université Laval, Quebec City, QC, Canada

Histone post-translational modifications and variants play crucial roles in the adaptability of chromatin structure, facilitating rapid responses necessary for biological processes such as transcription, replication, and DNA damage signaling. Notably, DNA double-strand break (DSB) signaling heavily relies on these histone modifications, with signal amplification and the recruitment of specific DNA repair factors being dictated by them. Among the histones, H2A and its variants are central to this response, with phosphorylation of the variant H2A.X being the initial and most characteristic histone mark deposit upon DNA damage detection. Additional post-translational modifications of H2A and its variants contribute to the selective recruitment of DNA repair factors and influence the choice of DNA repair pathways. This review provides a summary of current knowledge regarding the roles of histone H2A post-translational modifications and variants in DSB signaling and repair, with a particular emphasis on modifications and variants that impact the choice of repair pathways. Additionally, the involvement of histone chaperones, chromatin modifiers, and remodelers in these processes is discussed.

KEYWORDS

**double-strand break repair, histone H2A variants, chromatin modifiers, post-translational modification, chromatin readers, DNA repair pathway choice**

## Introduction

Preserving genomic integrity is crucial as cells are constantly confronted with multiple DNA-damaging agents from external and internal sources. Among different types of DNA damage, DNA double-strand breaks (DSBs) are the most toxic lesions. Indeed, if they are left unrepaired or not properly repaired, they can lead to mutations, chromosomal aberrations, and even cell death (Khanna and Jackson, 2001). Cells have developed sophisticated mechanisms to signal and repair the damage (Jackson and Bartek, 2009). In response to DSBs, two major repair mechanisms can occur: homologous recombination (HR), which mostly takes place in the late S and G2 phases of the cell cycle, and non-homologous end joining (NHEJ), which can occur throughout the interphase (Ingram et al., 2019). These mechanisms involve distinct actors that favor one mechanism *versus* another to promote a finely tuned signal.

In the nucleus, DNA is found in different levels of compaction depending on the genomic regions. The process of compaction is established by organizing the DNA around the nucleosome, the smallest subunit of the chromatin. It is composed of 147 bp of DNA

wrapped around two copies of the four canonical histones (H2A, H2B, H3 and H4) (Luger et al., 1997). In the nucleosome, histones can be modified by post-translational modifications (PTM) via protein complexes called writers, which add chemical groups (methyl, acetyl, phosphate) and/or peptides (Ubiquitin, SUMO) to their N-/C-terminal tails. These marks can be recognized as signals by readers and removed by erasers (Kornberg and Lorch, 2020). Moreover, canonical histones can be replaced by their non-allelic isoforms or histone variants, which give specific properties to the nucleosome and additional versatility in remodeling and signaling events. ATP-dependent remodelers can not only open chromatin by moving or evicting nucleosomes but can also replace specific histones within them (Eustermann et al., 2024). At the heart of this molecular dynamic, histone H2A and its variants play key roles in the response to DNA damage. Furthermore, these histones undergo post-translational modifications regulated and recognized by various molecular effectors through the signaling and repair process.

Specific chromatin modifiers/remodelers increase chromatin dynamics, sliding and/or removing of nucleosomes, allowing accessibility to the DNA, which is required at sites of damages for DNA repair processes (Hauer and Gasser, 2017; Clouaire and Legube, 2019). However, it is still poorly understood in mammalian cells how the specific chromatin remodelers that have been implicated in HR and NHEJ repair mechanisms are recruited and coordinated in their function. Post-translational modifications of H2A and its variants are known to influence chromatin dynamics, implicated in the selection between HR and NHEJ repair mechanisms. These modifications include, phosphorylation by the PI3-kinase-related kinase ATM (*ataxia telangectasia* mutated), ATR (*ATM and RAD3-related*), DNA-PKcs (*DNA-dependent protein kinase, catalytic subunit*), acetylation by histone acetyltransferase such as NuA4/TIP60 (*nucleosome acetyltransferase of H4/Tat-interactive protein, 60 kDa)* and ubiquitylation by enzymes such as RNF8 and RNF168 (*RING nuclear factor*) (Kolas et al., 2007; Doil et al., 2009; Stewart et al., 2009; Mattiroli et al., 2012; Jacquet et al., 2016; Lashgari et al., 2022). In this review, we aim to paint the landscape of the chromatin-modifying events that impact DNA repair pathway choice, and the role of PTMs on H2A and its variants in this process. We will discuss the role of the writer, reader, and chromatin remodeler in these processes. By gathering the current knowledge, we will present the underlying mechanisms that orchestrate DNA signaling and repair. This systematic review of current literature may unveil avenues for exploring and developing precise strategies to address genetic diseases and cancer that are driven by unproper repair of DNA breaks.

## The control of DSB repair choice

The DSB repair pathway choice is first dictated by the phase of the cell cycle (Hustedt and Durocher, 2017). HR is restricted to the S and G2 phases, implicating DNA end resection and homology search, as this process uses the newly synthesized double helix from the sister chromatid as a template to repair the damaged one, generally producing accurate repair product (Aylon et al., 2004; Ira et al., 2004). NHEJ, on the other hand, is a DSB repair mechanism that requires few or no processing as it brings together DNA ends by a multi-protein synaptic complex to directly ligate them (Lieber, 2010). This pathway can occur throughout interphase. HR and NHEJ are mutually exclusive, and disruption of either of the pathways sensitizes cells to DSB-inducing drugs and results in spontaneous chromosomal aberrations (Takata et al., 1998; van de Kooij et al., 2022). Thus, the first steps of the cellular response to DNA damage include the selection of the specific repair pathway.

Controlling the initiation of one repair pathway at the expense of the other ensures intrinsic genome integrity. Initiation of DSB repair by HR during the G1 phase can lead to aberrant repair using a template that is weakly homologous to the damaged sequence or fully random (Kasparek and Humphrey, 2011). Furthermore, NHEJ, if initiated in the G2 phase, disadvantages HR and the opportunity to repair DNA with high fidelity (Fugger and West, 2016; Choi et al., 2020). Thus, the DSB repair pathway choice is key in maintaining genome integrity and this choice is a dynamic process involving the recruitment of opposing factors at the DSB (anti-resection factors vs resection initiator) and the surrounding chromatin (Hustedt and Durocher, 2017; Sigismondo et al., 2023). Failure to properly repair DSBs can lead to pathological genomic alterations (Ceccaldi et al., 2016).

## The early response to DSBs is shared by NHEJ and HR pathways

The initial cellular response to DSBs shares common signaling events between repair pathways. Following a double-strand break, the MRN protein complex, consisting of MRE11 (*Meiotic Recombination 11*), RAD50 and NBS1 (*Nijmegen breakage syndrome 1 mutated*), is recruited to the lesion, forming a synapse point, i.e., holding DNA ends in close proximity (Rass et al., 2009; Reginato and Cejka, 2020; Rotheneder et al., 2023). This event leads to the activation of the PI3-kinase-related kinase (PIKK) ATM that phosphorylates the histone H2A variant H2A.X at its C-terminus (S139) in chromatin surrounding the break (~1 Mb), as well as proteins such as MDC1 (*Mediator of DNA damage checkpoint protein 1*) and MRE11 (Burma et al., 2001; Collins et al., 2020). Next, the E3 ubiquitin ligase RNF8 (RING finger protein 8) is recruited to the breakthrough the recognition of ATM-dependent phosphorylation of MDC1. RNF8 poly-ubiquitylates either histone linker H1 or L3MBTL2 (*lethal(3)malignant brain tumour-like protein 2*), the latter being also recruited by MDC1 at sites of damage (Huen et al., 2007; Thorslund et al., 2015; Nowsheen et al., 2018). This K63 poly-ubiquitin chains enable the subsequent recruitment of the E3 ubiquitin ligase RNF168 (*RING finger protein 168*) that ubiquitylates lysines 13 and 15 of histone H2A (H2AK13 or K15ub) and its variants (Mattiroli and Penengo, 2021; Kelliher et al., 2022). In parallel, depending on the cell cycle stage and genomic location, lysine 20 of histone H4 is unmodified, mono-, di- or tri-methylated (H4K20me0, me1, me2 or me3) (Mattiroli and Penengo, 2021). In the section below, we will discuss further the importance of this methylation state in the implementation of the

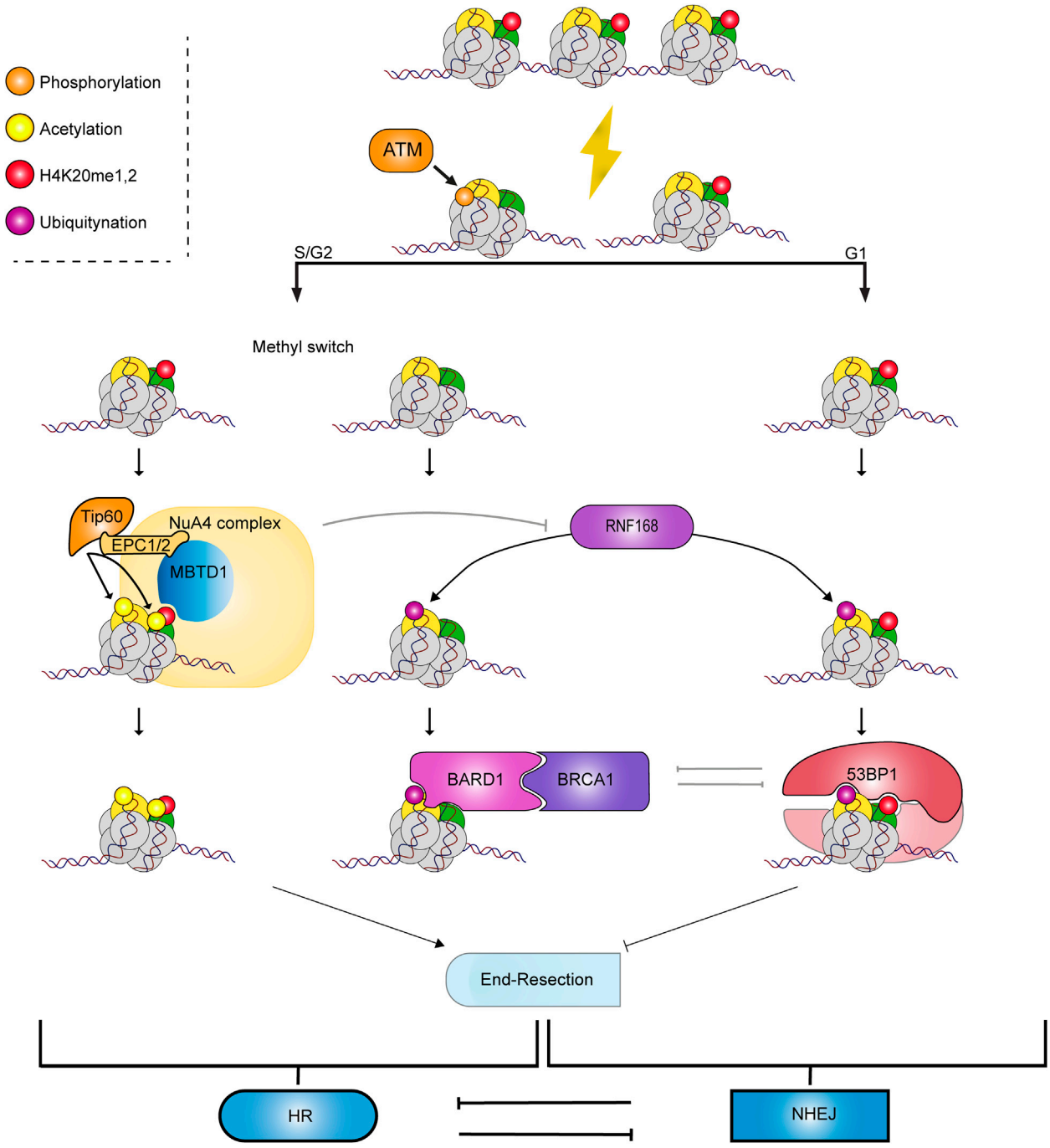


FIGURE 1
Crosstalk between H2A and H4 modifications to recruit chromatin readers to DNA breaks. When DSB occurs, MDC1 binds to H2A.X, which is phosphorylated by ATM (γH2A.X). ATM's phosphorylation of MDC1 leads to the recruitment of the E3 ubiquitin ligase RNF8 and RNF168. Depending on the methylation status of H4K20, different repair effectors are recruited, leading to the two main DSB repair pathways, which are mutually exclusive: HR mediated by the BARD1/BRCA1 complex and NHEJ through 53BP1.

repair pathway choice, either NHEJ or HR (Becker et al., 2021) as well as its crosstalk with H2A modifications at DSBs. Ultimately, the critical determinant of the repair pathway choice is whether a DSB undergoes 5' → 3′ resection, which is required for HR, while the resulting 3′ ssDNA overhang is a poor substrate for the NHEJ (Reviewed in: (Ceccaldi et al., 2016; Scully et al., 2019)) (Figure 1).

## Commitment to the NHEJ pathway

In the context of these chromatin modifications, NHEJ initiation is characterized by the recruitment of 53BP1 (*p53 Binding Protein 1*) through the collaboration of its oligomerization domain, its UDR (*Ubiquitin-dependent recruitment*) and its tandem Tudor domains in recognizing nucleosomal H2AK15Ub and H4K20me2 (Fradet-

Turcotte et al., 2013). 53BP1 is then bound by RIF-1 (*Replication Timing Regulatory Factor 1)*, and this interaction allows the recruitment of the Shieldin complex, composed of SHLD1, SHLD2, SHLD3 (*Shieldin Complex Subunit 1-2-3*) and REV7 (also known as *MAD2L2*) (Setiaputra and Durocher, 2019). The Shieldin complex is composed of two functional modules. The first one is SHLD1/2, which is a localization module, and the second one is SHLD3/REV7, which is the effector domain of the complex interacting with RIF1 (Gupta et al., 2018; Ghezraoui et al., 2018). The Shieldin complex appears to be a central component of NHEJ, protecting the DNA from the 5' → 3′ exonucleases activity, a critical step in the processing of the DNA ends during the early phases of HR (Mirman et al., 2018).

NHEJ is led by the proteins Ku70/80 that bind the broken ends, 20 to 200 bp of DNA flanking the damaged site (Walker et al., 2001; Zhang et al., 2001) and block resection. Ku70/80 interact with the DNA sugar backbone, ignoring specific DNA sequences (Downs and Jackson, 2004). The crystallographic structures of Ku70/80 present the heterodimer as a scaffolding complex allowing the recruitment of the PIKK-family DNA-PKcs. Ku70/80 heterodimer and DNA-PKcs forms DNA-PK, which serves as a platform that controls DNA-end sensing, protection and processing, before pairing and ligation (Jette and Lees-Miller, 2015). Then, the autophosphorylation of DNA-PKcs loosens the DNA-PK interaction with the DNA and restrains Artemis nuclease activity to avoid excessive DNA-end processing. This allows the recruitment of NHEJ factors XRCC4 (*X-ray repair cross-complementing protein 4)*, XLF (*RCC4-like factor)* factors, ligase IV and the APLF (*Aprataxin and PNKP like factor*) nuclease to process and ligate DNA ends (Rivera-Calzada et al., 2007; Liu et al., 2022). This complex enables the two DNA ends to be clamped to prevent rearrangements and chromosomal aberrations and the two non-homologous ends to be ligated by ligase IV (Chang et al., 2017).

## Commitment to the HR pathway

In the S/G2 phase, a DSB can be repaired using homologous recombination. This process uses the available sister chromatid as a template for repair. Resection of DNA-ends at the DSB generates a 3′ ssDNA overhang that invades the homologous chromatid to faithfully repair the damage (Jasin and Rothstein, 2013). The chromatin state surrounding the DNA breaks acts as a signaling hub by recruiting or inhibiting the recruitment of repair factors to direct repair to HR. HR is initiated by default in the absence of 53BP1, a DNA repair factor that guides repair toward NHEJ by preventing resection (Bunting et al., 2010). Indeed, knocking out 53BP1 in BRCA1 (*Breast Cancer gene 1*)-deficient cells rescues resection and subsequent homologous recombination (Bouwman et al., 2010). As previously mentioned, 53BP1 is recruited to chromatin ubiquitylated on H2AK15 and di-methylated on H4K20. However, during the S phase, newly synthesized histone H4 are unmethylated, which dilutes the presence of H4K20me1/2 from the parental nucleosome and concomitant recruitment of 53BP1 (Saredi et al., 2016; Escobar et al., 2021; Stewart-Morgan et al., 2023). H4K20 methylation status is thus important during the DSB repair pathway choice. The absence of 53BP1 on the nucleosome due to the absence of H4K20me1/2 allows the interaction of the BARD1 (*BRCA1-associated RING domain protein 1*)-BRCA1 complex with the nucleosome via the BARD1 ARD and BRCT domains that bind to H4K20me0 and H2AK15Ub, respectively (Nakamura et al., 2019; Becker et al., 2021; Dai et al., 2021; Hu et al., 2021; Witus et al., 2022; Burdett et al., 2023). After replication, H4K20 is rapidly mono-, di- or trimethylated by SET8 and SUV420H1/2, respectively (Pesavento et al., 2008; Jørgensen et al., 2013). In parallel, the H4K20me1/2 can be recognized by the MBTD1 (*mbt (malignant brain tumor) domain containing 1*) subunit of the NuA4/TIP60 acetyltransferase complex. Tip60 then acetylates lysines on the H2A and H4 tails, which hinders the interaction of 53BP1 with H4K20me1/2 (Tang et al., 2013; Jacquet et al., 2016; Lashgari et al., 2022). BARD1 promotes resection of the terminal ends via ubiquitylation of the endonuclease CtIP (*CtBP-interacting protein*) (Barber and Boulton, 2006). At the break, the heterodimer BRCA1/BARD1 poly-ubiquitylates residues K125, K127 and K129 of nucleosomal H2A (Kalb et al., 2014). Evidence showed that inhibiting this ubiquitylation, through USP48 (*Ubiquitin specific peptidase 48*) activity, restrains resection and consequently homologous recombination (Uckelmann et al., 2018). The ubiquitylation of H2A C-terminal residues allows end resection by EXO1 (*Exonuclease 1*) and DNA2/BLM (*Bloom syndrome protein*) helicase activities. The free 3′ ends are then rapidly coated by RPA (*Human Replication protein A*), a key protein in protecting the single-stranded DNA from degradation. RAD51 is subsequently loaded onto the DNA, replacing RPA. RAD51 loading involves BRCA2 in complex with PALB2 (*Partner and localizer of BRCA2*) (Davies et al., 2001; Ducy et al., 2019). RAD51 bound to the long overhang ssDNA forms a synapse to browse chromosomes. Once the search for homology is done, RAD51 opens the double helix and invades the complementary strand forming the D-loop through ATP hydrolysis, positioning of the damaged DNA at the homologous site (van der Heijden et al., 2008; Wald et al., 2022). This event recruits polymerases such as Pol δ that will fill the gap caused by the damage (Li et al., 2009). The displacement of the D-loop occurs through different sub-pathways of HR such as Single-Strand Annealing (SSA), Holliday junction HR (dHR) or Break-Induced Replication (BIR) (reviewed by Piazza and Heyer (Piazza and Heyer, 2019)) leading to the recovery of the genetic integrity at the site.

The chromatin landscape surrounding the break sites is directly involved in the whole process of repair. Nonetheless, the dynamic role of the different histone PTMs is still only partly understood and need to be further studied in the context of the repair pathway selection. Therefore, we gathered relevant knowledge related to H2A, its variants and their post-translational modifications after DSB that lead to the repair pathway choice.

## The histone H2A family

The histone H2A family is the most heterogeneous family of histones (Henikoff and Smith, 2015). H2A has numerous variants expressed in most cell types, such as H2A X, H2A Z.1, H2A Z.2 and macroH2A. H2A variants are encoded by paralogous genes harboring sequences that are highly conserved with canonical H2A but differ in their N- and C-termini.

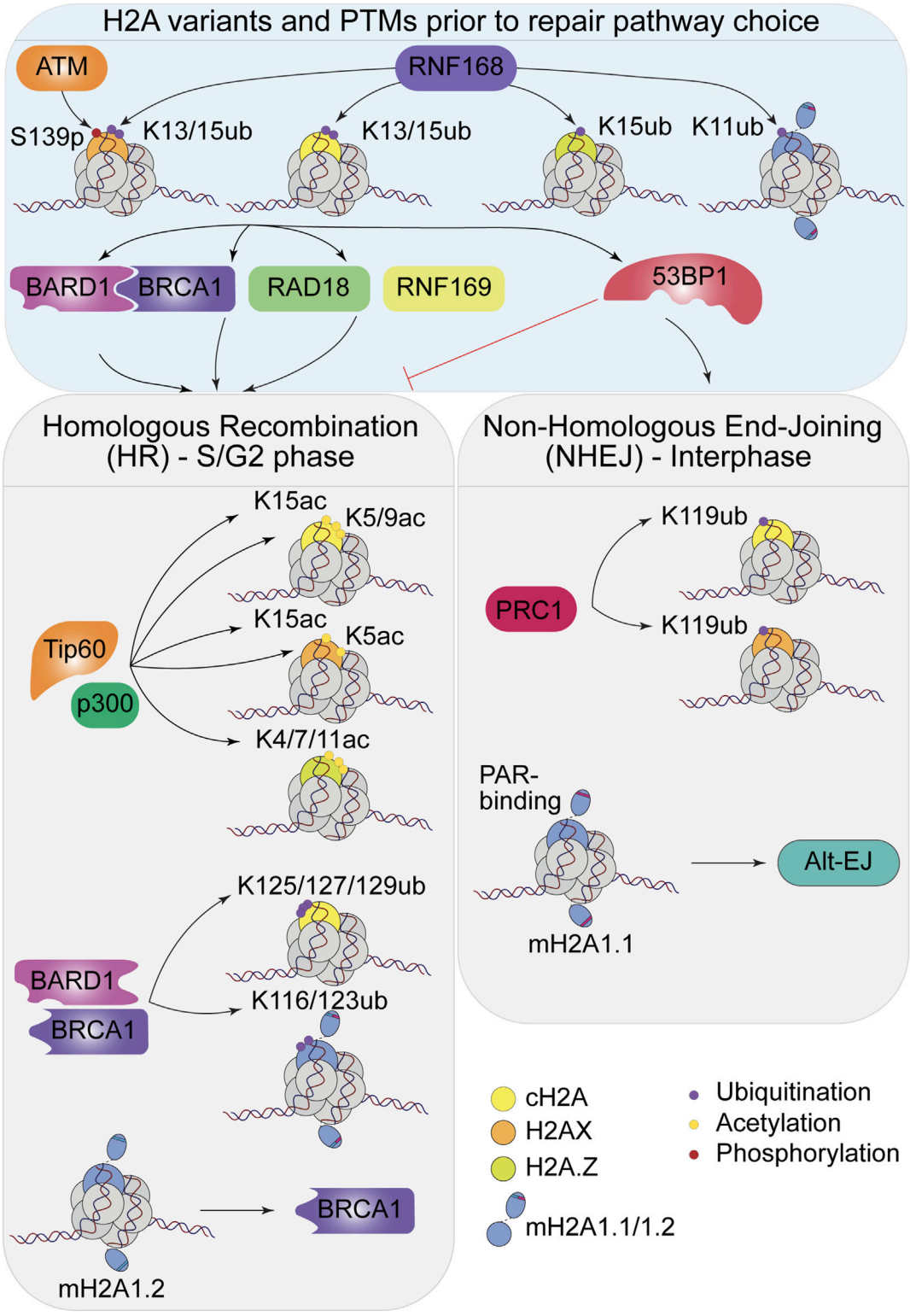


FIGURE 2
H2A variants and their PTMs impact the repair pathway choice. Top: Modifications happening prior to the choice, by ATM and RNF168 to recruit the DSB repair factors. Bottom: Choice between HR and NHEJ mediated by the repair factors, impact of the H2A variants and their PTMs.

The presence of H2A variants increases the diversity of the chromatin landscape and modulates the signals to various chromatin-modifying players such as RNF168, TIP60/NuA4 and BRCA1/BARD1. The inherent properties of those variants and their modifications refine the recruitment of key factors and the structure of chromatin itself during DSB signaling and DNA repair pathway

choice. The choreography of the writing, erasing, remodeling, and reading proteins along DSB signaling is determinant during the choice of the repair pathway. Histone H2A and its variants are thus key elements in the regulation of repair pathway choice (Figure 2).

## The canonical H2A

We previously discussed the role of the ubiquitylation of H2AK13/15 by RNF168 (Mattiroli et al., 2012) during DSB signaling, but several other modifications on this canonical histone also impact the outcome of repair. H2A lysine 119 is mono-ubiquitylated by the E3 ubiquitin ligase BMI1/RING1B, part of the Polycomb repressive complex 1 (PRC1), to prevent *de novo* transcription at damage sites (Ismail et al., 2010; Ginjala et al., 2011; Tamburri et al., 2020). Indeed, this mark is found on repressed genes, within H3K27me3-containing regions, deposited by the PRC2 methyltransferase complex (Schwartz and Pirrotta, 2013; Tamburri et al., 2020). Both PRC1 and PRC2 can be recruited to DSBs leading to neighboring gene repression to prevent conflict between transcription and the DNA repair machineries. Thus, H2AK119ub plays a role in transcription silencing in the damaged chromatin (Campbell et al., 2013). Additionally, BMI1-mediated mono-ubiquitylation of H2AK119 facilitates the recruitment of CtIP, promoting DNA end resection and allowing recruitment of key factors of the HR pathway, such as RPA, BRCA1 and RAD51 at DNA damage sites (Fitieh et al., 2022). In parallel, BAP1 (*BRCA1-associated protein 1*), the deubiquitinase of H2AK119, is phosphorylated in an ATM-dependent manner in response to DNA damage and is also required for efficient HR repair, highlighting the importance of highly dynamic H2AK119ub turnover at sites of DNA damage (Ismail et al., 2014). Canonical H2A possesses other lysines in its C-terminus, K125, K127 and K129. Interestingly, NMR studies revealed that these residues can be ubiquitylated by the heterodimer BRCA1/BARD1 (Witus et al., 2022). The E3 ligase is required for several functions of this heterodimer during DSB signaling (Barber and Boulton, 2006). Among them, ubiquitylation of H2AK125/127/129 recruits the ATP-dependent chromatin remodeler SMARCAD1 (*SWI/SNF-related, matrix-associated actin-dependent regulator of chromatin*), via its ubiquitin-binding CUE (*coupling of ubiquitin conjugation to ER degradation*) domains. SMARCAD1 is essential for nucleosome sliding and eviction at damaged sites, but also in 53BP1 repositioning, helping DNA end resection and processing with the CtIP nuclease (Densham et al., 2016; Sadek et al., 2022). Interestingly, loss of the specific deubiquitinase (DUB) for BRCA1/BARD1-dependent H2AK125/127/129ub, USP48, increases DNA end resection and RAD51 foci formation. USP48 thus serves as an antagonist of BRCA1 and limits RAD51 accumulation to ensure genomic stability (Uckelmann et al., 2018). Note that the BRCA1-BARD1 complex also ubiquitylates non-histone substrates such as CtIP (Yu et al., 2006; Wang et al., 2021; Bolck et al., 2022), highlighting the multifaceted role of proteins that act as histones writers and processing enzymes during initiation of the repair pathway.

Importantly, it has been very recently shown that canonical H2A di-acetylation on lysine 5 and 9 (K5/K9) by NuA4/TIP60 and p300 during the early stages of DSB signaling can create a non-permissive state of chromatin, impeding the NHEJ-end synapsis, thus promoting HR. Indeed, deacetylation of H2AK5/9ac by the mitotic deacetylase complex (MiDAC) suppresses hyper-accumulation of bromodomain-containing protein BRD4, which prevents proper DNA end synapsis, key to efficient NHEJ repair (Bao et al., 2024).

## H2A.X, the variant signaling repair

Upon detection of DSBs, activation of PIKKs ATM, ATR and DNA-PKcs lead to the addition of the first DSB-induced histone mark by phosphorylating the H2A.X variant at serine 139 (S139) (Rogakou et al., 1998), known as γH2AX. The phosphorylation of S139 of H2A.X is dispensable for the recruitment of DNA damage repair elements (Celeste et al., 2003) but its absence decreases the recruitment of BRCA1 and RAD51, two effectors of the DNA repair by HR (Bassing et al., 2002), and increases chromosomal aberrations leading to higher risk of tumor development in *H2AX* null mice (Celeste et al., 2002). Phosphorylation of H2A.X triggers a series of downstream modifications, being bound by MDC1 that is also phosphorylated by ATM and leading to the recruitment of RNF8. RNF8 catalyzes poly-ubiquitylation (K63 chain) of histone linker H1 or the protein L3MBTL2 (Huen et al., 2007; Kolas et al., 2007; Thorslund et al., 2015; Nowsheen et al., 2018), which is recognized by RNF168. The latter E3-ubiquitin ligase then mono-ubiquitylates lysines 13 and 15 (K13, K15) on histone H2A and H2A.X (Gatti et al., 2012; Mattiroli et al., 2012). Besides the phosphorylation of H2A.X on S139, the acetylation of H2A.X plays multiple roles in damage signaling. The acetylation of lysine 5 by Tip60 promotes the accumulation of NBS1 at double-strand breaks (Ikura et al., 2015). Indeed, loss of H2A.X acetylation at K5 leads to dispersed signal and improper accumulation of NBS1 onto damaged chromatin and increases γH2AX foci after DNA damage (Ikura et al., 2015). Conversely, Tip60 also modifies K15 on H2A and H2A.X, the same target as RNF168 required for the recruitment of 53BP1 and promotion of NHEJ repair (Jacquet et al., 2016). In the model proposed by *Jacquet et al.,* acetylation of the K15 by the NuA4/TIP60 complex blocks its ubiquitylation by RNF168, promoting HR over NHEJ (Fradet-Turcotte et al., 2013; Jacquet et al., 2016). However, a more recent model revealed that H2AK15ub also contributes to HR repair by driving element for repair pathway choice that comes from the methyl switch of H4K20 (Becker et al., 2021). The interplay for the accessibility and modification of H2AK15 in combination with H4K20 modification status still raises many questions and additional studies will be needed to define when and where H2AK15 is acetylated during cell cycle.

In addition to DNA repair protein, phosphorylation of H2A.X contributes to the recruitment of remodeling complexes SWI/SNF and INO80 through direct recognition of the modified histone at DSBs (Morrison et al., 2004; van Attikum et al., 2004; Park et al., 2006; Ogiwara et al., 2011; Harrod et al., 2020). While INO80 promotes resection, the current literature supports a role of SWI/SNF during strand invasion. Further studies will be required to characterize the role of these remodelers in DNA repair.

Interestingly, the NuA4/TIP60 complex has also been linked to the remodeling of H2A.X chromatin through an acetylation-linked

degradative poly-ubiquitylation as well as its SWI/SNF-family ATPase subunit p400 increasing chromatin accessibility for repair mechanisms (Ikura et al., 2007; 2015; Xu et al., 2010; Courilleau et al., 2012). In the yeast model, γH2A is removed from chromatin surrounding the break to allow resection and this implicates the initial action of NuA4 followed by remodelers (Cheng et al., 2018; Cheng et al., 2021). γH2A can also be replaced by the H2A variant H2A.Z, modulating the DNA repair signaling (Downs et al., 2004; van Attikum et al., 2007; Kalocsay et al., 2009; Horigome et al., 2014; Lee et al., 2014; Van et al., 2015). Moreover, NuA4/TIP60 subunit p400 catalyzes the exchange of γH2Av for H2Av in *D. melanogaster* (Kusch et al., 2004). H2Av is the fly ortholog of both H2A.X and H2A.Z, containing the SQ*Y domain at its C-terminus, which can be phosphorylated by ATM near DSBs, while its N-terminus and acidic patch is similar to H2A.Z (Bonisch and Hake, 2012). It has been suggested that the mammalian NuA4/TIP60 complex could remove γH2AX from the chromatin at DSBs and load H2A.Z (Altaf et al., 2010; Xu C. et al, 2012), as discussed further in the next section. For γH2AX to be able to recruit MDC1, its tyrosine 142 needs to be dephosphorylated by EYA (*Eyes absent*). This process is timely regulated by ZNF506 (*Zinc finger protein 506*) and allows the recruitment of downstream repair factors that amplify the repair signal (Cook et al., 2009; Nowsheen et al., 2018).

Among residues targeted for ubiquitylation in canonical H2A, K13, K15 and K119 are conserved in H2A.X and ubiquitylated upon the detection of DSBs (Pan et al., 2011; Wu et al., 2011; Mattiroli et al., 2012). H2A.X N-terminus is acetylated at its lysine K36 by CBP/p300 acetyltransferases, and this modification is required for cell survival after exposure to DNA damage, independently of γH2AX (Jiang et al., 2010). Indeed, mutants of K36 and T101, a site that is phosphorylated, lead to IR sensitivity, but rescued HR efficacy in *H2AX*−/− mouse ES cells at the same level that wild type H2A.X (Xie et al., 2010). This means that these residues contribute to IR resistance by a new, yet undiscovered, repair mechanism.

Elimination of γH2AX from the chromatin is essential for cell cycle progression after DSB repair (Fernandez-Capetillo et al., 2002; Nakamura et al., 2004; Shibata et al., 2010). Phosphatases PP2C and PP4 appear to be relevant candidates for this task (Chowdhury et al., 2005; Keogh et al., 2006; Nakada et al., 2008). Nonetheless, the question of whether dephosphorylation occurs on chromatin or after removal is still debated.

## H2A.Z, a key regulator of chromatin dynamics

Histone variant H2A.Z is ~60% homologous with canonical H2A. H2A.Z has more positive charged amino acids in its N-terminal tail, including two additional lysines, leading to a proposed intrinsic stabilization/destabilization of the nucleosome depending on the acetylation status (Abbott et al., 2001; Zhang et al., 2005; Zlatanova and Thakar, 2008; Draizen et al., 2016) (Figure 2). This variant also contains a more extended acidic patch, which is involved in regulating higher-order chromatin formation (Fan et al., 2004). H2A.Z is essential for the development and survival of mice as its depletion in mice leads to growth and metabolism defects (Belotti et al., 2024). H2A.Z is also a target of RNF168, demonstrated by *in vitro* and *in cellula* assays (O'Connor et al., 2015). The ubiquitylation profile of H2A.Z shows di-ubiquitylation like H2A and H2A.X. Lysine 15 of H2A.Z is the required first ubiquitylated residue, allowing ubiquitylation of other lysines (Fradet-Turcotte et al., 2013; Kelliher et al., 2020). Unfortunately, the identity of the other modified lysine(s) is not known. H2A.Z C-terminus is ubiquitylated and this modification has been associated with gene repression similar to canonical H2A (Sevilla and Binda, 2014). Reminiscent of canonical H2A, the C-terminal tail of H2A.Z is a substrate of the E3 ubiquitin ligase RING1B, and ubiquitylation of the K120, K121 and K125 residues is found at transcriptionally silent heterochromatin on the inactive X chromosome (Sarcinella et al., 2007).

Acetylation of H2A.Z is a key modification that occurs at the transcription start site (TSS) of active genes and is associated with epigenetic gene deregulation in tumorigenesis (as reviewed in (Giaimo et al., 2019). H2A.Z acetylation colocalizes with γH2AX at DSB (Hayakawa et al., 2017). K4, K7, K11 and K13 can be acetylated, playing a role in transcription, but di- or tri-acetylation is also observed in the context of DNA repair, conferring nucleosome destabilization and an open conformation (Colino-Sanguino et al., 2022). Loss of K7 acetylation, in TIP60-depleted cells, is sufficient to induce a p53-independent cell death (Wichmann et al., 2022). ChIP-seq mapping of chromatin composition/modifications after double-strand breaks showed different compositions of histone variants and PTMs depending on the genome location and the chosen repair pathway. It appears that total H2A.Z is significantly diminished during repair by HR, whereas H2A.Zac is unchanged, suggesting that ratio of H2A.Z acetylation greatly increases during HR (Taty-Taty et al., 2014; Clouaire et al., 2018). The genomic mapping approach demonstrated no significant changes of H2A.Z or H2A.Zac on chromatin during NHEJ repair (Clouaire et al., 2018). Besides, in the yeast model, SUMOylation of H2A.Z can lead to the recruitment of RAD51 (Kalocsay et al., 2009). Altogether, these data support a role of H2A.Z in the HR repair pathway. Nonetheless, knock-down/out H2A.Z cell lines show defective recruitment of Ku80 and downstream elements of NHEJ repair pathway (Belotti et al., 2024) as well as BRCA1 at damage sites (Xu C. et al, 2012).

H2A.Z has in fact two isoforms, H2A.Z.1 and H2A.Z.2, encoded by two different genes, that differ by only 3 amino acids (Kreienbaum et al., 2022). Studying specifically each isoform/amino acid variation may be key for a better understanding of H2A.Z involvement in the different repair pathways, as suggested by a recent study (Chen et al., 2023). It is known that the NuA4/TIP60 complex is a player in the deposition of H2A.Z and data on endogenous H2A.Z shows that NuA4/TIP60 has a preference for H2A.Z.2, while SRCAP, the other remodeler responsible for H2A.Z deposition, does not show such bias (Lamaa et al., 2020). Interestingly, it has been suggested that H2A.Z can serve as a recruitment platform for SUV420H1 to di-methylate H4K20, a crucial mark for 53BP1 binding and orientation towards the NHEJ repair pathway (Abini-Agbomson et al., 2023; Huang et al., 2023). Unfortunately, both H2A.Z isoforms are targeted in most studies, or only H2A.Z.1. The mechanism of H2A.Z removal from chromatin is controversial, but it has been shown that chaperone ANP32E (*Acidic nuclear phosphoprotein 32 family member E*) can remove H2A.Z from intact nucleosomes and is rapidly recruited to DSBs (Gursoy-Yuzugullu et al., 2015). It was

suggested to promote H4 acetylation, reshape the local chromatin and facilitate DNA repair. Loss of ANP32E leads to increased end-resection by CtIP, creating single-stranded DNA and increased repair by alternative NHEJ (Alt-EJ) (Gursoy-Yuzugullu et al., 2015). In parallel, the INO80 chromatin remodeler has been suggested to regulate H2A.Z dynamic in chromatin (Papamichos-Chronakis et al., 2011). INO80 is the first remodeler that has been shown to play a role at DSBs, assisting end resection by remodeling chromatin (Downs et al., 2004; Morrison et al., 2004; Van Attikum et al., 2004). Obviously, significant work is still needed to dissect H2A.Z dynamics and function at DSBs and how it can influence repair pathway choice.

## macroH2A, the largest histone

MacroH2A differs from other H2A variants by its distinct non-histone domain composed of a disordered linker region and a globular macrodomain. Three isoforms of macroH2A are produced from genes *H2AFY* and *H2AFY2*, also known as *MACROH2A1* and *MACROH2A2,* respectively (Pehrson and Fried, 1992; Costanzi and Pehrson, 2001). While only one mRNA is produced from *MACROH2A2, MACROH2A1* mRNA is alternatively spliced to produce macroH2A1.1 and macroH2A1.2 isoforms (Pehrson et al., 1997). Splicing occurs between two mutually exclusive variants of exon 6 of *MACROH2A1* mRNA, making isoforms that differ by only 33 amino acids within the macrodomain. This difference renders macroH2A1.1 capable of binding to poly (ADP-ribose) (PAR) (Karras et al., 2005; Kozlowski et al., 2018), an interaction that is essential for its role in the repression of transcription and DNA damage signaling on chromatin (Timinszky et al., 2009; Sebastian et al., 2020). MacroH2A1.2 and macroH2A2 show no affinity for PAR moieties, and no interactors of the macrodomain have been identified for macroH2A1.2 (Kustatscher et al., 2005; Kozlowski et al., 2018).

Structural studies show that macroH2A preferentially assembles into hybrid macroH2A-H2A nucleosomes in which protein-DNA and protein-protein interactions are more stable (Chakravarthy and Luger, 2006; Bowerman et al., 2019). MacroH2A is specifically incorporated in the chromatin by the LSH/HELLS (*Lymphoid-specific helicase/Helicase lymphocyte specific*) remodeler in an ATP-dependent manner, both *in vitro* and in cells (Ni et al., 2020; Ni and Muegge, 2021). In human genome, macroH2A accumulation is enriched at loci that exhibit high levels of replication stress, such as the common fragile sites (Kim et al., 2018) and at telomeres in cells where their replication is dependent of alternative lengthening of telomere (ALT) (Kim et al., 2019). Consistently, LSH/HELLS-depleted cells are prone to replication fork stalling and exhibit increased levels of DNA damage, a phenotype that is similar to the one observed in macroH2A-depleted cells (Kim et al., 2018; Xu et al., 2021). Depletion of LSH/HELLS, macroH2A1 or macroH2A2 lead to a reduction of RAD51 filament formation at stalled replication forks and to concomitant nuclease-dependent degradation of unprotected forks (Xu et al., 2021). Improper accumulation of 53BP1 at stalled forks contributes to this reduction as this phenotype is rescued by 53BP1 depletion in LSH/HELLS-deficient cells. Note that Xu et al., 2021 also report LSH/HELLS- and macroH2A1.2-dependent change in histone PTM at stalled forks (H3K4me3 and H4K20me2), suggesting that macroH2A loading at stalled replication forks impacts the chromatin environment. Other chaperones contribute to the efficient loading of macroH2A on chromatin as depletion of the histone chaperone complex associated with the replicative helicase, FACT (*FAcilitates Chromatin Transcription*), also impairs the deposition of macroH2A1.2 at sites of replication stress (Kim et al., 2018). In ALT cells, macroH2A1.2 incorporation at sites of replication stress is dependent on the chromatin remodeler ATRX, which negatively regulates the amount of macroH2A at telomeres (Ratnakumar et al., 2012; Kim et al., 2019).

MacroH2A1.2 and macroH2A1.1 were both originally described to accumulate on the mammalian inactive X chromosome (Xi) and promote the formation of the Xi macro-body (Costanzi and Pehrson, 1998). However, the role of macroH2A1.2 as a "replication-stress"-protective histone variant was recently shown to be important for the integrity of the Xi and associated female mice survival (Sebastian et al., 2020). At this locus, macroH2A1.2 actively counteracts Xi-specific anaphase defects and chromosomal instability that are induced by a macroH2A1.1-driven activation of Alt-EJ and thus, improper DNA repair pathway choice.

MacroH2A1.2 accumulates at the I-SceI-induced DSBs in an ATM-dependent manner (Khurana et al., 2014), while macroH2A1.1 accumulates in a PARP1-dependent manner at sites of damage (Timinszky et al., 2009; Xu Y. et al, 2012). The roles of macroH2A isoforms and their remodelers in DSBs signaling and repair have been studied using DNA repair reporter assays. In these assays, depletion of macroH2A1.2 reduces HR efficiency in a 53BP1-dependent manner, coherent with a model where macroH2A1.2 favors the recruitment of BRCA1 at DSBs (Khurana et al., 2014). A similar phenotype is observed at telomeres in ALT cells (Kim et al., 2019), a process that heavily relies on homology-driven repair. In the latter conditions, the depletion of macroH2A1.2 reduces the recruitment of BRCA1 at the telomeres and safeguards their genomic stability. In Khurana et al., 2014, depletion of the H3K9 methyltransferase PRDM2 also rescues the levels of HR, with no further impact upon co-depletion of macroH2A1. These findings suggest that, in addition to its role in regulating the recruitment of BRCA1, macroH2A's impact on DNA repair pathway choice at DSBs also relies in part on the compaction of the chromatin surrounding the break. While macroH2A1.2 promotes HR, efficient NHEJ repair has been associated with the PAR-binding capacity of macroH2A1.1 (Timinszky et al., 2009; Xu Y. et al, 2012; Sebastian et al., 2020). The mechanism by which macroH2A participated in the recruitment of NHEJ factors is unclear. At DNA break induced by laser stripes, the recruitment of GFP-Ku80 is reduced in LSH/HELLS knocked-out cell lines. Consistent with a role of macroH2A in NHEJ, depletion of LSH/HELLS reduces NHEJ levels in DNA repair reporter assays (Unoki et al., 2018). Other groups reported that accumulation of GFP-Ku70 at laser stripes is reduced in cells expressing macroH2A1.1, suggesting an inhibitory role in this condition (Timinszky et al., 2009). A possible explanation could be an indirect impact of macroH2A1.1 ectopic expression on chromatin compaction. Indeed, both the compaction of the chromatin and the interaction of macroH2A1.1 with DNA repair

factors such as PARP1, LIG3 and XRCC1 have been reported, making the dissociation of the two functions complex. Note the ectopic expression of macroH2A1.1 also leads to improper pathway choice by promoting Alt-EJ, a phenotype that may contribute to the acquisition of genomic instability in tumor cells (revised in (Oberdoerffer and Miller, 2023)).

As canonical histone H2A, macroH2A isoforms are targeted by histone-modifying enzymes in response to DNA damage. Co-transfection of Myc-RNF168 with SFB-macroH2A1 in HEK293T cells leads to the ubiquitylation of macroH2A1 (Kelliher et al., 2020). The ubiquitylation of macroH2A by RNF168 may offer additional docking platforms for recruiting DNA repair proteins to DNA damage. Similarly to what has been shown for H2AK129, the heterodimer BRCA1/BARD1 also ubiquitylates macroH2A on K123 (Kalb et al., 2014; Kim et al., 2017). Mutations of this site in cells lead to defective replicative senescence (Kim et al., 2017). However, a role for this modification in DNA repair is not excluded, as hypothesized for the ubiquitylation of canonical H2AK125/127/129 by BRCA1, further investigations are, nonetheless, required to clear this hypothesis. Interestingly, mass spectrometry analyses identified S137 of macroH2A1 linker region to be phosphorylated, for both splice variants. This modification is excluded from the Xi, but enriched in mitosis acting in chromatin condensation (Bernstein et al., 2008). Phosphorylation of the linker region, which is important for DNA interaction, might play a role in protein interactions (Muthurajan et al., 2011). Other mass spectrometry analyses observed that macroH2A1 splice variants have distinct modified sites. While macroH2A1.1 presents more T129 phosphorylation, S170 phosphorylation is enriched in macroH2A1.2, which could affect their folding, giving the role of the linker region in stabilizing heterochromatin architecture (Chakravarthy et al., 2012; Kozlowski et al., 2018; Giallongo et al., 2021). Those studies also revealed sites of acetylation (K7) or methylation (K18, K123 or K239) in macroH2A1, but none of them has been characterized for their impact in macroH2A's central role in maintaining nuclear integrity at DNA damage sites (Chu et al., 2006; Bernstein et al., 2008; Giallongo et al., 2021). Further investigations are required to decipher whether these PTMs are important for the function of macroH2A in DNA damage signaling and DNA repair, and to ascertain whether the specific modifications of macroH2A1 splice variants contribute to its markedly different functions in regulating tumorigenicity in humans (reviewed in Hsu et al., 2021).

## Conclusion and perspectives

The large H2A family has a major impact on the DSB repair pathway choice that is finely regulated by the histone variants and the PTMs that they are decorated with. The chromatin composition at DSBs is heterogenous and dynamic to ensure the signaling orientation and maximize the repair process at the different phases of the cell cycle. Each histone variant is giving additional properties modulated by the PTMs to recruit actors of the repair process, and each isoform of variants adds another layer of fine tuning, as discussed for H2AZ1/2 or macroH2A1.1/2. Past investigations focused on the writing and reading part of the chromatin dynamics at DSBs, while the role of specific remodelers on H2A variants-containing chromatin at DSBs is still debated. Some questions on the stoichiometry of variants-containing nucleosomes at DSBs also remain. Indeed, across many studies on histone variants and their roles in DDR, few mention the possibility of heterotypic nucleosomes. As an example, H2A.X-containing nucleosomes, signaling the damage, could also contain a macroH2A1.2, promoting or modulating the downstream signaling. Similar to the "histone code" hypothesis (Strahl and Allis, 2000; Jenuwein and Allis, 2001), the "variants code" may define the different patterns of recruitment of repair machinery. Besides H2A and its variants modulating DSB repair pathway choice, modifications of the other nucleosomal histones lead to crosstalk in regulating this choice. We mentioned that H4 methylation at lysine K20 by SUV420H1 promotes NHEJ, unless H4K16 is acetylated by Tip60. While unmethylated H4K20 recruits BARD1/BRCA1 to promote HR in S/G2 (Becker et al., 2021). Interestingly, H3K36me2 appears to promote NHEJ (Fnu et al., 2011) while the H3K36me3, a mark associated with transcribed regions, seems to prioritize HR repair (Aymard et al., 2014; Clouaire and Legube, 2015).

In the model of the "access, repair, restore" proposed by G. Almouzni (Green and Almouzni, 2002; Groth et al., 2007), modified as "prime, repair, restore" (Soria et al., 2012), the chromatin state needs to be "restored" after the repair, in a process that has been linked to cell cycle checkpoint release. The dephosphorylation of H2A.X by phosphatases like PP2AC or PP4C has been described but it remains debated if this occurs directly on chromatin or after removal of H2A.XS139ph by ATP-dependent remodelers, or both (Chowdhury et al., 2005; Keogh et al., 2006; van Attikum et al., 2007; Nakada et al., 2008). The deubiquitylation of H2AK15 by the USP51 is logically another event implicated in the restoration process (Wang et al., 2016; Ai et al., 2019) as well as the action of different histone deacetylases (Aricthota et al., 2022). It is less clear if erasers like USP48 and BAP1 also play roles in restoration beside their functions in the repair process itself, while it seems logical to argue a function of BAP1 to recover local transcription after repair. In addition, the action of the deubiquitinases on histone variants was not investigated, leaving questions unanswered. Overall, additional studies are needed to enrich our knowledge on the chromatin dynamics during completion of repair and chromatin state restoration.

Aside from the H2A variants we discussed, two others H2A variants emerged as playing roles in the DDR. H2A.J sequence is highly conserved with H2A, with two additional serines and one tyrosine while conserving lysines 125, 127 and 129 at the C-terminus (Tanaka et al., 2020). The SQ*KTKSK sequence is potentially phosphorylated as in the H2A.X variant. Moreover, similar to the C-terminal lysines in H2A being ubiquitylated by the BARD1-BRCA1 complex, it is likely that H2A.J is also modified by the complex. The H2A.J variant has been associated with the persistent DNA damages and appears to be correlated with senescence-associated secretory phenotype (Contrepois et al., 2017; Isermann et al., 2020). Another distant H2A variant, known as H2A.B (or H2A.Bbd), differs from canonical H2A with only 48% identity (González-Romero et al., 2008). In contrast to macroH2A, H2A.B is termed Barr body deficient (Bbd) because it is absent from the inactive X chromosome in females. It shows a preference for binding to regions with hyperacetylated H4, indicating

enrichment in active genomic regions and implying a role in gene regulation (Chadwick and Willard, 2001; Ishibashi et al., 2010). Nucleosomes containing H2A.B organize DNA less tightly and exhibit lower stability compared to canonical nucleosomes, resulting in a more relaxed and elongated structure (Arimura et al., 2013; Sansoni et al., 2014). Studies have uncovered potential roles of H2A.B in DNA repair. Indeed, H2A.B was found, through proteomic analysis, to transiently localize to sites of DNA synthesis during replication and DNA repair, potentially affecting cell cycle regulation and DNA damage sensitivity. Cells overexpressing H2A.B have a shortened S phase and are more prone to DNA damages, as observed in Hodgkin's lymphoma cells aberrantly expressing this variant (Sansoni et al., 2014).

Many cancers and pathologies involve histone H2A and its variants, including modifications that interact with specific readers after DNA double-strand break. Examples include ataxia telangiectasia and the RIDDLE syndrome linked with immunodeficiencies and increased risks of cancer development (McKinnon, 2004; Stewart et al., 2009; Lai and Chan, 2024). Improper or defective repair pathway in a particular cell context could be catastrophic. Thus, better understanding the regulation of the signals and the modulation of actors during the repair pathway orientation is a continuing challenge to address.

## Author contributions

EC: Investigation, Writing–original draft, Writing–review and editing. MG: Investigation, Validation, Writing–review and editing, AF-T: Funding acquisition, Supervision, Validation, Writing–review and editing. JC: Funding acquisition, Supervision, Validation, Writing–review and editing.

## Funding

The author(s) declare that financial support was received for the research, authorship, and/or publication of this article. Work in the Fradet-Turcotte and Côté labs is supported by grants from the Canadian Institutes of Health Research (CIHR; PJT-183708) and the National Science and Engineering Research Council of Canada (NSERC, RGPIN-2022-04530, RGPIN-2016-05844). EC and MG are supported by doctoral fellowships from the Fonds de Recherche du Québec - Santé (FRQ). AF-T and JC held Canada Research Chairs in Molecular Virology and Genomic Instability, and Chromatin Biology and Molecular Epigenetics, respectively. AF-T is supported by the Foundation J.-Louis Lévesque.

## Conflict of interest

The authors declare that the research was conducted in the absence of any commercial or financial relationships that could be construed as a potential conflict of interest.

The author(s) declared that they were an editorial board member of Frontiers, at the time of submission. This had no impact on the peer review process and the final decision.

## Publisher's note



## References

Abbott, D. W., Ivanova, V. S., Wang, X., Bonner, W. M., and Ausió, J. (2001). Characterization of the stability and folding of H2A.Z chromatin particles: Implications for transcriptional activation. *J. Biol. Chem.* 276, 41945–41949. doi:10.1074/jbc.m108217200

Abini-Agbomson, S., Gretarsson, K., Shih, R. M., Hsieh, L., Lou, T., De Ioannes, P., et al. (2023). Catalytic and non-catalytic mechanisms of histone H4 lysine 20 methyltransferase SUV420H1. *Mol. Cell* 83, 2872–2883.e7. doi:10.1016/j.molcel.2023.07.020

Ai, H., Guo, Y., Sun, D., Liu, S., Qi, Y., Guo, J., et al. (2019). Examination of the deubiquitylation site Selectivity of USP51 by using chemically synthesized ubiquitylated histones. *ChemBioChem* 20, 221–229. doi:10.1002/cbic.201800432

Altaf, M., Auger, A., Monnet-Saksouk, J., Brodeur, J., Piquet, S., Cramet, M., et al. (2010). NuA4-dependent acetylation of nucleosomal histones H4 and H2A directly stimulates incorporation of H2A.Z by the SWR1 complex. *J. Biol. Chem.* 285, 15966–15977. doi:10.1074/jbc.m110.117069

Aricthota, S., Rana, P. P., and Haldar, D. (2022). Histone acetylation dynamics in repair of DNA double-strand breaks. *Front. Genet.* 13, 926577. doi:10.3389/fgene.2022.926577

Arimura, Y., Kimura, H., Oda, T., Sato, K., Osakabe, A., Tachiwana, H., et al. (2013). Structural basis of a nucleosome containing histone H2A.B/H2A.Bbd that transiently associates with reorganized chromatin. *Sci. Rep.* 3, 3510. doi:10.1038/srep03510

Aylon, Y., Liefshitz, B., and Kupiec, M. (2004). The CDK regulates repair of double-strand breaks by homologous recombination during the cell cycle. *EMBO J.* 23, 4868–4875. doi:10.1038/sj.emboj.7600469

Aymard, F., Bugler, B., Schmidt, C. K., Guillou, E., Caron, P., Briois, S., et al. (2014). Transcriptionally active chromatin recruits homologous recombination at DNA double strand breaks. *Nat. Struct. Mol. Biol.* 21, 366–374. doi:10.1038/nsmb.2796

Bao, K., Ma, Y., Li, Y., Shen, X., Zhao, J., Tian, S., et al. (2024). A di-acetyl-decorated chromatin signature couples liquid condensation to suppress DNA end synapsis. *Mol. Cell.* 84, 1206–1223. doi:10.1016/j.molcel.2024.02.002

Barber, L. J., and Boulton, S. J. (2006). BRCA1 ubiquitylation of CtIP: just the tIP of the iceberg? *DNA Repair (Amst)* 5, 1499–1504. doi:10.1016/j.dnarep.2006.08.009

Bassing, C. H., Chua, K. F., Sekiguchi, J., Suh, H., Whitlow, S. R., Fleming, J. C., et al. (2002). Increased ionizing radiation sensitivity and genomic instability in the absence of histone H2AX. *Proc. Natl. Acad. Sci. U S A* 99, 8173–8178. doi:10.1073/pnas.122228699

Becker, J. R., Clifford, G., Bonnet, C., Groth, A., Wilson, M. D., and Chapman, J. R. (2021). BARD1 reads H2A lysine 15 ubiquitination to direct homologous recombination. *Nature* 596, 433–437. doi:10.1038/s41586-021-03776-w

Belotti, E., Lacoste, N., Iftikhar, A., Simonet, T., Papin, C., Osseni, A., et al. (2024). H2A.Z is involved in premature aging and DSB repair initiation in muscle fibers. *Nucleic Acids Res.* 52, 3031–3049. doi:10.1093/nar/gkae020

Bernstein, E., Muratore-Schroeder, T. L., Diaz, R. L., Chow, J. C., Changolkar, L. N., Shabanowitz, J., et al. (2008). A phosphorylated subpopulation of the histone variant macroH2A1 is excluded from the inactive X chromosome and enriched during mitosis. *Proc. Natl. Acad. Sci.* 105, 1533–1538. doi:10.1073/pnas.0711632105

Bolck, H. A., Przetocka, S., Meier, R., von Aesch, C., Zurfluh, C., Hänggi, K., et al. (2022). RNAi screening uncovers a synthetic sick interaction between CtIP and the BARD1 tumor suppressor. *Cells* 11, 643. doi:10.3390/cells11040643

Bönisch, C., and Hake, S. B. (2012). Histone H2A variants in nucleosomes and chromatin: more or less stable? *Nucleic Acids Res.* 40, 10719–10741. doi:10.1093/nar/gks865

Bouwman, P., Aly, A., Escandell, J. M., Pieterse, M., Bartkova, J., van der Gulden, H., et al. (2010). 53BP1 loss rescues BRCA1 deficiency and is associated with triple-negative

and BRCA-mutated breast cancers. *Nat. Struct. Mol. Biol.* 17, 688–695. doi:10.1038/nsmb.1831

Bowerman, S., Hickok, R. J., and Wereszczynski, J. (2019). Unique dynamics in asymmetric macroH2A-H2A hybrid nucleosomes result in increased complex stability. *J. Phys. Chem. B* 123, 419–427. doi:10.1021/acs.jpcb.8b10668

Bunting, S. F., Callén, E., Wong, N., Chen, H.-T., Polato, F., Gunn, A., et al. (2010). 53BP1 inhibits homologous recombination in brca1-deficient cells by blocking resection of DNA breaks. *Cell* 141, 243–254. doi:10.1016/j.cell.2010.03.012

Burdett, H., Foglizzo, M., Musgrove, L. J., Kumar, D., Clifford, G., Campbell, L. J., et al. (2023). BRCA1–BARD1 combines multiple chromatin recognition modules to bridge nascent nucleosomes. *Nucleic Acids Res.* 51, 11080–11103. doi:10.1093/nar/gkad793

Burma, S., Chen, B. P., Murphy, M., Kurimasa, A., and Chen, D. J. (2001). ATM phosphorylates histone H2AX in response to DNA double-strand breaks. *J. Biol. Chem.* 276, 42462–42467. doi:10.1074/jbc.c100466200

Campbell, S., Ismail, I. H., Young, L. C., Poirier, G. G., and Hendzel, M. J. (2013). Polycomb repressive complex 2 contributes to DNA double-strand break repair. *Cell Cycle* 12, 2675–2683. doi:10.4161/cc.25795

Ceccaldi, R., Rondinelli, B., and D'Andrea, A. D. (2016). Repair pathway choices and consequences at the double-strand break. *Trends Cell Biol.* 26, 52–64. doi:10.1016/j.tcb.2015.07.009

Celeste, A., Fernandez-Capetillo, O., Kruhlak, M. J., Pilch, D. R., Staudt, D. W., Lee, A., et al. (2003). Histone H2AX phosphorylation is dispensable for the initial recognition of DNA breaks. *Nat. Cell Biol.* 5, 675–679. doi:10.1038/ncb1004

Celeste, A., Petersen, S., Romanienko, P. J., Fernandez-Capetillo, O., Chen, H. T., Sedelnikova, O. A., et al. (2002). Genomic instability in mice lacking histone H2AX. *Science* 296, 922–927. doi:10.1126/science.1069398

Chadwick, B. P., and Willard, H. F. (2001). A novel chromatin protein, distantly related to histone H2a, is largely excluded from the inactive X chromosome. *J. Cell Biol.* 152, 375–384. doi:10.1083/jcb.152.2.375

Chakravarthy, S., and Luger, K. (2006). The histone variant macro-H2A preferentially forms 'hybrid nucleosomes. *J. Biol. Chem.* 281, 25522–25531. doi:10.1074/jbc.m602258200

Chakravarthy, S., Patel, A., and Bowman, G. D. (2012). The basic linker of macroH2A stabilizes DNA at the entry/exit site of the nucleosome. *Nucleic Acids Res.* 40, 8285–8295. doi:10.1093/nar/gks645

Chang, H. H. Y., Pannunzio, N. R., Adachi, N., and Lieber, M. R. (2017). Non-homologous DNA end joining and alternative pathways to double-strand break repair. *Nat. Rev. Mol. Cell Biol.* 18, 495–506. doi:10.1038/nrm.2017.48

Chen, C.-W., Zhang, L., Dutta, R., Niroula, A., Miller, P. G., Gibson, C. J., et al. (2023). SRCAP mutations drive clonal hematopoiesis through epigenetic and DNA repair dysregulation. *Cell Stem Cell* 30, 1503–1519.e8. doi:10.1016/j.stem.2023.09.011

Cheng, X., Cote, V. R., and Côte, J. (2021). NuA4 and SAGA acetyltransferase complexes cooperate for repair of DNA breaks by homologous recombination. *PLoS Genet.* 17, e1009459. doi:10.1371/journal.pgen.1009459

Cheng, X., Jobin-Robitaille, O., Billon, P., Buisson, R., Niu, H., Lacoste, N., et al. (2018). Phospho-dependent recruitment of the yeast NuA4 acetyltransferase complex by MRX at DNA breaks regulates RPA dynamics during resection. *Proc. Natl. Acad. Sci. U S A* 115, 10028–10033. doi:10.1073/pnas.1806513115

Choi, E.-H., Yoon, S., Koh, Y. E., Seo, Y.-J., and Kim, K. P. (2020). Maintenance of genome integrity and active homologous recombination in embryonic stem cells. *Exp. Mol. Med.* 52, 1220–1229. doi:10.1038/s12276-020-0481-2

Chowdhury, D., Keogh, M.-C., Ishii, H., Peterson, C. L., Buratowski, S., and Lieberman, J. (2005). γ-H2AX dephosphorylation by protein phosphatase 2A facilitates DNA double-strand break repair. *Mol. Cell* 20, 801–809. doi:10.1016/j.molcel.2005.10.003

Chu, F., Nusinow, D. A., Chalkley, R. J., Plath, K., Panning, B., and Burlingame, A. L. (2006). Mapping post-translational modifications of the histone variant MacroH2A1 using tandem mass spectrometry. *Mol. and Cell. proteomics MCP* 5, 194–203. doi:10.1074/mcp.M500285-MCP200

Clouaire, T., and Legube, G. (2015). DNA double strand break repair pathway choice: a chromatin based decision? *Nucleus* 6, 107–113. doi:10.1080/19491034.2015.1010946

Clouaire, T., and Legube, G. (2019). A snapshot on the cis chromatin response to DNA double-strand breaks. *Trends Genet.* 35, 330–345. doi:10.1016/j.tig.2019.02.003

Clouaire, T., Rocher, V., Lashgari, A., Arnould, C., Aguirrebengoa, M., Biernacka, A., et al. (2018). Comprehensive mapping of histone modifications at DNA double-strand breaks deciphers repair pathway chromatin signatures. *Mol. Cell* 72, 250–262.e6. doi:10.1016/j.molcel.2018.08.020

Colino-Sanguino, Y., Clark, S. J., and Valdes-Mora, F. (2022). The H2A.Z-nucleosome code in mammals: emerging functions. *Trends Genet.* 38, 273–289. doi:10.1016/j.tig.2021.10.003

Collins, P. L., Purman, C., Porter, S. I., Nganga, V., Saini, A., Hayer, K. E., et al. (2020). DNA double-strand breaks induce H2Ax phosphorylation domains in a contact-dependent manner. *Nat. Commun.* 11, 3158. doi:10.1038/s41467-020-16926-x

Contrepois, K., Coudereau, C., Benayoun, B. A., Schuler, N., Roux, P.-F., Bischof, O., et al. (2017). Histone variant H2A.J accumulates in senescent cells and promotes inflammatory gene expression. *Nat. Commun.* 8, 14995. doi:10.1038/ncomms14995

Cook, P. J., Ju, B. G., Telese, F., Wang, X., Glass, C. K., and Rosenfeld, M. G. (2009). Tyrosine dephosphorylation of H2AX modulates apoptosis and survival decisions. *Nature* 458, 591–596. doi:10.1038/nature07849

Costanzi, C., and Pehrson, J. R. (1998). Histone macroH2A1 is concentrated in the inactive X chromosome of female mammals. *Nature* 393, 599–601. doi:10.1038/31275

Costanzi, C., and Pehrson, J. R. (2001). MACROH2A2, a new member of the MACROH2A core histone family. *J. Biol. Chem.* 276, 21776–21784. doi:10.1074/jbc.m010919200

Courilleau, C., Chailleux, C., Jauneau, A., Grimal, F., Briois, S., Boutet-Robinet, E., et al. (2012). The chromatin remodeler p400 ATPase facilitates Rad51-mediated repair of DNA double-strand breaks. *J. Cell Biol.* 199, 1067–1081. doi:10.1083/jcb.201205059

Dai, L., Dai, Y., Han, J., Huang, Y., Wang, L., Huang, J., et al. (2021). Structural insight into BRCA1-BARD1 complex recruitment to damaged chromatin. *Mol. Cell* 81, 2765–2777.e6. doi:10.1016/j.molcel.2021.05.010

Davies, A. A., Masson, J. Y., McIlwraith, M. J., Stasiak, A. Z., Stasiak, A., Venkitaraman, A. R., et al. (2001). Role of BRCA2 in control of the RAD51 recombination and DNA repair protein. *Mol. Cell* 7, 273–282. doi:10.1016/s1097-2765(01)00175-7

Densham, R. M., Garvin, A. J., Stone, H. R., Strachan, J., Baldock, R. A., Daza-Martin, M., et al. (2016). Human BRCA1-BARD1 ubiquitin ligase activity counteracts chromatin barriers to DNA resection. *Nat. Struct. Mol. Biol.* 23, 647–655. doi:10.1038/nsmb.3236

Doil, C., Mailand, N., Bekker-Jensen, S., Menard, P., Larsen, D. H., Pepperkok, R., et al. (2009). RNF168 binds and amplifies ubiquitin conjugates on damaged chromosomes to allow accumulation of repair proteins. *Cell* 136, 435–446. doi:10.1016/j.cell.2008.12.041

Downs, J. A., Allard, S., Jobin-Robitaille, O., Javaheri, A., Auger, A., Bouchard, N., et al. (2004). Binding of chromatin-modifying activities to phosphorylated histone H2A at DNA damage sites. *Mol. Cell* 16, 979–990. doi:10.1016/j.molcel.2004.12.003

Downs, J. A., and Jackson, S. P. (2004). A means to a DNA end: the many roles of Ku. *Nat. Rev. Mol. Cell Biol.* 5, 367–378. doi:10.1038/nrm1367

Draizen, E. J., Shaytan, A. K., Mariño-Ramírez, L., Talbert, P. B., Landsman, D., and Panchenko, A. R. (2016). HistoneDB 2.0: a histone database with variants—an integrated resource to explore histones and their variants. *Database (Oxford)* 2016, baw014. doi:10.1093/database/baw014

Ducy, M., Sesma-Sanz, L., Guitton-Sert, L., Lashgari, A., Gao, Y., Brahiti, N., et al. (2019). The tumor suppressor PALB2: inside out. *Trends Biochem. Sci.* 44, 226–240. doi:10.1016/j.tibs.2018.10.008

Escobar, T. M., Loyola, A., and Reinberg, D. (2021). Parental nucleosome segregation and the inheritance of cellular identity. *Nat. Rev. Genet.* 22, 379–392. doi:10.1038/s41576-020-00312-w

Eustermann, S., Patel, A. B., Hopfner, K. P., He, Y., and Korber, P. (2024). Energy-driven genome regulation by ATP-dependent chromatin remodellers. *Nat. Rev. Mol. Cell Biol.* 25, 309–332. doi:10.1038/s41580-023-00683-y

Fan, J. Y., Rangasamy, D., Luger, K., and Tremethick, D. J. (2004). H2A.Z alters the nucleosome surface to promote HP1α-mediated chromatin fiber folding. *Mol. Cell* 16, 655–661. doi:10.1016/j.molcel.2004.10.023

Fernandez-Capetillo, O., Chen, H.-T., Celeste, A., Ward, I., Romanienko, P. J., Morales, J. C., et al. (2002). DNA damage-induced G2-M checkpoint activation by histone H2AX and 53BP1. *Nat. Cell Biol.* 4, 993–997. doi:10.1038/ncb884

Fitieh, A., Locke, A. J., Mashayekhi, F., Khaliqdina, F., Sharma, A. K., and Ismail, I. H. (2022). BMI-1 regulates DNA end resection and homologous recombination repair. *Cell Rep.* 38, 110536. doi:10.1016/j.celrep.2022.110536

Fnu, S., Williamson, E. A., De Haro, L. P., Brenneman, M., Wray, J., Shaheen, M., et al. (2011). Methylation of histone H3 lysine 36 enhances DNA repair by nonhomologous end-joining. *Proc. Natl. Acad. Sci. U S A* 108, 540–545. doi:10.1073/pnas.1013571108

Fradet-Turcotte, A., Canny, M. D., Escribano-Díaz, C., Orthwein, A., Leung, C. C. Y., Huang, H., et al. (2013). 53BP1 is a reader of the DNA damage-induced H2A Lys15 ubiquitin mark. *Nature* 499, 50–54. doi:10.1038/nature12318

Fugger, K., and West, S. C. (2016). Keeping homologous recombination in check. *Cell Res.* 26, 397–398. doi:10.1038/cr.2016.25

Gatti, M., Pinato, S., Maspero, E., Soffientini, P., Polo, S., and Penengo, L. (2012). A novel ubiquitin mark at the N-terminal tail of histone H2As targeted by RNF168 ubiquitin ligase. *Cell Cycle* 11, 2538–2544. doi:10.4161/cc.20919

Ghezraoui, H., Oliveira, C., Becker, J. R., Bilham, K., Moralli, D., Anzilotti, C., et al. (2018). 53BP1 cooperation with the REV7-shieldin complex underpins DNA structure-specific NHEJ. *Nature* 560 (7716), 122–127. doi:10.1038/s41586-018-0362-1

Giaimo, B. D., Ferrante, F., Herchenröther, A., Hake, S. B., and Borggrefe, T. (2019). The histone variant H2A.Z in gene regulation. *Epigenetics Chromatin* 12, 37. doi:10.1186/s13072-019-0274-9

Giallongo, S., Lo Re, O., Lochmanová, G., Parca, L., Petrizzelli, F., Zdráhal, Z., et al. (2021). Phosphorylation within intrinsic disordered region discriminates histone variant macroH2A1 splicing isoforms—macroH2A1.1 and macroH2A1.2. *Biol. (Basel)* 10, 659. doi:10.3390/biology10070659

Ginjala, V., Nacerddine, K., Kulkarni, A., Oza, J., Hill, S. J., Yao, M., et al. (2011). BMI1 is recruited to DNA breaks and contributes to DNA damage-induced H2A ubiquitination and repair. *Mol. Cell. Biol.* 31, 1972–1982. doi:10.1128/mcb.00981-10

González-Romero, R., Méndez, J., Ausió, J., and Eirín-López, J. M. (2008). Quickly evolving histones, nucleosome stability and chromatin folding: all about histone H2A.Bbd. *Gene* 413, 1–7. doi:10.1016/j.gene.2008.02.003

Green, C. M., and Almouzni, G. (2002). When repair meets chromatin. First in series on chromatin dynamics. *EMBO Rep.* 3, 28–33. doi:10.1093/embo-reports/kvf005

Groth, A., Rocha, W., Verreault, A., and Almouzni, G. (2007). Chromatin challenges during DNA replication and repair. *Cell* 128, 721–733. doi:10.1016/j.cell.2007.01.030

Gupta, R., Somyajit, K., Narita, T., Maskey, E., Stanlie, A., Kremer, M., et al. (2018). DNA repair network analysis reveals shieldin as a key regulator of NHEJ and PARP inhibitor sensitivity. *Cell* 173, 972–988.e23. doi:10.1016/j.cell.2018.03.050

Gursoy-Yuzugullu, O., Ayrapetov, M. K., and Price, B. D. (2015). Histone chaperone Anp32e removes H2A.Z from DNA double-strand breaks and promotes nucleosome reorganization and DNA repair. *Proc. Natl. Acad. Sci.* 112, 7507–7512. doi:10.1073/pnas.1504868112

Harrod, A., Lane, K. A., and Downs, J. A. (2020). The role of the SWI/SNF chromatin remodelling complex in the response to DNA double strand breaks. *DNA Repair (Amst)* 93, 102919. doi:10.1016/j.dnarep.2020.102919

Hauer, M. H., and Gasser, S. M. (2017). Chromatin and nucleosome dynamics in DNA damage and repair. *Genes Dev.* 31, 2204–2221. doi:10.1101/gad.307702.117

Hayakawa, K., Hirosawa, M., Tani, R., Yoneda, C., Tanaka, S., and Shiota, K. (2017). H2A O-GlcNAcylation at serine 40 functions genomic protection in association with acetylated H2AZ or γH2AX. *Epigenetics Chromatin* 10, 51. doi:10.1186/s13072-017-0157-x

Henikoff, S., and Smith, M. M. (2015). Histone variants and epigenetics. *Cold Spring Harb. Perspect. Biol.* 7, a019364. doi:10.1101/cshperspect.a019364

Horigome, C., Oma, Y., Konishi, T., Schmid, R., Marcomini, I., Hauer, M. H., et al. (2014). SWR1 and INO80 chromatin remodelers contribute to DNA double-strand break perinuclear anchorage site choice. *Mol. Cell* 55, 626–639. doi:10.1016/j.molcel.2014.06.027

Hsu, C.-J., Meers, O., Buschbeck, M., and Heidel, F. H. (2021). The role of MacroH2A histone variants in cancer. *Cancers (Basel)* 13, 3003. doi:10.3390/cancers13123003

Hu, Q., Botuyan, M. V., Zhao, D., Cui, G., Mer, E., and Mer, G. (2021). Mechanisms of BRCA1–BARD1 nucleosome recognition and ubiquitylation. *Nature* 596, 438–443. doi:10.1038/s41586-021-03716-8

Huang, L., Wang, Y., Long, H., Zhu, H., Wen, Z., Zhang, L., et al. (2023). Structural insight into H4K20 methylation on H2A.Z-nucleosome by SUV420H1. *Mol. Cell* 83, 2884–2895.e7. doi:10.1016/j.molcel.2023.07.001

Huen, M. S. Y., Grant, R., Manke, I., Minn, K., Yu, X., Yaffe, M. B., et al. (2007). RNF8 transduces the DNA-damage signal via histone ubiquitylation and checkpoint protein assembly. *Cell* 131, 901–914. doi:10.1016/j.cell.2007.09.041

Hustedt, N., and Durocher, D. (2017). The control of DNA repair by the cell cycle. *Nat. Cell Biol.* 19, 1–9. doi:10.1038/ncb3452

Ikura, M., Furuya, K., Matsuda, S., Matsuda, R., Shima, H., Adachi, J., et al. (2015). Acetylation of histone H2AX at lys 5 by the TIP60 histone acetyltransferase complex is essential for the dynamic binding of NBS1 to damaged chromatin. *Mol. Cell. Biol.* 35, 4147–4157. doi:10.1128/mcb.00757-15

Ikura, T., Tashiro, S., Kakino, A., Shima, H., Jacob, N., Amunugama, R., et al. (2007). DNA damage-dependent acetylation and ubiquitination of H2AX enhances chromatin dynamics. *Mol. Cell. Biol.* 27, 7028–7040. doi:10.1128/mcb.00579-07

Ingram, S. P., Warmenhoven, J. W., Henthorn, N. T., Smith, E. a. K., Chadwick, A. L., Burnet, N. G., et al. (2019). Mechanistic modelling supports entwined rather than exclusively competitive DNA double-strand break repair pathway. *Sci. Rep.* 9, 6359. doi:10.1038/s41598-019-42901-8

Ira, G., Pellicioli, A., Balijja, A., Wang, X., Fiorani, S., Carotenuto, W., et al. (2004). DNA end resection, homologous recombination and DNA damage checkpoint activation require CDK1. *Nature* 431, 1011–1017. doi:10.1038/nature02964

Isermann, A., Mann, C., and Rübe, C. E. (2020). Histone variant H2A.J marks persistent DNA damage and triggers the secretory phenotype in radiation-induced senescence. *Int. J. Mol. Sci.* 21, 9130. doi:10.3390/ijms21239130

Ishibashi, T., Li, A., Eirín-López, J. M., Zhao, M., Missiaen, K., Abbott, D. W., et al. (2010). H2A.Bbd: an X-chromosome-encoded histone involved in mammalian spermiogenesis. *Nucleic Acids Res.* 38, 1780–1789. doi:10.1093/nar/gkp1129

Ismail, I. H., Andrin, C., McDonald, D., and Hendzel, M. J. (2010). BMI1-mediated histone ubiquitylation promotes DNA double-strand break repair. *J. Cell Biol.* 191, 45–60. doi:10.1083/jcb.201003034

Ismail, I. H., Davidson, R., Gagné, J.-P., Xu, Z. Z., Poirier, G. G., and Hendzel, M. J. (2014). Germline mutations in BAP1 impair its function in DNA double-strand break repair. *Cancer Res.* 74, 4282–4294. doi:10.1158/0008-5472.can-13-3109

Jackson, S. P., and Bartek, J. (2009). The DNA-damage response in human biology and disease. *Nature* 461, 1071–1078. doi:10.1038/nature08467

Jacquet, K., Fradet-Turcotte, A., Avvakumov, N., Lambert, J.-P., Roques, C., Pandita, R. K., et al. (2016). The TIP60 complex regulates bivalent chromatin recognition by 53BP1 through direct H4K20me binding and H2AK15 acetylation. *Mol. Cell* 62, 409–421. doi:10.1016/j.molcel.2016.03.031

Jasin, M., and Rothstein, R. (2013). Repair of strand breaks by homologous recombination. *Cold Spring Harb. Perspect. Biol.* 5, a012740. doi:10.1101/cshperspect.a012740

Jenuwein, T., and Allis, C. D. (2001). Translating the histone code. *Science* 293, 1074–1080. doi:10.1126/science.1063127

Jette, N., and Lees-Miller, S. P. (2015). The DNA-dependent protein kinase: a multifunctional protein kinase with roles in DNA double strand break repair and mitosis. *Prog. Biophysics Mol. Biol.* 117, 194–205. doi:10.1016/j.pbiomolbio.2014.12.003

Jiang, X., Xu, Y., and Price, B. D. (2010). Acetylation of H2AX on lysine 36 plays a key role in the DNA double-strand break repair pathway. *FEBS Lett.* 584, 2926–2930. doi:10.1016/j.febslet.2010.05.017

Jørgensen, S., Schotta, G., and Sørensen, C. S. (2013). Histone H4 Lysine 20 methylation: key player in epigenetic regulation of genomic integrity. *Nucleic Acids Res.* 41, 2797–2806. doi:10.1093/nar/gkt012

Kalb, R., Mallery, D. L., Larkin, C., Huang, J. T. J., and Hiom, K. (2014). BRCA1 is a histone-H2A-specific ubiquitin ligase. *Cell Rep.* 8, 999–1005. doi:10.1016/j.celrep.2014.07.025

Kalocsay, M., Hiller, N. J., and Jentsch, S. (2009). Chromosome-wide Rad51 spreading and SUMO-H2a.z-dependent chromosome fixation in response to a persistent DNA double-strand break. *Mol. Cell* 33, 335–343. doi:10.1016/j.molcel.2009.01.016

Karras, G. I., Kustatscher, G., Buhecha, H. R., Allen, M. D., Pugieux, C., Sait, F., et al. (2005). The macro domain is an ADP-ribose binding module. *EMBO J.* 24, 1911–1920. doi:10.1038/sj.emboj.7600664

Kasparek, T. R., and Humphrey, T. C. (2011). DNA double-strand break repair pathways, chromosomal rearrangements and cancer. *Seminars Cell and Dev. Biol.* 22, 886–897. doi:10.1016/j.semcdb.2011.10.007

Kelliher, J., Ghosal, G., and Leung, J. W. C. (2022). New answers to the old RIDDLE: RNF168 and the DNA damage response pathway. *FEBS J.* 289 (9), 2467–2480. doi:10.1111/febs.15857

Kelliher, J. L., West, K. L., Gong, Q., and Leung, J. W. C. (2020). Histone H2A variants alpha1-extension helix directs RNF168-mediated ubiquitination. *Nat. Commun.* 11, 2462. doi:10.1038/s41467-020-16307-4

Keogh, M.-C., Kim, J.-A., Downey, M., Fillingham, J., Chowdhury, D., Harrison, J. C., et al. (2006). A phosphatase complex that dephosphorylates γH2AX regulates DNA damage checkpoint recovery. *Nature* 439, 497–501. doi:10.1038/nature04384

Khanna, K. K., and Jackson, S. P. (2001). DNA double-strand breaks: signaling, repair and the cancer connection. *Nat. Genet.* 27, 247–254. doi:10.1038/85798

Khurana, S., Kruhlak, M. J., Kim, J., Tran, A. D., Liu, J., Nyswaner, K., et al. (2014). A macrohistone variant links dynamic chromatin compaction to BRCA1-dependent genome maintenance. *Cell Rep.* 8, 1049–1062. doi:10.1016/j.celrep.2014.07.024

Kim, B.-J., Chan, D. W., Jung, S. Y., Chen, Y., Qin, J., and Wang, Y. (2017). The histone variant MacroH2A1 is a BRCA1 ubiquitin ligase substrate. *Cell Rep.* 19, 1758–1766. doi:10.1016/j.celrep.2017.05.027

Kim, J., Sturgill, D., Sebastian, R., Khurana, S., Tran, A. D., Edwards, G. B., et al. (2018). Replication stress shapes a protective chromatin environment across fragile genomic regions. *Mol. Cell* 69, 36–47.e7. doi:10.1016/j.molcel.2017.11.021

Kim, J., Sun, C., Tran, A. D., Chin, P.-J., Ruiz, P. D., Wang, K., et al. (2019). The macroH2A1.2 histone variant links ATRX loss to alternative telomere lengthening. *Nat. Struct. Mol. Biol.* 26, 213–219. doi:10.1038/s41594-019-0192-3

Kolas, N. K., Chapman, J. R., Nakada, S., Ylanko, J., Chahwan, R., Sweeney, F. D., et al. (2007). Orchestration of the DNA-damage response by the RNF8 ubiquitin ligase. *Science* 318, 1637–1640. doi:10.1126/science.1150034

Kornberg, R. D., and Lorch, Y. (2020). Primary role of the nucleosome. *Mol. Cell* 79, 371–375. doi:10.1016/j.molcel.2020.07.020

Kozlowski, M., Corujo, D., Hothorn, M., Guberovic, I., Mandemaker, I. K., Blessing, C., et al. (2018). MacroH2A histone variants limit chromatin plasticity through two distinct mechanisms. *EMBO Rep.* 19, e44445. doi:10.15252/embr.201744445

Kreienbaum, C., Paasche, L. W., and Hake, S. B. (2022). H2A.Z's 'social' network: functional partners of an enigmatic histone variant. *Trends Biochem. Sci.* 47, 909–920. doi:10.1016/j.tibs.2022.04.014

Kusch, T., Florens, L., Macdonald, W. H., Swanson, S. K., Glaser, R. L., Yates, J. R., et al. (2004). Acetylation by Tip60 is required for selective histone variant exchange at DNA lesions. *Science* 306, 2084–2087. doi:10.1126/science.1103455

Kustatscher, G., Hothorn, M., Pugieux, C., Scheffzek, K., and Ladurner, A. G. (2005). Splicing regulates NAD metabolite binding to histone macroH2A. *Nat. Struct. Mol. Biol.* 12, 624–625. doi:10.1038/nsmb956

Lai, P. M., and Chan, K. M. (2024). Roles of histone H2A variants in cancer development, prognosis, and treatment. *Int. J. Mol. Sci.* 25, 3144. doi:10.3390/ijms25063144

Lamaa, A., Humbert, J., Aguirrebengoa, M., Cheng, X., Nicolas, E., Côté, J., et al. (2020). Integrated analysis of H2A.Z isoforms function reveals a complex interplay in gene regulation. *Elife* 9, e53375. doi:10.7554/elife.53375

Lashgari, A., Kougnassoukou Tchara, P.-E., Lambert, J.-P., and Côté, J. (2022). New insights into the DNA repair pathway choice with NuA4/TIP60. *DNA Repair (Amst)* 113, 103315. doi:10.1016/j.dnarep.2022.103315

Lee, C.-S., Lee, K., Legube, G., and Haber, J. E. (2014). Dynamics of yeast histone H2A and H2B phosphorylation in response to a double-strand break. *Nat. Struct. Mol. Biol.* 21, 103–109. doi:10.1038/nsmb.2737

Li, X., Stith, C. M., Burgers, P. M., and Heyer, W.-D. (2009). PCNA is required for initiation of recombination-associated DNA synthesis by DNA polymerase δ. *Mol. Cell* 36, 704–713. doi:10.1016/j.molcel.2009.09.036

Lieber, M. R. (2010). The mechanism of double-strand DNA break repair by the nonhomologous DNA end-joining pathway. *Annu. Rev. Biochem.* 79, 181–211. doi:10.1146/annurev.biochem.052308.093131

Liu, L., Chen, X., Li, J., Wang, H., Buehl, C. J., Goff, N. J., et al. (2022). Autophosphorylation transforms DNA-PK from protecting to processing DNA ends. *Mol. Cell* 82, 177–189.e4. doi:10.1016/j.molcel.2021.11.025

Luger, K., Mäder, A. W., Richmond, R. K., Sargent, D. F., and Richmond, T. J. (1997). Crystal structure of the nucleosome core particle at 2.8 Å resolution. *Nature* 389, 251–260. doi:10.1038/38444

Mattiroli, F., and Penengo, L. (2021). Histone ubiquitination: an integrative signaling platform in genome stability. *Trends Genet*. 37 (6), 566–581. doi:10.1016/j.tig.2020.12.005

Mattiroli, F., Vissers, J. H. A., van Dijk, W., Ikpa, P., Citterio, E., Vermeulen, W., et al. (2012). RNF168 ubiquitinates K13-15 on H2A/H2AX to drive DNA damage signaling. *Cell* 150, 1182–1195. doi:10.1016/j.cell.2012.08.005

McKinnon, P. J. (2004). ATM and ataxia telangiectasia. *EMBO Rep.* 5, 772–776. doi:10.1038/sj.embor.7400210

Mirman, Z., Lottersberger, F., Takai, H., Kibe, T., Gong, Y., Takai, K., et al. (2018). 53BP1-RIF1-shieldin counteracts DSB resection through CST- and Polα-dependent fill-in. *Nature* 560, 112–116. doi:10.1038/s41586-018-0324-7

Morrison, A. J., Highland, J., Krogan, N. J., Arbel-Eden, A., Greenblatt, J. F., Haber, J. E., et al. (2004). INO80 and γ-H2AX interaction links ATP-dependent chromatin remodeling to DNA damage repair. *Cell* 119, 767–775. doi:10.1016/j.cell.2004.11.037

Muthurajan, U. M., McBryant, S. J., Lu, X., Hansen, J. C., and Luger, K. (2011). The linker region of MacroH2A promotes self-association of nucleosomal arrays. *J. Biol. Chem.* 286, 23852–23864. doi:10.1074/jbc.m111.244871

Nakada, S., Chen, G. I., Gingras, A.-C., and Durocher, D. (2008). PP4 is a γH2AX phosphatase required for recovery from the DNA damage checkpoint. *EMBO Rep.* 9, 1251–1026. doi:10.1038/embor.2008.204

Nakamura, K., Saredi, G., Becker, J. R., Foster, B. M., Nguyen, N. V., Beyer, T. E., et al. (2019). H4K20me0 recognition by BRCA1–BARD1 directs homologous recombination to sister chromatids. *Nat. Cell Biol.* 21, 311–318. doi:10.1038/s41556-019-0282-9

Nakamura, T. M., Du, L.-L., Redon, C., and Russell, P. (2004). Histone H2A phosphorylation controls Crb2 recruitment at DNA breaks, maintains checkpoint arrest, and influences DNA repair in fission yeast. *Mol. Cell. Biol.* 24, 6215–6230. doi:10.1128/mcb.24.14.6215-6230.2004

Ni, K., and Muegge, K. (2021). LSH catalyzes ATP-driven exchange of histone variants macroH2A1 and macroH2A2. *Nucleic Acids Res.* 49, 8024–8036. doi:10.1093/nar/gkab588

Ni, K., Ren, J., Xu, X., He, Y., Finney, R., Braun, S. M. G., et al. (2020). LSH mediates gene repression through macroH2A deposition. *Nat. Commun.* 11, 5647. doi:10.1038/s41467-020-19159-0

Nowsheen, S., Aziz, K., Aziz, A., Deng, M., Qin, B., Luo, K., et al. (2018). L3MBTL2 orchestrates ubiquitin signalling by dictating the sequential recruitment of RNF8 and RNF168 after DNA damage. *Nat. Cell Biol.* 20, 455–464. doi:10.1038/s41556-018-0071-x

Oberdoerffer, P., and Miller, K. M. (2023). Histone H2A Variants: diversifying chromatin to ensure genome integrity. *Seminars Cell and Dev. Biol.* 135, 59–72. doi:10.1016/j.semcdb.2022.03.011

O'Connor, H. F., Lyon, N., Leung, J. W., Agarwal, P., Swaim, C. D., Miller, K. M., et al. (2015). Ubiquitin-Activated Interaction Traps (UBAITs) identify E3 ligase binding partners. *EMBO Rep.* 16, 1699–1712. doi:10.15252/embr.201540620

Ogiwara, H., Ui, A., Otsuka, A., Satoh, H., Yokomi, I., Nakajima, S., et al. (2011). Histone acetylation by CBP and p300 at double-strand break sites facilitates SWI/SNF chromatin remodeling and the recruitment of non-homologous end joining factors. *Oncogene* 30, 2135–2146. doi:10.1038/onc.2010.592

Pan, M.-R., Peng, G., Hung, W.-C., and Lin, S.-Y. (2011). Monoubiquitination of H2AX protein regulates DNA damage response signaling. *J. Biol. Chem.* 286, 28599–28607. doi:10.1074/jbc.m111.256297

Papamichos-Chronakis, M., Watanabe, S., Rando, O. J., and Peterson, C. L. (2011). Global regulation of H2A.Z localization by the INO80 chromatin-remodeling enzyme is essential for genome integrity. *Cell* 144, 200–213. doi:10.1016/j.cell.2010.12.021

Park, J., Park, E., Lee, H., Kim, S. J., Hur, S., Imbalzano, A. N., et al. (2006). Mammalian SWI/SNF complexes facilitate DNA double-strand break repair by promoting γ-H2AX induction. *EMBO J.* 25, 3986–3997. doi:10.1038/sj.emboj.7601291

Pehrson, J. R., and Fried, V. A. (1992). MacroH2A, a core histone containing a large nonhistone region. *Science* 257, 1398–1400. doi:10.1126/science.1529340

Pesavento, J. J., Yang, H., Kelleher, N. L., and Mizzen, C. A. (2008). Certain and progressive methylation of histone H4 at lysine 20 during the cell cycle. *Mol. Cell. Biol.* 28, 468–486. doi:10.1128/mcb.01517-07

Piazza, A., and Heyer, W.-D. (2019). Homologous recombination and the formation of complex genomic rearrangements. *Trends Cell Biol.* 29, 135–149. doi:10.1016/j.tcb.2018.10.006

Rass, E., Grabarz, A., Plo, I., Gautier, J., Bertrand, P., and Lopez, B. S. (2009). Role of Mre11 in chromosomal nonhomologous end joining in mammalian cells. *Nat. Struct. Mol. Biol.* 16, 819–824. doi:10.1038/nsmb.1641

Ratnakumar, K., Duarte, L. F., LeRoy, G., Hasson, D., Smeets, D., Vardabasso, C., et al. (2012). ATRX-mediated chromatin association of histone variant macroH2A1 regulates α-globin expression. *Genes Dev.* 26, 433–438. doi:10.1101/gad.179416.111

Reginato, G., and Cejka, P. (2020). The MRE11 complex: a versatile toolkit for the repair of broken DNA. *DNA Repair (Amst)* 91–92, 102869. doi:10.1016/j.dnarep.2020.102869

Rivera-Calzada, A., Spagnolo, L., Pearl, L. H., and Llorca, O. (2007). Structural model of full-length human Ku70–Ku80 heterodimer and its recognition of DNA and DNA-PKcs. *EMBO Rep.* 8, 56–62. doi:10.1038/sj.embor.7400847

Rogakou, E. P., Pilch, D. R., Orr, A. H., Ivanova, V. S., and Bonner, W. M. (1998). DNA double-stranded breaks induce histone H2AX phosphorylation on serine 139. *J. Biol. Chem.* 273, 5858–5868. doi:10.1074/jbc.273.10.5858

Rotheneder, M., Stakyte, K., van de Logt, E., Bartho, J. D., Lammens, K., Fan, Y., et al. (2023). Cryo-EM structure of the Mre11-Rad50-Nbs1 complex reveals the molecular mechanism of scaffolding functions. *Mol. Cell* 83, 167–185.e9. doi:10.1016/j.molcel.2022.12.003

Sadek, M., Sheth, A., Zimmerman, G., Hays, E., and Vélez-Cruz, R. (2022). The role of SWI/SNF chromatin remodelers in the repair of DNA double strand breaks and cancer therapy. *Front. Cell Dev. Biol.* 10, 1071786. doi:10.3389/fcell.2022.1071786

Sansoni, V., Casas-Delucchi, C. S., Rajan, M., Schmidt, A., Bönisch, C., Thomae, A. W., et al. (2014). The histone variant H2A.Bbd is enriched at sites of DNA synthesis. *Nucleic Acids Res.* 42, 6405–6420. doi:10.1093/nar/gku303

Sarcinella, E., Zuzarte, P. C., Lau, P. N. I., Draker, R., and Cheung, P. (2007). Monoubiquitylation of H2A.Z distinguishes its association with euchromatin or facultative heterochromatin. *Mol. Cell. Biol.* 27, 6457–6468. doi:10.1128/mcb.00241-07

Saredi, G., Huang, H., Hammond, C. M., Alabert, C., Bekker-Jensen, S., Forne, I., et al. (2016). H4 K20me0 marks post-replicative chromatin and recruits the TONSL-MMS22L DNA repair complex. *Nature* 534, 714–718. doi:10.1038/nature18312

Schwartz, Y. B., and Pirrotta, V. (2013). A new world of Polycombs: unexpected partnerships and emerging functions. *Nat. Rev. Genet.* 14, 853–864. doi:10.1038/nrg3603

Scully, R., Panday, A., Elango, R., and Willis, N. A. (2019). DNA double-strand break repair-pathway choice in somatic mammalian cells. *Nat. Rev. Mol. Cell Biol.* 20, 698–714. doi:10.1038/s41580-019-0152-0

Sebastian, R., Hosogane, E. K., Sun, E. G., Tran, A. D., Reinhold, W. C., Burkett, S., et al. (2020). Epigenetic regulation of DNA repair pathway choice by macroH2A1 splice variants ensures genome stability. *Mol. Cell* 79, 836–845.e7. doi:10.1016/j.molcel.2020.06.028

Setiaputra, D., and Durocher, D. (2019). Shieldin - the protector of DNA ends. *EMBO Rep.* 20 (5), e47560. doi:10.15252/embr.201847560

Sevilla, A., and Binda, O. (2014). Post-translational modifications of the histone variant H2AZ. *Stem Cell Res.* 12, 289–295. doi:10.1016/j.scr.2013.11.004

Shibata, A., Barton, O., Noon, A. T., Dahm, K., Deckbar, D., Goodarzi, A. A., et al. (2010). Role of ATM and the damage response mediator proteins 53BP1 and MDC1 in the maintenance of G2/M checkpoint arrest. *Mol. Cell. Biol.* 30, 3371–3383. doi:10.1128/mcb.01644-09

Sigismondo, G., Arseni, L., Palacio-Escat, N., Hofmann, T. G., Seiffert, M., and Krijgsveld, J. (2023). Multi-layered chromatin proteomics identifies cell vulnerabilities in DNA repair. *Nucleic Acids Res.* 51, 687–711. doi:10.1093/nar/gkac1264

Soria, G., Polo, S. E., and Almouzni, G. (2012). Prime, repair, restore: the active role of chromatin in the DNA damage response. *Mol. Cell* 46, 722–734. doi:10.1016/j.molcel.2012.06.002

Stewart, G. S., Panier, S., Townsend, K., Al-Hakim, A. K., Kolas, N. K., Miller, E. S., et al. (2009). The RIDDLE syndrome protein mediates a ubiquitin-dependent signaling cascade at sites of DNA damage. *Cell* 136, 420–434. doi:10.1016/j.cell.2008.12.042

Stewart-Morgan, K. R., Requena, C. E., Flury, V., Du, Q., Heckhausen, Z., Hajkova, P., et al. (2023). Quantifying propagation of DNA methylation and hydroxymethylation with iDEMS. *Nat. Cell Biol.* 25, 183–193. doi:10.1038/s41556-022-01048-x

Strahl, B. D., and Allis, C. D. (2000). The language of covalent histone modifications. *Nature* 403, 41–45. doi:10.1038/47412

Takata, M., Sasaki, M. S., Sonoda, E., Morrison, C., Hashimoto, M., Utsumi, H., et al. (1998). Homologous recombination and non-homologous end-joining pathways of DNA double-strand break repair have overlapping roles in the maintenance of chromosomal integrity in vertebrate cells. *EMBO J.* 17, 5497–5508. doi:10.1093/emboj/17.18.5497

Tamburri, S., Lavarone, E., Fernández-Pérez, D., Conway, E., Zanotti, M., Manganaro, D., et al. (2020). Histone H2AK119 mono-ubiquitination is essential for polycomb-mediated transcriptional repression. *Mol. Cell* 77, 840–856.e5. doi:10.1016/j.molcel.2019.11.021

Tanaka, H., Sato, S., Koyama, M., Kujirai, T., and Kurumizaka, H. (2020). Biochemical and structural analyses of the nucleosome containing human histone H2A.J. *J. Biochem.* 167, 419–427. doi:10.1093/jb/mvz109

Tang, J., Cho, N. W., Cui, G., Manion, E. M., Shanbhag, N. M., Botuyan, M. V., et al. (2013). Acetylation limits 53BP1 association with damaged chromatin to promote homologous recombination. *Nat. Struct. Mol. Biol.* 20, 317–325. doi:10.1038/nsmb.2499

Taty-Taty, G.-C., Courilleau, C., Quaranta, M., Carayon, A., Chailleux, C., Aymard, F., et al. (2014). H2A.Z depletion impairs proliferation and viability but not DNA double-strand breaks repair in human immortalized and tumoral cell lines. *Cell Cycle* 13, 399–407. doi:10.4161/cc.27143

Thorslund, T., Ripplinger, A., Hoffmann, S., Wild, T., Uckelmann, M., Villumsen, B., et al. (2015). Histone H1 couples initiation and amplification of ubiquitin signalling after DNA damage. *Nature* 527, 389–393. doi:10.1038/nature15401

Timinszky, G., Till, S., Hassa, P. O., Hothorn, M., Kustatscher, G., Nijmeijer, B., et al. (2009). A macrodomain-containing histone rearranges chromatin upon sensing PARP1 activation. *Nat. Struct. Mol. Biol.* 16, 923–929. doi:10.1038/nsmb.1664

Uckelmann, M., Densham, R. M., Baas, R., Winterwerp, H. H. K., Fish, A., Sixma, T. K., et al. (2018). USP48 restrains resection by site-specific cleavage of the BRCA1 ubiquitin mark from H2A. *Nat. Commun.* 9, 229. doi:10.1038/s41467-017-02653-3

Unoki, M., Funabiki, H., Velasco, G., Francastel, C., and Sasaki, H. (2018). CDCA7 and HELLS mutations undermine nonhomologous end joining in centromeric instability syndrome. *J. Clin. Investigation* 129, 78–92. doi:10.1172/jci99751

Van, C., Williams, J. S., Kunkel, T. A., and Peterson, C. L. (2015). Deposition of histone H2A.Z by the SWR-C remodeling enzyme prevents genome instability. *DNA Repair (Amst)* 25, 9–14. doi:10.1016/j.dnarep.2014.10.010

Van Attikum, H., Fritsch, O., and Gasser, S. M. (2007). Distinct roles for SWR1 and INO80 chromatin remodeling complexes at chromosomal double-strand breaks. *EMBO J.* 26, 4113–4125. doi:10.1038/sj.emboj.7601835

Van Attikum, H., Fritsch, O., Hohn, B., and Gasser, S. M. (2004). Recruitment of the INO80 complex by H2A phosphorylation links ATP-dependent chromatin remodeling with DNA double-strand break repair. *Cell* 119, 777–788. doi:10.1016/j.cell.2004.11.033

van de Kooij, B., Kruswick, A., van Attikum, H., and Yaffe, M. B. (2022). Multi-pathway DNA-repair reporters reveal competition between end-joining, single-strand annealing and homologous recombination at Cas9-induced DNA double-strand breaks. *Nat. Commun.* 13, 5295. doi:10.1038/s41467-022-32743-w

van der Heijden, T., Modesti, M., Hage, S., Kanaar, R., Wyman, C., and Dekker, C. (2008). Homologous recombination in real time: DNA strand exchange by RecA. *Mol. Cell* 30, 530–538. doi:10.1016/j.molcel.2008.03.010

Wald, J., Fahrenkamp, D., Goessweiner-Mohr, N., Lugmayr, W., Ciccarelli, L., Vesper, O., et al. (2022). Mechanism of AAA+ ATPase-mediated RuvAB–Holliday junction branch migration. *Nature* 609, 630–639. doi:10.1038/s41586-022-05121-1

Walker, J. R., Corpina, R. A., and Goldberg, J. (2001). Structure of the Ku heterodimer bound to DNA and its implications for double-strand break repair. *Nature* 412, 607–614. doi:10.1038/35088000

Wang, X. S., Menolfi, D., Wu-Baer, F., Fangazio, M., Meyer, S. N., Shao, Z., et al. (2021). DNA damage-induced phosphorylation of CtIP at a conserved ATM/ATR site T855 promotes lymphomagenesis in mice. *Proc. Natl. Acad. Sci. U S A* 118, e2105440118. doi:10.1073/pnas.2105440118

Wang, Z., Zhang, H., Liu, J., Cheruiyot, A., Lee, J.-H., Ordog, T., et al. (2016). USP51 deubiquitylates H2AK13,15ub and regulates DNA damage response. *Genes Dev.* 30, 946–959. doi:10.1101/gad.271841.115

Wichmann, J., Pitt, C., Eccles, S., Garnham, A. L., Li-Wai-Suen, C. S. N., May, R., et al. (2022). Loss of TIP60 (KAT5) abolishes H2AZ lysine 7 acetylation and causes p53, INK4A, and ARF-independent cell cycle arrest. *Cell Death Dis.* 13, 627. doi:10.1038/s41419-022-05055-6

Witus, S. R., Zhao, W., Brzovic, P. S., and Klevit, R. E. (2022). BRCA1/BARD1 is a nucleosome reader and writer. *Trends Biochem. Sci.* 47, 582–595. doi:10.1016/j.tibs.2022.03.001

Wu, C.-Y., Kang, H.-Y., Yang, W.-L., Wu, J., Jeong, Y. S., Wang, J., et al. (2011). Critical role of monoubiquitination of histone H2AX protein in histone H2AX phosphorylation and DNA damage response. *J. Biol. Chem.* 286, 30806–30815. doi:10.1074/jbc.m111.257469

Xie, A., Odate, S., Chandramouly, G., and Scully, R. A. (2010). H2AX post-translational modifications in the ionizing radiation response and homologous recombination. *Cell Cycle* 9, 3602–3610. doi:10.4161/cc.9.17.12884

Xu, C., Xu, Y., Gursoy-Yuzugullu, O., and Price, B. D. (2012a). The histone variant macroH2A1.1 is recruited to DSBs through a mechanism involving PARP1. *FEBS Lett.* 586, 3920–3925. doi:10.1016/j.febslet.2012.09.030

Xu, X., Ni, K., He, Y., Ren, J., Sun, C., Liu, Y., et al. (2021). The epigenetic regulator LSH maintains fork protection and genomic stability via MacroH2A deposition and RAD51 filament formation. *Nat. Commun.* 12, 3520. doi:10.1038/s41467-021-23809-2

Xu, Y., Ayrapetov, M. K., Xu, C., Gursoy-Yuzugullu, O., Hu, Y., and Price, B. D. (2012b). Histone H2A.Z controls a critical chromatin remodeling step required for DNA double-strand break repair. *Mol. Cell* 48, 723–733. doi:10.1016/j.molcel.2012.09.026

Xu, Y., Sun, Y., Jiang, X., Ayrapetov, M. K., Moskwa, P., Yang, S., et al. (2010). The p400 ATPase regulates nucleosome stability and chromatin ubiquitination during DNA repair. *J. Cell Biol.* 191, 31–43. doi:10.1083/jcb.201001160

Yu, X., Fu, S., Lai, M., Baer, R., and Chen, J. (2006). BRCA1 ubiquitinates its phosphorylation-dependent binding partner CtIP. *Genes Dev.* 20, 1721–1726. doi:10.1101/gad.1431006

Zhang, H., Roberts, D. N., and Cairns, B. R. (2005). Genome-Wide dynamics of Htz1, a histone H2A variant that poises repressed/basal promoters for activation through histone loss. *Cell* 123, 219–231. doi:10.1016/j.cell.2005.08.036

Zhang, Z., Zhu, L., Lin, D., Chen, F., Chen, D. J., and Chen, Y. (2001). The three-dimensional structure of the C-terminal DNA-binding domain of human Ku70. *J. Biol. Chem.* 276, 38231–38236. doi:10.1074/jbc.m105238200

Zlatanova, J., and Thakar, A. (2008). H2A.Z: view from the top. *Structure* 16, 166–179. doi:10.1016/j.str.2007.12.008

frontiers | Frontiers in Epigenetics and Epigenomics

TYPE Brief Research Report
PUBLISHED 04 September 2024
DOI 10.3389/freae.2024.1427399



OPEN ACCESS

EDITED BY
Raul Mostoslavsky,
Massachusetts General Hospital Cancer Center, United States

REVIEWED BY
Yiannis Drosos,
University of Patras, Greece
Alexandre Gaspar Maia,
Mayo Clinic, United States

*CORRESPONDENCE
Sara Patrizi,
sara.patrizi@opbg.net
Evelina Miele,
evelina.miele@opbg.net

†These authors have contributed equally to this work and share last authorship

RECEIVED 03 May 2024
ACCEPTED 13 August 2024
PUBLISHED 04 September 2024

CITATION
Patrizi S, Vallese S, Pedace L, Nardini C, Stracuzzi A, Barresi S, Giovannoni I, Abballe L, Antonacci C, Russo I, Di Giannatale A, Alaggio R, Locatelli F, Milano GM and Miele E (2024) Quantification of tumour-infiltrating immune cells through deconvolution of DNA methylation data in Ewing sarcomas. *Front. Epigenet. Epigenom.* 2:1427399. doi: 10.3389/freae.2024.1427399



# Quantification of tumour-infiltrating immune cells through deconvolution of DNA methylation data in Ewing sarcomas

Sara Patrizi[1]*, Silvia Vallese[2], Lucia Pedace[1], Claudia Nardini[1], Alessandra Stracuzzi[2], Sabina Barresi[2], Isabella Giovannoni[2], Luana Abballe[1], Celeste Antonacci[1], Ida Russo[1], Angela Di Giannatale[1], Rita Alaggio[2], Franco Locatelli[1†], Giuseppe Maria Milano[1†] and Evelina Miele[1*†]

[1]Onco-Hematology, Cell Therapy, Gene Therapies and Hemopoietic Transplant, Bambino Gesù Children's Hospital, IRCCS, Rome, Italy, [2]Pathology Unit, Bambino Gesù Children's Hospital, IRCCS, Rome, Italy

Ewing Sarcomas (EWS, OMIM#612219) presents a major challenge in pediatric oncology due to its aggressive nature and poor prognosis, particularly in metastatic cases. Genetic fusions involving the *EWSR1* gene and ETS family transcription factors are common in EWS, though other rarer fusions have also been identified. Current standard techniques like immunohistochemistry have failed to fully characterize the immune tumor microenvironment of EWS, hindering insights into tumor development and treatment strategies. Recent efforts apply gene expression datasets to quantify tumor-infiltrating immune cells in EWS. Similar deconvolution techniques can be also applied to DNA methylation (DNAm) arrays, which are much more stable compared to RNA-based methods. This study aims to characterize immune cell infiltration in EWS using DNAm array data. We collected 32 EWS samples from 32 consecutive patients referred to Bambino Gesù Children's Hospital. DNAm analysis was performed by EPIC arrays; data loading, normalization, deconvolution and survival analysis were then performed in R programming environment. We observed a higher content of dendritic cells and longer overall survival in samples with *EWSR1::FLI1* translocation compared to samples with rarer fusions. Moreover, T-memory lymphocytes and monocytes emerged as a significant predictor of overall survival. This study underscores the potential of DNAm arrays in providing robust insights into EWS immune profiles, offering a promising avenue for future research. Further investigations with larger cohorts are warranted to validate these findings and explore additional immune cell types influencing EWS outcomes.

KEYWORDS

**Ewing sarcoma, DNA methylation, immune microenvironment, deconvolution, immunotherapy**

# 1 Introduction

Ewing sarcomas (EWS) most often affect the bones and soft tissues in children and young adults and are known for their aggressive nature and their dismal prognosis when diagnosed in the metastatic stage. From a histological perspective, these tumors fall within the category of "undifferentiated small round blue cell sarcomas of bone and soft tissue (WHO 2020 and WHO 2022)." They consist of small, monotonous round cells exhibiting nuclei with finely dispersed chromatin and thin rim of cytoplasm. The cells are arranged in sheets with occasional rosette formation and frequent necrotic areas (Yoshida, 2023; Sbaraglia et al., 2021; Pfister et al., 2022). The differential diagnosis from other Ewing-like sarcomas (ELS), requires molecular characterization (Llombart-Bosch et al., 2009; Italiano et al., 2012; Antonescu, 2014). EWS are characterized by genetic fusions involving an *EWS* gene and an ETS family transcription factor (Delattre et al., 1992). The most frequent fusion involves *EWSR1* (OMIM*133450) and *FLI1* (OMIM*193067), but other rarer rearrangements with the same biological behavior have also been identified (Sorensen and Triche, 1996; Arvand and Denny, 2001).

So far, standard techniques like immunohistochemistry have been unsuccessful in providing a complete characterization of the immune tumour microenvironment of EWS (Paydas et al., 2016; Berghuis et al., 2011). Some efforts have been made using single-cell RNA sequencing (Visser et al., 2023; Cillo et al., 2022), a technique that still presents several challenges and limitations (Robinson et al., 2022). An accurate quantification of tumour-infiltrating immune cells (TIICs), however, would be valuable to shed light on the development and aggressiveness of these tumours and provide new avenues for treatment (Evdokimova et al., 2022).

Recently, Stahl et al. analysed microarray gene expression datasets of primary EWS samples using the CIBERSORT deconvolution algorithm to determine the proportion of 22 immune cell types within bulk tumour tissue (Stahl et al., 2019).

Such deconvolution can be also inferred from DNA methylation (DNAm) arrays, which are more robust than gene expression arrays given the higher stability of DNA compared with RNA (Alberts et al., 2002). Moreover, DNAm data is known to be less influenced by copy number variation than gene expression (Stranger et al., 2007; Houseman et al., 2009), a relevant concern in the field of oncology where most samples display copy number variations. Lastly, DNAm arrays are currently widely used to aid soft tissue sarcoma diagnosis through machine-learning based classifiers (Koelsche et al., 2021), while RNA sequencing currently lacks diagnostic applications. Thus, performing both diagnostic profiling and tumor microenvironment characterization on the same data appears convenient.

The aim of this study is to characterize the relative abundance of immune cells infiltrated in EWS using DNAm array, a technique that is already implemented in the diagnostic workflow of challenging sarcoma cases at our Institution, and to correlate it with patients' survival.

# 2 Methods

We selected 32 EWS samples from 32 patients with challenging diagnosis referred to our institution and analysed for DNAm profiling (from 2020 to 2024) and, after acquiring informed consent from either the patient or their legal guardian, retrieved their follow-up information from clinical records (study protocol number 2126_OPBG_2020, reviewed and approved by the Bambino Gesù Children's Hospital Ethical Committee). We reviewed 30/32 cases with available tissue, evaluating parameters that could affect the tumor purity. In detail, we quantified the percentage of inflammatory cells, by CD45 antibody staining (mouse monoclonal antibody, clone 2B11+PD7/26, ready to use, Dako) performed on DAKO OMNIS platform scoring it 0 (<1%), 1 (1–2%), 2 (3–5%), or 3 (>5%); the presence (Yoshida, 2023) or absence (0) of necrosis and collagenized stroma. We calculated a final "total infiltration score" from the sum of the previously described parameters and correlated it with the tumor purity calculated from DNAm deconvolution data.

We extracted both RNA (by ReliaPrep™ FFPE Total RNA kit, Promega) and DNA (by MagPurix FFPE DNA Extraction Kit, Zzinexts, Life Science Corporation, New Taipei City, Taiwan) from unstained sections of paraffin blocks containing at least 70% tumour cells.

We used either whole-transcriptome RNA sequencing (in 3/32 cases), RT-PCR or Archer FusionPlex custom panel to detect the presence of gene fusions, as described previously (Patrizi et al., 2024).

We carried out DNA methylation (DNAm) analysis using the Human MethylationEPIC v1.0 and v2.0 BeadChip arrays (Illumina), according to the manufacturer's instructions, as previously reported (Salgado et al., 2023).

We analyzed raw BeadChip data with R package ChAMP (version 2.26.0) (Tian et al., 2017), that was chosen because it conveniently integrates existing analysis tools into a single pipeline. We loaded v1.0 and v2.0 data separately with method "minfi" (Aryee et al., 2014) and filtering out probes with detection $p$-value > 0.01. Then, we merged v1.0 and v2.0 raw beta values according to probe name and genomic position. We normalized the merged raw methylation beta values using the BMIQ method (Teschendorff et al., 2013), confirmed the absence of confounding batch factors with function champ. SVD, and performed immune cell deconvolution through package MethylResolver (Arneson et al., 2020). This deconvolution method can resolve fractions of 11 immune cell types, both in terms of relative abundance to the total amount of immune cells and of absolute abundance scaled according to tumor purity (the percentage of tumor cells in the total tissue), without the need to develop a cancer-specific signature.

We used two-tailed heteroschedastic Student's T-test to evaluate the statistical significance of differences in immune cell content between sample groups, and Kaplan-Meier analysis performed with R package survival (https://CRAN.R-project.org/package=survival) to assess the relationship between immune cell content and overall survival. For Kaplan-Meier analysis, we determined the optimal cutpoint for each continuous variable using function surv_cutpoint from package survminer (https://CRAN.R-project.org/package=survminer), that uses the maximally selected rank statistics from the maxstat R package to divide a continuous variable in order to obtain the most significant correlation with survival.

# 3 Results

The study cohort includes 32 tumors with histological diagnosis of Ewing sarcoma from 32 consecutive patients less than 30 years old

10.3389/freae.2024.1427399

TABLE 1 Characteristics of the selected EWS samples, including gender, age at diagnosis, status at last follow up (DOD = Dead of Disease, NA = Not Available), translocation, and translocation type.

| Case # | Gender (M/F) | Age at diagnosis (years) | Status at last follow up | Overall survival (years) | Translocation |
|---|---|---|---|---|---|
| 1 | M | 5 | NA | NA | EWSR1::ETV4 |
| 2 | F | | NA | NA | EWSR1::FLI1 |
| 3 | F | 14 | DOD | 1.58 | EWSR1::FLI1 |
| 4 | M | 16 | ALIVE | 4.17 | EWSR1::FLI1 |
| 5 | M | 12 | ALIVE | 1.42 | EWSR1::FLI1 |
| 6 | F | 5 | ALIVE | 4.25 | EWSR1::FLI1 |
| 7 | M | 11 | DOD | 3.75 | EWSR1::FLI1 |
| 8 | F | 12 | DOD | 2.08 | EWSR1::FLI1 |
| 9 | F | 17 | ALIVE | 4.92 | EWSR1::FLI1 |
| 10 | F | 9 | NA | NA | EWSR1::FLI1 |
| 11 | F | 34 | NA | NA | EWSR1::FLI1 |
| 12 | M | 10 | DOD | 0.08 | EWSR1::FLI1 |
| 13 | M | 6 | DOD | 1.08 | EWSR1::ERG |
| 14 | F | 18 | DOD | 0.58 | EWSR1::FLI1 |
| 15 | M | 11 | NA | NA | EWSR1::FLI1 |
| 16 | F | 4 | NA | NA | EWSR1::FLI1 |
| 17 | F | 9 | NA | NA | EWSR1::FLI1 |
| 18 | F | 27 | NA | NA | EWSR1::FLI1 |
| 19 | F | 10 | DOD | 0.58 | EWSR1::ERG |
| 20 | F | 13 | ALIVE | 1.25 | EWSR1::FLI1 |
| 21 | F | 16 | ALIVE | 1.17 | EWSR1::FLI1 |
| 22 | F | 10 | ALIVE | 1.08 | EWSR1::FLI1 |
| 23 | M | 1 | ALIVE | 0.83 | EWSR1::FLI1 |
| 24 | M | 2 | ALIVE | 0.83 | EWSR1::ETV4 |
| 25 | M | 6 | ALIVE | 0.67 | EWSR1::FLI1 |
| 26 | M | 9 | ALIVE | 0.92 | EWSR1::FLI1 |
| 27 | M | 7 | ALIVE | 0.67 | EWSR1::FLI1 |
| 28 | M | 11 | DOD | 2.58 | EWSR1::FLI1 |
| 29 | M | 16 | ALIVE | 0.42 | EWSR1::FLI1 |
| 30 | F | 13 | ALIVE | 0.25 | EWSR1::FLI1 |
| 31 | M | 15 | ALIVE | 0.50 | EWSR1::FLI1 |
| 32 | F | 5 | ALIVE | 4.83 | EWSR1::FLI1 |

at the time of diagnosis. Patients' characteristics are summarized in Table 1. The cohort included 17 females (53%) and 15 males (47%). The median age was 11 years old. Most samples (28/32) had the *EWSR1::FLI1* fusion, while 4 had other translocations involving *EWSR1* (2 *EWSR1::ERG*, 2 *EWSR1::ETV4*). In 30/32 cases the tissue was obtained at the moment of diagnosis of the primary tumor. One case was a very late relapse, while for 1 this information was not available (Supplementary Table S1). The level of immune infiltration observable through histological review was generally extremely low and did not allow the quantification of specific cell types (Supplementary Table S1; Supplementary Figure S1). We also evaluated further histological aspects that could influence tumor purity, observing necrosis/haemorragy in 15/30 and fibrosis in 13/30 cases. However, we observed no correlation between the total infiltration score and DNAm-inferred tumor purity (correlation score 0.26).

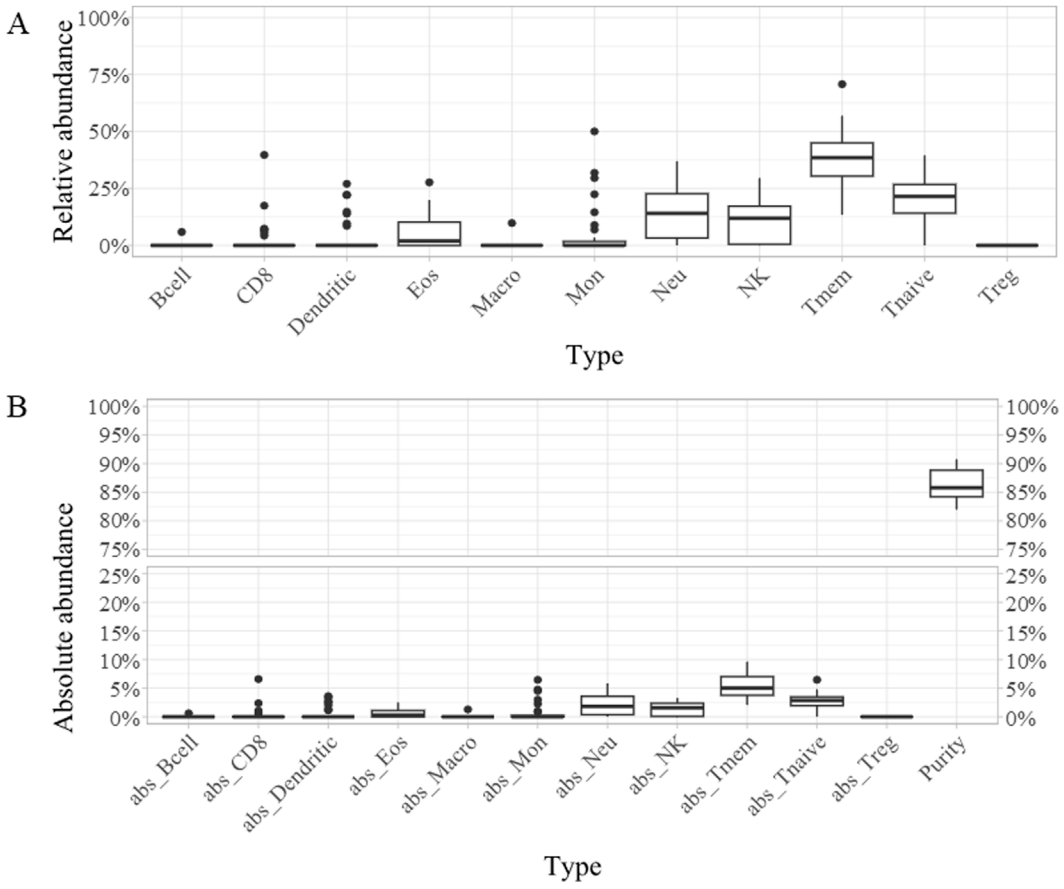


FIGURE 1
Boxplots representing the relative **(A)** and absolute ["abs," **(B)**] abundance of each of the 11 cell types detected across the whole cohort: B cells (Bcell), CD8 lymphocytes (CD8), dendritic cells (Dendritic), eosinophiles (Eos), macrophages (Macro), monocytes (Mon), neutrophils (Neu), natural killer cells (NK), T-memory lymphcytes (Tmem), T-naive lymphocytes (Tnaive), T-regulatory lymphocytes (Treg), tumor purity (Purity).

The immune cell deconvolution returned the abundance of 11 cell types, both relatively to the total amount of immune cells (relative abundance) and to the total tissue (absolute abundance).

Across the whole cohort, the most abundant cell types were T-memory lymphocytes ("Tmem," mean percentage 37.49%), T-naïve lymphocytes (mean percentage 20.56%), neutrophils (mean percentage 14.10%), and natural killer (NK) cells (mean percentage 10.44%) (Figures 1A, B; Supplementary Table S1). When compared to *EWSR::FLI1* rearranged, samples with rarer translocations displayed a significantly lower mean content of dendritic cells, both absolute (0% versus 0.61%) and relative to the immune component (0% versus 4.37%) (Figures 2A, B; Supplementary Table S1).

Follow-up was available for 24/32 patients (Table 1). Samples with *EWSR1::FLI1* translocation showed a significantly longer overall survival than samples with rarer alterations (Supplementary Table S1). Moreover, Kaplan-Meier analysis revealed two variables significantly associated with overall survival in the whole cohort. One was the absolute content of T-memory lymphocytes, that correlated with better outcomes (Bonferroni $p$-value = 0.04) when it was higher than 2.05% (Figure 3A), and the other was the absolute content of monocytes, that was associated with higher overall survival when lower than 0.82% (Figure 3B; Supplementary Table S2). Moreover, patients with tumor purity lower than 83.73% had a higher survival probability, although not significantly (Bonferroni $p$-value = 0.11) (Supplementary Table S2).

## 4 Discussion

Our cohort included 32 patients with a median age of 11 years at diagnosis, which reflects the age of peak incidence of Ewing sarcoma. However, we did not observe the same male prevalence that is reported in literature (Durer et al., 2024). The immune cell deconvolution showed that the most abundant cell types across the cohort were lymphocytes, representing 60.63% of all TIICs considering Tmem, T-naïve and CD8 lymphocytes (2.54%), followed by neutrophils (mean percentage 14.10%). This result differs from the prevalence of macrophages detected from RNA sequencing data by Stahl et al. Lymphocyte prevalence has been reported as a characteristic of tumours with "hot" immune microenvironment (Wang et al., 2023), whereas Ewing sarcoma is known as a "cold" tumour, with low expression of neoantigens and low leucocyte infiltration (Evdokimova et al., 2022). The low and

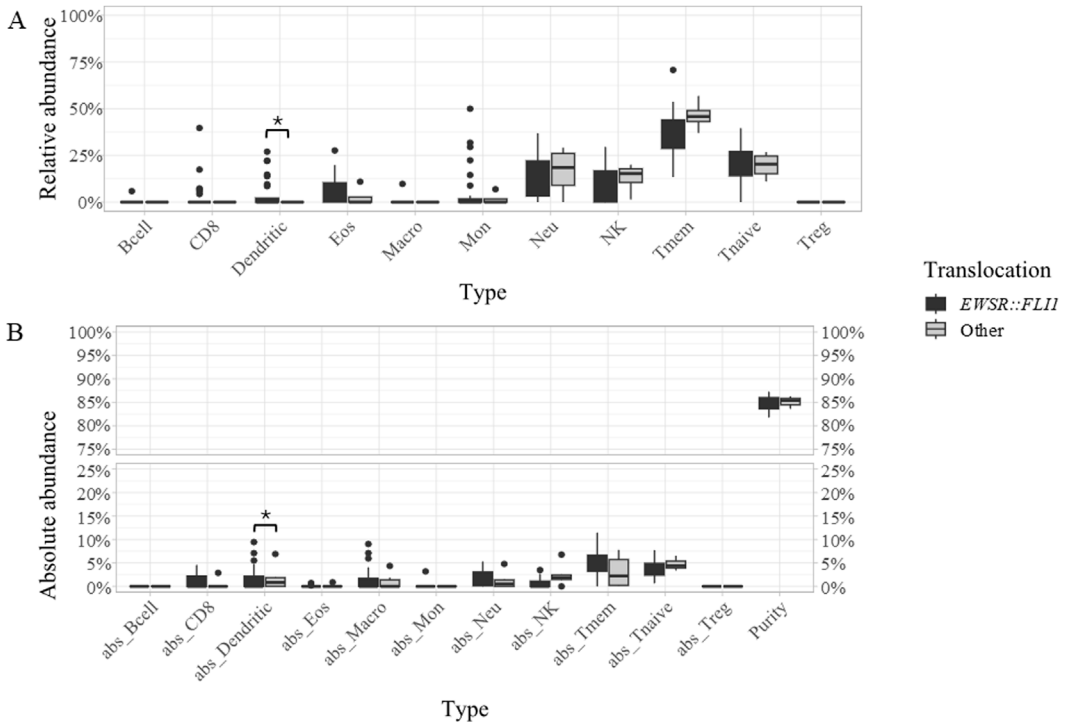


FIGURE 2
Boxplots representing the relative **(A)** and absolute ["abs," **(B)**] abundance of each of the 11 cell types detected in samples with EWSR::FLI1 translocation (dark grey) or other rearrangements (light grey). The immune cell types include B cells (Bcell), CD8 lymphocytes (CD8), dendritic cells (Dendritic), eosinophiles (Eos), macrophages (Macro), monocytes (Mon), neutrophils (Neu), natural killer cells (NK), T-memory lymphcytes (Tmem), T-naive lymphocytes (Tnaive), T-regulatory lymphocytes (Treg), tumor purity (Purity). Statistically significant differences between patient groups are labeled by an asterisk.

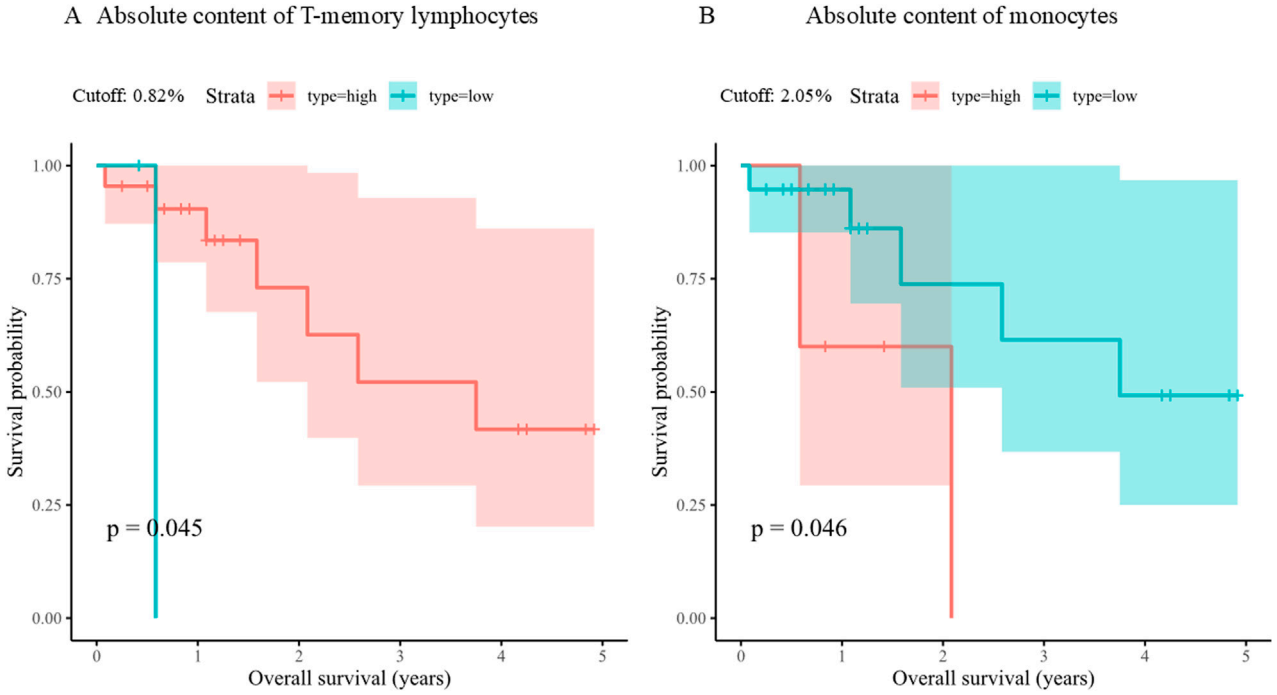


FIGURE 3
Kaplan-Meier plots of overall survival based on absolute content of T-memory lymphocytes **(A)** and monocytes **(B)**. For each continuous variable, the cohort was divided in two groups (Strata) according to its value (high or low) relatively to its optimal cutpoint (Cutoff).

homogenous absolute immune cell content measured for each sample in our cohort supports the latter concept.

In our cohort, samples with *EWSR1::FLI1* translocation presented significantly longer overall survival and higher dendritic cells content (both relative and absolute) than the cases with different translocations. Since dendritic cells are known to play an important role in presenting tumour antigens to the immune system, and are often downregulated in metastatic and aggressive cancers (Del Prete et al., 2023), these two observations could be correlated. However, functional studies on a larger cohort would be needed to reach a definite conclusion.

We also found a significant correlation of longer overall survival with higher relative Tmem content, which supports previous reports of their important anti-tumor role (Liu et al., 2020). In some contexts, however, the presence of tissue-resident memory T cells has been related to a stronger recruitment of other immune cells, causing a loss of MHC class I protein expression on tumour cells and thus favoring their escape from immune response (Weeden et al., 2023). Therefore, the role of Tmem in the immune microenvironment of EWS appears intriguing and worthy of further investigations. Patients with lower tumor purity (and in consequence with higher immune infiltrate) also had better outcomes, albeit not significantly, which leads us to hypothesize that, even in a cold tumor microenvironment, an immune response can limit the cancerous cell proliferation.

Our study shows that TIICs proportions in EWS can be inferred from DNA methylation data, thus providing an alternative to traditional techniques or gene expression arrays. A weakness of our study is the lack of correlation between DNAm-inferred tumor purity and our total infiltration score derived from histopathological evaluation. We can speculate that this could be due to the selection of a different histological section for DNA methylation and histological review, or to method-specific biases. Further specific studies on larger sample groups are needed, to better assess the correlation between deconvolution results from different data sources and histopathology, and to confirm the cell types we identified as directly or inversely correlated with survival.

## Data availability statement

The data presented in the study are deposited in the NCBI GEO repository, accession number GSE276012.

## Ethics statement

The studies involving humans were approved by Comitato Etico Ospedale Pediatrico Bambino Gesù. The studies were conducted in accordance with the local legislation and institutional requirements. Written informed consent for participation in this study was provided by the participants' legal guardians/next of kin.

## Author contributions

SP: Conceptualization, Writing–original draft, Writing–review and editing, Formal Analysis, Visualization. SV: Data curation, Resources, Writing–review and editing. LP: Investigation, Writing–review and editing. CN: Investigation, Writing–review and editing. AS: Resources, Data curation, Writing–review and editing. SB: Investigation, Writing–review and editing. IG: Investigation, Writing–review and editing. LA: Investigation, Writing–review and editing. CA: Investigation, Writing–review and editing. IR: Data curation, Resources, Writing–review and editing. AD: Data curation, Resources, Writing–review and editing. RA: Supervision, Writing–review and editing. FL: Supervision, Writing–review and editing. GM: Conceptualization, Data curation, Funding acquisition, Resources, Supervision, Writing–original draft, Writing–review and editing. EM: Conceptualization, Data curation, Funding acquisition, Resources, Supervision, Writing–original draft, Writing–review and editing.

## Funding

The author(s) declare that financial support was received for the research, authorship, and/or publication of this article. This research was supported by the Italian Ministry of Health with "Current Research funds" (202005_ONCO_MIELE to EM; and 202203_FBG_MILANO.1.15 to GM).

## Acknowledgments

The authors thank Associazione il Cuore grande di Flavio for their support. SP and LA were supported by Fondazione Umberto Veronesi.

## Conflict of interest

The authors declare that the research was conducted in the absence of any commercial or financial relationships that could be construed as a potential conflict of interest.

The author(s) declared that they were an editorial board member of Frontiers, at the time of submission. This had no impact on the peer review process and the final decision.

## Publisher's note



## Supplementary material

The Supplementary Material for this article can be found online at: https://www.frontiersin.org/articles/10.3389/freae.2024.1427399/full#supplementary-material

# References


Alberts, B., Bray, D., Lewis, J., Raff, M., and Roberts, K. (2002). *The molecular biology of the cell*. New York: Garland Science.

Antonescu, C. (2014). Round cell sarcomas beyond Ewing: emerging entities. *Histopathology* 64 (1), 26–37. doi:10.1111/his.12281

Arneson, D., Yang, X., and Wang, K. (2020). MethylResolver—a method for deconvoluting bulk DNA methylation profiles into known and unknown cell contents. *Commun. Biol.* 3 (1), 422–513. doi:10.1038/s42003-020-01146-2

Arvand, A., and Denny, C. T. (2001). Biology of EWS/ETS fusions in Ewing's family tumors. *Oncogene* 20 (40), 5747–5754. doi:10.1038/sj.onc.1204598

Aryee, M. J., Jaffe, A. E., Corrada-Bravo, H., Ladd-Acosta, C., Feinberg, A. P., Hansen, K. D., et al. (2014). Minfi: a flexible and comprehensive Bioconductor package for the analysis of Infinium DNA methylation microarrays. *Bioinformatics* 30 (10), 1363–1369. doi:10.1093/bioinformatics/btu049

Berghuis, D., Santos, S. J., Baelde, H. J., Taminiau, A. H., Maarten Egeler, R., Schilham, M. W., et al. (2011). Pro-inflammatory chemokine-chemokine receptor interactions within the Ewing sarcoma microenvironment determine CD8(+) T-lymphocyte infiltration and affect tumour progression. *J. Pathology* 223 (3), 347–357. doi:10.1002/path.2819

Cillo, A. R., Mukherjee, E., Bailey, N. G., Onkar, S., Daley, J., Salgado, C., et al. (2022). Ewing sarcoma and osteosarcoma have distinct immune signatures and intercellular communication networks. *Clin. Cancer Res.* 28 (22), 4968–4982. doi:10.1158/1078-0432.ccr-22-1471

Delattre, O., Zucman, J., Plougastel, B., Desmaze, C., Melot, T., Peter, M., et al. (1992). Gene fusion with an ETS DNA-binding domain caused by chromosome translocation in human tumours. *Nature* 359 (6391), 162–165. doi:10.1038/359162a0

Del Prete, A., Salvi, V., Soriani, A., Laffranchi, M., Sozio, F., Bosisio, D., et al. (2023). Dendritic cell subsets in cancer immunity and tumor antigen sensing. *Cell Mol. Immunol.* 20 (5), 432–447. doi:10.1038/s41423-023-00990-6

Durer, S., Gasalberti, D. P., and Shaikh, H. (2024). "Ewing sarcoma," in *StatPearls* (Treasure Island (FL): StatPearls Publishing). Available at: http://www.ncbi.nlm.nih.gov/books/NBK559183/.

Evdokimova, V., Gassmann, H., Radvanyi, L., and Burdach, S. E. G. (2022). Current state of immunotherapy and mechanisms of immune evasion in ewing sarcoma and osteosarcoma. *Cancers* 15 (1), 272. doi:10.3390/cancers15010272

Houseman, E. A., Christensen, B. C., Karagas, M. R., Wrensch, M. R., Nelson, H. H., Wiemels, J. L., et al. (2009). Copy number variation has little impact on bead-array-based measures of DNA methylation. *Bioinformatics* 25 (16), 1999–2005. doi:10.1093/bioinformatics/btp364

Italiano, A., Sung, Y. S., Zhang, L., Singer, S., Maki, R. G., Coindre, J. M., et al. (2012). High prevalence of CIC fusion with double-homeobox (DUX4) transcription factors in EWSR1-negative undifferentiated small blue round cell sarcomas. *Genes, Chromosomes Cancer* 51 (3), 207–218. doi:10.1002/gcc.20945

Koelsche, C., Schrimpf, D., Stichel, D., Sill, M., Sahm, F., Reuss, D. E., et al. (2021). Sarcoma classification by DNA methylation profiling. *Nat. Commun.* 12, 498. doi:10.1038/s41467-020-20603-4

Liu, Q., Sun, Z., and Chen, L. (2020). Memory T cells: strategies for optimizing tumor immunotherapy. *Protein Cell* 11 (8), 549–564. doi:10.1007/s13238-020-00707-9

Llombart-Bosch, A., Machado, I., Navarro, S., Bertoni, F., Bacchini, P., Alberghini, M., et al. (2009). Histological heterogeneity of Ewing's sarcoma/PNET: an immunohistochemical analysis of 415 genetically confirmed cases with clinical support. *Virchows Arch.* 455 (5), 397–411. doi:10.1007/s00428-009-0842-7

Patrizi, S., Miele, E., Falcone, L., Vallese, S., Rossi, S., Barresi, S., et al. (2024). Malignant peripheral nerve sheath tumor (MPNST) and MPNST-like entities are defined by a specific DNA methylation profile in pediatric and juvenile population. *Clin. Epigenetics* 16, 9. doi:10.1186/s13148-023-01621-7

Paydas, S., Bagir, E. K., Deveci, M. A., and Gonlusen, G. (2016). Clinical and prognostic significance of PD-1 and PD-L1 expression in sarcomas. *Med. Oncol.* 33 (8), 93. doi:10.1007/s12032-016-0807-z

Pfister, S. M., Reyes-Múgica, M., Chan, J. K. C., Hasle, H., Lazar, A. J., Rossi, S., et al. (2022). A summary of the inaugural WHO classification of pediatric tumors: transitioning from the optical into the molecular era. *Cancer Discov.* 12 (2), 331–355. doi:10.1158/2159-8290.cd-21-1094

Robinson, E. L., Baker, A. H., Brittan, M., McCracken, I., Condorelli, G., Emanueli, C., et al. (2022). Dissecting the transcriptome in cardiovascular disease. *Cardiovasc. Res.* 118 (4), 1004–1019. doi:10.1093/cvr/cvab117

Salgado, C. M., Alaggio, R., Ciolfi, A., Zin, A., Diomedi Camassei, F., Pedace, L., et al. (2023). Pediatric BCOR-altered tumors from soft tissue/kidney display specific DNA methylation profiles. *Mod. Pathol.* 36 (2), 100039. doi:10.1016/j.modpat.2022.100039

Sbaraglia, M., Bellan, E., and Tos, A. P. D. (2021). The 2020 WHO classification of soft tissue tumours: news and perspectives. *Pathol. - J. Ital. Soc. Anat. Pathol. Diagn Cytopathol.* 113, 70–84. doi:10.32074/1591-951X-213

Sorensen, P. H., and Triche, T. J. (1996). Gene fusions encoding chimaeric transcription factors in solid tumours. *Semin. Cancer Biol.* 7 (1), 3–14. doi:10.1006/scbi.1996.0002

Stahl, D., Gentles, A. J., Thiele, R., and Gütgemann, I. (2019). Prognostic profiling of the immune cell microenvironment in Ewing´s Sarcoma Family of Tumors. *Oncoimmunology* 8 (12), e1674113. doi:10.1080/2162402x.2019.1674113

Stranger, B. E., Forrest, M. S., Dunning, M., Ingle, C. E., Beazley, C., Thorne, N., et al. (2007). Relative impact of nucleotide and copy number variation on gene expression phenotypes. *Science* 315 (5813), 848–853. doi:10.1126/science.1136678

Teschendorff, A. E., Marabita, F., Lechner, M., Bartlett, T., Tegner, J., Gomez-Cabrero, D., et al. (2013). A beta-mixture quantile normalization method for correcting probe design bias in Illumina Infinium 450 k DNA methylation data. *Bioinformatics* 29 (2), 189–196. doi:10.1093/bioinformatics/bts680

Tian, Y., Morris, T. J., Webster, A. P., Yang, Z., Beck, S., Feber, A., et al. (2017). ChAMP: updated methylation analysis pipeline for Illumina BeadChips. *Bioinformatics* 33 (24), 3982–3984. doi:10.1093/bioinformatics/btx513

Visser, L. L., Bleijs, M., Margaritis, T., van de Wetering, M., Holstege, F. C. P., and Clevers, H. (2023). Ewing sarcoma single-cell transcriptome analysis reveals functionally impaired antigen-presenting cells. *Cancer Res. Commun.* 3 (10), 2158–2169. doi:10.1158/2767-9764.crc-23-0027

Wang, L., Geng, H., Liu, Y., Liu, L., Chen, Y., Wu, F., et al. (2023). Hot and cold tumors: immunological features and the therapeutic strategies. *MedComm* 4 (5), e343. doi:10.1002/mco2.343

Weeden, C. E., Gayevskiy, V., Marceaux, C., Batey, D., Tan, T., Yokote, K., et al. (2023). Early immune pressure initiated by tissue-resident memory T cells sculpts tumor evolution in non-small cell lung cancer. *Cancer Cell* 41 (5), 837–852.e6. doi:10.1016/j.ccell.2023.03.019

Yoshida, A. (2023). Ewing and Ewing-like sarcomas: a morphological guide through genetically-defined entities. *Pathol. Int.* 73 (1), 12–26. doi:10.1111/pin.13293

frontiers | Frontiers in Epigenetics and Epigenomics

TYPE Original Research
PUBLISHED 02 October 2024
DOI 10.3389/freae.2024.1435634



OPEN ACCESS

EDITED BY
Ting Wang,
Washington University in St. Louis, United States

REVIEWED BY
Hana Hall,
Purdue University, United States
Mushan Li,
The Pennsylvania State University (PSU), United States

*CORRESPONDENCE
Richard S. Lee,
rlee8@jh.edu

RECEIVED 20 May 2024
ACCEPTED 23 August 2024
PUBLISHED 02 October 2024

CITATION
Lee RS, Santos A, Garrison-Desany H, Aulinas A, Carey JL, Vives-Gilabert Y, Cox OH, Cuilan G, Webb SM and Resmini E (2024) Blood DNA methylation of *CRF* and its association with amygdala volume and mood in Cushing's syndrome.
*Front. Epigenet. Epigenom.* 2:1435634.
doi: 10.3389/freae.2024.1435634



# Blood DNA methylation of *CRF* and its association with amygdala volume and mood in Cushing's syndrome

Richard S. Lee[1]*, Alicia Santos[2,3], Henri Garrison-Desany[4], Anna Aulinas[2,5], Jenny L. Carey[1], Yolanda Vives-Gilabert[2,6], Olivia H. Cox[1], Gabriel Cuilan[1], Susan M. Webb[2,3] and Eugenia Resmini [2]

[1]Department of Psychiatry, Johns Hopkins University School of Medicine, Baltimore, MD, United States, [2]Department of Endocrinology, Hospital de la Santa Creu I Sant Pau, Research Center for Pituitary Diseases, Institut de Recerca Sant Pau (IR-Sant Pau), EndoERN, CIBERER Unit 747, ISCIII, Barcelona, Spain, [3]Department of Medicine, Universitat Autonoma de Barcelona, Barcelona, Spain, [4]Department of Mental Health, Johns Hopkins Bloomberg School of Public Health, Baltimore, MD, United States, [5]Department of Medicine, Universitat de Vic-Universitat Central de Catalunya, Vic, Spain, [6]Intelligent data analysis laboratory (IDAL), Electronic Engineering Department, Escuela técnica superior de ingeniería (ETSE), Universidad de Valencia (UV), Valencia, Spain

**Objective:** The impact of chronic exposure to stress or glucocorticoids on psychiatric symptoms has been exemplified by cases of iatrogenic or endogenous hypercortisolism such as Cushing's syndrome (CS). The amygdala plays an important role in mediating both stress and affective responses, and one of the key factors that link stress response and psychiatric symptoms is the corticotropin-releasing factor (CRF). Epigenetic changes, especially those occurring on CpG dinucleotides in DNA of glucocorticoid target genes in blood, have been previously implicated as potential predictors of glucocorticoid-related events in the central nervous system (CNS). In this study, we examined amygdala volume and mood symptoms in CS patients and aimed at evaluating whether these parameters were associated with blood DNA methylation of *CRF*.

**Methods:** In this cross-sectional study, 32 CS patients and 32 healthy controls matched for age, sex, and years of education underwent an MRI scan, a Beck Depression Inventory-II, and a State-Trait Anxiety Inventory. Genomic DNA extracted from total leukocytes were used for DNA methylation analysis of several CpG dinucleotides at the *CRF* promoter region.

**Results:** Significant associations between *CRF* methylation vs. amygdala volume (CpG-1, $P = 0.006$) and depression scores (CpG-2, $P = 0.01$) were found. To assess whether the promoter CpG methylation has functional consequences, we examined RNA and DNA extracted from non-CS, postmortem amygdala tissues. A significant association between CpG methylation and gene expression (CpG-1, $P = 0.004$) was observed.

**Abbreviations:** BDI, Beck Depression Inventory; CRF, human protein; CRF, human gene; CRF, mouse protein; *Crf*, mouse gene; FKBP5 FK506, Binding Protein 5; PTSD post-traumatic stress disorder; STAI, State-Trait Anxiety Inventory.

**Conclusion:** These results demonstrate that methylation levels of the *CRF* promoter CpGs are associated with amygdala volume in CS and related mood symptoms. Methylation levels may also be associated with *CRF* expression. This finding supports the feasibility of using epigenetic patterns in blood as a surrogate for assessing GC-related pathologies in the brain.

KEYWORDS

Cushing's syndrome, hypercortisolism, corticotropin-releasing factor, DNA methylation, amygdala

## Introduction

Cushing's syndrome (CS) is a rare disease caused by chronic glucocorticoid (GC) excess. It is characterized by central obesity, moon face, muscle weakness, red or purple striae, easy bruising, bone loss, hypertension, fatigue, emotional lability, anxiety, and depression (Starkman et al., 1981; Sonino and Fava, 2001; Arnaldi et al., 2003; Nieman et al., 2008). While many of the symptoms improve following the resolution of hypercortisolism, other symptoms persist, especially GCs' deleterious effects on the brain. Several studies have documented cognitive impairments and reduced brain volume in CS patients even months and years after biochemical or surgical cure (Bourdeau et al., 2005; Tiemensma et al., 2010; Resmini et al., 2012; Andela et al., 2015; Santos et al., 2015). These findings highlight the enduring, yet unidentified factors that mediate the effects of chronic hypercortisolism on brain function and justify the use of CS as an appropriate human model for understanding the impact of chronic cortisol and stress exposure in the general population.

Previously, we have demonstrated in a mouse model of CS that hypercortisolism is associated with epigenetic changes in the stress response and mood disorder gene *Fkbp5* (Scammell et al., 2001; Binder et al., 2004; Lee et al., 2010; Attwood et al., 2011; Klengel et al., 2013). These epigenetic changes consist of, but are not limited to, the addition or removal of methyl groups to cytosine and guanine (CpGs) dinucleotide sequence of DNA at regulatory regions such as gene promoters, enhancers, and disease- and tissue-specific regions (Irizarry et al., 2009). At *Fkbp5*, DNA methylation levels were significantly associated with several GC-induced parameters such as increase in adiposity, hyperglycemia, atrophy of specific organs, and changes in behavior (Lee et al., 2011). Specifically, exposure to excess glucocorticoids (GCs) was associated with DNA methylation changes at intronic CpGs located near GC response elements (GREs) within the gene (Lee et al., 2010), and GC-induced CpG methylation assessed at the *Fkbp5* locus in blood correlated significantly with its methylation and expression levels in the brain (Ewald et al., 2014). A more comprehensive, genome-wide study using the same mouse model showed that GC-induced methylation changes detected at a large number of genes in blood also occurred at the same genes in the brain (Seifuddin et al., 2017).

In human CS, we also showed that hypercortisolism is associated with the reduction of intronic DNA methylation of *FKBP5* in blood, which in turn correlated with memory impairment and hippocampal volume (Resmini et al., 2016). Since GCs have been shown to site-specifically alter DNA methylation and gene function, genes that are targeted by GCs and play a mechanistic role in CS pathology may be good candidates as peripheral biomarkers that can reflect physiological processes occurring in the central nervous system (CNS).

An important neuroendocrine factor that governs GC-related behaviors and thus can serve as a candidate peripheral biomarker of hypercortisolism is corticotropin-releasing factor (CRF or CRH for corticotropin-releasing hormone). CRF is a neuropeptide that serves as one of the core components of the hypothalamus-pituitary-adrenal (HPA) axis that mediates the body's stress response. In response to stress exposure, the hypothalamic release of CRF causes the pituitary release of ACTH (adrenocorticotropic hormone), which culminates in the adrenal release of cortisol. Due to its involvement in the HPA axis and abundant expression in the brain, CRF also plays a central role in stress-related psychiatric disorders. CRF hyperactivity is often associated with depression and anxiety, and exposure to early-life stress serves as a risk factor for anxiety and mood disorders by causing persistent dysregulation of *CRF* (Arborelius et al., 1999; Heim and Nemeroff, 2001). In addition, CRF can contribute to negative emotional states that can drive cycles of drug addiction and relapse (Koob, 1999).

Importantly, it is thought that CRF signaling beyond its direct role within the hypothalamus-pituitary-adrenal (HPA) axis such as in the amygdala (Hostetler and Ryabinin, 2013) may be responsible for some of the GC-borne mood disorder symptoms such as those observed in CS. In fact, reduction in amygdala volume has been observed in CS patients and associated with alterations in mood symptoms (Santos et al., 2017). In mice, stress exposure and neurodevelopmental alterations involve epigenetic mechanisms, namely DNA methylation, in governing *Crf* expression and anxiety-like behaviors (McGill et al., 2006; Elliott et al., 2010). Further, CRF and downstream signaling through its interacting receptor CRFR1 have been shown to play a central role in the amygdala in contextual fear conditioning and anxiety-related behaviors, such as post-traumatic stress disorder (PTSD) (Hollis et al., 2016; Itoga et al., 2016). Therefore, we hypothesize that CRF signaling in the amygdala may be associated with some of the behavioral symptoms observed in CS patients.

In this study, we examined amygdala volume and mood scores in CS patients and aimed at evaluating whether these parameters were associated with blood DNA methylation of the *CRF* gene. A secondary goal of the study was to test the role of DNA methylation in *Crf* expression by using postmortem amygdala tissues from which both DNA methylation and mRNA could be measured. Demonstrating that some of the CS-related pathologies could be linked to blood CRF methylation, similar to what has been reported with *FKBP5* and hippocampal volume, would further support the feasibility of using epigenetic patterns in blood as a surrogate for assessing GC-related pathologies in the brain.

# Materials and methods

## CS patients and controls

In this cross-sectional study, 32 right-handed CS patients clinically followed at the Hospital Sant Pau (Barcelona, Spain), and 32 healthy controls matched for age, sex, and years of education were included. Control subjects were recruited among right-handed healthy volunteers who had previously participated in clinical studies at the Hospital Sant Pau. They had no history of excess GC exposure and were free of medications.

At the time of the study, 9 CS patients were hypercortisolemic (active disease), with 7 cases of pituitary and 2 of adrenal origins. All were on medical therapy, 4 on metyrapone, and 5 on ketoconazole. Four of nine were awaiting surgery (2 adrenal and 2 pituitary). The remaining 5 of the nine had previously undergone unsuccessful pituitary transsphenoidal neurosurgery. Twenty-three patients were in remission (biochemically cured), with 18 cases of pituitary and 5 of adrenal origins. All cured CS of pituitary origin had undergone transsphenoidal surgery (12) or pituitary radiotherapy (6). Unilateral adrenalectomy was performed in the 5 CS patients of adrenal origin. Four patients had adrenal insufficiency at the time of the study and required hydrocortisone replacement therapy, whereas the remaining 19 did not require chronic substitution therapy.

CS was considered in remission if patients achieved adrenal insufficiency or morning cortisol suppression (<50 nmol/L; <1.8 μg/dL) after 1 mg dexamethasone overnight and repeatedly normal 24-h urinary free cortisol levels (measured by radioimmunoassay following urine extraction with an organic solvent; normal <280 nmol/24 h). The mean time of biochemical cure at the study date was 7.1 ± 2.2 years (mean ± STD). Patients exhibited poorer verbal and visual memory performance than controls, as previously described (Resmini et al., 2012). The duration of hypercortisolism was considered as the time from symptom onset until remission of hypercortisolism after treatment and was assessed by the endocrinologist in charge. At diagnosis, the duration of hypercortisolism was estimated by personal interview, detailed review of medical records, and photographs of patients. All information was written or kept in clinical records, together with data regarding the achievement of the biochemical cure. The mean duration of hypercortisolism was 5.1 ± 2.8 years. CS patients with diabetes mellitus and growth hormone deficiency were excluded since cognitive deficits and brain volume reductions have also been described in these conditions (den Heijer et al., 2003; Popovic et al., 2004; Gold et al., 2007; Bruehl et al., 2009). All patients and controls signed an informed consent after study approval by the Hospital Ethics Committee. None of the participants had a past medical history of head injury, cerebrovascular disease, psychiatric disorders, or use of tranquilizers.

## Mood scores and MRI

Beck Depression Inventory-II (BDI-II) is a self-reported measure of the severity of depressive symptoms (Beck and Beamesderfer, 1974; Beck et al., 1996). It has 21 items with a four-point scale ranging from 0 to 3. The total score is the sum of each item rating, ranging from 0 to 63. The manual states that higher scores indicate more severe depressive symptoms. Scores 0–13 indicate minimal depression, 14–19 indicate mild depression, 20–28 indicate moderate depression, and 29–63 indicate severe depression. State-Trait Anxiety Inventory (STAI) is a self-reported measure that includes two subscales to evaluate two types of anxiety: state anxiety (anxiety related to current events) and trait anxiety (anxiety as a personal characteristic) (Spielberger et al., 1983). Each subscale has 20 questions with a four-point scale ranging from 0 to 3. The total score for each subscale is the sum of each item rating and can range from 0 to 60. Higher scores indicate higher levels of anxiety. MRI was obtained using a 3-Tesla Philips Achieva facility (software version 2.1.3.2). All volumetric scores were obtained and normalized to the estimated intracranial volume of each individual, as previously described (Resmini et al., 2012; Santos et al., 2017).

## Postmortem amygdala samples

Postmortem amygdala tissues from controls (N = 20) without any psychiatric disorders were obtained from the Maryland Psychiatric Research Center. The cohort demographics are as follows: 43.8 ± 14.7 years of age; 17 Whites, 2 Blacks, and 1 Hispanic; and 13 females and 7 males. The purpose of these samples was to examine the relationship between promoter methylation and expression of *CRF*.

## Genomic DNA extraction from total leukocytes and brain tissues

Genomic DNA extraction from total leukocytes was carried out using an adapted proteinase K and phenol protocol in all CS and age-matched control subjects (Sambrook et al., 1989). Blood samples from patients were collected in EDTA tubes to reduce blood clotting and DNA degradation. White blood cells were isolated from the buffy coat, pelleted, and stored at −80°C. Genomic DNA was isolated from the white blood cell pellet using a buffer containing 0.1 M $MgCl_2$, 0.02 M EDTA, 0.5% SDS, 0.01 M Tris, pH 8.0, and 1 mg/mL of proteinase K at 37°C overnight. The lysates were homogenized by passing through a blunt 20-gauge needle (0.9 mm diameter) at 4°C, and DNA was purified by phenol:chloroform:isoamyl alcohol (25:24:1) extraction followed by ethanol precipitation. For the postmortem amygdala tissues, DNA was extracted using the Allprep DNA/RNA Micro Kit according to the manufacturer's instructions (Qiagen, Germantown, MD). Finally, genomic DNA from blood and brain was resuspended or eluted in Tris–EDTA buffer and quantified by Qubit Fluorometer (ThermoScientific, Waltham, MA).

## Bisulfite PCR and pyrosequencing

DNA methylation was measured by pyrosequencing of the PCR products, which measures methylation variation at >90% precision (Colella et al., 2003). Two hundred and fifty ng of DNA was bisulfite-converted using the EZ DNA Methylation-Gold kit, according to the manufacturer's protocol (Zymo Research, Irvine, CA). Two sets of

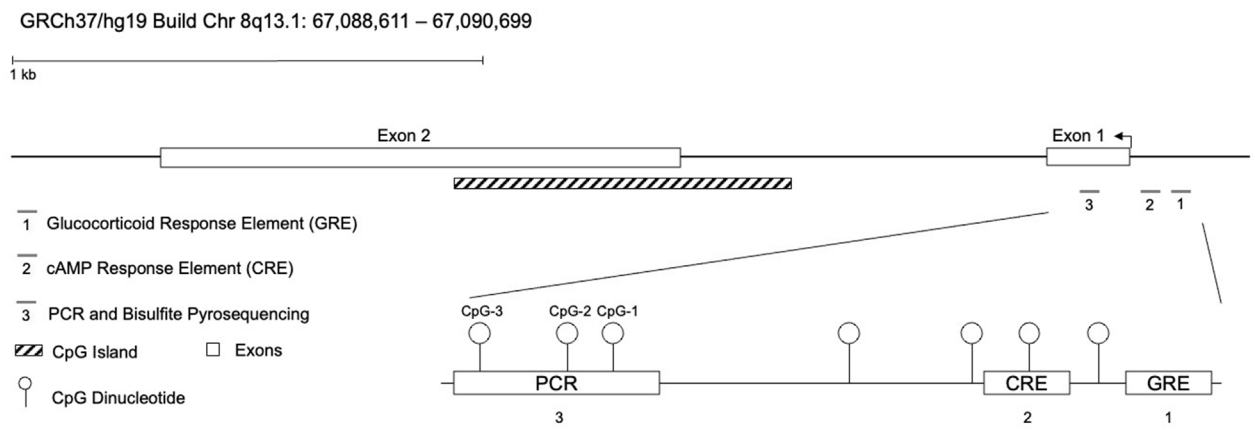


FIGURE 1
Genomic organization of the corticotropin-releasing factor (*CRF*) locus. The *CRF* gene is 2.2 kilobases in size and consists of 2 exons. It is located on the negative strand of human chromosome 8q13.1 (UCSC: GRCh37/hg19 assembly). The diagram depicts the promoter and 5′-UTR CpGs assayed, as well as two putative cAMP- and glucocorticoid-response elements.

primers were designed to amplify a 248-bp promoter region of the human *CRF* gene:

Outside – A: TTAATGGATTTGGTTTTT GAGTT;
Outside – B: ACACACCCCTAATATAACCTTTCA;
Nested – A: TTTAGAGTTT GGAGTGGGATT; and
Nested – B: AAACCCTTCCATTTTAAAACTC.

The genomic organization of *CRF* and three promoter CpG dinucleotides targeted by bisulfite pyrosequencing are shown in Figure 1. The human genomic sequence that harbors the three CpGs, including 20 basepairs flanking both sides of the CpGs, share 100% sequence identity with those of the mouse and rat. Genomic coordinates of the three consecutive CpGs are CpG-1 (67,090,798), CpG-2 (67,090,792), and CpG-3 (67,090,776) on chromosome 8q13.1, according to the UCSC Genome Browser GRCh37/hg19 assembly. Further, the CpGs are functionally significant, based on their proximity to a putative glucocorticoid response element and a previous study implicating them to stress-induced changes in methylation (Elliott et al., 2010). Thermocycling was carried out using the Veriti thermal cycler (Life Technologies, Carlsbad, CA), and 25 ng of bisulfite-treated DNA was used for each PCR reaction. An additional nested PCR was performed with 2 μL of the previous PCR reaction and biotinylated Nested–A primer (Nested–B being unmodified). Amplification for both PCR steps consisted of 40 cycles (94°C for 1 min, 53°C for 30 s, 72°C for 1 min). PCR products were confirmed on agarose gels. Pyro Gold reagents were used to prepare samples for pyrosequencing according to the manufacturer's instructions (Qiagen). For each sample, the biotinylated PCR product was mixed with streptavidin-coated sepharose beads (GE Healthcare, Waukesha, WI), binding buffer, and Milli-Q water and shaken at room temperature. A vacuum prep tool was used to isolate the sepharose bead-bound single-stranded PCR products. The attached DNAs were released into a PSQ HS 96-plate containing pyrosequencing primer (*CRF* Pyro: CCTATAATTTAT ACAAAAAC) in annealing buffer. Pyrosequencing reactions were performed on the PyroMark MD System (Qiagen). CpG methylation quantification was performed with the Pyro Q-CpGt 1.0.9 software (Qiagen). An internal quality-control step was employed to disqualify any assays that contained unconverted DNA. The percentage of methylation at each CpG, as determined by pyrosequencing, was compared among DNA samples from Control, cured CS and active CS patients.

## RNA extraction and quantitative real-time PCR (qPCR)

RNA was extracted from ~25 mg of postmortem amygdala samples using the Allprep DNA/RNA Micro Kit according to the manufacturer's instructions (Qiagen). The total RNA eluted from the Allprep columns was quantified by TapeStation 2.0 bioanalyzer (Agilent Technologies, Santa Clara, CA), and 5 out of 25 samples with RIN numbers less than 7 were excluded from gene expression analysis. The QuantiTect Reverse Transcription Kit (Qiagen) was used to generate cDNA for quantitative real-time PCR. *CRF* expression analysis was carried out in triplicate using 1X Taqman Universal Master Mix (Applied Biosystems, Foster City, CA), 1 μL Taqman probes for *CRF* or house-keeping gene β-actin (*ACTB*) for normalization, and 30 ng of cDNA template in a total volume of 20 μL. Real-time reactions were performed on an Applied Biosystems QuantStudio 5 real-time PCR system with standard PCR conditions (50°C for 2 min; 95°C for 10 min; and 95°C for 15 s and 60°C for 1 min for 40 cycles). Each set of triplicates was checked to ensure that the threshold cycle (Ct) values were all within 0.5 Ct of each other. To determine relative expression values, the -ΔΔCt method was used (Applied Biosystems).

## Statistical analysis

Data were analyzed using the statistical software Stata 15.1 (StataCorp, 2017; R Core Team, 2018). *P*-values were corrected for multiple testing across methylation sites using a Bonferroni correction for each CpG locus, resulting in an adjusted cutoff for significance of 0.02. An exploratory analysis was conducted between CS cases (active

TABLE 1 Demographics, amygdala volumes, and affective symptom scores in CS patients and controls.

| | Controls (N = 32) | Cushing's syndrome (N = 32) | *P*-value |
|---|---|---|---|
| Age (yrs) | 43.8 (11.0) | 44.5 (11.6) | 0.79 |
| Sex (Male: Female) | 7:25 | 6:26 | 0.23 |
| Education (yrs) | 13.8 (3.6) | 13.2 (3.5) | 0.45 |
| Right Amg. Vol. ($cm^3$) | 2,167.8 (255.8) | 2,050.7 (366.4) | 0.14 |
| Left Amg. Vol. ($cm^3$) | 1,865.4 (254.1) | 1,871.5 (301.0) | 0.93 |
| Total Amg. Vol. ($cm^3$) | 4,033.2 (485.3) | 3,922.3 (642.6) | 0.44 |
| BDI | 2.6 (3.5) | 9.3 (5.6) | $2.7 \times 10^{-7}$ |
| STAI – State | 10.2 (7.6) | 19.7 (12.9) | $7.0 \times 10^{-4}$ |
| STAI – Trait | 11.2 (6.6) | 24.5 (11.3) | $2.7 \times 10^{-7}$ |

Data are presented as mean (standard deviation). *P*-values reflect statistical significance between healthy controls and Cushing's syndrome that includes both active and cured cases. *P*-values for quantitative traits are derived from Student's t-test. *P*-values from categorical traits are derived from $Chi^2$ test.

and cured) and controls to assess potential confounders to the comparability of cases and controls. Major sociodemographic factors, including age, gender, and education, as well as biological and mental health characteristics, such as amygdala volume and scores on the BDI-II and STAI, were tested for differences, with crude associations calculated using Student's t-test for quantitative traits and Chi-squared tests for categorical traits.

Association between *CRF* promoter methylation across the three CpG sites and CS case status was conducted using both crude Pearson's correlation adjusting for age, gender, and education level of participants and linear regression adjusting for age, gender, and years of education. Given the tendency of nearby CpG dinucleotides to be similarly methylated (Martin et al., 2015), the methylation values across the three CpGs were averaged, and the regression was run again as a sensitivity analysis of global methylation in the region. Then, the difference in methylation between active CS cases only and healthy controls was examined with linear regression, as well as differences between active CS cases and cured CS cases to examine any effects treatment may have on methylation status.

The relationship between *CRF* methylation and mental health metric scores was also assessed using Pearson's correlation and adjusted linear regression. This was repeated for the state and trait anxiety (STAI) subscales as a sensitivity analysis. Then, *CRF* methylation and amygdala volume were examined using similar statistical tests as described above, using right, left, and total amygdala volumes as the outcome of interest for the linear regression analysis.

Finally, using post-mortem amygdala tissues from healthy individuals, DNA methylation was assessed against gene expression levels of *CRF*, and Pearson's correlation was calculated between relative *CRF* expression and each CpG site.

# Results

## Sociodemographic and biometric data for CS patients and controls

Exploratory analysis found no statistically significant differences between CS cases and healthy controls on major sociodemographic and clinical variables. The mean age of controls was 43.8 ± 11.0 years compared to 44.5 ± 11.6 years for CS ($P = 0.79$, Table 1). Gender distributions were also similar, with 21.9% (N = 7) of controls and 18.8% (N = 6) of CS cases being males ($P = 0.23$). Differences in the years of education attained was 0.6 years ($P = 0.45$). Amygdala volumes showed no significant differences between controls and CS, although CS volumes were somewhat smaller: right amygdala volume (2167.8 ± 255.8 vs. 2050.7 ± 366.4 $cm^3$, $P = 0.14$); left (1865.4 ± 254.1 vs. 1871.5 ± 301.0 $cm^3$, $P = 0.93$); and total (4033.2 ± 485.3 vs. 3922.3 ± 642.6 $cm^3$, $P = 0.44$). It should be noted that when comparing active CS cases and controls, mean difference in the right amygdala volume was borderline significant (2167.8 ± 255.8 vs. 1944.2 ± 501.6 $cm^3$, $P = 0.073$). In contrast, all three mental health scores showed highly significant associations via the t-test, with the BDI scores in controls on average 2.6 ± 3.5 and 9.3 ± 5.6 among CS cases ($P < 0.0001$). The state score for anxiety had a difference of 9.5 ($P = 0.0007$), and the trait score had a difference of 13.3 between controls and CS ($P < 0.0001$).

## CRF promoter methylation in CS patients and controls

We determined DNA methylation levels of three stress-relevant, consecutive CpG dinucleotides at the *CRF* promoter (Figure 1) in the CS patients and healthy controls. Bisulfite pyrosequencing showed a trend of reduced methylation in CS samples across all three CpGs, with only CpG-3 achieving statistical significance: CpG-1 (−2.5%, $P = 0.18$); CpG-2 (−1.6%, $P = 0.39$), and CpG-3 (−2.9%, $P = 0.009$) (Figure 2A). Adjusting for common sociodemographic factors (age, gender, and education), similar effects were observed: CpG-1 (−2.5%, $P = 0.15$); CpG-2 (−1.7%, $P = 0.33$), CpG-3 (−3.1%, $P = 0.002$) (Table 2). Mean methylation levels across the three CpGs between the groups were also significantly different (−2.3%, $P = 0.04$). CS samples further stratified into active vs. cured status showed consistent reduction in the active CS compared to cured CS samples across all three CpGs, but none of the reductions were

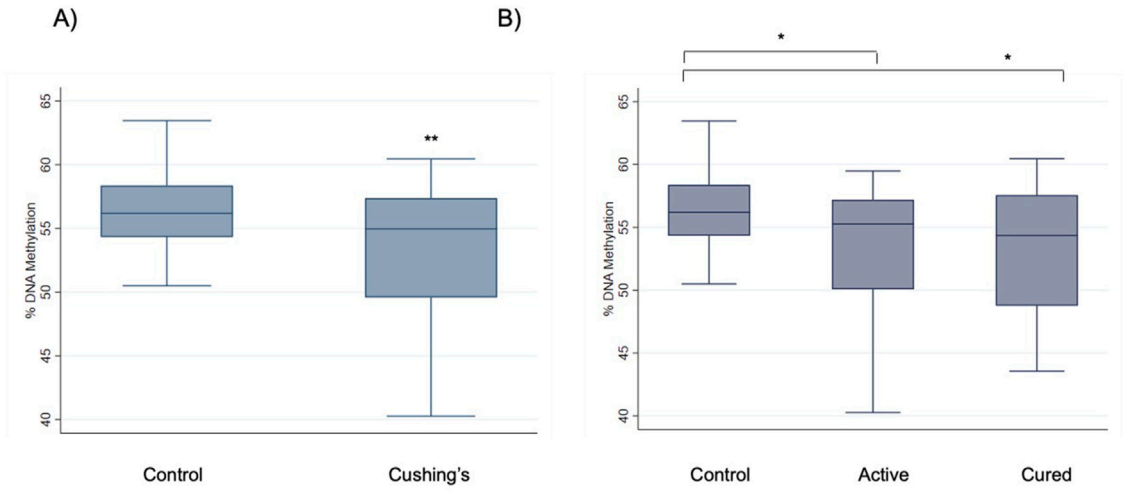


FIGURE 2
Reduction of *CRF* methylation in Cushing's syndrome. **(A)** The boxplot shows a comparison of methylation differences between healthy controls (N = 32) and CS patients (N = 32) at the *CRF* promoter CpG-3 in leukocytes. The CS patients include both active (N = 9) and cured patients (N = 23). **(B)** CpG-3 methylation levels were also analyzed after case samples were further segregated into active CS vs. cured CS. *$P < 0.05$ and **$P < 0.01$ using Student's t-test.

significant (methylation difference <3.7%, $P > 0.27$). Notably, CpG-3 showed differences in methylation between active CS vs. controls (−3.5%, $P = 0.03$) and cured CS vs. controls (−2.7%, $P = 0.02$) (Figure 2B). Examining only the active CS cases vs. healthy controls and adjusting for age, gender, and education showed similar patterns as active and cured CS compared to controls: CpG-1 (−2.0%, $P = 0.27$), CpG-2 (−0.6%, $P = 0.75$), and CpG-3 (−2.91%, $P = 0.006$).

## Association between *CRF* methylation and mood data

We then evaluated whether the methylation levels correlated with data obtained from the Beck Depression Inventory (BDI-II) and State-Trait Anxiety Inventory (STAI). Significant correlations were observed across CpG-2 (r = −0.29, $P = 0.01$) and CpG-3 (r = −0.23, $P = 0.01$), and borderline correlation was observed at CpG-1 (r = −0.22, $P = 0.06$) when *CRF* methylation was compared against BDI-II scores. Linear regression analysis was also performed, and results for CpG-2 vs. BDI-II scores is shown in Figure 3A. In linear regression analysis adjusting for sociodemographic variables, BDI-II scores were significantly associated with CpG-2 (−0.26, $P = 0.01$) and CpG-3 (−0.45, $P = 0.01$), while their association with CpG-1 had a point estimate (−0.20) and *P*-value ($P = 0.06$) similar to those prior to adjustment (Table 2). In contrast, none of the CpGs were significantly associated with neither the STAI Trait ($|r|<0.16$, $P > 0.20$) nor the STAI State ($|r|<0.19$, $P > 0.12$) scores. Figure 3B shows the linear regression analysis between CpG-2 methylation levels and STAI State scores. Using linear regression and adjusting for age, education, and gender, the STAI State subscale scores were only significantly associated with CpG-2 (−0.41, $P = 0.05$ and $P > 0.21$ for CpG-1 and CpG-3). None of the three CpGs were significantly associated with the Trait subscale, with CpG-1 being the most significant (−0.32, $P = 0.13$).

## Association between *CRF* methylation and amygdala volume

Given a previous study linking anxiety and depression scores with amygdala volume (Santos et al., 2017), *CRF* methylation was compared to amygdala volume. For all study participants, methylation levels were first compared to total amygdala volume consisting of both left and right regions and then each right or left region separately. Interestingly, we observed significant, positive associations with CpG-1 methylation when it was compared to total (r = 0.37, $P = 0.003$, Figure 4A), right (r = 0.36, $P = 0.004$, Figure 4B), and left (r = 0.34, $P = 0.006$, Figure 4C) amygdala volumes. Methylation levels at CpG-2 and CpG-3 were not correlated with any of the volume metrics ($r \leq 11.92$, $P \geq P.51$). For CpG-1, these relationships remained significant after adjusting for age, sex, and education in all three amygdala volume measurements using linear regression: total (28.20, $P = 0.P06$), left (11.87, $P = 0.02$), and right (16.33, P = *P*.005) amygdala volumes (Table 2).

## Association between DNA methylation and gene expression

Finally, since only blood DNA samples were available from the CS patients, it was not possible to determine whether the methylation levels of the three CpGs were generally associated with *CRF* gene expression. To demonstrate this association, amygdala tissues from twenty deceased individuals with no diagnosis of psychiatric disorders or CS were examined. Genomic DNA and messenger RNA extracted simultaneously from the same tissue were used for *CRH* methylation analysis and gene expression, respectively. Analysis using Pearson's coefficient showed a negative correlation between gene expression and methylation at all three CpGs: CpG-1 (−0.62, $P = 0.004$, Figure 5A), CpG-2 (−0.40, $P = 0.08$,

TABLE 2 Individual and mean *CRF* methylation across three CpG sites vs. CS case status, depression scores (assessed continuously and dichotomously), and amygdala volumes (assessed as total, left, and right amygdala volumes), adjusting for age, sex, and education.

| | Cushing's syndrome case[a] | | Beck depression Inventory-II (BDI-II) score[b] | | | | Amygdala volume ($cm^3$)[c] | | | | | |
|---|---|---|---|---|---|---|---|---|---|---|---|---|
| | | | BDI continuous score | | BDI qualitative score | | Total volume | | Left volume | | Right volume | |
| | Adjusted coefficient (95% CI) | *P*-value | Adjusted coefficient (95% CI) | *P*-value | Adjusted coefficient (95% CI) | *P*-value | Adjusted coefficient (95% CI) | *P*-value | Adjusted coefficient (95% CI) | *P*-value | Adjusted coefficient (95% CI) | *P*-value |
| Mean CpG | −2.45 (−4.76, −0.13) | **0.04** | **−0.31 (-0.52, -0.11)** | **0.003** | **0.81 (0.67, 0.98)** | **0.03** | 26.76 (−3.39, 56.91) | 0.08 | 12.09 (−2.54, 26.71) | 0.10 | 14.68 (−2.47, 31.82) | 0.09 |
| CpG1 | −2.52 (−5.97, 0.92) | 0.15 | −0.20 (−0.40, 0.004) | 0.06 | 0.94 (0.84, 1.04) | 0.23 | **28.20 (8.35, 48.05)** | **0.006** | **11.87 (2.12, 21.63)** | **0.02** | **16.33 (5.09, 27.57)** | **0.005** |
| CpG2 | −1.71 (−5.17, 1.75) | 0.33 | **−0.26 (-0.46, -0.06)** | **0.01** | **0.86 (0.76, 0.97)** | **0.02** | 5.33 (−15.92, 26.58) | 0.62 | 3.16 (−7.10, 13.42) | 0.54 | 2.18 (−9.90, 14.25) | 0.72 |
| CpG3 | −3.11 (−5.00, −1.22) | **0.002** | **−0.45 (-0.79, -0.10)** | **0.01** | 0.84 (0.70, 1.03) | 0.09 | 11.92 (−24.09, 47.93) | 0.51 | 5.74 (−11.67, 23.15) | 0.51 | 6.18 (−14.28, 26.63) | 0.55 |

Note: Statistically significant associations are highlighted in bold.

[a]Cushing's case status was used as an outcome with *CRF*, methylation being used as the predictor in logistic regression.

[b]Depression was the outcome with *CRF* methylation as a predictor in linear regression for continuous BDI score and logistic regression for qualitative scoring (using score ≥ 20 points).

[c]Amygdala volume was used as an outcome with *CRF* methylation as a predictor. All models were adjusted for age (years), gender (female), and education (years).





10.3389/freae.2024.1435634

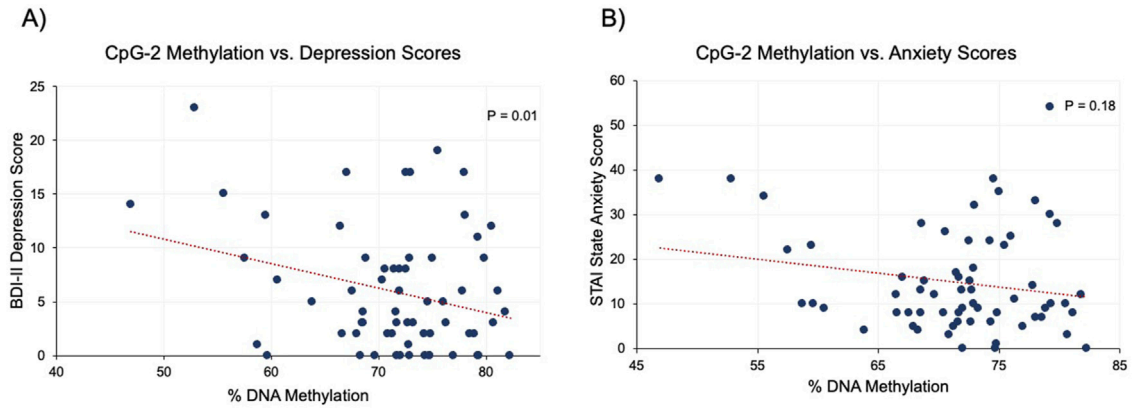


FIGURE 3
Association between mood and anxiety scores vs. *CRF* methylation at CpG-2. **(A)** Linear regression analysis showed a significant, negative association between CRF methylation and depression scores (BDI-II). **(B)** The association between *CRF* methylation and STAI State scores were non-significant.

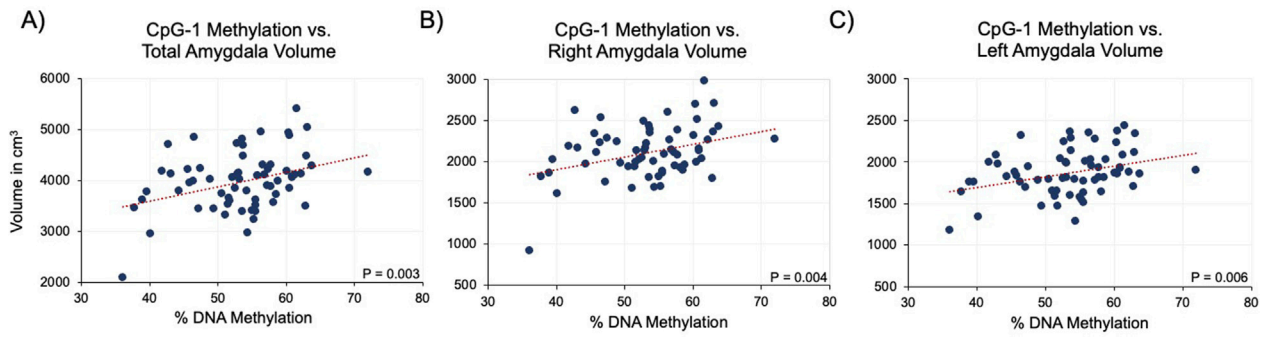


FIGURE 4
Association between *CRF* methylation at CpG-1 and amygdala volume. Linear regression analysis showed a significant, positive association between *CRF* methylation and total **(A)**, right **(B)**, and left **(C)** amygdala volumes.

Figure 5B), and CpG-3 (−0.53, $P$ = 0.02, Figure 5C) with the strongest correlation at CpG-1.

## Discussion

In the current study, we explored the relationship among *CRF* promoter CpG methylation, amygdala volume, and mood status in CS patients, aimed at assessing whether DNA from a peripheral tissue such as blood could be used to inform us about the detrimental consequences of chronic hypercortisolemia on the amygdala and mood.

We observed for the first time a consistent decrease in DNA (CpG) methylation levels in CS patients, with healthy controls showing the highest *CRF* methylation levels and cured CS samples showing lower levels, followed by active CS samples showing the lowest. The disease status-dependent decrease in *CRF* methylation is reminiscent of the intronic methylation levels observed at the *FKBP5* locus, which also showed a CS-associated decrease in methylation (Resmini et al., 2016). In both cases, the cured CS group showed methylation levels that were between those of the active CS cases and controls, suggesting that GC-induced loss of methylation in blood may only be partially reversible. Such methylation patterns underscore the durability of GC-induced epigenetic changes and may reflect similarly irreversible CS symptomatology.

Postmortem amygdala tissues from deceased healthy individuals were used to establish a functional role for the *CRF* CpGs by showing that these CpGs may play a role in influencing gene expression by conferring methylation-sensitive binding of transcription factors to the *CRF* promoter. Since leukocyte mRNA was not collected from the CS cohort, it was not possible to assess whether CpG methylation levels associated with *CRF* expression levels. Further, since we had compared methylation levels in blood to volumetric and psychometric measurements associated with the amygdala, we sought to determine whether methylation correlated with gene expression in this relevant tissue. A significant relationship that was observed between *CRF* gene expression and CpG methylation suggests that methylation levels of at least two of the three CpGs likely influence *CRF* expression in the amygdala. All three CpGs tested are conserved across species and located approximately 200 bases downstream of negative GC and cAMP response

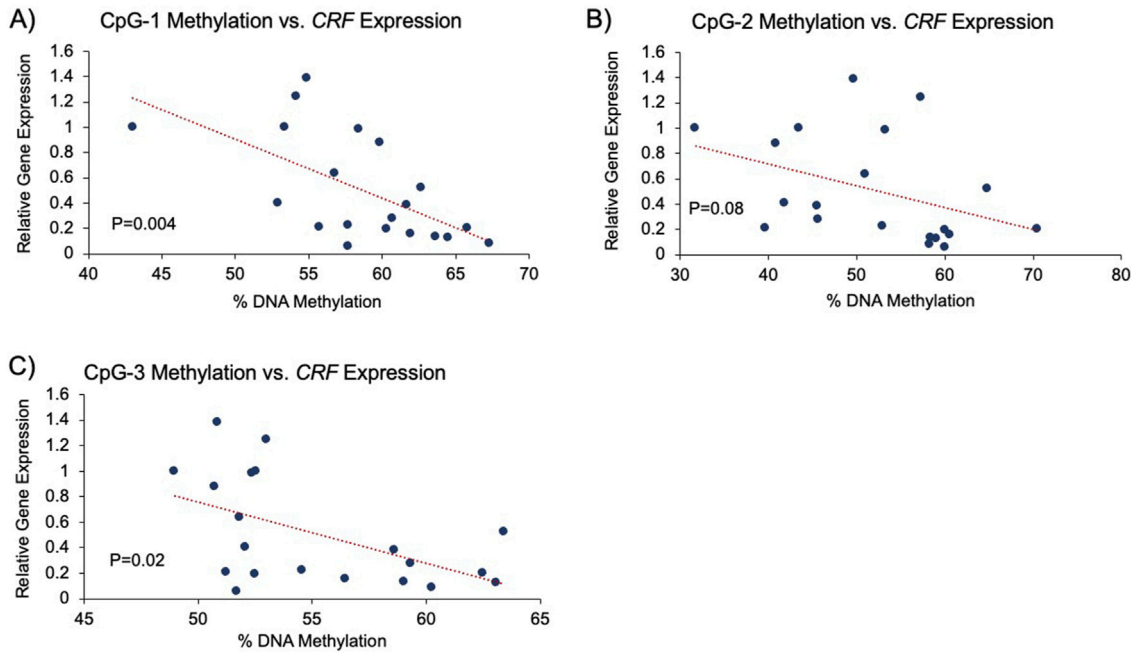


FIGURE 5
Association between *CRF* expression and promoter methylation. Analysis using Pearson's correlation coefficient showed a significant, negative correlation between gene expression and DNA methylation in postmortem amygdala tissues of healthy controls. **(A–C)** Pearson's correlation analysis between CRF expression and CpGs 1-3, respectively, is shown.

elements that are thought to mediate cortisol- and stress-induced regulation of the *CRF* gene (Malkoski et al., 1997). Importantly, data from another group demonstrated that these three CpGs underwent significant loss of methylation in mice that were susceptible to stress, and these CpGs conferred methylation-sensitive gene expression in an *in vitro* reporter assay (Elliott et al., 2010). Loss of *CRF* methylation in CS implies that hypercortisolism may lead to increased *CRF* expression in the amygdala. While exposure to excess GCs leads to the downregulation of CRF in the hippocampus and the hypothalamus as part of the negative feedback mechanism of the HPA axis (Lee et al., 2010), there is a positive feedback in the amygdala (Gold and Chrousos, 2002), where GC administration activates *CRF*, especially in the central amygdala (Makino et al., 1999; Shepard et al., 2000; Kolber et al., 2008; Tran and Greenwood-Van Meerveld, 2012). Taken together, our results suggest that methylation of *CRF* promoter could be a functional, peripheral biomarker of mood and amygdala volume in CS patients.

We also examined the association between *CRF* methylation and mood data. While a significant association was observed between BDI-II depression scores and *CRF* methylation, there was no significant association between the STAI anxiety scores and methylation. This finding was surprising given the central role that CRF plays on anxiety in the amygdala. However, CRF and anxiety may be involved in the context of chronic stress rather than in elevated GC exposure alone and thus may involve additional neuroendocrine factors, such as noradrenaline (Tanaka et al., 2000).

Finally, we observed a positive relationship between DNA methylation levels of *CRF* and total amygdala volume. Specifically, higher CpG-1 methylation levels were associated with higher amygdala volumes and *vice versa*, and this association held when left and right amygdala volumes were analyzed separately. Since reduced methylation levels were associated with hypercortisolism and increased *CRF* expression, this finding suggests a potential role for *CRF* expression in amygdala, the volume reduction of which has been previously observed in our CS cohort (Santos et al., 2017) and in patients receiving chronic, exogenous GC administration (Brown et al., 2008). Consistent decrease in amygdala volume was also documented in unmedicated major depression patients in a meta-analysis study (Hamilton et al., 2008). However, association studies of amygdala volume with other stress-related pathologies such as anxiety disorder and PTSD have yielded mixed results, largely owing to differences in age, sex, and nature and duration of the stressors. Considering our findings, additional work is necessary to demonstrate the role of *CRF* expression on amygdala volumes in the context of these other psychopathologies.

Our study has several limitations. The sample size of our cohort is relatively small, but this is difficult to avoid in a rare disease such as CS, especially in cohorts where multidimensional data such as brain volume, psychometric, and cognitive data have been collected. Also, our study population included patients with pituitary-dependent CS and adrenal CS. We did not segregate the two types of CS, since doing so would further reduce the sample size, and they both shared chronic exposure to endogenous hypercortisolism, which we assumed would be detrimental to the brain regardless of CS etiology. Nine subjects with active CS were taking ketoconazole, which could have also led to a potential confound.

In addition, although significant relationships were observed between blood DNA methylation and processes related to the brain, there were several experimental steps in between that could not be performed. Previous work in mice showed that treatment with high-dose GCs caused similar methylation changes in both blood and

brain tissues (Ewald et al., 2014; Seifuddin et al., 2017). In these studies, the use of an animal model enabled the investigation of GC-treated blood and brain tissues from the same animals so that biologically meaningful correlations could be derived between the two tissues. In the current clinical cohort, while an attempt was made to demonstrate that the same set of CpGs in the amygdala were associated with gene expression, the question of whether CS-associated methylation levels in the blood correlated with methylation changes in the amygdala remains undetermined. To answer this question, both blood and brain tissues from the same patients are needed to elucidate this relationship, which is not feasible in living CS patients. We also acknowledge that unlike the significant relationship that we observed between *CRF* methylation and gene expression in the control postmortem brains, there may be additional factors and mechanisms that can contribute to *CRF* expression in CS patients.

Another limitation was the inability to distinguish epigenetic changes that reflect a reduction in DNA methylation from those which may be due to changes in the cellular composition of blood. During chronic exposure to high-dose GCs, there occurs a substantial shift in the cellular proportion of blood. For instance, when mice are exposed to high-dose GCs, neutrophils assume a greater percentage of circulating white blood cells in a process known as demargination (Seifuddin et al., 2017). Since each cell type exhibits distinct methylation patterns across its genome, GC-induced changes in methylation may also capture the increasing contribution of methylation content from a cell type, such as those from neutrophils that increases in proportion in the GC-exposed blood. While there are several statistical methods for estimating cell type proportion changes based on unique methylation signature of each cell type, these methods rely on the use of genome-wide methylation platforms such as the Illumina 450K or EPIC arrays, with hundreds of CpG probes being used for each cell-type signature (Houseman et al., 2012). We acknowledge that our analysis of *CRF* precluded the use of such an array. However, we note that a whole blood cell count performed in cured CS patients in this cohort showed similar percentage of neutrophil and lymphocyte counts as those of the controls (Aulinas et al., 2014). This implies that for at least the cured CS samples, none of the analysis that involves DNA methylation are likely to be due to a shift in the cellular composition of blood. Finally, we acknowledge the relatively small effect size in DNA methylation differences between CS and controls. We observed a bigger effect size when testing GC-induced DNA methylation changes in the mouse blood. However, the bigger effect size in mice was due to the combination of demargination and loss of DNA methylation in the post GC-treatment period that was not as prominent in human CS (Seifuddin et al., 2017). We speculate that methylation differences in CS blood may be smaller due, in part, to the smaller percentage of lymphocytes in humans (30–50%) compared to mice (75–90%) (Doeing et al., 2003; Mestas and Hughes, 2004). A previous study by our group has shown that GC-induced loss of methylation occurs primarily in T-cells, implying that mice with a larger percentage of T-cells in the blood than humans will show greater changes in DNA methylation (Seifuddin et al., 2017). Nevertheless, we observed significant correlations between CRF methylation and CS status, BDI-II scores, and amygdala volume, underscoring the unlikelihood that these methylation differences are spurious findings. In addition, our effect sizes are similar to or greater than those (methylation M-values) obtained from a recent methylomic study of Cushing's disease using the EPIC methylation platform (Armignacco et al., 2022).

Despite these limitations, our study shows that epigenetic patterns at the *CRF* locus could be associated with mood and amygdala volume alterations in CS patients. Our findings support the feasibility of using epigenetic patterns in blood as a surrogate for assessing GC-related pathologies in the brain.

## Data availability statement

The datasets presented in the study are publicly available. This data can be found here: https://figshare.com/articles/dataset/_b_Blood_DNA_methylation_of_b_b_b_b_i_CRF_i_b_b_b_b_and_its_association_with_amygdala_volume_and_mood_in_Cushing_s_syndrome_b_/27084100?file=49350520, DOI: https://10.6084/m9.figshare.27084100.

## Ethics statement

Studies involving humans were approved by Hospital Ethics Committee of Hospital de la Santa Creu I Sant Pau. Studies were conducted in accordance with the local legislation and institutional requirements. Participants provided their written informed consent to participate in this study.

## Author contributions

RL: Conceptualization, Data curation, Funding acquisition, Investigation, Methodology, Project administration, Resources, Supervision, Writing–original draft, Writing–review and editing. AS: Data curation, Funding acquisition, Methodology, Writing–review and editing. HG-D: Formal Analysis, Methodology, Writing–review and editing. AA: Data curation, Methodology, Writing–review and editing. JC: Data curation, Supervision, Writing–review and editing. YV-G: Data curation, Methodology, Writing–review and editing. OC: Data curation, Supervision, Writing–review and editing. GC: Data curation, Validation, Writing–review and editing. SW: Data curation, Funding acquisition, Methodology, Writing–review and editing. ER: Conceptualization, Data curation, Funding acquisition, Methodology, Writing–original draft, Writing–review and editing.

## Funding

The author(s) declare that financial support was received for the research, authorship, and/or publication of this article. This study is supported by grants from: the James Wah Mood Disorders Scholar Fund via the Charles T. Bauer Foundation, the Baker Foundation, and the Project Match Foundation awarded to RSL and grants from the Instituto de Salud Carlos III, Spanish Ministry of Science and Innovation (MICINN, FIS080302), and the European Commission (ERCUSYN PHP800200) awarded to ER, AS, and SW.

## Conflict of interest

The authors declare that the research was conducted in the absence of any commercial or financial relationships that could be construed as a potential conflict of interest.

The author(s) declared that they were an editorial board member of Frontiers, at the time of submission. This had no impact on the peer review process and the final decision.

## Publisher's note



## References

Andela, C. D., van Haalen, F. M., Ragnarsson, O., Papakokkinou, E., Johannsson, G., Santos, A., et al. (2015). Mechanisms in Endocrinology: Cushing's syndrome causes irreversible effects on the human brain: a systematic review of structural and functional magnetic resonance imaging studies. *Eur. J. Endocrinol.* 173 (1), R1–R14. doi:10.1530/EJE-14-1101

Arborelius, L., Owens, M. J., Plotsky, P. M., and Nemeroff, C. B. (1999). The role of corticotropin-releasing factor in depression and anxiety disorders. *J. Endocrinol.* 160 (1), 1–12. doi:10.1677/joe.0.1600001

Armignacco, R., Jouinot, A., Bouys, L., Septier, A., Lartigue, T., Neou, M., et al. (2022). Identification of glucocorticoid-related molecular signature by whole blood methylome analysis. *Eur. J. Endocrinol.* 186 (2), 297–308. doi:10.1530/EJE-21-0907

Arnaldi, G., Angeli, A., Atkinson, A. B., Bertagna, X., Cavagnini, F., Chrousos, G. P., et al. (2003). Diagnosis and complications of Cushing's syndrome: a consensus statement. *J. Clin. Endocrinol. and Metabolism* 88 (12), 5593–5602. doi:10.1210/jc.2003-030871

Attwood, B. K., Bourgognon, J. M., Patel, S., Mucha, M., Schiavon, E., Skrzypiec, A. E., et al. (2011). Neuropsin cleaves EphB2 in the amygdala to control anxiety. *Nature* 473 (7347), 372–375. doi:10.1038/nature09938

Aulinas, A., Ramirez, M. J., Barahona, M. J., Valassi, E., Resmini, E., Mato, E., et al. (2014). Telomere length analysis in Cushing's syndrome. *Eur. J. Endocrinol.* 171 (1), 21–29. doi:10.1530/EJE-14-0098

Beck, A. T., and Beamesderfer, A. (1974). Assessment of depression: the depression inventory. *Mod. problems pharmacopsychiatry* 7 (0), 151–169. doi:10.1159/000395074

Beck, A. T., Steer, R. A., Ball, R., and Ranieri, W. (1996). Comparison of Beck depression inventories -IA and -II in psychiatric outpatients. *J. Personality Assess.* 67 (3), 588–597. doi:10.1207/s15327752jpa6703_13

Binder, E. B., Salyakina, D., Lichtner, P., Wochnik, G. M., Ising, M., Putz, B., et al. (2004). Polymorphisms in FKBP5 are associated with increased recurrence of depressive episodes and rapid response to antidepressant treatment. *Nat. Genet.* 36 (12), 1319–1325. doi:10.1038/ng1479

Bourdeau, I., Bard, C., Forget, H., Boulanger, Y., Cohen, H., and Lacroix, A. (2005). Cognitive function and cerebral assessment in patients who have Cushing's syndrome. *Endocrinol. Metabolism Clin. N. Am.* 34 (2), 357–369. doi:10.1016/j.ecl.2005.01.016

Brown, E. S., Woolston, D. J., and Frol, A. B. (2008). Amygdala volume in patients receiving chronic corticosteroid therapy. *Biol. Psychiatry* 63 (7), 705–709. doi:10.1016/j.biopsych.2007.09.014

Bruehl, H., Wolf, O. T., and Convit, A. (2009). A blunted cortisol awakening response and hippocampal atrophy in type 2 diabetes mellitus. *Psychoneuroendocrinology* 34 (6), 815–821. doi:10.1016/j.psyneuen.2008.12.010

Colella, S., Shen, L., Baggerly, K. A., Issa, J. P., and Krahe, R. (2003). Sensitive and quantitative universal Pyrosequencing methylation analysis of CpG sites. *Biotechniques* 35 (1), 146–150. doi:10.2144/03351md01

den Heijer, T., Vermeer, S. E., van Dijk, E. J., Prins, N. D., Koudstaal, P. J., Hofman, A., et al. (2003). Type 2 diabetes and atrophy of medial temporal lobe structures on brain MRI. *Diabetologia* 46 (12), 1604–1610. doi:10.1007/s00125-003-1235-0

Doeing, D. C., Borowicz, J. L., and Crockett, E. T. (2003). Gender dimorphism in differential peripheral blood leukocyte counts in mice using cardiac, tail, foot, and saphenous vein puncture methods. *BMC Clin. Pathol.* 3 (1), 3. doi:10.1186/1472-6890-3-3

Elliott, E., Ezra-Nevo, G., Regev, L., Neufeld-Cohen, A., and Chen, A. (2010). Resilience to social stress coincides with functional DNA methylation of the Crf gene in adult mice. *Nat. Neurosci.* 13 (11), 1351–1353. doi:10.1038/nn.2642

Ewald, E. R., Wand, G. S., Seifuddin, F., Yang, X., Tamashiro, K. L., Potash, J. B., et al. (2014). Alterations in DNA methylation of Fkbp5 as a determinant of blood-brain correlation of glucocorticoid exposure. *Psychoneuroendocrinology* 44, 112–122. doi:10.1016/j.psyneuen.2014.03.003

Gold, P. W., and Chrousos, G. P. (2002). Organization of the stress system and its dysregulation in melancholic and atypical depression: high vs low CRH/NE states. *Mol. Psychiatry* 7 (3), 254–275. doi:10.1038/sj.mp.4001032

Gold, S. M., Dziobek, I., Sweat, V., Tirsi, A., Rogers, K., Bruehl, H., et al. (2007). Hippocampal damage and memory impairments as possible early brain complications of type 2 diabetes. *Diabetologia* 50 (4), 711–719. doi:10.1007/s00125-007-0602-7

Hamilton, J. P., Siemer, M., and Gotlib, I. H. (2008). Amygdala volume in major depressive disorder: a meta-analysis of magnetic resonance imaging studies. *Mol. Psychiatry* 13 (11), 993–1000. doi:10.1038/mp.2008.57

Heim, C., and Nemeroff, C. B. (2001). The role of childhood trauma in the neurobiology of mood and anxiety disorders: preclinical and clinical studies. *Biol. Psychiatry* 49 (12), 1023–1039. doi:10.1016/s0006-3223(01)01157-x

Hollis, F., Sevelinges, Y., Grosse, J., Zanoletti, O., and Sandi, C. (2016). Involvement of CRFR1 in the basolateral amygdala in the immediate fear extinction deficit. *eNeuro* 3 (5), ENEURO.0084–16.2016. doi:10.1523/ENEURO.0084-16.2016

Hostetler, C. M., and Ryabinin, A. E. (2013). The CRF system and social behavior: a review. *Front. Neurosci.* 7, 92. doi:10.3389/fnins.2013.00092

Houseman, E. A., Accomando, W. P., Koestler, D. C., Christensen, B. C., Marsit, C. J., Nelson, H. H., et al. (2012). DNA methylation arrays as surrogate measures of cell mixture distribution. *BMC Bioinforma.* 13, 86. doi:10.1186/1471-2105-13-86

Irizarry, R. A., Ladd-Acosta, C., Wen, B., Wu, Z., Montano, C., Onyango, P., et al. (2009). The human colon cancer methylome shows similar hypo- and hypermethylation at conserved tissue-specific CpG island shores. *Nat. Genet.* 41 (2), 178–186. doi:10.1038/ng.298

Itoga, C. A., Roltsch Hellard, E. A., Whitaker, A. M., Lu, Y. L., Schreiber, A. L., Baynes, B. B., et al. (2016). Traumatic stress promotes hyperalgesia via corticotropin-releasing factor-1 receptor (CRFR1) signaling in central amygdala. *Neuropsychopharmacology* 41 (10), 2463–2472. doi:10.1038/npp.2016.44

Klengel, T., Mehta, D., Anacker, C., Rex-Haffner, M., Pruessner, J. C., Pariante, C. M., et al. (2013). Allele-specific FKBP5 DNA demethylation mediates gene-childhood trauma interactions. *Nat. Neurosci.* 16 (1), 33–41. doi:10.1038/nn.3275

Kolber, B. J., Roberts, M. S., Howell, M. P., Wozniak, D. F., Sands, M. S., and Muglia, L. J. (2008). Central amygdala glucocorticoid receptor action promotes fear-associated CRH activation and conditioning. *Proc. Natl. Acad. Sci. U. S. A.* 105 (33), 12004–12009. doi:10.1073/pnas.0803216105

Koob, G. F. (1999). Stress, corticotropin-releasing factor, and drug addiction. *Ann. N. Y. Acad. Sci.* 897, 27–45. doi:10.1111/j.1749-6632.1999.tb07876.x

Lee, R. S., Tamashiro, K. L., Yang, X., Purcell, R. H., Harvey, A., Willour, V. L., et al. (2010). Chronic corticosterone exposure increases expression and decreases deoxyribonucleic acid methylation of Fkbp5 in mice. *Endocrinology* 151 (9), 4332–4343. doi:10.1210/en.2010-0225

Lee, R. S., Tamashiro, K. L., Yang, X., Purcell, R. H., Huo, Y., Rongione, M., et al. (2011). A measure of glucocorticoid load provided by DNA methylation of Fkbp5 in mice. *Psychopharmacol. Berl.* 218 (1), 303–312. doi:10.1007/s00213-011-2307-3

Makino, S., Shibasaki, T., Yamauchi, N., Nishioka, T., Mimoto, T., Wakabayashi, I., et al. (1999). Psychological stress increased corticotropin-releasing hormone mRNA and content in the central nucleus of the amygdala but not in the hypothalamic paraventricular nucleus in the rat. *Brain Res.* 850 (1-2), 136–143. doi:10.1016/s0006-8993(99)02114-9

Malkoski, S. P., Handanos, C. M., and Dorin, R. I. (1997). Localization of a negative glucocorticoid response element of the human corticotropin releasing hormone gene. *Mol. Cell. Endocrinol.* 127 (2), 189–199. doi:10.1016/s0303-7207(96)04004-x

Martin, T. C., Yet, I., Tsai, P. C., and Bell, J. T. (2015). coMET: visualisation of regional epigenome-wide association scan results and DNA co-methylation patterns. *BMC Bioinforma.* 16, 131. doi:10.1186/s12859-015-0568-2

McGill, B. E., Bundle, S. F., Yaylaoglu, M. B., Carson, J. P., Thaller, C., and Zoghbi, H. Y. (2006). Enhanced anxiety and stress-induced corticosterone release are associated with increased Crh expression in a mouse model of Rett syndrome. *Proc. Natl. Acad. Sci. U. S. A.* 103 (48), 18267–18272. doi:10.1073/pnas.0608702103

Mestas, J., and Hughes, C. C. (2004). Of mice and not men: differences between mouse and human immunology. *J. Immunol.* 172 (5), 2731–2738. doi:10.4049/jimmunol.172.5.2731

Nieman, L. K., Biller, B. M., Findling, J. W., Newell-Price, J., Savage, M. O., Stewart, P. M., et al. (2008). The diagnosis of cushing's syndrome: an endocrine society clinical practice guideline. *J. Clin. Endocrinol. and Metabolism* 93 (5), 1526–1540. doi:10.1210/jc.2008-0125

Popovic, V., Pekic, S., Pavlovic, D., Maric, N., Jasovic-Gasic, M., Djurovic, B., et al. (2004). Hypopituitarism as a consequence of traumatic brain injury (TBI) and its possible relation with cognitive disabilities and mental distress. *J. Endocrinol. Invest.* 27 (11), 1048–1054. doi:10.1007/bf03345308

R Core Team (2018). *R: a language and environment for statistical computing*. Vienna, Austria: R Foundation.

Resmini, E., Santos, A., Aulinas, A., Webb, S. M., Vives-Gilabert, Y., Cox, O., et al. (2016). Reduced DNA methylation of FKBP5 in Cushing's syndrome. *Endocrine* 54 (3), 768–777. doi:10.1007/s12020-016-1083-6

Resmini, E., Santos, A., Gomez-Anson, B., Vives, Y., Pires, P., Crespo, I., et al. (2012). Verbal and visual memory performance and hippocampal volumes, measured by 3-Tesla magnetic resonance imaging, in patients with Cushing's syndrome. *J. Clin. Endocrinol. and Metabolism* 97 (2), 663–671. doi:10.1210/jc.2011-2231

Sambrook, J., Fritsch, E. F., and Maniatis, T. (1989). *Molecular cloning: a laboratory manual*. Second Edition. New York: Cold Spring Harbor Laboratory Press.

Santos, A., Granell, E., Gomez-Anson, B., Crespo, I., Pires, P., Vives-Gilabert, Y., et al. (2017). Depression and anxiety scores are associated with amygdala volume in Cushing's syndrome: preliminary study. *BioMed Res. Int.* 2017, 1–7. doi:10.1155/2017/2061935

Santos, A., Resmini, E., Gomez-Anson, B., Crespo, I., Granell, E., Valassi, E., et al. (2015). Cardiovascular risk and white matter lesions after endocrine control of Cushing's syndrome. *Eur. J. Endocrinol.* 173 (6), 765–775. doi:10.1530/EJE-15-0600

Scammell, J. G., Denny, W. B., Valentine, D. L., and Smith, D. F. (2001). Overexpression of the FK506-binding immunophilin FKBP51 is the common cause of glucocorticoid resistance in three New World primates. *General Comp. Endocrinol.* 124 (2), 152–165. doi:10.1006/gcen.2001.7696

Seifuddin, F., Wand, G., Cox, O., Pirooznia, M., Moody, L., Yang, X., et al. (2017). Genome-wide Methyl-Seq analysis of blood-brain targets of glucocorticoid exposure. *Epigenetics* 12 (8), 637–652. doi:10.1080/15592294.2017.1334025

Shepard, J. D., Barron, K. W., and Myers, D. A. (2000). Corticosterone delivery to the amygdala increases corticotropin-releasing factor mRNA in the central amygdaloid nucleus and anxiety-like behavior. *Brain Res.* 861 (2), 288–295. doi:10.1016/s0006-8993(00)02019-9

Sonino, N., and Fava, G. A. (2001). Psychiatric disorders associated with Cushing's syndrome. Epidemiology, pathophysiology and treatment. *CNS Drugs* 15 (5), 361–373. doi:10.2165/00023210-200115050-00003

Spielberger, C. D., Gorsuch, R. L., Lushene, R., Vagg, P. R., and Jacobs, G. A. (1983). *Manual for the state-trait anxiety inventory*. Palo Alto, CA: Consulting Psychologists Press.

Starkman, M. N., Schteingart, D. E., and Schork, A. M. (1981). Depressed mood and other psychiatric manifestations of Cushing's syndrome: relationship to hormone levels. *Psychosom. Med.* 43 (1), 3–18. doi:10.1097/00006842-198102000-00002

StataCorp (2017). *Stata statistical software: release 15*. College Station, TX: StataCorp LLC.

Tanaka, M., Yoshida, M., Emoto, H., and Ishii, H. (2000). Noradrenaline systems in the hypothalamus, amygdala and locus coeruleus are involved in the provocation of anxiety: basic studies. *Eur. J. Pharmacol.* 405 (1-3), 397–406. doi:10.1016/s0014-2999(00)00569-0

Tiemensma, J., Kokshoorn, N. E., Biermasz, N. R., Keijser, B. J., Wassenaar, M. J., Middelkoop, H. A., et al. (2010). Subtle cognitive impairments in patients with long-term cure of Cushing's disease. *J. Clin. Endocrinol. and Metabolism* 95 (6), 2699–2714. doi:10.1210/jc.2009-2032

Tran, L., and Greenwood-Van Meerveld, B. (2012). Altered expression of glucocorticoid receptor and corticotropin-releasing factor in the central amygdala in response to elevated corticosterone. *Behav. Brain Res.* 234 (2), 380–385. doi:10.1016/j.bbr.2012.07.010

frontiers | Frontiers in Epigenetics and Epigenomics

TYPE Review
PUBLISHED 14 October 2024
DOI 10.3389/freae.2024.1464276



OPEN ACCESS

EDITED BY
Sandipan Brahma,
University of Nebraska Medical Center,
United States

REVIEWED BY
Boxun Li,
Duke University, United States
Mushan Li,
The Pennsylvania State University (PSU),
United States
Anna Maria Giuseppina Poma,
University of L'Aquila, Italy

*CORRESPONDENCE
Lei Cao-Lei,
lcao5@uottawa.ca

RECEIVED 13 July 2024
ACCEPTED 19 September 2024
PUBLISHED 14 October 2024

CITATION
Roe EA, Khov E, Kim H, Demelo B, Zavitz S and Cao-Lei L (2024) The impact of climate change-related disasters on mental health and epigenetics: a narrative review.
*Front. Epigenet. Epigenom.* 2:1464276.
doi: 10.3389/freae.2024.1464276



# The impact of climate change-related disasters on mental health and epigenetics: a narrative review

Emma Antonina Roe, Engluy Khov, Hannah Kim, Beth Demelo, Savannah Zavitz and Lei Cao-Lei*

Faculty of Health Sciences, University of Ottawa, Ottawa, ON, Canada

Climate change has contributed to an increase in the frequency and intensity of natural disasters such as droughts, wildfires, hurricanes, and floods, leading to both immediate physical harm and long-term mental health consequences. Survivors often experience psychological distress, including anxiety, depression, and post-traumatic stress disorder (PTSD), as a result of these traumatic events. This narrative review explores the intersection of climate change-related disasters, mental health outcomes, and epigenetic modifications. Specifically, we summarize recent findings on how environmental stressors influence both mental health and epigenetic changes, such as DNA methylation. Emerging evidence suggests that epigenetic mechanisms, particularly DNA methylation, could mediate the effects of climate change-related stress on mental health, potentially contributing to the onset of mental disorders like depression, panic disorder, autism spectrum disorder, and attention deficit hyperactivity disorder. We also discuss other epigenetic mechanisms, such as histone modifications and non-coding RNAs, and emphasize the importance of longitudinal studies to capture the dynamic nature of epigenetic changes over time. Finally, we propose future research directions to deepen our understanding of the complex relationships between climate change-related disasters, mental health outcomes, and epigenetic mechanisms, which will pave the way for more effective mental health interventions and policy integration.

KEYWORDS

**climate change, disaster, mental health, epigenetics, prevention and intervention**

## Introduction

Climate change has become an overwhelming issue over the last few decades. In 2023, the Intergovernmental Panel on Climate Change (IPCC) released its Sixth Assessment, report, declaring that the global climate is in a code red status and that "we are way off track" on reducing its impact. Consequently, there has been an increase in natural disasters, such as earthquakes, hurricanes, and floods, among other similar events. Those affected will often face physical or emotional damage through injury, death, relocation, and loss of livelihood (Masson-Delmotte et al., 2021).

Mental health is integral to a person's health and can be altered due to stressful life events, such as climate change-related disasters. Climate change directly and indirectly impacts the frequency and intensity of these natural disasters, causing immediate physical

damage and long-term effects on mental health and wellbeing. Survivors often experience stress, anxiety, depression, and post-traumatic stress disorder (PTSD) due to the psychological trauma associated with these events (Saeed and Gargano, 2022).

Epigenetics refers to heritable changes in gene expression that do not alter the underlying DNA sequence but can profoundly affect how genes are turned on or off, influencing an individual's development, physiology, and disease susceptibility (Bird, 2007). These modifications, such as DNA methylation, histone modification, and non-coding RNAs, regulate gene expression by altering chromatin structure or modifying RNA stability, enabling genes to respond to environmental stimuli (Allis and Jenuwein, 2016). Epigenetic changes are also reversible, offering therapeutic potential through drugs like DNMT and HDAC inhibitors that target aberrant epigenetic states linked to diseases (Singh et al., 2022). Understanding these mechanisms provides crucial insights into how environmental factors, including climate change-related disasters, impact health at the molecular level. As research progresses, it highlights the dynamic role of the epigenome in shaping health risks and offers new avenues for both public health interventions and novel treatments.

The objective of this narrative review is to explore the intersection of climate change, natural disasters, mental health, and epigenetics. Specifically, we summarize recent findings on the impact of common climate change-related disasters on both mental health and epigenetic changes. Additionally, we propose future research directions and offer perspectives to deepen the understanding of the complex relationships between climate change-related disasters, mental health outcomes, and epigenetic mechanisms.

## Climate change and related disasters

Climate change refers to significant and long-term changes in Earth's temperature, precipitation patterns, and atmospheric conditions, driven largely by human activities such as burning fossil fuels, deforestation, and industrial processes (IPCC, 2018; Nema et al., 2012). These activities have accelerated the accumulation of greenhouse gases like carbon dioxide and methane in the atmosphere, leading to global warming—a phenomenon that disrupts weather patterns and increases the frequency and severity of natural disasters (Masson-Delmotte et al., 2021). Natural disasters, which include sudden and severe events caused by environmental factors, pose significant threats to human health, safety, and wellbeing (Alexander, 2018). The increase in global temperatures has resulted in more frequent and severe disaster events, including droughts, storms, extreme heat, and heavy rainfall. In the following sections, we provide an overview of several common types of these disasters.

1) Droughts are prolonged periods of deficient rainfall exacerbated by rising temperatures and shifting precipitation patterns (Trenberth et al., 2014). They have severe consequences for agriculture, water supply, and ecosystems, impacting food security and livelihoods (He et al., 2019). Drought can impact respiratory health, mental health, and illnesses related to exposure to toxins, food/water security, rates of injury and infectious diseases (including food-, water- and vector-borne diseases) (Yusa et al., 2015). 2) Wildfires are exacerbated by climate change due to higher temperatures, drier conditions, and prolonged droughts (Di Virgilio et al., 2019). For instance, the devastating 2019-2020 Australian bushfires burned over 18.6 million hectares, causing substantial loss of life and biodiversity, underscoring climate change's impact on wildfire behavior (Haque et al., 2021). 3) Extreme precipitation events, intensified by climate change, result from warmer oceans holding more moisture, leading to more intense storms like hurricanes, typhoons, and cyclones (Trenberth, 2007). These storms bring heavy downpours and powerful winds, causing catastrophic flooding, landslides, and infrastructure damage, resulting in significant human and economic losses (Gordon and Young, 2021). 4) Floods occur when water submerges dry land, often due to heavy rainfall, rapid snowmelt, or storm surges from tropical cyclones. The 2010 floods in Pakistan, affecting over 20 million people, illustrate the widespread damage to infrastructure and displacement of communities caused by climate-induced flooding (Jacquet et al., 2016). 5) Ice storms, influenced by warmer ocean temperatures and altered precipitation patterns, can lead to heavy ice accumulation, resulting in widespread power outages, infrastructure damage, and hazardous travel conditions, as demonstrated during the 1998 Quebec ice storm (Germain and Martin, 2011). 6) Earthquakes, primarily caused by tectonic forces, can be indirectly influenced by climate change through factors like droughts, increased rainfall, melting glaciers, ice caps, and human activities such as fracking (Sadhukhan et al., 2022).

It is crucial to continuously monitor the trends in the frequency and intensity of climate change over time to inform public health and further research into the impact of climate change on the human population.

## The effect of climate change-related disasters on mental health

In the following section, we summarize recent publications that investigate the impact of various climate change-related disasters on mental health.

### Drought and heat waves

A systematic review conducted by Thompson et al. (2018) describes the mental health effects of high ambient temperature and heat waves. It investigates whether heat-related morbidity and mortality are increased among individuals with known mental disorders. This review concluded that high temperatures have a wide range of mental health effects, with the strongest evidence linking them to increased risk of suicide. Similarly, Hanigan and Chaston (2022) examined the impact of drought on suicide rates in rural New South Wales, Australia, and found that drought increases suicide rates among rural males aged 10–29 and 30–49 while decreasing rates among rural females aged 30–49. The exacerbating effects of climate change on these trends highlight the need for targeted interventions such as counseling services, community support networks, financial aid, and public health messaging. Addressing the mental health challenges posed by

drought requires multidisciplinary approaches and policy development to enhance community resilience. Furthermore, Varshney et al. (2023) provided a systematic review examining the global mental health outcomes of vulnerable populations affected by natural hazards such as drought and bushfires. They highlighted that such events disproportionately affect these groups, exacerbating pre-existing mental health issues and socioeconomic challenges, leading to increased anxiety, depression, PTSD, and suicidality. This review emphasizes the necessity for tailored mental health interventions and policies that address structural barriers and provide long-term support, promoting resilience and recovery in vulnerable communities. In a similar vein, Luong et al. (2021) investigated the intricate relationship between prolonged drought exposure and mental health among rural communities in New South Wales, Australia, showing that psychological distress initially rises during the early years of drought, but people gradually adapt, leading to decreased distress over time. However, this adaptation does not equate to complete recovery, as overall life satisfaction declines with long-term drought exposure. The study highlights the necessity for continuous support, resilient communities, and proactive drought management to address the persistent and complex mental health challenges posed by drought conditions. Adding to this body of research, Sewell et al. (2024) examined how concurrent heatwaves and droughts significantly increase mental health risks in children, adolescents, and young adults in North Carolina. Their findings showed that these climate events had a clear impact on emergency department visits for mood disorders and suicidality, especially among those in socioeconomically disadvantaged communities. The authors suggest targeted public health interventions and policy measures to enhance community resilience, improve access to resources, and address the social determinants of health to mitigate these impacts.

## Wildfires

The increasing frequency and intensity of wildfires, driven in part by climate change, have profound effects on mental health. Several studies have explored these impacts, revealing a range of psychological outcomes and identifying factors that contribute to mental health challenges following wildfire exposure. For instance, a study conducted by Cowlishaw et al. (2024) analyzed the relationship between Australian bushfires and mental health during the COVID-19 pandemic. Through semi-structured interviews and focus groups, the researchers assessed mental health outcomes following fire exposure. Their findings revealed six broad themes that helped situate the impacts of the pandemic within the context of adjustment and recovery processes after bushfires. This study underscores the compound nature of disasters and their multifaceted effects on mental health. Similarly, Isaac et al. (2023) investigated the impacts of wildfire on anxiety, insomnia, and trauma symptoms across participants from Australia, the United States, and Canada. Their research found that wildfire exposure led to negative outcomes in these areas, with participants in the USA reporting higher severity of symptoms. Moreover, female subjects exhibited higher rates of PTSD compared to their male counterparts, highlighting gender differences in psychological vulnerability to wildfire exposure. Several studies have specifically considered PTSD as an outcome of wildfire exposure. For example, Macleod et al. (2024) assessed levels of anxiety, depression, stress, PTSD, psychological wellbeing, and resilience following exposure to the 2019 Australian bushfires. Their results indicated that certain demographic factors, including sex, finances, and pre-existing mental health diagnoses, influenced mental health outcomes. Approximately half of the participants, regardless of direct exposure to the bushfires, met the clinical cutoff for depression and anxiety, with 35% of those directly affected meeting the PTSD cutoff criteria. This suggests that wildfire exposure has widespread mental health impacts that transcend direct physical harm. In a related study, Mellish et al. (2024) examined the psychological outcomes of direct and indirect exposure to the 2019/2020 Australian bushfires. The researchers found that 25% of the nonclinical group met the PTSD diagnosis cutoff criteria. Interestingly, those indirectly exposed exhibited higher rates of maladaptive and avoidant coping strategies and lower rates of posttraumatic growth. Furthermore, individuals indirectly exposed reported similar levels of distress as those directly exposed, indicating that even indirect experiences of wildfire can lead to significant psychological distress. The impact of wildfires on vulnerable populations has also been a focus of recent research. Saberi et al. (2023) analyzed the impact of the Northern California wildfires on people with HIV (PWH) and the clinicians providing care to them. The study reported heightened rates of anxiety, hypervigilance, stress, depression, sleep disturbances, and mental health-related coping strategies among PWH following wildfire exposure. Additionally, clinicians noted that their practice had been directly impacted by the wildfires for 2 years after the event, highlighting the long-term implications for healthcare providers and patients alike. Moreover, Watts et al. (2023) investigated PTSD rates and precipitating factors following South Australian bushfire exposure. Their study found that PTSD rates declined over time. However, predictive factors for PTSD included fear for one's life, loss of a loved one to the fires, loss of property, lower education levels, major life stressors, and being female. Notably, relocation following the fires was identified as a significant stressor for PTSD at the 2-year mark of self-reports, indicating that the process of recovery and adaptation continues long after the immediate disaster.

Collectively, these studies highlight the severe and varied mental health impacts of wildfires. Factors such as gender, direct versus indirect exposure, pre-existing conditions, and demographic characteristics influence psychological outcomes. Understanding these factors is crucial for developing effective interventions and support systems to mitigate the mental health consequences of wildfires.

## Hurricane and typhoon

A study conducted by Burrows et al. (2023) investigated the impact of the physical environment, specifically environmental greenness, on psychological distress outcomes following hurricane exposures. The results indicated significant connections between residential environmental greenness and distress levels, with perceived control over their environment being a notable influential factor on the participants. This study underscores the

importance of environmental factors in mitigating psychological distress post-disaster. Building on this, Acierno et al. (2006) analyzed the long-term impacts of hurricane exposure on trauma and mental health outcomes through a longitudinal study. Their findings concluded that older age was associated with a lower intensity of PTSD and depressive symptoms following exposure, highlighting the influence of age and recovery stressors on symptom intensity. These results align with the notion that recovery processes and personal attributes significantly impact mental health outcomes after a hurricane. Similarly, Cohen et al. (2023) conducted a study on the rates of depression and PTSD among Houston residents exposed to Hurricane Harvey during the pandemic. They determined that both stressors and traumas affected PTSD, with stressors acting as a primary influence on depressive symptoms. Miller et al. (2023) analyzed suicide mortality rates following Hurricane Florence and found an overall rate of 15.53 deaths per 100,000 people across a 4-year span for those aged ten and above who were affected by the hurricane. Interestingly, suicide mortality rates initially increased among the exposed group but later decreased to match those of the unexposed group. This trend indicates the complex and evolving nature of mental health impacts following hurricanes. In Puerto Rico, Sackey et al. (2023) investigated the influence of hurricane exposure on symptoms of depression, anxiety, and PTSD among teachers and students. The results revealed that experiences of loss, disruption of life, and an objective threat from the disaster were significant factors in determining the severity of mental health symptoms. A notable sex-effect indicated that participants identifying as female experienced more peritraumatic symptoms and measurable anxiety, emphasizing the role of gender in mental health outcomes post-disaster. Short et al. (2023) gathered data on parent-child dyads affected by Hurricane Harvey and assessed parental anxiety and depressive symptoms, children's emotional distress, and psychosocial tendencies. They found that parental mental health significantly influenced their children's emotional outcomes, with parental experiences of disruption and loss being predictive of emotional distress in the child. This highlights the intergenerational transmission of trauma and the importance of addressing family dynamics in post-disaster mental health interventions. Further, Wertis et al. (2023) investigated the influence of Hurricane Ida on community substance use, suicidal ideations, stress/anxiety, and bereavement. Data collected using a free Crisis Text Line (CTL) accessed by community members before and after Hurricane Ida revealed that the number of daily conversations through the CTL service peaked post-hurricane exposure. Reports of suicidal ideations, substance use, stress/anxiety, and bereavement were highest in the period after the hurricane, illustrating the widespread and immediate mental health impacts of such disasters. Lastly, Wang et al. (2023) analyzed the outcomes of parental PTSD on children's mental health following Typhoon Lekima. They found that the trajectory of parental PTSD directly correlated with the child's symptoms of PTSD and depression, impacting their feelings of safety. This study highlights the possibility of generational outcomes following exposure to natural disasters and underscores the need for family-centered mental health interventions.

In conclusion, these studies provide comprehensive insights into the mental health impacts of hurricanes and typhoons. They emphasize the importance of environmental, demographic, and familial factors in understanding and addressing the mental health needs of affected populations. The findings underscore the necessity for tailored interventions and ongoing support to mitigate the long-term psychological effects of such natural disasters.

## Flood

Brock et al. (2015) examined the impact of prenatal exposure to the 2008 Iowa floods on perinatal depression and maternal wellbeing and found that increased flood exposure during pregnancy was associated with increased depressive symptoms, significantly mediated by peritraumatic distress, and decreased wellbeing. These findings underscore the need for early psychological interventions to address distress in disaster-exposed populations and mitigate long-term mental health impacts. Similarly, Kingston et al. (2019) studied family resilience after the 2013 Alberta flood using longitudinal data. They found that children's adverse outcomes depended on factors such as genetics and home environment. Resilience was linked to changes in stress biomarkers, including cortisol, immune function, and metabolomics. This study highlights the importance of developing accurate resilience screening tools by comparing cortisol biomarkers, linking needs to interventions, understanding genetic influences, and informing mental health policy. In Germany, Schürr et al. (2023) investigated the short-term and long-term mental health impacts of the 2016 flood in Simbach am Inn on adolescents through a qualitative interview study. They identified key stressors such as family safety concerns, the extent of damage, and disrupted routines, while protective factors included strong family and community support. These findings emphasize the need for comprehensive mental health care, including educational programs, long-term support, and enhanced training for responders to better address adolescents' mental health needs post-disaster. Turning to Pakistan, Nadeem et al. (2023) addressed the mental and maternal health challenges faced by women in flood-affected communities. They highlighted the increased vulnerability to mental health issues such as PTSD, anxiety, and depression, along with unique maternal health challenges. This underscores the need for integrated, culturally relevant mental health support, mobile health units, and gender-sensitive disaster response strategies. In another study from Pakistan, Mahesar et al. (2024) investigated the profound impact of the 2022 floods on suicidal behavior by analyzing newspaper reports. The high prevalence of suicides, particularly among males and young adults in flood-affected regions, highlights the need for targeted mental health interventions, culturally sensitive approaches, and collaborative efforts between the government and nongovernmental organizations (NGOs) to address the unique psychological and socio-economic stressors faced by these populations. Integrating mental health support into disaster preparedness and response strategies will help mitigate the long-term mental health consequences of future disasters. Longman et al. (2019) examined the mental health impacts of the April 2017 floods in rural New South Wales, Australia. They found significant psychological distress and probable PTSD among individuals, especially among vulnerable groups such as the elderly, young, socio-economically disadvantaged, and Indigenous populations.

This study emphasizes the critical role of effective community and organizational responses in disaster situations. It advocates for integrating mental health considerations into disaster planning and policy development to enhance resilience and recovery in flood-affected communities. In Japan, Miyaji et al. (2022) explored the role of cognitive social capital in reducing the odds of developing PTSD among victims of heavy rainfall and flooding. They found that while cognitive social capital uniformly benefits mental health, the effects of structural social capital vary based on age and sex, with elderly women benefiting and elderly men potentially experiencing adverse effects. This study highlights the importance of using social capital interventions to improve mental health resilience after disasters. Finally, Cherry et al. (2023) explained the significant impact of severe weather events, like floods, on the mental health of middle-aged and older adults. They emphasized the role of various factors, such as age, social support, state hope, recovery stressors, and prior lifetime trauma, in predicting mental health outcomes like PTSD, depression, and worry. This study underscores the importance of mental health services, social support systems, and interventions based on hope theory to mitigate the adverse effects of disasters and promote resilience among affected individuals.

Taken together, these studies provide comprehensive insights into the mental health impacts of floods. They highlight the significance of early intervention, resilience factors, community support, and tailored mental health services in addressing the psychological aftermath of flooding. By integrating mental health considerations into disaster response strategies, it is possible to enhance the resilience and wellbeing of affected populations.

## Ice storm

Li et al. (2023) examined the long-term impacts of prenatal maternal stress (PNMS) resulting from the 1998 Quebec ice storm on brain structure and function in young adults. They discovered that individuals exposed to PNMS had larger gray matter volumes and increased functional connectivity in several brain regions compared to non-exposed controls. This study highlights the significant and lasting effects of prenatal stress on brain development, particularly emphasizing the timing of exposure and maternal cognitive appraisal. Cao-Lei et al. (2021) analyzed the impact of PNMS from the same natural disaster on hippocampal volumes in adolescents. Their research revealed significant gene-by-environment interactions, showing that PNMS affects hippocampal development differently in boys and girls, moderated by COMT and BDNF genetic variants. While objective hardship influenced hippocampal volume in both sexes, subjective distress had a sex-specific effect. These findings underscore the importance of considering genetic susceptibility and the nature of prenatal stressors in understanding brain development.

## Earthquakes

Recent studies have highlighted the significant impact of earthquakes on mental health, with increased risks of depression, PTSD, anxiety disorders, sleep disorders, and stress among survivors.

Research on the 2023 earthquakes in Turkey and Syria has provided valuable insights into these effects across different survivor groups. For instance, in a study on university students in Amman, Alfuqaha et al. (2023) investigated PTSD following an earthquake, finding that 26.20% reported extreme PTSD symptoms, coupled with low levels of meaning in life (ML) and social support (SS). Female students were particularly vulnerable to PTSD symptoms and faced challenges in seeking ML and SS. Complementing these findings, another study by Alpay and Aydın (2024) explored the predictive value of early peritraumatic reactions (e.g., dissociation, distress) for PTSD and depression among general survivors in Turkey, identifying dissociation as the strongest predictor for both conditions. Additionally, in Syria, Ataya et al. (2024) reported increased rates of depression, sleep problems, and anxiety disorders following the earthquake, with women being more susceptible to sleep disorders and depression, and young adults more vulnerable to sleep disorders.

Regarding the 2020 Turkey earthquake, Tanrıkulu et al. (2024) found that healthy subjects had a higher prevalence of earthquake-related PTSD compared to schizophrenia patients, with female gender increasing the risk among healthy subjects. This highlights the differential impact of earthquakes on mental health based on pre-existing conditions and demographics.

The long-term mental health impacts of the 2008 Wenchuan earthquake in China have also been extensively studied. For example, Chen et al. (2023a) identified three patterns of social support among survivors, finding that moderate and high support improved quality of life by reducing depressive symptoms. Another study by Chen et al. (2023b) demonstrated that accumulated stressful events exacerbated mental health problems, even with social support. Adding to this, Ma Z. et al. (2023) identified distinct PTSD trajectory groups among survivors, with specific symptoms predicting remission or chronic dysfunction in different groups. Research on the 1976 Tangshan earthquake in China has also provided valuable insights. Lu et al. (2023) revealed that prenatal exposure to earthquake stress increased the risk of depressive symptoms in adulthood, especially among females. Further, Ma W. et al. (2023) observed that earthquake-related experiences did not affect the severity of schizophrenia or PTSD, but older age and marital changes were linked to more severe PTSD symptoms.

Japan has experienced significant mental health impacts from earthquakes and tsunamis. Studies by Hikichi et al. (2023a); Hikichi et al. (2023b) on the 2011 earthquake and tsunami found correlations between housing damage, present bias, and delayed-onset posttraumatic stress symptoms (PTSS) among older adults. Notably, a higher sense of coherence (SOC) improved mental wellbeing in those with minor property damage. Following the 2016 Kumamoto earthquake, Matsuoka et al. (2023) reported that relocating to temporary housing had mixed effects on major depressive episodes, without clear links to PTSD symptoms.

In Korea, a study by Han (Han, 2023) investigated the impact of the 2016 Kyungju earthquake on mental health, finding that residents, particularly women, low-income individuals, and those near the epicenter, had a higher risk of mood disorders post-earthquake. This underscores the importance of considering

TABLE 1 Summary of studies investigating the association between climate change-related disasters and epigenetics.

| Authors | Exposure/Disaster | Participants | Sample | Methods | Results |
|---|---|---|---|---|---|
| Straight et al. (2022) | Maternal exposed to drought in Kenya in 2009 | 213 children, 104 exposed and 109 non-exposed controls (1.8–9.6 years old) | Saliva | Illumina Infinium MethylationEPIC Beadchip | 16 CpG sites were differently methylated, predominantly in metabolism and immune functioning. A CpG mediator, cg03771070 had a significant indirect effect of drought exposure on child body weight |
| Qiao et al. (2024) | Maternal exposed to drought in Kenya in 2009 | 213 children, 104 exposed and 109 non-exposed controls (1.8–9.6 years old) | Saliva | Illumina Infinium MethylationEPIC Beadchip | Three epigenetic clocks were seen to be altered: Hannum's (1st generation), GrimAge (2nd generation) and DNAm based telomere length (DNAmTL) clock (2nd generation). These have implications in chronic diseases and longevity |
| Xu et al. (2023) | Women exposed to wildfire | 479 Australian women, 132 female twin pairs, and 215 of their sisters (40–70 years old) | Blood | HumanMethylation450K Beadchip | The $PM_{2.5}$ from the exposed group was associated with DNA methylation measures. 26 CpGs and 33 DMRs were found associated with inflammatory regulation and platelet regulation |
| Kello et al. (2023) | Matenal exposure to Hurricane Maria in 2017 | 32 mother (16 High PNMS group and 16 low PNMS group) (average 31.2 ± 4.8 years) 32 children (26 male and 6 female (average 17.1 ± 4.3 months)) | Blood | Illumina Infinium MethylationEPIC Beadchip | 47 significant DMPs were identified, with 30 associated with gestational stage. Most DMPs were hypermethylated, clustering on chromosomes 1–4. DNA methylation differences were also linked to maternal mental status and property damage after the hurricane |
| Cao-Lei et al. (2014) | Matenal objective hardship resulted from 1998 Quebec ice storm | 34 children prenatally exposed to Quebec ice storm | T cells | Illumina Infinium Methylation450K Beadchip | Objective hardship was correlated with DNA methylation levels of 957 genes (1,675 CpGs) predominantly related to immune function |
| Cao-Lei et al. (2015) | Matenal cognitive appraisal resulted from 1998 Quebec ice storm | 34 children prenatally exposed to Quebec ice storm | T cells | Illumina Infinium Menthylation450K Beadchip | Cognitive appraisal was associated with 1564 different genes (2872 CpGs) predominantly related to immune function |
| Wang et al. (2022) | Prenatal Tangshan earthquake stress exposure | Prenatal exposed group (N = 100), Control group (N = 76) | Blood | Bisulfite sequencing | Prenatal earthquake exposure, particularly during the second trimester, was associated with higher NR3C1 methylation levels and impaired working memory. A moderate negative correlation was found between CpG1 methylation and working memory in the second trimester group |
| Mendoza-Ortega et al. (2021) | Maternal earthquake stress in Mexico City, 2017 | 83 mother-infant pairs (22 control infants, 24 pregnancies during earthquake and 37 concieved afterwards) | Umbilical cord blood | Quantitative real-time PCR | Newborns exposed *in utero* or conceived after the earthquake had significantly higher mtDNAcn compared to unexposed newborns |

socioeconomic factors in understanding the mental health impacts of earthquakes.

Salawali et al. (2020) highlighted posttraumatic growth (PTG) in adolescent survivors of the 2018 Palu earthquake, tsunami, and liquefaction in Indonesia. The study emphasized resilience and positive change facilitated by cognitive and acceptance commitment therapies, alongside social support, demonstrating the potential for growth even in the aftermath of disasters.

The combined impact of COVID-19 and earthquakes in Croatia during 2020 has been studied in different cohort groups. During the COVID-19 pandemic and the 2020 Croatia earthquake, Levaj et al. (2023) compared mental health outcomes and healthcare use among patients with severe mental illness, finding that additional care through Community Mental Health Teams (CMHTs) improved social support and healthcare access. In a complementary study, Šagud et al. (2023) reported higher levels of depression, stress, and fear related to COVID-19 and the 2020 Croatia earthquake among psychiatric patients, with individuals with depression and/or anxiety disorders being more vulnerable.

These studies provide valuable insights into the far-reaching impacts of climate change-induced earthquakes on mental health. They emphasize the importance of tailored interventions that address the specific needs of different age groups, genders, and demographic cohorts, highlighting the significance of mental health prevention and ongoing support in the face of traumatic events.

## The effect of climate change-related disasters on epigenetic modification

In the subsequent section, we explore the intricate associations between several climate change-related disasters and epigenetic modifications (Table 1).

### Drought

Straight et al. (2022) used a cohort of children who had been exposed to a drought *in utero* to investigate the long-term epigenetic effects. Through DNA methylation arrays, they discovered 16 CpG differences between the exposed cohort, and the same-sex control siblings. The CpG differences were linked mainly to metabolism and immune system pathways, leading to higher adipositivity in children exposed, as well as decreased immune function. They also found a different CpG mediator known as cg03771070 which was significantly associated with lowered body weight in the exposed group. A recent study by Qiao et al. (2024), suggests that droughts may be able to cause accelerated epigenetic aging *in utero*, due to the stress experienced by the mother. Through blood samples of children who were affected by droughts, and compared against their same-sex unexposed siblings, a positive association with epigenetic age acceleration (EAA) through two epigenetic clocks was found: Hannum's clock (Hannum et al., 2013), a first-generation epigenetic clock that serves as a lifespan predictor and GrimAge's clock (Lu et al., 2019), a second-generation clock known for predicting disease risk. A negative association with EAA was found with another second-generation clock: DNA methylation-based telomere length (DNAmTL) clock. The combined effect of these associations leads to increased risk of chronic diseases and loss of genetic longevity due to the stress experienced by the mothers during a drought.

### Wildfire

A recent study has identified biological markers indicating changes to the human epigenome following wildfire smoke exposure. A research group (Xu et al., 2023) studied the associations between long-term exposure to wildfire related-PM2.5 and blood DNA methylation in 479 Australian women, including 132 female twin pairs and 215 of their sisters. Using the HumanMethylation450K Beadchip, the study revealed that long-term exposure to wildfire-related PM2.5 (>3 years) was associated with differences in blood DNA methylation of 26 CpGs and 33 differentially methylated regions (DMRs). These genomic regions were mapped to 47 genes enriched for pathways related to inflammatory regulation and platelet activation, and were linked to various human diseases and phenotypes, including cancer, mental disorders, diabetes, obesity, asthma, and blood pressure. This study underscores the potential for wildfire smoke exposure to induce epigenetic changes, which may contribute to the development of mental health problems. Understanding these mechanisms is crucial for developing targeted interventions to mitigate the adverse mental health effects of wildfire exposure.

### Hurricane

Kello et al. (2023) investigated hurricane Maria, which was one of the largest natural disasters to affect Puerto Rico. The authors reported that 47 significant differentially methylated probes (DMPs) were associated with various hurricane-related variables, with 30 significant DMPs specifically linked to the gestational stage at the time of the hurricane. Most of the DMPs associated with the timing of exposure were hypermethylated, and the most significant clusters were located on chromosomes 1–4. Additionally, maternal mental status and property damage following the hurricane were associated with notable variations in DNA methylation patterns. These findings suggest that both the timing of prenatal exposure and post-hurricane stressors may influence DNA methylation, potentially affecting long-term health outcomes.

### Ice storm

A study investigating genome-wide DNA methylation levels in adolescents found that maternal objective hardship led to methylation changes in genes involved in immune function, whereas maternal subjective distress did not impact genome-wide methylation profiles (Cao-Lei et al., 2014). Using blood samples from 13-year-olds, T cell DNA was analyzed with the Illumina HumanMethylation450K Beadchip, revealing comparability of methylation profiles across T cells, saliva, and peripheral blood mononuclear cells (PBMCs). Additionally, maternal cognitive

appraisal was linked to methylation changes in immune-related genes (Cao-Lei et al., 2015). The overlap in genes and biological pathways associated with cognitive appraisal and objective hardship suggests distinct yet interconnected pathways through which different aspects of prenatal stress affect methylation.

### Earthquake

Wang et al. (2022) investigated the association between prenatal exposure to stress caused by the 1976 Tangshan earthquake in China and the methylation of CpG sites within the NR3C1 exon 1F promoter. The researchers also explored how these epigenetic modifications may impact working memory in adulthood. The findings indicated that individuals prenatally exposed to the earthquake exhibited significantly higher NR3C1 methylation levels compared to those who were not exposed to such stress. Notably, among those exposed, individuals in the second trimester showed significantly higher methylation levels than those in the third trimester. Additionally, impaired working memory was observed in subjects exposed to prenatal earthquakes during the second trimester. The study found a moderate negative correlation between methylated CpG1 in the NR3C1 exon 1F promoter and working memory specifically in the second trimester group, suggesting that CpG1 methylation may play a role in the relationship between earthquake-related prenatal stress and long-term effects on working memory. Moreover, a study from the OBESO perinatal cohort in Mexico City investigated the impact of acute gestational stress from the 2017 earthquake on mitochondrial DNA copy number (mtDNAcn) (Mendoza-Ortega et al., 2021). The researchers compared mtDNAcn in umbilical cord blood from infants born before the earthquake, those whose mothers were pregnant during the earthquake, and those conceived after the earthquake. Using quantitative real-time PCR, they found that newborns exposed to the earthquake *in utero* or conceived afterward had significantly higher mtDNAcn than those not exposed, suggesting mtDNAcn as a potential biomarker for acute stress. The study emphasizes the importance of long-term monitoring of children born to mothers who experienced prenatal stress, especially from natural disasters.

## The potential role of epigenetics in prevention and intervention

Integrating epigenetic research into therapeutic and preventive strategies for mental health offers promising opportunities to develop personalized interventions aimed at mitigating the adverse effects of climate change on mental wellbeing. Epigenetic markers act as accessible and dynamic biosensors, capturing both biological and biographical risks for mental disorders, making them valuable not only as indicators but also as targets for preventive measures (Domschke, 2021). Musci and Schlomer (2018) emphasize the importance of including genetic and epigenetic research in preventive medicine, arguing that understanding these factors allows for the creation of individualized interventions that can prevent the onset of mental disorders.

Domschke (Domschke, 2021) further suggests that targeting epigenetic markers in prevention could foster resilience against mental disorders, potentially halting their transmission to future generations. This concept of "epigenetic memory" for environmental adaptations is particularly relevant given evidence that epigenetically imprinted trauma can be passed across generations through the germline (Bohacek and Mansuy, 2015). Such findings raise the possibility of "transgenerational prevention" where successful interventions embodied in epigenetic signatures could equip future generations with an enhanced ability to adapt to environmental stressors, including those linked to climate change.

Moreover, research by Hong and Efferth (2016) demonstrated a link between epigenetic modifications and PTSD risk and memory function in survivors of the Wenchuan earthquake, highlighting the need for further studies on patient-specific criteria, social support roles, and alternative treatments such as Chinese medicine. Olson et al. (2019) also stress the need to explore the epigenetic changes triggered by natural disasters, particularly in terms of adverse effects on pregnancy and fetal development, which could have lasting, transgenerational impacts.

By deepening our understanding of the genetic and epigenetic mechanisms underlying mental health disorders and their environmental triggers, more effective strategies can be developed to build resilience and prevent the transmission of these disorders across generations. Future research should prioritize early interventions, policy integration, and public health strategies that address the large-scale risk factors posed by climate change-related disasters, paving the way for more robust mental health prevention and intervention efforts.

## Perspectives

Despite significant strides in understanding the impacts of climate change-related disasters on mental health and epigenetic modifications, several critical gaps persist in the current literature.

### Sex effect

The influence of climate change on natural disasters cannot be overlooked, as it directly and indirectly impacts the occurrence of such events. Above-mentioned studies have revealed that various disasters have an impact on women more than men, and women are more susceptible to experiencing poor sleep quality, depression disorders, mood disorders, and PTSD in comparison to men (Alfuqaha et al., 2023; Ataya et al., 2024; Chen et al., 2023b; Han, 2023; Hikichi et al., 2023a; Lu et al., 2023). Research indicates that biological sex can influence susceptibility to stress and subsequent epigenetic alterations, yet studies often do not disaggregate findings by sex. Future research should systematically examine how sex differences influence the manifestation of epigenetic changes and mental health responses.

### Vulnerable populations

Climate shifts have increased the range and seasonality of vector-borne diseases, creating global public health challenges

and affecting vulnerable populations (Romanello et al., 2021). Children are more likely to be susceptible to the health impacts of climate change-related disasters, such as respiratory issues, heat stress, and infectious diseases (Romanello et al., 2021). With their developing bodies, children breathe more air, drink more water, and spend more time outdoors relative to their body weight, making them more susceptible to environmental hazards like air and water contamination (Makharia et al., 2023). Older adults face greater risks from reduced physiological resilience and often pre-existing health conditions. There is increased sensitivity to environmental changes and exposures as a by-product of lowered physiological reserve capacity, slower metabolism, and a slower immune system (Carnes et al., 2014). Moreover, low-income communities are disproportionately affected by the health and environmental consequences of climate change (Levy and Patz, 2015). They are more likely to be exposed to environmental hazards without the proper resources to reduce the impact. People with lower socioeconomic status are more likely to live in regions highly exposed to the risk of climate change (e.g., flood-prone regions), areas with poor air quality, or near industrial sites, which negatively impact health (Makharia et al., 2023). Furthermore, Indigenous communities around the world continue to face political, economic, and racial marginalization, further burdened by the effects of climate change (Redvers et al., 2023). Environmental changes from climate change, such as the loss of traditional lands and ecosystems, were found to significantly impact the mental health of Indigenous peoples living in their traditional territories. It included acute psychological stress from environmental changes, climate-related disasters, and cultural and spiritual dislocation due to the loss of traditional lands and practices (Grande et al., 2023). It heightened social and economic pressures that exacerbate existing health inequalities. Despite these challenges, Indigenous communities show resilience, using their knowledge and social networks to adapt to the adverse effects of climate change. Climate policies and interventions should understand the Indigenous perspectives and needs, implementing culturally tailored mental health services and support systems. Therefore, more attention should be given to the unique experiences and coping mechanisms of vulnerable populations in the face of climate change in order to develop effective strategies that prioritize their wellbeing and sustainability.

## Combined effects of disasters

The difficulty of studying the combined effects of multiple disasters, such as extreme temperatures and pandemics, presents significant challenges in understanding and addressing their mental health and epigenetic impacts. The occurrence of disasters, like those observed during the COVID-19 pandemic, exacerbates the complexity of these effects. In addition, according to the 2021 IPCC report, it is anticipated that as global warming progresses, extreme temperatures will become more frequent. All data models indicate a 1.5-degree Celsius rise in global temperatures by 2050, which will likely increase the frequency and intensity of heatwaves and other extreme weather events (2021). Recent studies underscore this trend, revealing a significant increase in the frequency of heatwaves since the mid-twentieth century, particularly in regions already vulnerable to climate change (Perkins-Kirkpatrick and Lewis, 2020). Additionally, research by Sanches et al. observed a rise in the intensity and frequency of surface air temperature extremes along the western South Atlantic coast over the past 40 years, further highlighting the escalating threat posed by extreme temperatures (Sanches et al., 2023). Addressing the mental health and epigenetic impacts of these climate change-induced disasters, especially in the context of concurrent events, requires a multifaceted approach. Research must consider the interplay between various stressors and their cumulative effects on mental health and epigenetic modifications. This holistic understanding is crucial for developing effective intervention strategies to mitigate the adverse health impacts of climate change-related disasters.

## Potential mediating role of epigenetics

As previously discussed, we have provided evidence demonstrating how these climate change-related disasters influence both mental health outcomes and epigenetic changes. Epigenetic mechanisms, particularly DNA methylation, offer a dynamic system by which environmental factors, such as stress induced by natural disasters, can regulate gene expression and contribute to long-term psychological impacts.

Recent studies have highlighted the potential of DNA methylation as a significant contributor to various mental disorders, including depressive disorder, panic disorder, autism spectrum disorder (ASD), attention deficit hyperactivity disorder (ADHD), and borderline personality disorder. For instance, Barbu et al. (2021) established a Methylation Risk Score (MRS) for Major Depressive Disorder (MDD), which was correlated with both current and future depression. This score demonstrated associations with lifestyle factors, such as smoking and alcohol use, both of which are known to influence DNA methylation and contribute to depression (Barbu et al., 2021). In line with these findings, Czamara et al. (2022) investigated the relationship between DNA methylation, panic disorder (PD), and MDD in response to stressful life events. Their results showed that gene expression alterations in PYROXD1 and GFOD2 were significantly associated with PD and MDD (Czamara et al., 2022). Furthermore, the InterGEN study involving Black women provided evidence that psychosocial stressors could induce alterations in DNA methylation, which were linked to depressive symptoms. The study identified several genes, including GLRX5, CLEC1B, and NBPF8, among others, that were associated with depressive symptoms and neurological diseases (Taylor et al., 2024). Additional research has also supported the role of epigenetics in mediating mental health outcomes related to other environmental stressors. Chrétienneau et al. (2024) found distinct DNA methylation patterns in the OXTR, CRH, and NTF3 genes in individuals with substance use disorders (SUD) who had experienced paternal abuse, linking these patterns to an elevated risk of suicidal behavior (Chrétienneau et al., 2024). Similarly, Zhu et al. (2022) demonstrated that placental DNA methylation of the NHIP gene is associated with increased ASD risk in high-risk cohorts (Zhu et al., 2022). Feil et al. (2023) also explored the relationship between air pollution and neurodevelopmental

delays, showing that DNA methylation in genes such as GOPC and DYRK1A mediated the effects of air pollution on cognitive development (Feil et al., 2023). Another noteworthy example is the study by Fotopoulos et al. (2024), which combined neuroimaging and epigenetics to investigate the impact of prenatal smoking on children with ADHD. The findings revealed significant reductions in cortical surface area in brain regions linked to attention regulation and impulsivity, suggesting that epigenetic markers can be used to assess prenatal smoking exposure and its subsequent effects on brain development and ADHD (Fotopoulos et al., 2024).

These findings provide evidence that epigenetic modifications, particularly DNA methylation, could mediate the impact of various environmental stressors on mental health. As research in this field continues to evolve, the role of epigenetics in linking environmental factors, such as climate change-related disasters, to mental health outcomes becomes increasingly clear. Future research should focus on expanding our understanding of these epigenetic pathways and identifying potential therapeutic targets for mitigating the mental health consequences of such environmental stressors.

## Other mechanisms of epigenetics and the need for longitudinal studies

While much of the current research has focused on DNA methylation, it is essential to recognize that other epigenetic mechanisms, such as histone modifications and non-coding RNAs, are also crucial regulators of gene expression. These mechanisms may play significant roles in mediating responses to environmental stressors, including those related to climate change. To gain a more comprehensive understanding of the long-term mental health impacts of such stressors, future research should expand beyond DNA methylation and explore the broader epigenetic landscape. This includes investigating histone modifications, chromatin remodeling, and non-coding RNA interactions, all of which may contribute to the complex regulatory networks that influence mental health.

Moreover, there is a pressing need for longitudinal studies that track individuals over extended periods to capture the dynamic nature of epigenetic changes and their interaction with genetic and environmental factors. Longitudinal designs can reveal whether initial epigenetic modifications persist or evolve in response to ongoing stressors, potentially serving as biomarkers for long-term mental health risks exacerbated by climate-related disasters. These studies should also consider developmental windows of vulnerability, examining how disaster exposure shapes epigenetic profiles and mental health trajectories across the lifespan. By monitoring these changes over time, researchers can identify critical periods of susceptibility and resilience, informing the development of more targeted and personalized interventions to mitigate the adverse mental health effects of climate-related stress.

Integrating multi-omics approaches into longitudinal studies will further enhance our understanding of how various epigenetic mechanisms contribute to mental health outcomes, ultimately paving the way for more effective prevention and intervention strategies in the context of environmental stress.

# Conclusion

The review underscores the complex interplay between climate change-related disasters, mental health outcomes, and epigenetic modifications. While much of the current research has focused on DNA methylation, it is crucial to explore other epigenetic mechanisms, such as histone modifications and non-coding RNAs, to gain a more comprehensive understanding of how these mechanisms mediate the long-term mental health effects of environmental stressors. The evidence suggests that epigenetic markers serve not only as indicators of mental health risks but also as potential targets for personalized preventive interventions, which may help build resilience against mental disorders and mitigate their transmission to future generations. However, significant gaps remain in the literature, particularly regarding the combined effects of multiple disasters and the long-term impact of these events on epigenetic changes. Future research should focus on integrating multi-omics approaches, conducting longitudinal studies, and developing tailored interventions that address the unique needs of vulnerable populations. By advancing our understanding of these epigenetic pathways, we can create more effective strategies for preventing and mitigating the mental health consequences of climate change-related disasters.

# Author contributions

ER: Investigation, Resources, Writing–original draft, Writing–review and editing. EK: Investigation, Resources, Writing–original draft, Writing–review and editing. HK: Investigation, Resources, Writing–original draft, Writing–review and editing. BD: Investigation, Resources, Writing–original draft, Writing–review and editing. SZ: Investigation, Resources, Writing–original draft, Writing–review and editing. LC-L: Conceptualization, Investigation, Supervision, Writing–original draft, Writing–review and editing.

# Funding

The author(s) declare that no financial support was received for the research, authorship, and/or publication of this article.

# Conflict of interest

The authors declare that the research was conducted in the absence of any commercial or financial relationships that could be construed as a potential conflict of interest.

# Publisher's note

# References


Acierno, R., Ruggiero, K. J., Kilpatrick, D. G., Resnick, H. S., and Galea, S. (2006). Risk and protective factors for psychopathology among older versus younger adults after the 2004 Florida hurricanes. *Am. J. Geriatr. Psychiatry* 14 (12), 1051–1059. doi:10.1097/01.JGP.0000221327.97904.b0

Alexander, D. (1993). *Natural disasters*. 1st Edn. Routledge. doi:10.4324/9781315859149

Alfuqaha, O. A., Al-Masarwah, U. M., Farah, R. I., Yasin, J. A., Alkuttob, L. A., Muslieh, N. I., et al. (2023). The impact of Turkey and Syria earthquakes on university students: posttraumatic stress disorder symptoms, meaning in life, and social support. *Behav. Sci.* 13, 587. doi:10.3390/bs13070587

Allis, C. D., and Jenuwein, T. (2016). The molecular hallmarks of epigenetic control. *Nat. Rev. Genet.* 17, 487–500. doi:10.1038/nrg.2016.59

Alpay, E. H., and Aydın, A. (2024). Effects of peritraumatic reactions on post-traumatic stress among Kahramanmaras earthquake survivors. *Nordic J. Psychiatry* 78, 153–161. doi:10.1080/08039488.2023.2291548

Ataya, J., Soqia, J., Ataya, J., AlMhasneh, R., Batesh, D., Alkhadraa, D., et al. (2024). Sleep quality and mental health differences following Syria-Turkey earthquakes: a cross-sectional study. *Int. J. Soc. Psychiatry* 70, 700–708. doi:10.1177/00207640231223432

Barbu, M. C., Shen, X., Walker, R. M., Howard, D. M., Evans, K. L., Whalley, H. C., et al. (2021). Epigenetic prediction of major depressive disorder. *Mol. Psychiatry* 26, 5112–5123. doi:10.1038/s41380-020-0808-3

Bird, A. (2007). Perceptions of epigenetics. *Nature* 447, 396–398. doi:10.1038/nature05913

Bohacek, J., and Mansuy, I. M. (2015). Molecular insights into transgenerational non-genetic inheritance of acquired behaviours. *Nat. Rev. Genet.* 16, 641–652. doi:10.1038/nrg3964

Brock, R. L., O'Hara, M. W., Hart, K. J., McCabe-Beane, J. E., Williamson, J. A., Brunet, A., et al. (2015). Peritraumatic distress mediates the effect of severity of disaster exposure on perinatal depression: the Iowa flood study. *J. Trauma Stress* 28, 515–522. doi:10.1002/jts.22056

Burrows, K., Fong, K. C., Lowe, S. R., Fussell, E., and Bell, M. L. (2023). The impact of residential greenness on psychological distress among Hurricane Katrina survivors. *PLoS One* 18, e0285510. doi:10.1371/journal.pone.0285510

Cao-Lei, L., Elgbeili, G., Massart, R., Laplante, D. P., Szyf, M., and King, S. (2015). Pregnant women's cognitive appraisal of a natural disaster affects DNA methylation in their children 13 years later: Project Ice Storm. *Transl. Psychiatry* 5 (2), e515. doi:10.1038/tp.2015.13

Cao-Lei, L., Massart, R., Suderman, M. J., Machnes, Z., Elgbeili, G., Laplante, D. P., et al. (2014). DNA methylation signatures triggered by prenatal maternal stress exposure to a natural disaster: Project Ice Storm. *PLoS One* 9, e107653. doi:10.1371/journal.pone.0107653

Cao-Lei, L., Yogendran, S., Dufoix, R., Elgbeili, G., Laplante, D. P., and King, S. (2021). Prenatal maternal stress from a natural disaster and hippocampal volumes: gene-by-environment interactions in young adolescents from Project ice storm. *Front. Behav. Neurosci.* 15, 706660. doi:10.3389/fnbeh.2021.706660

Carnes, B. A., Staats, D., and Willcox, B. J. (2014). Impact of climate change on elder health. *Journals Gerontology Ser. A* 69, 1087–1091. doi:10.1093/gerona/glt159

Chen, X. Y., Shi, X., Li, C., and Fan, F. (2023a). Longitudinal associations between social support trajectories and quality of life mediated by depressive symptoms: a 10-year cohort study of Wenchuan earthquake. *J. Adolesc.* 95, 1702–1714. doi:10.1002/jad.12239

Chen, X. Y., Wang, D., Liu, X., Shi, X., Scherffius, A., and Fan, F. (2023b). Cumulative stressful events and mental health in young adults after 10 years of Wenchuan earthquake: the role of social support. *Eur. J. Psychotraumatology* 14, 2189399. doi:10.1080/20008066.2023.2189399

Cherry, K. E., Miller, L. R., Bordes, P. J., Calamia, M. R., Elliott, E. M., Sampson, L., et al. (2023). Longitudinal assessment of mental health after a flood: roles of social support, hope, recovery stressors, and prior lifetime trauma. *Aging and Ment. Health* 27, 2446–2456. doi:10.1080/13607863.2023.2191927

Chrétienneau, C., Spindola, L. M., Vorspan, F., Lagerberg, T. V., Marie-Claire, C., Bellivier, F., et al. (2024). An epigenetic candidate-gene association study of parental styles in suicide attempters with substance use disorders. *Addict. Biol.* 29, e13392. doi:10.1111/adb.13392

Cohen, G. H., Wang, R., Sampson, L., Lowe, S. R., Ettman, C. K., Abdalla, S. M., et al. (2023). Depression and PTSD among Houston residents who experienced hurricane Harvey and COVID-19: implications for urban areas affected by multiple disasters. *J. Urban Health* 100, 860–869. doi:10.1007/s11524-023-00767-2

Cowlishaw, S., O'Dwyer, C., Bowd, C., Sadler, N., O'Donnell, M., Forbes, D., et al. (2024). Pandemic impacts and experiences after disaster in Australia: qualitative study of compound impacts following the Black Summer bushfires. *BJPsych Open* 10, e43. doi:10.1192/bjo.2023.648

Czamara, D., Neufang, A., Dieterle, R., Iurato, S., Arloth, J., Martins, J., et al. (2022). Effects of stressful life-events on DNA methylation in panic disorder and major depressive disorder. *Clin. Epigenetics* 14, 55. doi:10.1186/s13148-022-01274-y

Di Virgilio, G., Evans, J. P., Blake, S. A., Armstrong, M., Dowdy, A. J., Sharples, J., et al. (2019). Climate change increases the potential for extreme wildfires. *Geophys. Res. Lett.* 46, 8517–8526. doi:10.1029/2019gl083699

Domschke, K. (2021). Prevention in psychiatry: a role for epigenetics? *World Psychiatry* 20, 227–228. doi:10.1002/wps.20854

Feil, D., Abrishamcar, S., Christensen, G. M., Vanker, A., Koen, N., Kilanowski, A., et al. (2023). DNA methylation as a potential mediator of the association between indoor air pollution and neurodevelopmental delay in a South African birth cohort. *Clin. Epigenetics* 15, 31. doi:10.1186/s13148-023-01444-6

Fotopoulos, N. H., Chaumette, B., Devenyi, G. A., Karama, S., Chakravarty, M., Labbe, A., et al. (2024). Maternal smoking during pregnancy and cortical structure in children with attention-deficit/hyperactivity disorder. *Psychiatry Res.* 334, 115791. doi:10.1016/j.psychres.2024.115791

Germain, D., and Martin, J.-P. (2011). The vulnerability of northern cities to weather-related hazards: case studies from the Province of Quebec, eastern Canada. *Adv. Environ. Res.* 22, 143–160.

Gordon, G. A., and Young, R. R. (2021). "Natural hazards: hurricanes, cyclones, and typhoons," in *Encyclopedia of security and emergency management*, 676–683.

Grande, A. J., Dias, I., Jardim, P. T. C., Vieira Machado, A. A., Soratto, J., da Rosa, M. I., et al. (2023). Climate change and mental health of Indigenous peoples living in their territory: a concept mapping study. *Front. Psychiatry* 14, 1237740. doi:10.3389/fpsyt.2023.1237740

Han, C. (2023). Seismic activity and development of mood disorders: findings from the 2016 Kyungju earthquake. *Sci. Total Environ.* 867, 161328. doi:10.1016/j.scitotenv.2022.161328

Hanigan, I. C., and Chaston, T. B. (2022). Climate change, drought and rural suicide in New South Wales, Australia: future impact scenario projections to 2099. *Int. J. Environ. Res. Public Health* 19, 7855. doi:10.3390/ijerph19137855

Hannum, G., Guinney, J., Zhao, L., Zhang, L., Hughes, G., Sadda, S., et al. (2013). Genome-wide methylation profiles reveal quantitative views of human aging rates. *Mol. Cell* 49, 359–367. doi:10.1016/j.molcel.2012.10.016

Haque, M. K., Azad, M. A. K., Hossain, M. Y., Ahmed, T., Uddin, M., and Hossain, M. M. (2021). Wildfire in Australia during 2019-2020, its impact on health, biodiversity and environment with some proposals for risk management: a review. *J. Environ. Prot.* 12, 391–414. doi:10.4236/jep.2021.126024

He, X., Estes, L., Konar, M., Tian, D., Anghileri, D., Baylis, K., et al. (2019). Integrated approaches to understanding and reducing drought impact on food security across scales. *Curr. Opin. Environ. Sustain.* 40, 43–54. doi:10.1016/j.cosust.2019.09.006

Hikichi, H., Sawada, Y., Aida, J., Kondo, K., and Kawachi, I. (2023a). Association between housing damage, present bias and delayed-onset post-traumatic stress symptoms among older adults 9 years after a natural disaster. *J. Epidemiol. Community Health* 77, 494–500. doi:10.1136/jech-2022-220218

Hikichi, H., Shiba, K., Aida, J., Kondo, K., and Kawachi, I. (2023b). Association between sense of coherence and health and well-being among older survivors of a natural disaster: a prospective outcome-wide study. *Sci. Rep.* 13, 16385. doi:10.1038/s41598-023-43672-z

Hong, C., and Efferth, T. (2016). Systematic review on post-traumatic stress disorder among survivors of the wenchuan earthquake. *Trauma Violence Abuse* 17, 542–561. doi:10.1177/1524838015585313

IPCC (2018). "Global Warming of 1.5° C. An IPCC Special Report on the impacts of global warming of 1.5° C above pre-industrial levels and related global greenhouse gas emission pathways," in *The context of strengthening the global response to the threat of climate change, sustainable development, and efforts to eradicate poverty* (Geneva: ipcc).

Isaac, F., Toukhsati, S. R., Klein, B., Di Benedetto, M., and Kennedy, G. A. (2023). Differences in anxiety, insomnia, and trauma symptoms in wildfire survivors from Australia, Canada, and the United States of America. *Int. J. Environ. Res. Public Health* 21, 38. doi:10.3390/ijerph21010038

Jacquet, G. A., Kirsch, T., Durrani, A., Sauer, L., and Doocy, S. (2016). Health care access and utilization after the 2010 Pakistan floods. *Prehospital disaster Med.* 31, 485–491. doi:10.1017/s1049023x16000716

Kello, E., Vieira, A. R., Rivas-Tumanyan, S., Campos-Rivera, M., Martinez-Gonzalez, K. G., Buxó, C. J., et al. (2023). Pre- and peri-natal hurricane exposure alters DNA methylation patterns in children. *Sci. Rep.* 13, 3875. doi:10.1038/s41598-023-30645-5

Kingston, D., Mughal, M. K., Arshad, M., Kovalchuk, I., Metz, G. A. S., Wynne-Edwards, K., et al. (2019). Prediction and understanding of resilience in albertan families: longitudinal study of disaster responses (PURLS) - protocol. *Front. Psychiatry* 10, 729. doi:10.3389/fpsyt.2019.00729

Levaj, S., Medved, S., Grubišin, J., Tomašić, L., Brozić, K., Shields-Zeeman, L., et al. (2023). The impact of the COVID-19 pandemic and earthquake on mental health of persons with severe mental illness: a survey study among people receiving community

mental health care versus treatment as usual in Croatia. *Int. J. Soc. Psychiatry* 69, 653–663. doi:10.1177/00207640221130966

Levy, B. S., and Patz, J. A. (2015). Climate change, human rights, and social justice. *Ann. Glob. Health* 81, 310–322. doi:10.1016/j.aogh.2015.08.008

Li, X., Qureshi, M. N. I., Laplante, D. P., Elgbeili, G., Jones, S. L., Long, X., et al. (2023). Atypical brain structure and function in young adults exposed to disaster-related prenatal maternal stress: Project Ice Storm. *J. Neurosci. Res.* 101, 1849–1863. doi:10.1002/jnr.25246

Longman, J. M., Bennett-Levy, J., Matthews, V., Berry, H. L., Passey, M. E., Rolfe, M., et al. (2019). Rationale and methods for a cross-sectional study of mental health and wellbeing following river flooding in rural Australia, using a community-academic partnership approach. *BMC Public Health* 19, 1255. doi:10.1186/s12889-019-7501-y

Lu, A. T., Quach, A., Wilson, J. G., Reiner, A. P., Aviv, A., Raj, K., et al. (2019). DNA methylation GrimAge strongly predicts lifespan and healthspan. *Aging (Albany NY)* 11, 303–327. doi:10.18632/aging.101684

Lu, W. T., Zhao, X. C., Wang, R., Li, N., Song, M., Wang, L., et al. (2023). Long-term effects of early stress due to earthquake exposure on depression symptoms in adulthood: a cross-sectional study. *Injury* 54, 207–213. doi:10.1016/j.injury.2022.07.047

Luong, T. T., Handley, T., Austin, E. K., Kiem, A. S., Rich, J. L., and Kelly, B. (2021). New insights into the relationship between drought and mental health emerging from the Australian rural mental health study. *Front. Psychiatry* 12, 719786. doi:10.3389/fpsyt.2021.719786

Ma, W., Lei, R., Sun, Y., Liang, X., Zhang, S., Wang, C., et al. (2023a). A study of post-traumatic stress disorder in schizophrenic patients 35 years after experiencing the Tangshan earthquake. *Brain Behav.* 13, e2963. doi:10.1002/brb3.2963

Ma, Z., Wang, D., Fu, X., Tao, Y., Zhang, Y., Liu, W., et al. (2023b). Prospective network of post-traumatic stress disorder (PTSD) symptoms across adolescent survivors with distinct trajectories of PTSD: a cohort study of the Wenchuan earthquake. *J. Anxiety Disord.* 99, 102767. doi:10.1016/j.janxdis.2023.102767

Macleod, E., Heffernan, T., Greenwood, L. M., Walker, I., Lane, J., Stanley, S. K., et al. (2024). Predictors of individual mental health and psychological resilience after Australia's 2019-2020 bushfires. *Aust. N. Z. J. Psychiatry* 58, 58–69. doi:10.1177/00048674231175618

Mahesar, R. A., Khalil, H., Shaikh, S., Kalhoro, A., Rajar, A. B., Memon, M. A., et al. (2024). Exploring suicidality in the aftermath of the 2022 flood in Pakistan: insights from newspaper reports. *CNS Spectr.* 29, 1–3. doi:10.1017/s1092852923002419

Makharia, G. K., Sadeghi, A., Leddin, D., and Costello, A. (2023). Impact of climate change on vulnerable populations. *Gut* 72, 2201–2204. doi:10.1136/gutjnl-2023-331195

Masson-Delmotte, V., Zhai, P., Pirani, A., Connors, S. L., Péan, C., Berger, S., et al. (2021). Climate change 2021: the physical science basis. Contribution of working group I to the sixth assessment report of the intergovernmental panel on climate change. *Chem. Int.* 43, 22–23.

Masson-Delmotte, V., Zhai, P., Pirani, A., Connors, S. L., Péan, C., Berger, S., et al. (2021). Climate change 2021: the physical science basis. Contribution of working group I to the sixth assessment report of the intergovernmental panel on climate change. *Chem. Int.* 2, 2391. doi:10.1017/9781009157896

Matsuoka, Y., Haseda, M., Kanamori, M., Sato, K., Amemiya, A., Ojima, T., et al. (2023). Does disaster-related relocation impact mental health via changes in group participation among older adults? Causal mediation analysis of a pre-post disaster study of the 2016 Kumamoto earthquake. *BMC Public Health* 23, 1982. doi:10.1186/s12889-023-16877-0

Mellish, S., Ryan, J. C., and Litchfield, C. A. (2024). Short-term psychological outcomes of Australia's 2019/20 bushfire season. *Psychol. Trauma Theory, Res. Pract. Policy* 16, 292–302. doi:10.1037/tra0001323

Mendoza-Ortega, J. A., Reyes-Muñoz, E., Nava-Salazar, S., Rodríguez-Martínez, S., Parra-Hernández, S. B., Schnaas, L., et al. (2021). Mitochondrial DNA copy number adaptation as a biological response derived from an earthquake at intrauterine stage. *Int. J. Environ. Res. Public Health* 18, 11771. doi:10.3390/ijerph182211771

Miller, V. E., Pence, B. W., Fitch, K. V., Swilley-Martinez, M., Kavee, A. L., Dorris, S., et al. (2023). Hurricane Florence and suicide mortality in North Carolina: a controlled interrupted time-series analysis. *Inj. Prev.* 29, 180–185. doi:10.1136/ip-2022-044709

Miyaji, C., Takao, S., Noguchi, M., Okazaki, T., Sato, S., and Yorifuji, T. (2022). Social capital and post-traumatic stress disorder among heavy rainfall and flood victims in Japan. *Acta Med. Okayama* 76, 439–446. doi:10.18926/AMO/63903

Musci, R. J., and Schlomer, G. (2018). The implications of genetics for prevention and intervention programming. *Prev. Sci.* 19, 1–5. doi:10.1007/s11121-017-0837-6

Nadeem, A., Ahsan, A., Tariq, R., and Basaria, A. A. A. (2023). Addressing women's mental and maternal well-being in the aftermath of flood disasters: a focus on flood-affected communities in Pakistan. *Med. Confl. Surviv.* 39, 356–363. doi:10.1080/13623699.2023.2255847

Nema, P., Nema, S., and Roy, P. (2012). An overview of global climate changing in current scenario and mitigation action. *Renew. Sustain. Energy Rev.* 16, 2329–2336. doi:10.1016/j.rser.2012.01.044

Olson, D. M., Brémault-Phillips, S., King, S., Metz, G. A. S., Montesanti, S., Olson, J. K., et al. (2019). Recent Canadian efforts to develop population-level pregnancy intervention studies to mitigate effects of natural disasters and other tragedies. *J. Dev. Orig. Health Dis.* 10, 108–114. doi:10.1017/s2040174418001113

Perkins-Kirkpatrick, S. E., and Lewis, S. C. (2020). Increasing trends in regional heatwaves. *Nat. Commun.* 11, 3357. doi:10.1038/s41467-020-16970-7

Qiao, X., Straight, B., Ngo, D., Hilton, C. E., Owuor Olungah, C., Naugle, A., et al. (2024). Severe drought exposure *in utero* associates to children's epigenetic age acceleration in a global climate change hot spot. *Nat. Commun.* 15, 4140. doi:10.1038/s41467-024-48426-7

Redvers, N., Aubrey, P., Celidwen, Y., and Hill, K. (2023). Indigenous Peoples: traditional knowledges, climate change, and health. *PLOS Glob. Public Health* 3, e0002474. doi:10.1371/journal.pgph.0002474

Romanello, M., McGushin, A., Di Napoli, C., Drummond, P., Hughes, N., Jamart, L., et al. (2021). The 2021 report of the Lancet Countdown on health and climate change: code red for a healthy future. *Lancet* 398, 1619–1662. doi:10.1016/s0140-6736(21)01787-6

Saberi, P., Ming, K., Arnold, E. A., Leddy, A. M., and Weiser, S. D. (2023). Extreme weather events and HIV: development of a conceptual framework through qualitative interviews with people with HIV impacted by the California wildfires and their clinicians. *BMC Public Health* 23, 950. doi:10.1186/s12889-023-15957-5

Sackey, E. T., Stewart, R. W., Young, J., and Orengo-Aguayo, R. (2023). Disaster exposure and mental health among Puerto Rican teachers after Hurricane Maria. *J. Trauma. Stress* 36, 1066–1076. doi:10.1002/jts.22973

Sadhukhan, B., Chakraborty, S., and Mukherjee, S. (2022). Investigating the relationship between earthquake occurrences and climate change using RNN-based deep learning approach. *Arabian J. Geosciences* 15, 31. doi:10.1007/s12517-021-09229-y

Saeed, S. A., and Gargano, S. P. (2022). Natural disasters and mental health. *Int. Rev. psychiatry* 34, 16–25. doi:10.1080/09540261.2022.2037524

Šagud, M., Janović, M. B., Ćusa, Z. V., Jakšić, N., Krakan, L. B., Begić, D., et al. (2023). Depression and stress levels in patients with different psychiatric disorders during concurrent early-phase COVID-19 pandemic and earthquake in Croatia. *BMC Psychiatry* 23, 798. doi:10.1186/s12888-023-05302-w

Salawali, S. H., Susanti, H., Daulima, N. H. C., and Putri, A. F. (2020). Posttraumatic growth in adolescent survivors of earthquake, tsunami, and liquefaction in Palu Indonesia: a phenomenological study. *Pediatr. Rep.* 12, 8699. doi:10.4081/pr.2020.8699

Sanches, F. H. C., Martins, F. R., Conti, W. R. P., and Christofoletti, R. A. (2023). The increase in intensity and frequency of surface air temperature extremes throughout the western South Atlantic coast. *Sci. Rep.* 13, 6293. doi:10.1038/s41598-023-32722-1

Schürr, A., Elbel, J., Hieronimi, A., Auer, I., Coenen, M., and Böse-O'Reilly, S. (2023). Mental health in adolescents after experiencing a flood event in Bavaria, Germany-A qualitative interview study. *Front. Public Health* 11, 1210072. doi:10.3389/fpubh.2023.1210072

Sewell, K., Paul, S., De Polt, K., Sugg, M. M., Leeper, R. D., Rao, D., et al. (2024). Impacts of compounding drought and heatwave events on child mental health: insights from a spatial clustering analysis. *Discov. Ment. Health* 4, 1. doi:10.1007/s44192-023-00055-0

Short, M. B., Kaye, S., Knight, C., Riobueno-Naylor, A., Lai, B., Elkins, S., et al. (2023). Parental influence on child mental health post-hurricane Harvey. *J. Child and Adolesc. Trauma* 16, 853–867. doi:10.1007/s40653-023-00554-w

Singh, M., Kumar, V., Sehrawat, N., Yadav, M., Chaudhary, M., Upadhyay, S. K., et al. (2022). Current paradigms in epigenetic anticancer therapeutics and future challenges. *Seminars Cancer Biol.* 83, 422–440. doi:10.1016/j.semcancer.2021.03.013

Straight, B., Qiao, X., Ngo, D., Hilton, C. E., Olungah, C. O., Naugle, A., et al. (2022). Epigenetic mechanisms underlying the association between maternal climate stress and child growth: characterizing severe drought and its impact on a Kenyan community engaging in a climate change-sensitive livelihood. *Epigenetics* 17, 2421–2433. doi:10.1080/15592294.2022.2135213

Tanrıkulu, A. B., Kaya, H., Örüm, M. H., and Akyıldırım, S. (2024). Prevalence and determinants of post-traumatic stress disorder in patients with schizophrenia 2 years after an earthquake in Turkey. *Int. J. Psychiatry Med.* 59, 65–82. doi:10.1177/00912174231180467

Taylor, B., Zhao, Y., Perez, N. B., Potts-Thompson, S., Crusto, C., Creber, R. M., et al. (2024). Epigenome-wide association study of depressive symptoms in Black women in the InterGEN study. *Int. J. Mol. Sci.* 25, 7681. doi:10.3390/ijms25147681

Thompson, R., Hornigold, R., Page, L., and Waite, T. (2018). Associations between high ambient temperatures and heat waves with mental health outcomes: a systematic review. *Public Health* 161, 171–191. doi:10.1016/j.puhe.2018.06.008

Trenberth, K. E. (2007). Warmer oceans, stronger hurricanes. *Sci. Am.* 297, 44–51. doi:10.1038/scientificamerican0707-44

Trenberth, K. E., Dai, A., Van Der Schrier, G., Jones, P. D., Barichivich, J., Briffa, K. R., et al. (2014). Global warming and changes in drought. *Nat. Clim. Change* 4, 17–22. doi:10.1038/nclimate2067

Varshney, K., Makleff, S., Krishna, R. N., Romero, L., Willems, J., Wickes, R., et al. (2023). Mental health of vulnerable groups experiencing a drought or bushfire: a systematic review. *Glob. Ment. Health (Camb)* 10, e24. doi:10.1017/gmh.2023.13

Wang, R., Wang, J., Xu, S., Wang, L., Song, M., An, C., et al. (2022). Prenatal earthquake stress exposure in different gestational trimesters is associated with methylation changes in the glucocorticoid receptor gene (NR3C1) and long-term working memory in adulthood. *Transl. Psychiatry* 12, 176. doi:10.1038/s41398-022-01945-7

Wang, X., Huang, J., Yang, X., Liu, Z., and Zhou, X. (2023). Trajectories of parental posttraumatic stress disorder and children's mental health following Super Typhoon Lekima: the mediating role of feeling of safety. *J. Adolesc.* 95, 1590–1602. doi:10.1002/jad.12228

Watts, R., Liu, W. M., Hooff, M. V., McFarlane, A., Sekhar, V., Kathiravan, T., et al. (2023). Incidence and factors impacting PTSD following the 2005 Eyre Peninsula bushfires in South Australia - a 7 year follow up study. *Aust. J. Rural Health* 31, 132–137. doi:10.1111/ajr.12909

Wertis, L., Runkle, J. D., Sugg, M. M., and Singh, D. (2023). Examining hurricane ida's impact on mental health: results from a quasi-experimental analysis. *Geohealth* 7, e2022GH000707. doi:10.1029/2022gh000707

Xu, R., Li, S., Wu, Y., Yue, X., Wong, E. M., Southey, M. C., et al. (2023). Wildfire-related PM(2.5) and DNA methylation: an Australian twin and family study. *Environ. Int.* 171, 107704. doi:10.1016/j.envint.2022.107704

Yusa, A., Berry, P., J Cheng, J., Ogden, N., Bonsal, B., Stewart, R., et al. (2015). Climate change, drought and human health in Canada. *Int. J. Environ. Res. Public Health* 12, 8359–8412. doi:10.3390/ijerph120708359

Zhu, Y., Gomez, J. A., Laufer, B. I., Mordaunt, C. E., Mouat, J. S., Soto, D. C., et al. (2022). Placental methylome reveals a 22q13.33 brain regulatory gene locus associated with autism. *Genome Biol.* 23, 46. doi:10.1186/s13059-022-02613-1

# Frontiers in
# Epigenetics and Epigenomics

**Explores breakthroughs in Epigenetics and Epigenomics**

An interdisciplinary journal at the forefront of epigenetic science, advancing our understanding of cell biology, development, and disease by uncovering the fundamental processes of epigenetics and epigenomics.

---

## Discover the latest Research Topics

See more →

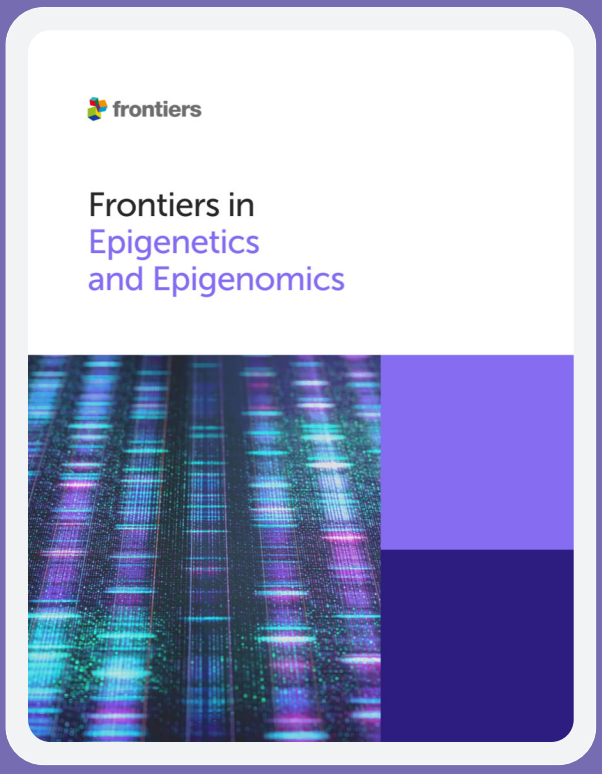


**Frontiers**

Avenue du Tribunal-Fédéral 34
1005 Lausanne, Switzerland
frontiersin.org

**Contact us**

+41 (0)21 510 17 00
frontiersin.org/about/contact